

DISSERTATION

ENERGY STORAGE AND CONVERSION MATERIALS: PART 1: SYNTHESIS AND
CHARACTERIZATION OF RUTHENIUM TRIS-BIPYRIDINE BASED FULLERENE
CHARGE TRANSFER SALTS AS A NEW CLASS OF TUNABLE THERMOELECTRIC
MATERIALS; PART 2: SYNTHESIS AND CHARACTERIZATION OF POLYMER THIN
FILMS FOR USE AS A LITHIUM ION BATTERY SEPARATOR

Submitted by

Daniel James Bates

Department of Chemistry

In partial fulfillment of the requirements

For the Degree of Doctor of Philosophy

Colorado State University

Fort Collins, Colorado

Spring 2013

Doctoral Committee:

Advisor: C. Michael Elliott

Co-Advisor: Amy L. Prieto

Richard G. Finke

Alan Van Orden

Debbie C. Crans

David S. Dandy

ABSTRACT

ENERGY STORAGE AND CONVERSION MATERIALS: PART 1: SYNTHESIS AND CHARACTERIZATION OF RUTHENIUM TRIS-BIPYRIDINE BASED FULLERENE CHARGE TRANSFER SALTS AS A NEW CLASS OF TUNABLE THERMOELECTRIC MATERIALS; PART 2: SYNTHESIS AND CHARACTERIZATION OF POLYMER THIN FILMS FOR USE AS A LITHIUM ION BATTERY SEPARATOR MATERIAL

PART 1: SYNTHESIS AND CHARACTERIZATION OF RUTHENIUM TRIS-BIPYRIDINE BASED FULLERENE CHARGE-TRANSFER SALTS AS A NEW CLASS OF TUNABLE THERMOELECTRIC MATERIALS

The need for clean and efficient energy has never been as great as today. One class of materials that may help address this problem is thermoelectric materials. Thermoelectric (TE) materials can convert thermal energy into electrical energy and, conversely, convert electrical energy into thermal energy. Devices made from thermoelectric materials are composed of solid-state elements with no moving parts. Common uses of TE devices today include cooling systems that cannot tolerate vibrations, such as lasers, and electrical production on space probes and shuttles. The main reason TE devices are not more commonly used is due to their low efficiency.

To address this issue, a class of highly tunable charge-transfer salts was used to investigate relationships between structure and thermoelectric properties. The ultimate goal of the project was to find methods of tuning the electrical conductivity of a material independent of the thermal conductivity. This goal was to be achieved by synthesizing a host of charge transfer fullerene salts of the general form $[ML_n^{p+}]_a(C_{60}^{a-})_p$ where M is ruthenium, L is a bipyridine based

ligand; $p+ = 1+, 2+$; and $a- = 1-$. These salts were expected to exhibit semiconductor behavior and large Seebeck coefficients. Structural data were collected on single crystals through XRD but only three crystals afforded publishable data due to the fullerene being disordered in the crystal lattice. Seebeck coefficients and electrical conductivity values were calculated from a two probe measurement on pressed powders. Values ranging from 100 to $-400 \mu\text{V/K}$ for Seebeck coefficient and 5.6×10^{-2} to 3.3×10^{-5} S/cm for electrical conductivity were achieved. Seebeck values varied significantly from one batch to the next, showing how sensitive Seebeck coefficients were to doping levels.

PART 2: SYNTHESIS AND CHARACTERIATION OF POLYMER THIN FILMS FOR USE AS A LITHIUM-ION BATTERY SEPARATOR MATERIAL

With the increasing price of petroleum based fuels and pressure to move toward a greener economy, the demand for electric vehicles has never been so great. Batteries are used to power electric vehicles and larger vehicles require batteries with greater power density. This has created a large demand for a high-power-density lithium-ion battery. To increase the power of a battery, the time it takes to charge/discharge must be decreased. For a given amount of energy, if it takes longer to get the energy, via discharging, then less power will be achieved. To increase the speed at which a battery can be charged/discharged, two approaches can be taken. If the anode and cathode are made into high surface area electrodes (such as 3-D nanostructures), the surface to volume ratio is increased and the distance that lithium must diffuse into the cathode/anode are decreased, making the charging/discharging process occur faster. The second approach is to make the separation between the anode and cathode smaller, that is, to decrease the separator

thickness. By decreasing the separator thickness, the lithium ions do not have to travel as far from one electrode to the other and the time lithium takes to transport is decreased. The limiting factor holding back the next generation high-surface-area nanostructured lithium-ion batteries is the separator.

The first system explored was a radical initiated aqueous electrodeposition of poly(ethylene glycol) diacrylate. Initial work was done in a glove box with harsh organic solvents, so the first goal was to transition the technique to an aqueous solution on the bench-top. Once optimized, poly(ethylene glycol) diacrylate was deposited onto indium tin oxide planar, copper antimonide planar and 3-D structured electrodes. Monitoring film thickness as a function of deposition time, temperature, and monomer concentration was also achieved. Film thickness was measured using SEM imaging from freeze fractured samples. Impedance spectroscopy was used to determine the ionic conductivity of the solid polymer electrolyte, which was 6.1×10^{-7} S/cm. Film thickness was controllable and films as thin as 2 microns were achieved for this system. A half cell was constructed and cycling was demonstrated, but only when the separator was plasticized.

The second system explored was the direct electrodeposition of diazonium salts to achieve an ultra-thin separator material. The goal of this project was a conformal coating that was under 100 nm thick and grafted to the electrode surface. The goal was chosen because the first project afforded films on the micron scale that were not grafted, which led to many shorted cells plus a thickness that was not practical for nanostructured batteries. In this project, a new class of diazonium salts with poly(ethylene glycol) moieties were synthesized and characterized by NMR and IR spectroscopy. The salts were electrodeposited onto glassy carbon electrodes, showing remarkable self-limiting properties. During a fifteen minute deposition, current dropped

up to 5 orders in magnitude due to the self-limiting nature of diazonium salts. Redox probe experiments confirmed a conformal and pinhole-free film was deposited. Redox probe experiments also show permeation of the film is possible and likely has a size dependency, which is favorable for lithium permeation. Impedance spectroscopy was used to determine the resistance and thickness of the films, around 5-10 k Ω and 3 nm, respectively.

ACKNOWLEDGEMENTS

I am always grateful for the help I have received over the years that has allowed me to get as far as I have come. Over the last 5 years, many people have supported me along my journey and I would like to take a second to acknowledge them.

First, I would like to thank two great advisors, Dr. Mike Elliott and Dr. Amy Prieto, for continued support, funding, and guidance throughout my graduate career. I am truly grateful to have had such great advisors that were always available for questions and patient with my writing, or lack thereof. I would also like to thank Mike and his wife for letting me stay in their basement for a few months, not many advisors would be that gracious, but you and your wife are.

I would like to thank my fiancé, Rebecca Bayer, for her patience and support through all the hard work and late hours. You are a great person and have been a tremendous help, thank you.

I would like to thank my friends and family for their continued support and love through this difficult process. I couldn't do all of this without your support.

I would like to thank a few special individuals that directly helped me with useful discussions throughout my graduate work: Matthew Rawls, Derek Johnson, Tim Arthur, James Mosby, Daniel DiRocco, Megan Lazorski, Ray Taylor, and Richard G. Finke.

I would also like to thank a few special individuals that directly helped me with instrument training and data acquisition: Don Heyse, Pat McCurdy, Jeff Ince, Brian Newell, and Sandeep Kohli.

I would like to thank Jennifer Lippert for her support and love through the first 3 years of my graduate career. You are a great person and I wish you the best in life.

Finally, I would like to thank all my lab-mates for a great experience over the last five years that made graduate school more enjoyable. It will be hard to say goodbye to such a great group of people.

TABLE OF CONTENTS

| | |
|--|-----|
| PART 1: SYNTHESIS AND CHARACTERIZATION OF RUTHENIUM TRIS-BIPYRIDINE BASED FULLERENE CHARGE-TRANSFER SALTS AS A NEW CLASS OF TUNABLE THERMOELECTRIC MATERIALS..... | 1 |
| CHAPTER 1: RUTHENIUM TRIS(BIPYRIDINE) BASED FULLERENE CHARGE-TRANSFER SALTS AS A NEW CLASS OF TUNABLE THERMOELECTRIC MATERIALS | 2 |
| INTRODUCTION | 2 |
| EXPERIMENTAL..... | 18 |
| SYNTHESIS..... | 21 |
| RESULTS AND DISCUSSION..... | 32 |
| CONCLUSION..... | 43 |
| REFERENCES | 45 |
| APPENDIX 1..... | 47 |
| PART 2: SYNTHESIS AND CHARACTERIATION OF POLYMER THIN FILMS FOR USE AS A LITHIUM-ION BATTERY SEPARATOR MATERIAL..... | 110 |
| CHAPTER 2: AQUEOUS ELECTRODEPOSITION OF POLY(ETHYLENE GLYCOL) DIACRYLATE FOR USE AS A LITHIUM-ION BATTERY SEPARATOR MATERIAL.... | 111 |
| INTRODUCTION | 111 |
| EXPERIMENTAL..... | 123 |
| RESULTS AND DISCUSSION..... | 125 |
| CONCLUSION..... | 148 |
| REFERENCES | 151 |
| CHAPTER 3: SYNTHESIS AND CHARACTERIZATION OF DIAZONIUM SALTS WITH A POLY(ETHYLENE GLYCOL) APPENDAGE AND FILMS AFFORDED BY ELECTRODEPOSITION FOR USE AS A LITHIUM-ION BATTERY SEPARATOR MATERIAL..... | 154 |
| INTRODUCTION | 154 |
| EXPERIMENTAL..... | 157 |
| SYNTHESES..... | 158 |
| RESULTS AND DISCUSSION..... | 164 |
| CONCLUSION..... | 176 |
| REFERENCES | 180 |

**PART 1: SYNTHESIS AND CHARACTERIZATION OF RUTHENIUM TRIS-
BIPYRIDINE BASED FULLERENE CHARGE-TRANSFER SALTS AS A NEW CLASS
OF TUNABLE THERMOELECTRIC MATERIALS**

CHAPTER 1: RUTHENIUM TRIS(BIPYRIDINE) BASED FULLERENE CHARGE-TRANSFER SALTS AS A NEW CLASS OF TUNABLE THERMOELECTRIC MATERIALS

INTRODUCTION

The demand for energy continues to grow in our society and around the globe. Alongside this demand is the realization that pollution has detrimental effects on our land, air, and water that should be minimized or avoided. To satisfy the demand for energy, while minimizing environmental effects, a two-pronged approach must be taken. First, energy resources need to be broadened with a focus on cleaner sources such as wind and solar which currently account for 1.36 % of energy production as seen in Figure 1.1.¹ Second, energy must be used more efficiently or recycled from inefficient systems. One method that has great potential for increasing energy efficiency is recycling waste heat. More than half of the energy consumed nationwide is lost as heat, seen in Figure 1.1.¹ If even a small percentage of heat could be recovered, the global effect would be significant.

One class of materials that may help address the energy efficiency problem is thermoelectric materials. Thermoelectric (TE) materials can convert thermal energy into electrical energy and, conversely, electrical energy into thermal energy. Devices made from thermoelectric materials are composed of solid-state elements with no moving parts.²⁻⁴ Common uses of TE devices today include cooling systems in situations that cannot tolerate vibrations, such as lasers, and electrical production on space probes and shuttles.²⁻⁴ The main reason TE devices are not more commonly used is due to their low efficiency.^{2,4}

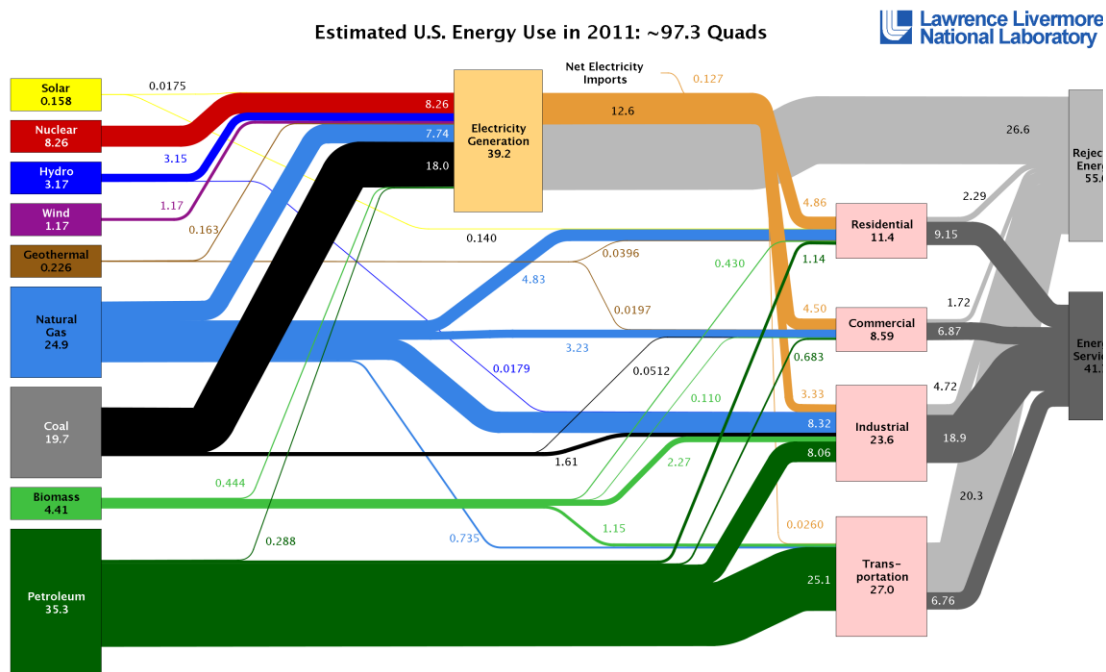


Figure 1.1. A diagram showing energy production and consumption for the United States in 2011. All energy is on a quadrillion BTU scale, with production separated by resource and consumption by sector. Over half the energy produced has no end use and is rejected energy in the form of waste-heat. Figure reproduced from reference 1.

To understand why TE materials have low efficiency, some background information is needed. Shown in Figure 1.2 is a thermoelectric couple, composed of n-doped and p-doped semiconductors that are placed parallel to each other physically and in series electrically.⁵ Heat is then applied to one end, typically waste heat, and the other side is a heat sink, typically air. At the hot end of the material, charge carriers (electrons or holes) are thermally excited into higher energy states. At the cold end the charge carriers are not. Electrons from the n-doped material diffuse to the lower energy states on the cold end of the material; the same effect happens with the holes of the p-doped material. The effect causes a charge build-up across the material and a resultant voltage that can be harnessed in the form of electrical energy.

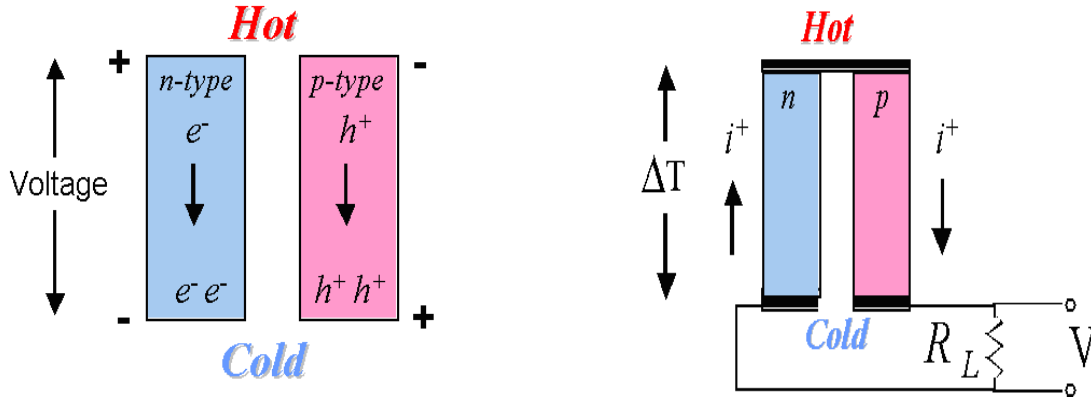


Figure 1.2. Illustration of a thermoelectric couple, composed of a p-type and n-type material, used for power generation. When a temperature difference is applied across the couple, charges build up and current will flow if the elements are connected in a circuit. Figure reproduced from reference 2.

The efficiency of TE materials can be described by 3 equations.⁶

$$\eta = \eta_{carnot} + \eta^* \quad (\text{Eq. 1.1})$$

$$\eta_{carnot} \leq 1 - T_C / T_H \quad (\text{Eq. 1.2})$$

$$\eta^* = ((T_H - T_C) / T_H) * (((ZT + 1)^{1/2} - 1) / ((ZT + 1)^{1/2} + T_C / T_H)) \quad (\text{Eq. 1.3})$$

In the equations above, η = efficiency, T_H = temperature at the hot end (heat applied), T_C = temperature at the cold end (heat sink), and Z = figure of merit (K^{-1}). The efficiency can be increased by increasing η_{carnot} or η^* (thermoelectric efficiency). The Carnot efficiency can be maximized by inducing the largest temperature difference across the material. The larger the T_H relative to T_C , the smaller the ratio T_C/T_H becomes. Although the practical limits of ΔT depend on the material (decomposition temperature and thermal conductivity), maximizing ΔT is not the focus of this chapter. In addition to a large ΔT , the value η^* can also be maximized by increasing the figure of merit (ZT), which is where this work focuses.

The figure of merit is a product of intrinsic property measurements including thermal and electrical conductivity, see equation 4 below. It is worth noting that Z is the figure of merit with units of K^{-1} , while ZT is the dimensionless figure of merit. The dimensionless figure of merit is used as a scale to compare TE materials, with a desired threshold of 4. A figure of merit threshold of 4 was chosen because a $ZT = 4$ would correspond to a Carnot efficiency of *ca.* 30 %, comparable to current refrigeration technology (household scale refrigeration not industrial scale since efficiency scales with size).⁴ A $ZT=1$ corresponds to a Carnot efficiency of *ca.* 10 %.⁴ The equation for ZT is given below.

$$ZT = S^2 \sigma T / \kappa \quad (\text{Eq. 1.4})$$

S = Seebeck coefficient ($\mu\text{V}/\text{K}$), σ = electrical conductivity (S/cm), T = average of temperature difference applied (K), and κ = thermal conductivity (W/Kcm). The Seebeck coefficient and thermal conductivities can be expanded further by the equations below.

$$S = V / \Delta T \quad (\text{Eq. 1.5})$$

$$\kappa = \kappa_{el} + \kappa_{ph} \quad (\text{Eq. 1.6})$$

$$\kappa_{el} = L \sigma T \quad (\text{Eq. 1.7})$$

For the equations above, V is the voltage (V) that forms when a temperature difference (ΔT) across the semi-conductor is applied. The thermal conductivity (κ) is comprised of two parts: κ_{el} is the electron contribution to the thermal conductivity and κ_{ph} is the phonon contribution. The electron contribution to κ is the thermal energy transferred through electrons as they move. The phonon contribution is due to vibrations of the atoms that transmit thermal energy through the

material. The electron contribution can be related to the electrical conductivity by the Wiedemann-Franz relation (Eq. 7) where L = Lorentz number ($W\Omega/K^2$) and T = temperature (K).

From equations 1 and 3, as Z approaches infinity, η^* approaches unity, and the efficiency of the device approaches the Carnot limit.⁶ Unfortunately, the best TE materials to date have ZT values approaching 2.5.^{7,8} Based on equation 4 an ideal thermoelectric material would have a high Seebeck coefficient allowing for a high electrical potential per temperature difference, a high electrical conductivity to maximize electric flow through the device, and a low thermal conductivity to retain a maximum temperature difference. Another way of stating this is that the perfect TE material would be a cross between a phonon glass and an electron crystal.

The term phonon glass refers to a material that is amorphous and therefore has many scattering sites that dissipate and interfere with phonons. An electron crystal refers to a material with long range order that facilitates electron mobility while minimizing defects (scatter sites) and trap states. Combining these ideas affords an ideal TE material. In reality, balancing the properties to find a “sweet spot” is needed since metals exhibit high electrical conductivity while insulators exhibit high Seebeck coefficients and low thermal conductivity, see Figure 1.3.⁹

The Seebeck coefficient is a measure of the voltage that forms when a temperature difference is applied. At the hot end of the material, charge carriers are thermally excited into higher energy states. Some of the carriers retreat toward the cold end of the material, *vide supra*. Not all charge carriers retreat to the cold end of the material due to entropy; some charge carriers remain at the hot end of the material in more energetic states. The Seebeck coefficient is a measure of this phenomenon.

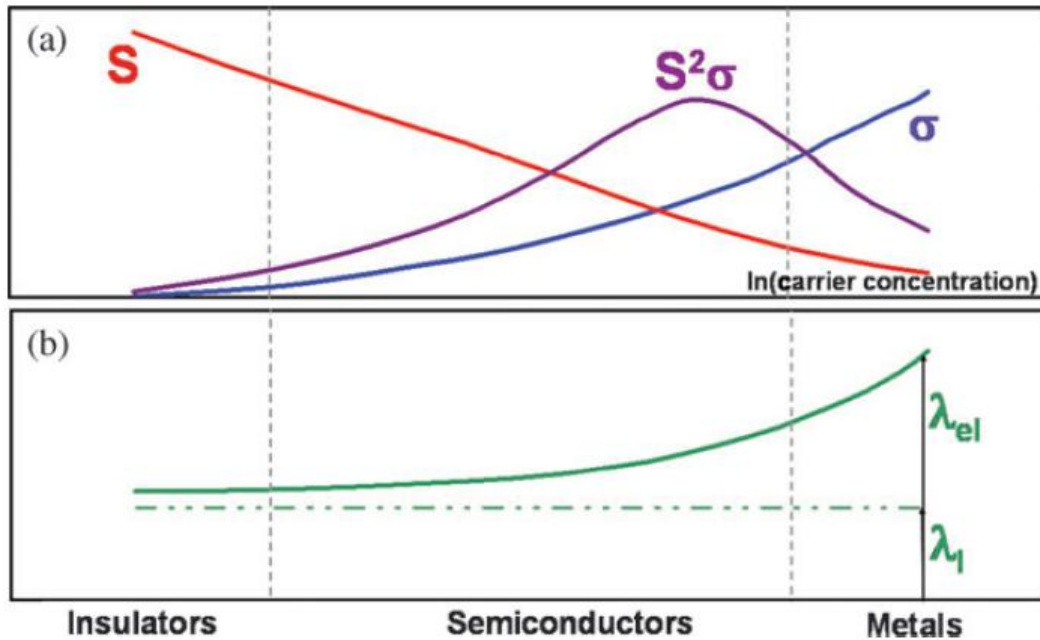


Figure 1.3. Graph illustrating important parameters for TE materials based on material type: metals, semiconductors, and insulators. Figure reproduced from reference 6.

Equations 6 and 7 mathematically describe the limitations of thermoelectric materials for power generation. The equations describe the direct relationship between electrical and thermal conductivity. If the electrical conductivity of a material is increased, so is the electron contribution to the thermal conductivity (κ_{el}). To minimize the thermal conductivity without affecting the electrical conductivity, the phonon contribution to the thermal conductivity must be minimized. Deconvolution of the electrical and thermal conductivity is achieved by independent tuning of κ_{ph} . Three different approaches have been used with moderate success.¹⁰⁻¹⁸

The first method involves doping semiconductors with heavy elements, which introduce atomic scale defects, see Figure 1.4.^{8,10,12} The effect is a scattering of short mean path phonons. Heavier elements vibrate at a lower frequency than lighter elements. This is related by the equation below; f = frequency, k = spring constant, and m = mass.

$$f = (1/2\pi) * (k/m)^{1/2} \quad (\text{Eq. 1.8})$$

Phonons are discrete energy packets of the elastic field in a particular mode.¹⁹ In other words, the energy of a particular phonon mode is quantized. Since energy is quantized, the frequency of vibration for a particular element is dependent upon mass. Therefore, when the phonons interact with the heavy elements, the elements vibrate at a lower frequency

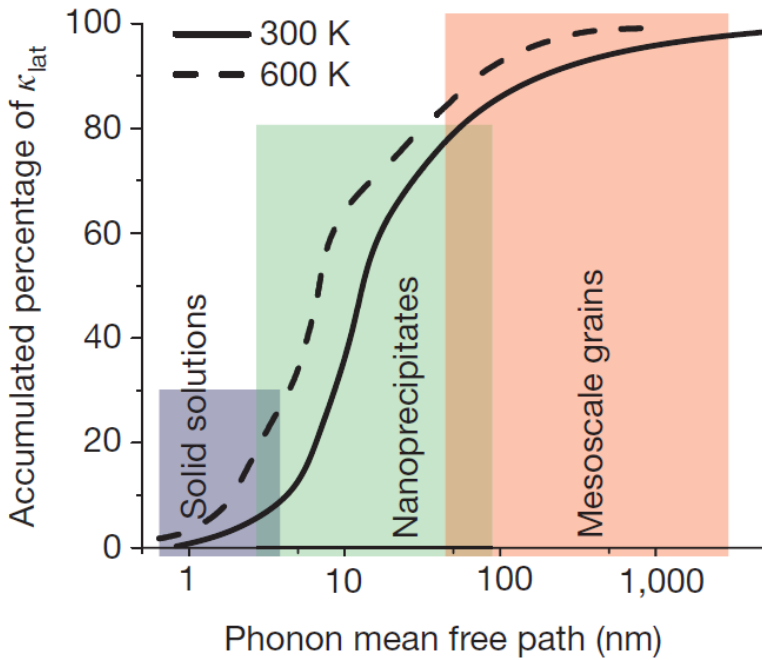


Figure 1.4. Graph showing contributions of phonons with different mean free paths to cumulative κ_{lat} for PbTe. Phonons with short, medium, and long mean free paths can be scattered by atomic-scale defects, nanoscale precipitates, and meso-scale grain boundaries, respectively. Figure reproduced from reference 5.

compared to the rest of the material. The mismatched vibrations lead to destructive interference and phonon scattering, which results in a dampening of the high frequency (low mean free path) phonon vibrations and therefore the phonon contribution to the thermal conductivity. Ideally, the net effect is a lowering of the thermal conductivity without significantly altering the electrical conductivity. In reality, doping alters the electrical conductivity as well, but the net effect is an increased ZT.

The second method involves skutterudites or clathrates that possess a weakly bound atom inside the structure.^{11,15,16} Skutterudites/clathrates are a class of crystalline solids that consist of complex cage-like structures. By putting a weakly bound atom inside the cage-like structure, the atom can rattle around inside the cage and scatter the phonon vibrations randomly. The phonon contribution is lowered because the phonon vibrations are scattered and less directional, thus decreasing the thermal conductivity.

The third method is to use quantum confinement, that is to make very thin films, (2D), nanowires (1D) or nanoparticles (0D) of thermoelectric materials.^{13,14,17,18,20} In the case of wires, it has been shown that by making the wires small enough that quantum size effects are prevalent, the thermal conductivity can be decreased. The lack of atoms in the wires' cross-section (e.g. only 10's of atoms thick) lowers the phonon vibrations in those dimensions and the phonon vibrations approach 1D. Since there are a high percentage of atoms on the edge, when looking at a cross section a large fraction of the phonon vibrations are dampened due to a lack of a medium for propagation. Additionally, due to quantum-size effects the density of states near the Fermi level is increased, which increases the power factor ($S^2\sigma$), see Eq 4.²¹ In the case of nanoparticles, the particles afford phonon scattering sites, but only phonons of similar length scale to the particles (3-100 nm).⁸ Therefore, long wavelength phonons (>100 nm) are largely

unaffected by nanoscale architectures, see Figure 1.4. Still, phonon contributions have been diminished enough to afford ZT in the range of 1.5-1.8.⁸ Recently, a variation of this approach has been reported with great success. By incorporating nanoparticles and mesoscale interfaces, both small wavelength and long wavelength phonons were scattered affording a ZT greater than 2, as seen in Figure 1.5.⁸

Although great success has been had in the field of thermoelectric materials, *vide supra*, much remains to be accomplished. In all cases mentioned, the materials and synthetic methods permit only minimal tuning or structural manipulations. Doping with heavy elements is limited to dopant type and amount. Clathrates and skutterudites allow for slightly better tuning. Atom substitution can be performed on the cage structure where the type of rattling atom(s) and amount can be varied.²²⁻²⁴ The rattling atom is generally restricted to alkali and alkali-earth metals where there can be 0, 1, or 2 rattling atoms per cage.^{23,24}

Nanostructured TE materials are also limited. Although nanostructured materials allow for large variation through manipulation of composition, size, and shape of the nanoparticles, systematic small changes to elucidate structure-property relationships would be extremely difficult and has not been reported.^{25,26} To determine, understand, and optimize structure-property relationships, current TE materials may not be a good choice based on the lack of tunability of the conventional solid-state materials.

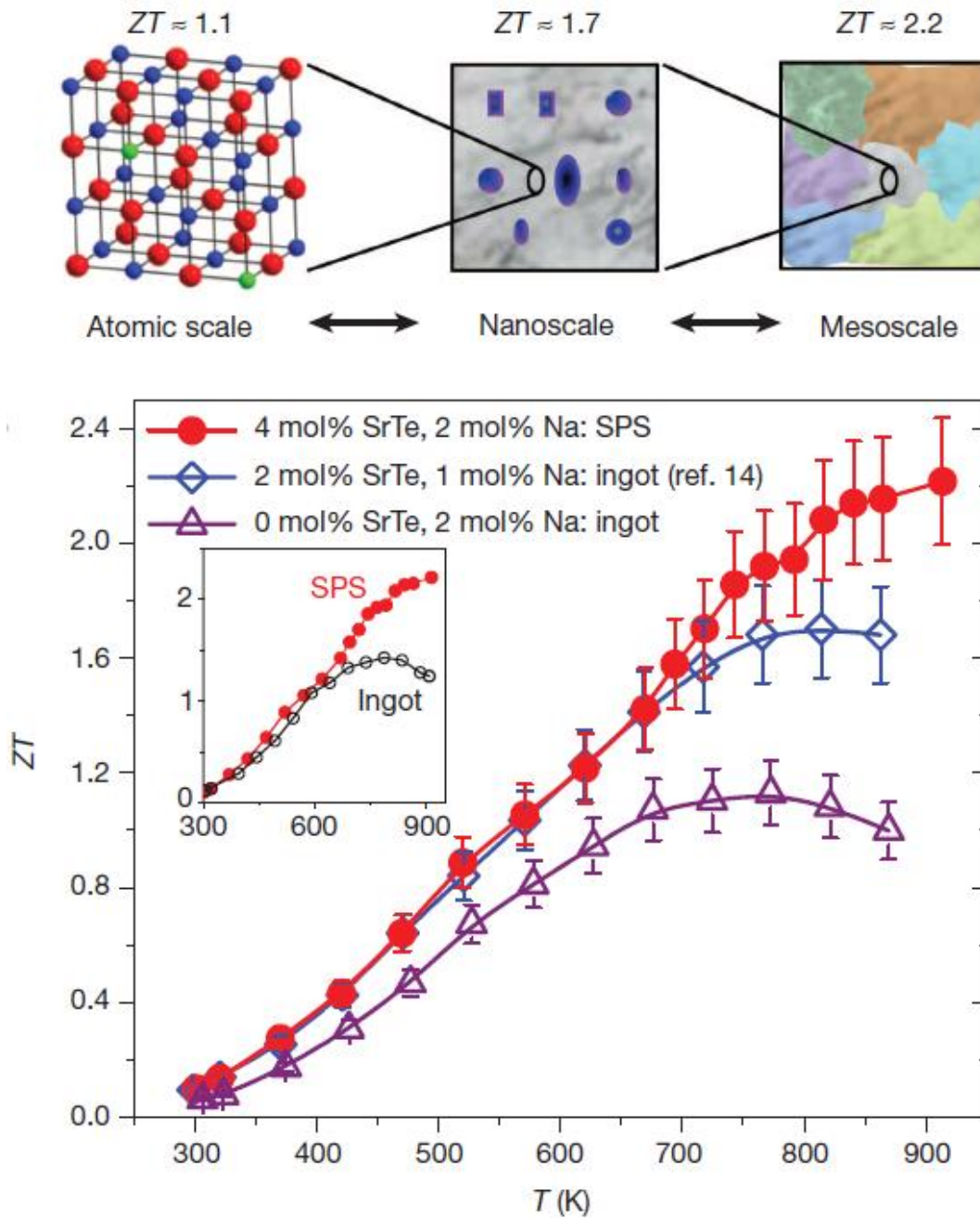


Figure 1.5. ZT as a function of temperature for an ingot of PbTe doped with 2 mol% Na (atomic scale scattering), PbTe-SrTe (2 mol%) doped with 1 mol% Na (atomic plus nanoscale scattering), and spark-plasma-sintered (SPS) PbTe-SrTe (4 mol%) doped with 2 mol% Na (atomic, nano, and mesoscale scattering). Measurement uncertainty is 10 %, as shown by the error bars provided. Figure reproduced from reference 8.

A new class of highly tunable charge transfer salts are proposed that allow for a more fundamental understanding of how structure affects TE properties. In brief, the size of the cation can be tuned by choice of metal and ligand size which should influence phonon contribution to the thermal conductivity, while the carrier concentration can be tuned by the electronic properties of the ligand and metal center. Furthermore, two different stoichiometries can be generated which allows for a second method of tuning carrier concentration through disproportionation. The ultimate goal is to understand how to decouple the thermal and electrical conductivity for this new class of materials, and then tune them independently. The project is unique because it allows for synthetic variation and manipulation that has never been applied to a thermoelectric system and is not typically possible for traditional extended solids. The highly tunable charge transfer salts have the general form $[ML_n^{p+}]_a(C_{60}^{a-})_p$ where M is Fe, Cr, or Ru, L is a bipyridine, terpyridine, or phenanthroline (substituted or unsubstituted); $p+ = 1+, 2+, \text{ or } 3+$; and $a- = 1-, 2-, \text{ or } 3-$. The salts were proposed because they were expected to exhibit semiconductor behavior (*vide infra*), since the synthetic expertise for making ruthenium tris(bipyridine) complexes already existed in C.M. Elliott's group, and because of the multiple tuning pathways expected to be available. The breadth of the project is large. Therefore, in an attempt to focus on proof-of-concept, only bipyridine-based ligands and ruthenium-centered complexes were synthesized.

There are some good reasons for using tris-bipyridine or bis-terpyridine metal complexes. First, they all exhibit multiple reversible redox-couples in the absence of moisture and air, as shown in Figure 1.6.^{27,28} The rich electrochemistry allows for the synthesis of multiple oxidation states from the parent material by means of simple electrochemical or chemical reduction. With each successive reduction the formal charge decreases by one unit. It is known that the reducing electrons go into the ligand based π^* orbitals.^{29,30} The second reason for using these polypyridine

complexes is the semiconductor behavior they exhibit in reduced oxidation states. For instance, $[\text{Ru}(\text{bpy})_3]^0$ has an electrical conductivity of $1.5 \times 10^{-1} \text{ S/cm}$ at $25 \text{ }^\circ\text{C}$.³¹ Since the reducing electron(s) occupies a π^* orbital, there is a net effect of raising the highest occupied molecular orbital (HOMO) of the complex, affording a lower bandgap. With a smaller band gap the reduced ruthenium complexes exhibit semiconductor behavior. Semiconducting charge transfer salts composed of fullerene and ruthenium polypyridine have already been reported by Foss *et al.*³² Hong *et al.* has reported semiconducting behavior for $[\text{Ru}^{2+}(\text{bpy})_3](\text{C}_{60}^{1-})_2$, $[\text{Ru}^{1+}(\text{bpy})_3](\text{C}_{60}^{1-})$, and $[\text{Ru}^{1+}(\text{bpy})_3]_2(\text{C}_{60}^{2-})$ as well.³³ Aside from rich electrochemistry, ruthenium tris(bipyridine) based complexes have a roughly spherical shape of comparable size to C_{60} .^{20,34}

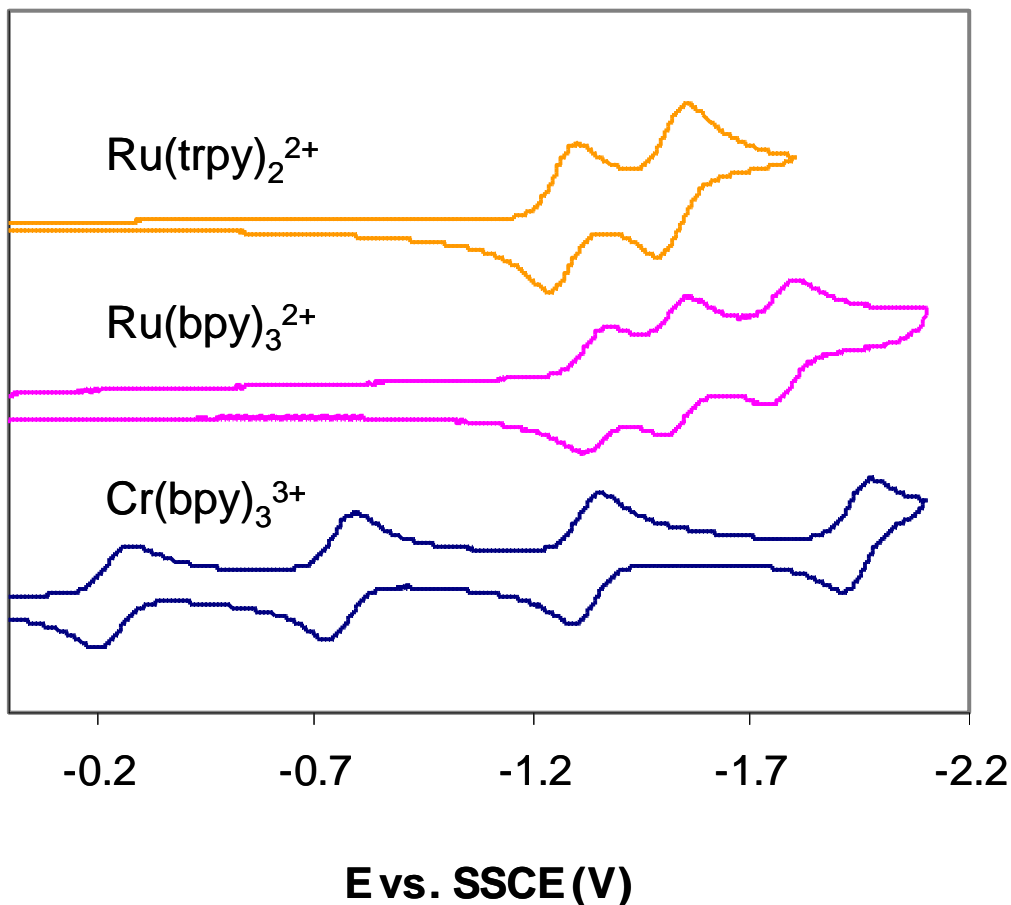
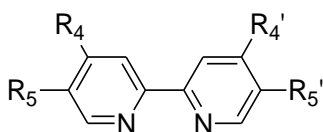
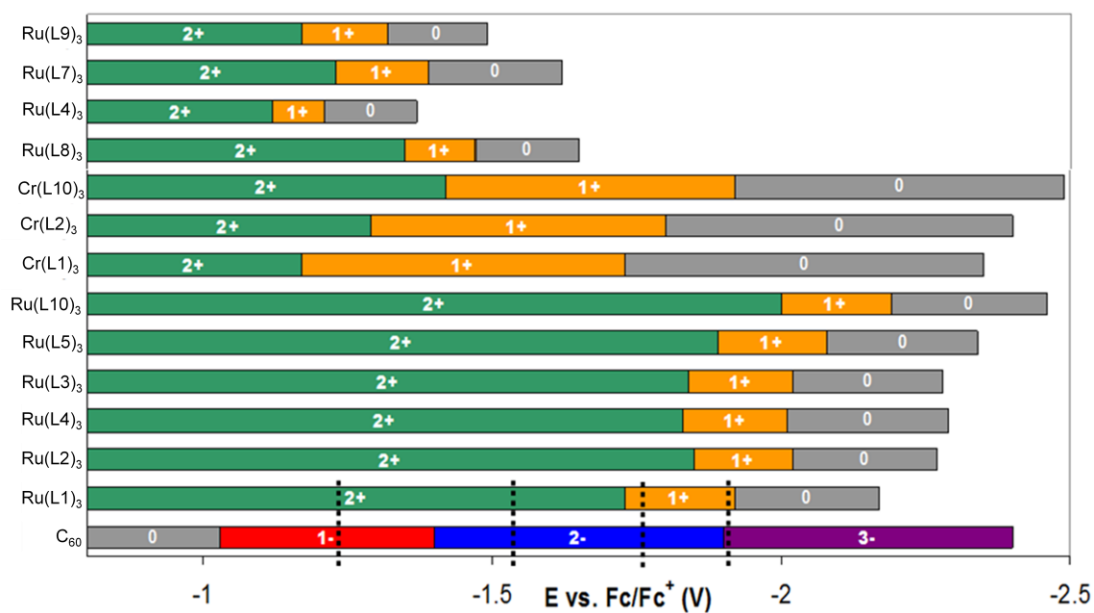


Figure 1.6. Voltammograms for three complexes: $\text{Ru}(\text{bpy})_3^{2+}$, $\text{Ru}(\text{trpy})_2^{2+}$ and $\text{Cr}(\text{bpy})_3^{3+}$. Figure reproduced from reference 28.

There are four reasons for using C_{60} . First, as already mentioned, is the size and shape, which we hypothesized would facilitate crystal growth. The second reason is that C_{60} exhibits semiconductor behavior when doped with alkali metals. For instance, $\text{K}_3(\text{C}_{60})$ has an electrical conductivity of $5 \times 10^2 \text{ S/cm}$.³⁵ The third reason for using C_{60} is the extremely low thermal conductivity values reported for samples doped with Co, Al, or Bi/P co-doped.³⁶ The fourth reason for using C_{60} is because C_{60} exhibits up to six sequential $1e^-$ reductions in solution, and

can form stable anions.³⁷ More importantly, the first four reductions occur over the same potential region that ruthenium (II) trisbipyridines are reduced, (-0.5 to -2.5 V vs Fc/Fc⁺) allowing for variation in the overall salt stoichiometry, see Figure 1.7.

Figure 1.7, in which the X-axis is the potential scale, can be used to predict the possible stoichiometric salts that could be generated based on solution redox potentials. Each horizontal bar corresponds to the complex on the left (L_x, x=1-10). The color of the bar indicates the dominant oxidation state in solution within the potential range. The vertical marks (between oxidation states) indicate each respective E_{1/2} in solution. The data for C₆₀ are at the bottom of the chart. The four dashed lines are examples of possible salt stoichiometries predicted for Ru(bpy)₃. They are [Ru(bpy)₃²⁺](C₆₀¹⁻)₂, [Ru(bpy)₃²⁺](C₆₀²⁻), [Ru(bpy)₃¹⁺]₂(C₆₀²⁻), and [Ru(bpy)₃¹⁺]₃(C₆₀³⁻). The current method used to produce these salts is quite simple. First the metal complex is electrochemically reduced to ML_n⁰ in an inert atmosphere box, isolated, and then used as a reducing agent for C₆₀. With [Ru(bpy)₃]⁰ as an example, addition of 1:1 stoichiometric amounts of [Ru(bpy)₃]⁰:C₆₀ would result in a 2e⁻ reduction of the C₆₀ and a 2e⁻ oxidation of the [Ru(bpy)₃]⁰, affording [Ru(bpy)₃²⁺](C₆₀²⁻). Furthermore, if twice as much C₆₀ was added, keeping all other parameters constant, the [Ru(bpy)₃]⁰ would undergo an 1e⁻ oxidation by two different C₆₀, affording [Ru(bpy)₃²⁺](C₆₀¹⁻)₂. Once again, due to the breadth of the project, only ligands L6-L9, or variations of L6 and L7, were synthesized. Furthermore, charge transfer salts were only synthesized from L6, L7, or a variation of L6 and L7 ligands.



| Lx | R₄ | R₄' | R₅ | R₅' |
|-----------|----------------------|-----------------------|----------------------|-----------------------|
| 1 | H | H | H | H |
| 2 | Me | Me | H | H |
| 3 | <i>i</i> -prop | <i>i</i> -prop | H | H |
| 6 | <i>t</i> -but | <i>t</i> -but | H | H |
| 5 | H | H | Me | Me |
| 8 | COOEt | COOEt | H | H |
| 4 | H | H | COOEt | COOEt |
| 7 | CF ₃ | CF ₃ | H | H |
| 9 | H | H | CF ₃ | CF ₃ |
| 10 | Me | Me | Me | Me |

Figure 1.7. Possible fullerene salts that could be generated based on solution redox potentials. Bipyridine structure is shown for charity. Table inset, above, lists substitution at 4,4' and 5,5' positions. Reproduced from ref. 28.

Electrical conductivity in Ru/C₆₀ based charge transfer salts has been described using an electron-hopping model on an immobilized polyvalent redox system.³³ The electron hopping model is governed by two main factors, the distance between acceptor and donor sites and the relative concentration of the sites. Because the redox potential of the ruthenium complex can be altered predictably, Ru/C₆₀ salts have the ability to tune the concentration of acceptor and donor sites, which will be discussed in more detail below. The size of the ruthenium complex can be altered by synthesizing different sized ligands, also discussed below. Varying ligand size should allow for modifying the distance between donor and acceptor sites, allowing for two approaches to tune the electrical conductivity independently of each other.

In summary, the hypothesis for part 1 of this thesis is that ruthenium tris(bipyridine)/C₆₀-based charge-transfer salts will be a new class of superior thermoelectric materials in terms of tunability and will allow for the fundamental study of structure-to-thermoelectric property relationships. The hypothesis will be judged by measurements of Seebeck coefficient, electrical conductivity, ligand tunability through NMR, and ruthenium complex and charge-transfer salt tunability through CV and UV-Vis-NIR respectively.

EXPERIMENTAL

Ligand and ruthenium complex reactions were conducted under atmospheric conditions. Electrochemical reductions and C₆₀ salt reactions were conducted in an inert atmosphere box. Ligands were characterized by ¹H NMR spectroscopy. Metal complexes were characterized by ¹H NMR spectroscopy, cyclic voltammetry (CV), and UV-visible spectroscopy. Fullerene salts generated were characterized by UV-vis-NIR spectroscopy. Single crystal measurements were performed using a Bruker Kappa Apex 2 CCD diffractometer under a N₂ stream. Data were collected using graphite-monochromatized Mo K α radiation ($\lambda = 0.71703 \text{ \AA}$). Absorption corrections were performed with SADABS.³⁸ The structures were solved using SHELXTL software.³⁹ All chemicals (solvents, supporting electrolytes, and starting materials) were received commercially and used as received unless stated. Benzonitrile, hexane, and heptane were dried over Na metal for 12 hrs prior to distilling, and then stored in an inert atmosphere box. Acetonitrile was obtained from a Pure-Solv solvent purification system and stored in an inert atmosphere box.

The general overall procedure for forming the charge transfer salts is as follows. Ligand esterification reactions were performed on 5,5'-dicarboxy-2,2'-bipyridine or 4,4'-dicarboxy-2,2'-bipyridine. Ru(DMSO)₄Cl₂ was used as the starting material for the complexation reactions with 3.3 eq. ligand in ethylene glycol. The mixture was heated to 120 °C for 20 min. Ruthenium complexes were reduced to overall zero charge by performing bulk electrolysis. Ruthenium fullerene salts were synthesized by adding stoichiometric amounts in benzonitrile. Figure 1.8 below outlines the syntheses for ligands and salt complexes. Detailed syntheses start on page 18.

Solvated single crystals were grown for X-ray analysis. Slow vapor diffusion of heptane or hexane into benzonitrile was most fruitful, although single crystal growth was difficult with C₆₀. Crystals were commonly twinned and often the disorder of the fullerene could not be solved.

Seebeck coefficients and resistivity values were measured in an inert atmosphere box. A polycarbonate block constructed with copper plugs was used for the measurements, see Figure 1.9. The copper plugs could be heated independently and thermocouples were used to monitor the temperature of each plug. Powder samples were pressed between the plugs while heating one plug. The voltage was then measured across the plugs. The thickness and two-point electrical resistance were measured, allowing for the calculation of resistivity.

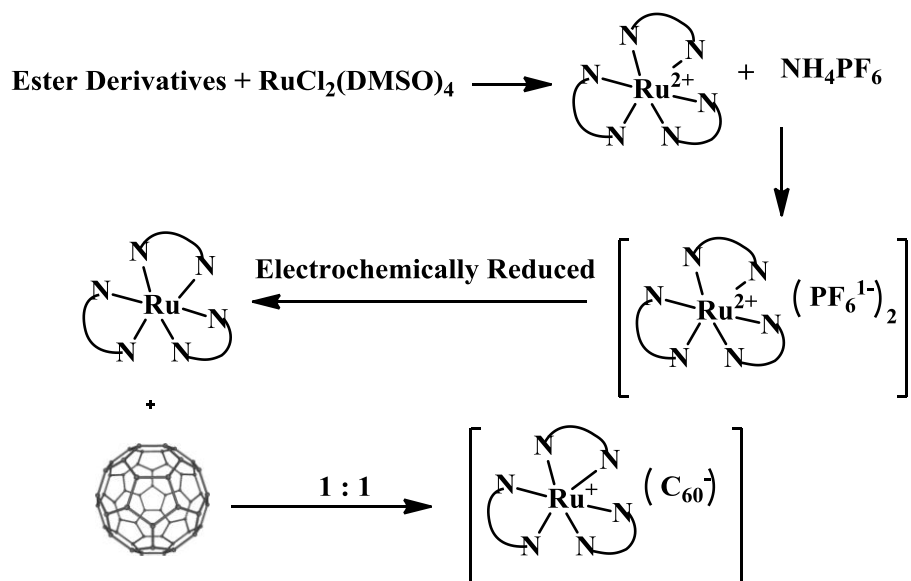
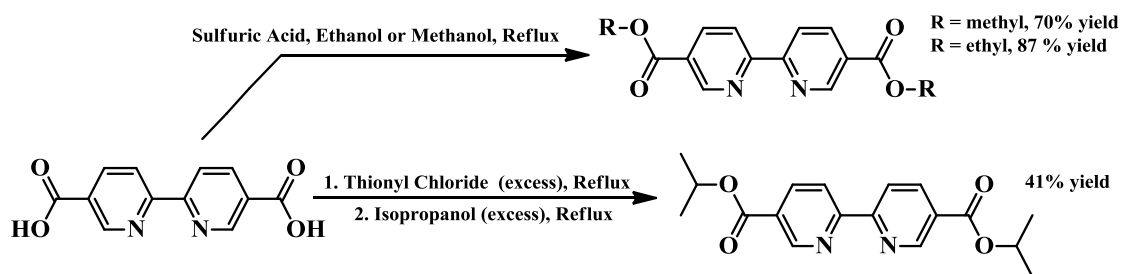


Figure 1.8. Synthetic scheme for ligands and charge-transfer salts.

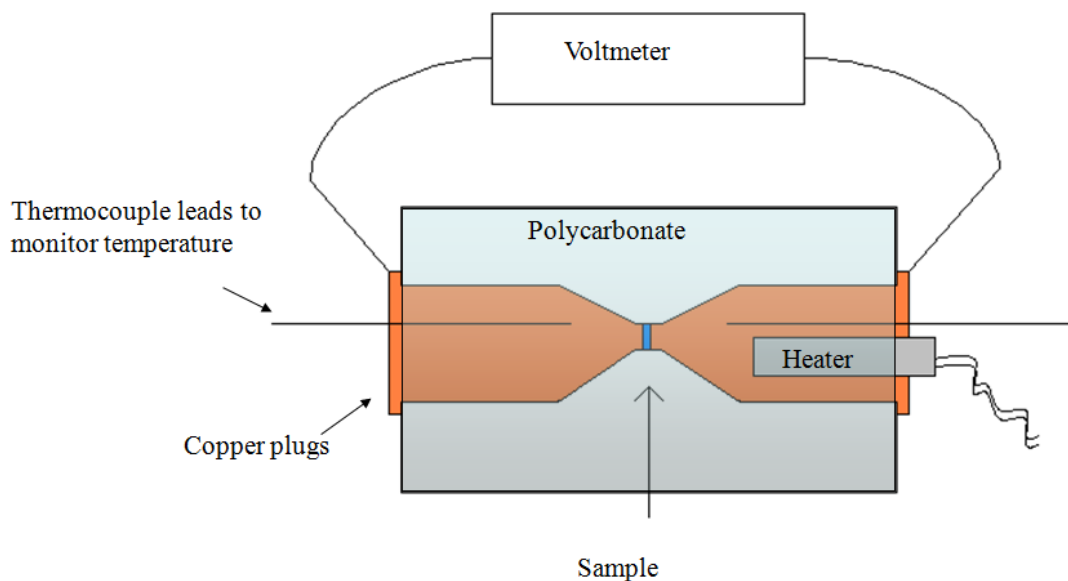


Figure 1.9. Device used to determine Seebeck coefficient and electrical resistivity.

SYNTHESIS

All reduction potentials are reported vs Ag/Ag^+ (1 M AgNO_3 in DMSO).

5,5'-dicarboxy-2,2'-bipyridine (L1). 5,5'-dimethyl-2,2'-bipyridine (8.70 g, 0.0472 mol) was dissolved in 225 mL of 95 % sulfuric acid. $\text{NaCr}_2\text{O}_7 \cdot 2\text{H}_2\text{O}$ (38.2 g, 0.139 mol) was added slowly over 3 hours while an ice bath was used to maintain a temperature below 80 °C. The reaction mixture turned forest green. Once cooled to room temperature, the solution was added to 500 mL of ice. Distilled water was added until the total volume was 1000 mL. A pale off-white solid precipitated over time (12 hr). The solid was isolated, rinsed thoroughly with distilled water, and dried. A pale white solid was recovered, 7.33 g (63.0 % yield). No NMR was taken due to very limited solubility.

4,4'-dicarboxy-2,2'-bipyridine(L2) was synthesized following the procedure by Elliott *et al.*²⁷

5,5'-bis(methoxycarbonyl)-2,2'-bipyridine (L3) was synthesized following the procedure by Elliott *et al.*²⁷ ¹H NMR (300 MHz, CDCl₃, δ): 9.29 (s, 2H), 8.60 (d, 2H), 8.45 (d, 2H), 3.99 (s, 6H). A white crystalline solid was recovered, 0.828 g (70.1 % yield).

5,5'-bis(ethoxycarbonyl)-2,2'-bipyridine (L4) was synthesized following the procedure by Elliott *et al.*²⁷ ¹H NMR (300 MHz, CDCl₃, δ): 9.30 (s, 2H), 8.57 (d, 2H), 8.45 (d, 2H), 4.44 (q, 4H), 1.45 (t, 6H). A white crystalline solid was recovered, 1.54 g (63.3 % yield).

5,5'-bis(isopropoxycarbonyl)-2,2'-bipyridine (L5) A sample of **L1** (2.00 g, 0.00819 mol) was refluxed in 10 mL of thionyl chloride for 24 hr, by which point all of the solid dissolved. Thionyl chloride was evaporated off under reduced pressure (extreme care should be taken to properly trap and neutralize thionyl chloride) using Schlenk line techniques. The resulting solid was refluxed in isopropanol for 48 hrs affording an amber solution. Solvent was removed and the residue redissolved in dichloromethane and filtered. An insoluble brown solid, possible impurity was removed by filtration. Solvent was removed once again and the residue was recrystallized using ethanol. This yielded 1.82 g (67.7 % yield) of white needles. ¹H NMR (300 MHz, CDCl₃, δ): 9.33 (s, 2H), 8.62 (d, 2H), 8.48 (d, 2H), 5.36 (m, 2H), 1.47 (d, 12H).

5,5'-bis(trifluoromethyl)-2,2'-bipyridine (L6) was prepared using a method described in literature.⁴⁰ The only deviation was the column chromatography. The column, a silica stationary phase, was flushed with chloroform (eluent) after running the column as detailed by Furue *et al.* and the product recrystallized using hexanes. Flushing the column increased the yield ~ 2 fold. A white solid was recovered, 0.463 g (53.7 % yield). ¹H NMR (300 MHz, CDCl₃, δ): 8.99 (s, 2H), 8.66 (d, 2H), 8.13 (d, 2H).

4,4'-bis(methoxycarbonyl)-2,2'-bipyridine (L7) was synthesized following the procedure by Elliott *et al.*²⁷ ¹H NMR (300 MHz, CDCl₃, δ): 9.29 (s, 2H), 8.60 (d, 2H), 8.45 (d, 2H), 3.99 (s, 6H). A crystalline white solid was recovered, 0.483 g (43.0 % yield).

4,4'-bis(ethoxycarbonyl)-2,2'-bipyridine (L8) was synthesized following the procedure by Elliott *et al.*²⁷ ¹H NMR (300 MHz, CDCl₃, δ): 8.94 (s, 2H), 8.86 (d, 2H), 7.91 (d, 2H), 4.47 (q, 4H), 1.45 (t, 6H). A crystalline white solid was recovered, 2.10 g (85.1 % yield).

4,4'-bis(isopropoxycarbonyl)-2,2'-bipyridine (L9). A sample of **L2** (1.59 g, 6.50 mmol) was refluxed in 30 mL of thionyl chloride for 5 days, by which point the solid had dissolved. Thionyl chloride was evaporated off under reduced pressure (extreme care should be taken to properly trap and neutralize thionyl chloride) and the resulting solid was refluxed in isopropanol for 24 hr. After 24 hr the mixture had become a transparent solution. Solvent was removed and the residue redissolved in chloroform and filtered. An insoluble solid was removed during this process and discarded. Solvent was removed once again and the residue was recrystallized using ethanol. This yielded 1.67 g (78.3 % yield) of white needles. ¹H NMR (300 MHz, CDCl₃, δ): 8.92 (s, 2H), 8.86 (d, 2H), 7.89 (d, 2H), 5.32 (m, 2H), 1.43 (d, 12H).

4,4'-bis(trifluoromethyl)-2,2'-bipyridine (L10) was prepared using a method described in literature.⁴⁰ A white crystalline solid was recovered, 0.121 g (29.9 % yield). ¹H NMR (300 MHz, CDCl₃, δ): 8.90 (d, 2H), 8.74 (s, 2H), 7.61 (d, 2H).

RuCl₂(DMSO)₄ (C1) was prepared using a method described in literature.⁴¹

[Ru(L3)₃](PF₆)₂ (C2) was synthesized using a modified method published by Hong *et al.*³³ A sample of **L3** (0.372 g, 1.36 mmol) was added to 40 mL ethylene glycol. Then 0.201 g (0.415 mmol) of RuCl₂(DMSO)₄ was added. The mixture was heated to 120 °C and held for 20 min at

that temperature. As the mixture heated the color changed from light yellow to dark greenish black before finally turning dark red. The solution was cooled to room temperature before adding 50 mL distilled water and excess NH_4PF_6 . A red solid precipitated immediately. The red solid was filtered, rinsed with water and dried before refluxing in methanol overnight. The methanol mixture was cooled in an ice bath before filtering. The resulting red solid was recrystallized using a mixed solution of acetone and ethanol. This yielded a red solid, 0.351 g (.291 mmol, 70.1 % yield). ^1H (300 MHz, CD_3CN , δ): 8.72 (d, 2H), 8.60 (d, 2H), 8.13 (s, 2H), 3.80 (s, 6H). The 2+ oxidation state of ruthenium was confirmed by UV-vis ($\lambda_{\text{max}} = 465, 505$ nm in acetonitrile).²⁷

[Ru(L4)₃](PF₆)₂ (C3) was synthesized using the same method as **C2**. A sample of **L4** was used instead of **L3** and the final reflux was done in ethanol rather than methanol. A red crystalline solid was recovered at 96.5 % yield. ^1H NMR (300 MHz, CD_3CN , δ): 8.68 (d, 2H), 8.57 (d, 2H), 8.11 (s, 2H), 4.23 (q, 4H), 1.21 (t, 6H). The 2+ oxidation state of ruthenium was confirmed by UV-vis ($\lambda_{\text{max}} = 465, 505$ nm in acetonitrile).²⁷

[Ru(L5)₃](PF₆)₂ (C4) was synthesized using the same method as **C2**. A sample of **L5** was used instead of **L3** and the final reflux was done in isopropanol rather than methanol. A red crystalline solid was recovered at 60.2 % yield. ^1H NMR (300 MHz, CD_3CN , δ): 8.67 (d, 2H), 8.58 (d, 2H), 8.08 (s, 2H), 5.06 (m, 2H), 1.21 (d, 12H). The 2+ oxidation state of ruthenium was confirmed by UV-vis ($\lambda_{\text{max}} = 465, 505$ nm in acetonitrile).²⁷

[Ru(L7)₃](PF₆)₂ (C5) was synthesized using the same method as **C2**. A sample of **L7** was used instead of **L3**. A red crystalline solid was recovered at 52.8 % yield. ^1H NMR (300 MHz, CD_3CN , δ): 9.07 (s, 2H), 7.86 (d, 2H), 7.82 (d, 2H), 3.99 (s, 6H). The 2+ oxidation state of ruthenium was confirmed by UV-vis ($\lambda_{\text{max}} = 442, 471$ nm in acetonitrile).²⁷

[Ru(L8)₃](PF₆)₂ (C6) was synthesized using the same method as **C2**. A sample of **L8** was used instead of **L3** and the final reflux was done in ethanol rather than methanol. A red crystalline solid was recovered at 73.2 % yield. ¹H NMR (300 MHz, CD₃CN, δ): 9.06 (s, 2H), 7.85 (d, 2H), 7.83 (d, 2H), 4.46 (q, 4H), 1.40 (t, 6H). The 2+ oxidation state of ruthenium was confirmed by UV-vis ($\lambda_{\text{max}} = 442, 471$ nm in acetonitrile).²⁷

[Ru(L9)₃](PF₆)₂ (C7) was synthesized using the same method as **C2**. A sample of **L9** was used instead **L3** and the final reflux was done in isopropanol rather than methanol. A red crystalline solid was recovered at 87.5 % yield. ¹H NMR (300 MHz, CD₃CN, δ): 9.05 (s, 2H), 7.85 (d, 2H), 7.82 (d, 2H), 5.29 (m, 2H), 1.39 (d, 12H). The 2+ oxidation state of ruthenium was confirmed by UV-vis ($\lambda_{\text{max}} = 442, 471$ nm in acetonitrile).²⁷

[Ru(L3)₃]⁰ (C8) was synthesized using a modified method published by Hong *et al.*³³ An electrochemical reduction was performed on [Ru(L3)₃](PF₆)₂ (0.104 g, 0.0864 mmol). The electrolyte solution consisted of 1.12 g tetramethylammonium hexafluorophosphate (TMAPF₆) in 60 mL acetonitrile. A CV was taken to determine the reduction potential, which was -1.175 V. The reduction potential was calculated by averaging the reduction potentials for the +1/0 and 0/-1 couples. The reduction was performed until the current was ≤ 50 μA . A total of 17.1 C of charge passed (expected 16.7 C). Solution turned from red to a dark blue color with the formation of precipitates. The mixture was filtered and a dark blue solid was isolated and rinsed with neat acetonitrile. A dark blue solid was recovered, 0.0172 g (0.0187 mmol, 21.7 % yield). The zero oxidation state of the product was confirmed by UV-vis ($\lambda_{\text{max}} = 414$ and 632 nm in acetonitrile).²⁷

[Ru(L4)₃]⁰ (C9) was synthesized using the same method as **C8**. The differences being that the electrolyte solution consisted of 1.23 g sodium perchlorate (NaClO₄) in 100 mL acetonitrile, a potential of -1.19 V was applied, and 45.6 C of charge were passed (expected 44.7 C). Furthermore, a dark blue solution was isolated and removed of solvent. Then dichloromethane was added to the resulting residue and the mixture was filtered to remove supporting electrolyte. The filtrate was removed of solvent and a dark blue solid was isolated, 0.151 g (0.151 mmol, 64.8 % yield). The zero oxidation state of the product was confirmed by UV-vis (λ_{max} = 415 and 632 nm in acetonitrile).²⁷

[Ru(L5)₃]⁰ (C10) was synthesized using the same method as **C9**. A dark blue solid was recovered, 0.162 g (0.149 mmol, 69.7 % yield). The zero oxidation state of the product was confirmed by UV-vis (λ_{max} = 415 and 628 nm in acetonitrile).²⁷

[Ru(L7)₃]⁰ (C11) was synthesized using the same method as **C8**. The voltage was set to -1.3675 V. A dark brownish black solid was recovered, 0.0607 g (0.0661 mmol, 57.5 % yield). The zero oxidation state of the product was confirmed by UV-vis (λ_{max} = 427 and 540 nm in acetonitrile).²⁷

[Ru(L8)₃]⁰ (C12) was synthesized using the same method as **C8**. The voltage was set to -1.430 V. A dark brownish black solid was recovered, 0.148 g (0.147 mmol, 84.7 % yield). The zero oxidation state of the product was confirmed by UV-vis (λ_{max} = 432 and 550 nm in acetonitrile).²⁷

[Ru(L9)₃]⁰ (C13) was synthesized using the same method as **C8**. The voltage was set to -1.440 V. A dark brownish black solid was recovered, 0.0465 g (0.0428 mmol, 48.1 % yield). The zero oxidation state of the product was confirmed by UV-vis (λ_{max} = 428 and 545 nm in acetonitrile).²⁷

[Ru(L3)₃]¹⁺(C₆₀¹⁻) (S1) was synthesized using a modified method of the one published by Hong *et al.*³³ To 10 mL of benzonitrile was added **C8** (0.0509 g, 0.0555 mmol). Once dissolved, 0.0387 g C₆₀ (0.0537 mmol) was added. This mixture stirred overnight before adding *ca.* 30 mL of hexane. A solid precipitated. The solid was collected by filtration, rinsed with hexane, and dried. A dark purple solid was recovered, 0.0597 g (0.0364 mmol, 69.6 % yield). UV-vis-NIR in benzonitrile confirms the presence of [Ru(L3)₃]¹⁺ (λ_{max} = 410 and 550 nm) and the presence of C₆₀¹⁻ (λ_{max} = 1081 nm).^{27,42}

[Ru(L4)₃]¹⁺(C₆₀¹⁻) (S2) was synthesized using the same method as **S1**. A dark purple solid was recovered, 0.154 g (0.0892 mmol, 89.5 % yield). UV-vis-NIR in benzonitrile confirms the presence of [Ru(L4)₃]¹⁺ (λ_{max} = 414 and 540 nm) and the presence of C₆₀¹⁻ (λ_{max} = 1080 nm).^{27,42}

[Ru(L5)₃]¹⁺(C₆₀¹⁻) (S3) was synthesized using the same method as **S1**. A dark purple solid was recovered, 0.154 g (0.0853 mmol, 79.0 % yield). UV-vis-NIR in benzonitrile confirms the presence of [Ru(L5)₃]¹⁺ (λ_{max} = 411 and 550 nm) and the presence of C₆₀¹⁻ (λ_{max} = 1080 nm).^{27,42}

[Ru(L7)₃]¹⁺(C₆₀¹⁻) (S4) was synthesized using the same method as **S1**. A dark reddish brown solid was recovered, 0.0416 g (0.0254 mmol, 37.7 % yield). UV-vis-NIR in benzonitrile confirms the presence of [Ru(L7)₃]¹⁺ (λ_{max} = 375 and 502 nm) and the presence of C₆₀¹⁻ (λ_{max} = 1081 nm).^{27,42}

[Ru(L8)₃]¹⁺(C₆₀¹⁻) (S5) was synthesized using the same method as **S1**. A dark reddish brown solid was recovered, 0.0349 g (0.0202 mmol, 27.9 % yield). UV-vis-NIR in benzonitrile confirms the presence of [Ru(L8)₃]¹⁺ (λ_{max} = 373 and 502 nm) and the presence of C₆₀¹⁻ (λ_{max} = 1081 nm).^{27,42}

[Ru(L9)₃]¹⁺(C₆₀¹⁻) (S6) was synthesized using the same method as **S1**. A dark reddish brown solid was recovered, 0.0341 g (0.0244 mmol, 74.4 % yield). UV-vis-NIR in benzonitrile confirms the presence of **[Ru(L7)₃]¹⁺** ($\lambda_{\text{max}} = 373$ and 501 nm) and the presence of C₆₀¹⁻ ($\lambda_{\text{max}} = 1080$ nm).^{27,42}

[Ru(L3)₃]²⁺(C₆₀¹⁻)₂ (S7) was synthesized using the same method as **S1** except a 1:2 ratio of **C8**:C₆₀ was used. A dark red solid was recovered, 0.0732 g (0.0310 mmol, 61.9 % yield). UV-vis-NIR in benzonitrile confirms the presence of **[Ru(L3)₃]²⁺** ($\lambda_{\text{max}} = 505$ nm) and the presence of C₆₀¹⁻ ($\lambda_{\text{max}} = 1081$ nm).^{27,42}

[Ru(L4)₃]²⁺(C₆₀¹⁻)₂ (S8) was synthesized using the same method as **S1** except a 1:2 ratio of **C9**:C₆₀ was used. A dark red solid was recovered, 0.105 g (0.0429 mmol, 91.4 % yield). UV-vis-NIR in benzonitrile confirms the presence of **[Ru(L4)₃]²⁺** ($\lambda_{\text{max}} = 505$ nm) and the presence of C₆₀¹⁻ ($\lambda_{\text{max}} = 1080$ nm).^{27,42}

[Ru(L5)₃]²⁺(C₆₀¹⁻)₂ (S9) was synthesized using the same method as **S1** except a 1:2 ratio of **C10**:C₆₀ was used. A dark red solid was recovered, 0.0771 g (0.0305 mmol, 53.4 % yield). UV-vis-NIR in benzonitrile confirms the presence of **[Ru(L5)₃]²⁺** ($\lambda_{\text{max}} = 504$ nm) and the presence of C₆₀¹⁻ ($\lambda_{\text{max}} = 1080$ nm).^{27,42}

[Ru(L7)₃]²⁺(C₆₀¹⁻)₂ (S10) was synthesized using the same method as **S1** except a 1:2 ratio of **C11**:C₆₀ was used. A dark red brown solid was recovered, 0.134 g (0.0568 mmol, 86.6 % yield). UV-vis-NIR in benzonitrile confirms the presence of **[Ru(L7)₃]²⁺** ($\lambda_{\text{max}} = 442$ and 471 nm) and the presence of C₆₀¹⁻ ($\lambda_{\text{max}} = 1081$ nm).^{27,42}

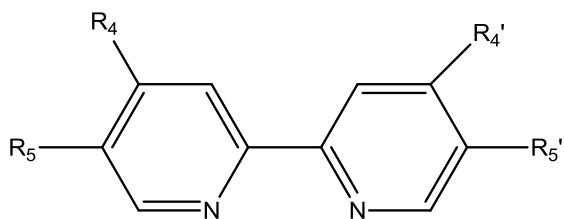
$[\text{Ru}(\text{L8})_3]^{2+}(\text{C}_{60}^{1-})_2$ (**S11**) was synthesized using the same method as **S1** except a 1:2 ratio of **C12**: C_{60} was used. A dark red brown solid was recovered, 0.0731 g (0.0298 mmol, 70.5 % yield). UV-vis-NIR in benzonitrile confirms the presence of $[\text{Ru}(\text{L8})_3]^{2+}$ ($\lambda_{\text{max}} = 442$ and 471 nm) and the presence of C_{60}^{1-} ($\lambda_{\text{max}} = 1080$ nm).^{27,42}

$[\text{Ru}(\text{L9})_3]^{2+}(\text{C}_{60}^{1-})_2$ (**S12**) was synthesized using the same method as **S1** except a 1:2 ratio of **C13**: C_{60} was used. A dark red brown solid was recovered, 0.117 g (0.0463 mmol, 87.0 % yield). UV-vis-NIR in benzonitrile confirms the presence of $[\text{Ru}(\text{L7})_3]^{2+}$ ($\lambda_{\text{max}} = 438$ and 470 nm) and the presence of C_{60}^{1-} ($\lambda_{\text{max}} = 1080$ nm).^{27,42}

SYNTHESIS SUMMARY

Below are tables that summarize the 10 ligands, 6 zero-valent complexes, and 12 salts that have been synthesized.

Table 1.1. Summary of ligands synthesized. Bipyridine structure is shown for clarity.



| Ligand | R ₄ | R ₄ ' | R ₅ | R ₅ ' |
|--------|-----------------|------------------|-----------------|------------------|
| L1 | H | H | COOH | COOH |
| L2 | COOH | COOH | H | H |
| L3 | H | H | COOMe | COOMe |
| L4 | H | H | COOEt | COOEt |
| L5 | H | H | COOi-pr | COOi-pr |
| L6 | H | H | CF ₃ | CF ₃ |
| L7 | COOMe | COOMe | H | H |
| L8 | COOEt | COOEt | H | H |
| L9 | COOi-pr | COOi-pr | H | H |
| L10 | CF ₃ | CF ₃ | H | H |

Table 1.2. Summary of complexes and salts synthesized

| Reduced Ruthenium Complex | Ru : C ₆₀ stoich. | Salt generated |
|---|------------------------------|--|
| Ru ⁰ (diisopropyl-2,2'-bipyridine-5,5'-dicarboxylate) ₃ (C10) | 1:1 | Ru ¹⁺ diisopropyl-2,2'-bipyridine-5,5'-dicarboxylate) ₃ : C ₆₀ ¹⁻ (S3) |
| Ru ⁰ (diisopropyl-2,2'-bipyridine-5,5'-dicarboxylate) ₃ (C10) | 1:2 | Ru ²⁺ diisopropyl-2,2'-bipyridine-5,5'-dicarboxylate) ₃ : (C ₆₀ ¹⁻) ₂ (S9) |
| Ru ⁰ (diethyl-2,2'-bipyridine-5,5'-dicarboxylate) ₃ (C9) | 1:1 | Ru ¹⁺ (diethyl-2,2'-bipyridine-5,5'-dicarboxylate) ₃ : C ₆₀ ¹⁻ (S2) |
| Ru ⁰ (diethyl-2,2'-bipyridine-5,5'-dicarboxylate) ₃ (C9) | 1:2 | Ru ²⁺ (diethyl-2,2'-bipyridine-5,5'-dicarboxylate) ₃ : (C ₆₀ ¹⁻) ₂ (S8) |
| Ru ⁰ (dimethyl-2,2'-bipyridine-5,5'-dicarboxylate) ₃ (C8) | 1:1 | Ru ¹⁺ (dimethyl-2,2'-bipyridine-5,5'-dicarboxylate) ₃ : C ₆₀ ¹⁻ (S1) |
| Ru ⁰ (dimethyl-2,2'-bipyridine-5,5'-dicarboxylate) ₃ (C8) | 1:2 | Ru ²⁺ (dimethyl-2,2'-bipyridine-5,5'-dicarboxylate) ₃ : (C ₆₀ ¹⁻) ₂ (S7) |
| Ru ⁰ (diisopropyl-2,2'-bipyridine-4,4'-dicarboxylate) ₃ (C13) | 1:1 | Ru ¹⁺ (diisopropyl-2,2'-bipyridine-4,4'-dicarboxylate) ₃ : C ₆₀ ¹⁻ (S6) |
| Ru ⁰ (diisopropyl-2,2'-bipyridine-4,4'-dicarboxylate) ₃ (C13) | 1:2 | Ru ²⁺ (diisopropyl-2,2'-bipyridine-4,4'-dicarboxylate) ₃ : (C ₆₀ ¹⁻) ₂ (S12) |
| Ru ⁰ (diethyl-2,2'-bipyridine-4,4'-dicarboxylate) ₃ (C12) | 1:1 | Ru ¹⁺ (diethyl-2,2'-bipyridine-4,4'-dicarboxylate) ₃ : C ₆₀ ¹⁻ (S5) |
| Ru ⁰ (diethyl-2,2'-bipyridine-4,4'-dicarboxylate) ₃ (C12) | 1:2 | Ru ²⁺ (diethyl-2,2'-bipyridine-4,4'-dicarboxylate) ₃ : (C ₆₀ ¹⁻) ₂ (S11) |
| Ru ⁰ (dimethyl-2,2'-bipyridine-4,4'-dicarboxylate) ₃ (C11) | 1:1 | Ru ¹⁺ (dimethyl-2,2'-bipyridine-4,4'-dicarboxylate) ₃ : C ₆₀ ¹⁻ (S4) |
| Ru ⁰ (dimethyl-2,2'-bipyridine-4,4'-dicarboxylate) ₃ (C11) | 1:2 | Ru ²⁺ (dimethyl-2,2'-bipyridine-4,4'-dicarboxylate) ₃ : (C ₆₀ ¹⁻) ₂ (S10) |

RESULTS AND DISCUSSION

The hypothesis for part 1 of this thesis was that ruthenium tris(bipyridine)/C₆₀-based charge-transfer salts would be a new class of superior thermoelectric materials in terms of tunability and would allow for fundamental study of structure-to-thermoelectric property relationships. The hypothesis was judged by measurements of Seebeck coefficient and electrical conductivity through two-point contact electrical measurements (voltage and resistance respectively), ligand tunability through NMR spectroscopy, and ruthenium complex and charge-transfer salt tunability through CV and UV-Vis-NIR respectively.

By changing the ligand, specifically changing the electron donating or accepting abilities of the ligand substituents, the redox potentials of the [ML₃]^{P+} species were altered predictably. For instance, in Figure 1.7, Ru(L8)₃ and Ru(L4)₃, which correspond to [Ru^{P+}(diethyl-2,2'-bipyridine-4,4'-dicarboxylate)₃] and [Ru^{P+}(diethyl-2,2'-bipyridine-5,5'-dicarboxylate)₃] respectively, differ only by the position of the ethyl carboxylate groups on the bipyridine. Since the reducing electrons occupy π* orbitals on the bipyridine-based ligands, the reduction potential is governed by the energy level of the π* orbitals. In the 5,5' position on the bipyridine, π* orbitals of the ligand can delocalize more effectively into the electron withdrawing ester groups compared to the 4,4' position which allows for better stabilization of the reduced complex. The net effect is that 5,5' substitutions reduce at less negative potentials than 4,4' substitutions because of increased stabilization of the reduced complex (assuming the same type of substitution, i.e. an ethyl ester). The shift in reduction potentials based on ligand substitution can be seen in Figure 1.7 (compare L8 and L4).

Since the mechanism of electron conduction through the charge transfer salts involves electron hopping, the concentration of acceptor/donor sites is expected to greatly influence the electrical conductivity. Shifting the redox potential changes the degree of disproportionation and charge-transfer, in accordance with the Nernst equation and the electrical neutrality principle (Figure 1.10), and the electrical conductivity.³³ Shifting the redox potential of the salt closer to the redox potentials of the cation and/or anion increase the degree of disproportionation, while shifting to a more negative value increases the charge-transfer in the salt because C_{60}^{2-} formation becomes easier to achieve. This principle was only confirmed in a few cases when comparing all 12 salts synthesized, for instance $[Ru^{1+}(\text{dimethyl-2,2'-bipyridine-5,5'-dicarboxylate})_3]C_{60}^{1-}$ and $[Ru^{1+}(\text{dimethyl-2,2'-bipyridine-4,4'-dicarboxylate})_3]C_{60}^{1-}$, seen in Table 1.3. $[Ru^{1+}(\text{dimethyl-2,2'-bipyridine-4,4'-dicarboxylate})_3]C_{60}^{1-}$ can undergo significantly more disproportionation and charge-transfer than $[Ru^{1+}(\text{dimethyl-2,2'-bipyridine-5,5'-dicarboxylate})_3]C_{60}^{1-}$ and exhibited a larger electrical conductivity. It is likely that non-ideal stoichiometries were isolated as the products in many of the fullerene salt syntheses, *vide infra*, and the mixed oxidation state salts were affording data that was difficult to interpret. With the higher energy π^* orbitals of 4,4' position on the bipyridine, the reduction potential is shifted to more negative values compared with 5,5' positions, see Figure 1.7. At a more negative potential, the ruthenium complex is a strong enough reducing agent to allow for C_{60}^{2-} formation, via charge-transfer, in the salt. In summary, shifting the reduction potential of the cation to more negative values should increase the amount of charge-transfer and disproportionation, which should increase the electrical conductivity.

$$\begin{aligned}
[\text{RuL}_3^{2+}] + [\text{RuL}_3^{1+}] + [\text{RuL}_3^0] &= 1 && \text{(stoichiometric balance)} \\
[\text{C}_{60}^0] + [\text{C}_{60}^{1-}] + [\text{C}_{60}^{2-}] &= 1 && \text{(stoichiometric balance)} \\
[\text{Ru}^{1+}] + 2[\text{Ru}^{2+}] &= [\text{C}_{60}^{1-}] + 2[\text{C}_{60}^{2-}] && \text{(charge neutrality)} \\
E_{\text{eq}} &= E_{0/1+}^0 - (RT/F)\ln([\text{RuL}_3^0]/[\text{RuL}_3^{1+}]) && \text{(nernst eq.)} \\
E_{\text{eq}} &= E_{1+/2+}^0 - (RT/F)\ln([\text{RuL}_3^{1+}]/[\text{RuL}_3^{2+}]) && \text{(nernst eq.)} \\
E_{\text{eq}} &= E_{1-/0}^0 - (RT/F)\ln([\text{C}_{60}^{1-}]/[\text{C}_{60}^0]) && \text{(nernst eq.)} \\
E_{\text{eq}} &= E_{2-/1-}^0 - (RT/F)\ln([\text{C}_{60}^{2-}]/[\text{C}_{60}^{1-}]) && \text{(nernst eq.)}
\end{aligned}$$

Figure 1.10. Equations for calculating disproportionated redox species for $[\text{Ru}^{1+}(\text{diethyl-2,2'-bipyridine-5,5'-dicarboxylate})_3]\text{C}_{60}^{1-}$ in solution with the assumption that $[\text{Ru}(\text{diethyl-2,2'-bipyridine-5,5'-dicarboxylate})_3]^0$ and C_{60}^0 were mixed in exact 1:1 ratio.

Table 1.3. Summary of Seebeck coefficients and conductivity values for all 12 charge transfer salts, Bi₂Te₃, a leading TE material near room temperature, is listed for comparison.

| Charge Transfer Salt | Seebeck (μV/K) | Conductivity (S/cm) |
|--|----------------|------------------------------|
| [Ru ¹⁺ (diisopropyl-2,2'-bipyridine-5,5'-dicarboxylate) ₃]C ₆₀ ¹⁻ | 16 ± 4 | 2.5 ± 0.5 x 10 ⁻² |
| [Ru ¹⁺ (diethyl-2,2'-bipyridine-5,5'-dicarboxylate) ₃]C ₆₀ ¹⁻ | -17 ± 4 | 1.1 ± 0.2 x 10 ⁻³ |
| [Ru ¹⁺ (dimethyl-2,2'-bipyridine-5,5'-dicarboxylate) ₃]C ₆₀ ¹⁻ | -10 ± 1 | 2.2 ± 0.4 x 10 ⁻³ |
| [Ru ²⁺ (diisopropyl-2,2'-bipyridine-5,5'-dicarboxylate) ₃](C ₆₀ ¹⁻) ₂ | -170 ± 25 | 1.3 ± 0.3 x 10 ⁻² |
| [Ru ²⁺ (diethyl-2,2'-bipyridine-5,5'-dicarboxylate) ₃](C ₆₀ ¹⁻) ₂ | -400 ± 140 | 2.4 ± 0.5 x 10 ⁻³ |
| [Ru ²⁺ (dimethyl-2,2'-bipyridine-5,5'-dicarboxylate) ₃](C ₆₀ ¹⁻) ₂ | -120 ± 10 | 5.6 ± 1.1 x 10 ⁻⁵ |
| [Ru ¹⁺ (diisopropyl-2,2'-bipyridine-4,4'-dicarboxylate) ₃]C ₆₀ ¹⁻ | -130 ± 30 | 1.4 ± 0.3 x 10 ⁻³ |
| [Ru ¹⁺ (diethyl-2,2'-bipyridine-4,4'-dicarboxylate) ₃]C ₆₀ ¹⁻ | -120 ± 20 | 6.2 ± 1.2 x 10 ⁻³ |
| [Ru ¹⁺ (dimethyl-2,2'-bipyridine-4,4'-dicarboxylate) ₃]C ₆₀ ¹⁻ | -160 ± 40 | 1.5 ± 0.3 x 10 ⁻² |
| [Ru ²⁺ (diisopropyl-2,2'-bipyridine-4,4'-dicarboxylate) ₃](C ₆₀ ¹⁻) ₂ | -17 ± 4 | 5.6 ± 1.1 x 10 ⁻² |
| [Ru ²⁺ (diethyl-2,2'-bipyridine-4,4'-dicarboxylate) ₃](C ₆₀ ¹⁻) ₂ | 100 ± 8 | 8.3 ± 1.7 x 10 ⁻⁵ |
| [Ru ²⁺ (dimethyl-2,2'-bipyridine-4,4'-dicarboxylate) ₃](C ₆₀ ¹⁻) ₂ | 58 ± 8 | 3.3 ± 0.7 x 10 ⁻⁵ |
| Bi ₂ Te ₃ (Spark plasma sintered) | 150 | 1.9 x 10 ⁷ |

In an attempt to increase the electrical conductivity, disproportionation was forced by thoroughly mixing 1:1 molar ratios of $[\text{Ru}^{1+}(\text{diethyl-2,2'}\text{-bipyridine-5,5'-dicarboxylate})_3]\text{C}_{60}^{1-}$ ($\sigma = 1.1 \times 10^{-3}$ S/cm) and $[\text{Ru}^{2+}(\text{diethyl-2,2'}\text{-bipyridine-5,5'-dicarboxylate})_3](\text{C}_{60}^{1-})_2$ ($\sigma = 2.4 \times 10^{-3}$ S/cm) in a mortar and pestle. The resulting salt exhibited an electrical conductivity of 5.0×10^{-2} S/cm, an increase of greater than one order of magnitude versus the starting materials.

Electrical conductivity measurements were also investigated as a function of pressure on the sample. Electrical conductivity increased with increased pressure, in one case increasing by 16%. Because of this variance in conductivity with pressure, and because sample pressure was not measured along with the conductivity, an estimated error of 20% was assigned to the conductivity measurements. Also, only two point conductivity measurements were performed, so contact resistance was not taken into account, but was minimized through the use of conductive copper plugs.

The size of the $[\text{RuL}_3]^{\text{p}+}$ was also altered. By changing the methyl group on 5,5'-bis(methoxy carbonyl)-2,2'-bipyridine to ethyl or isopropyl, the size of the ruthenium complex was changed significantly. One effect of increasing the size of the complex was a lowering of the charge density. It also would change the distance for electron hopping, discussed *vide infra*. We hypothesized that a lower charge density would lead to a lower phonon contribution due to the presence of weaker electrostatic interactions. Since many of the phonons in salts travel through electrostatic interactions, decreased charge density was expected to lower the phonon contribution.⁴³ Increasing the cation size should also increase the unit cell, all other parameters being constant. Thermal conductivity measurements have not been performed because the measurement is nontrivial, particularly for air sensitive samples, and electrical conductivity

values were low for the samples. Therefore, future work will be needed to support or refute the hypothesis that a decreased charge density lowers the phonon contribution to the thermal conductivity.

Structural data were collected for three salts: $[\text{Ru}^{1+}(\text{dimethyl-2,2'-bipyridine-5,5'-dicarboxylate})_3]\text{C}_{60}^{1-}$, $[\text{Ru}^{1+}(\text{diethyl-2,2'-bipyridine-5,5'-dicarboxylate})_3]\text{C}_{60}^{1-}$, and $[\text{Ru}^{1+}(\text{diisopropyl-2,2'-bipyridine-5,5'-dicarboxylate})_3]\text{C}_{60}^{1-}$ which can be found in Appendix 1 (pg 47). The structural data showed that the isopropyl based salt packs such that ruthenium-ruthenium distances were reduced compared to ethyl or methyl analogues, with methyl the next closest. This is an unexpected result that may help explain the electrical conductivities of the different salts. The conductivity follows the same trend from highest to lowest: isopropyl, methyl, and then ethyl, seen in Table 1.4. We hypothesize that the closer ruthenium distances in the structure allow for better electron hopping and more mixed valency in the overall salt affording higher electrical conductivity.

Table 1.4. Comparison of ruthenium-ruthenium distances with electrical conductivity for the 3 crystal structures.

| Salt | Ru-Ru Distance (Å) | Conductivity (S/cm) |
|---|--------------------|------------------------------|
| [Ru ¹⁺ (diethyl-2,2'-bipyridine-5,5'-dicarboxylate) ₃]/C ₆₀ ¹⁻ | 18.534(3) | 1.1 ± 0.2 x 10 ⁻³ |
| [Ru ¹⁺ (dimethyl-2,2'-bipyridine-5,5'-dicarboxylate) ₃]/C ₆₀ ¹⁻ | 14.4091(3) | 2.2 ± 0.4 x 10 ⁻³ |
| [Ru ¹⁺ (diisopropyl-2,2'-bipyridine-5,5'-dicarboxylate) ₃]/C ₆₀ ¹⁻ | 10.08(3) | 2.5 ± 0.5 x 10 ⁻² |

Salt stoichiometry was also varied in the experiments. Based on the redox potentials of the ruthenium complexes synthesized, two stoichiometries could be synthesized, 1:1 and 1:2, Ru:C₆₀. This is highlighted in Figure 1.11 with two horizontal, dashed, blue lines. The C₆₀ image in Figure 1.11 is courtesy of the Nanotechnology lab at Georgia Tech Research Institute.⁴⁴ The salt stoichiometry was shown to affect the electrical conductivity, likely due to disproportionation. Salts with 1:2 stoichiometry, or Ru²⁺/(C₆₀¹⁻)₂, exhibited the lowest electrical conductivity on average and also underwent the least amount of disproportionation because formation of Ru³⁺ is energetically unfavorable.

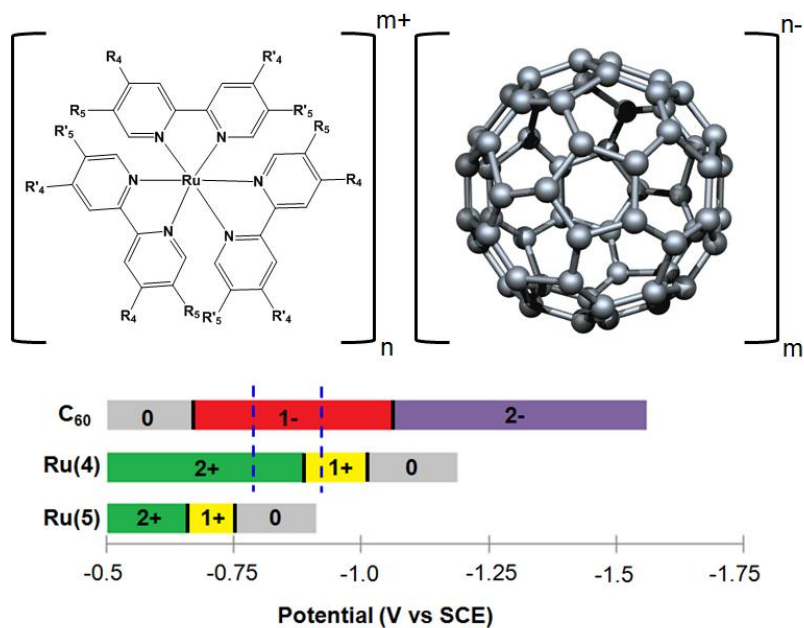


Figure 1.11. Generic structure of ruthenium tris(bipyridine)/C₆₀ salt highlighting 4,4' and 5,5' positions. Also shown are redox potential regions for [Ru^{m+}(diethyl-2,2'-bipyridine-5,5'-dicarboxylate)₃] (**Ru(5)**), [Ru^{m+}(diethyl-2,2'-bipyridine-4,4'-dicarboxylate)₃] (**Ru(4)**), and C₆₀ vs SCE. Vertical lines separating different colored regions of the horizontal bars indicate E_{1/2} for the respective redox couple. Blue dashed lines represent potentials where 1:1 and 1:2 stoichiometries exist for Ru(4):C₆₀ respectively.

Seebeck coefficients ranging from 100 to -400 $\mu\text{V}/\text{K}$ were measured for the 12 salts that have been synthesized, seen in Table 1.3. This is a large range of values for a small group of salts, with Seebeck coefficients larger than Bi₂Te₃, a leading room temperature TE material. It is interesting that both hole and electron carrier materials were synthesized, although it should be noted that the positive and negative Seebeck coefficients could be due to non-ideal stoichiometries that were isolated as the products from the fullerene salt syntheses (*vide infra*), and thus behaving as doped samples. The range of values is promising, but further study is needed with higher purity materials (non mixed-oxidation-state salts).

The Seebeck coefficient was variable from batch to batch, in the case of $[\text{Ru}^{2+}(\text{diethyl-2,2'-bipyridine-5,5'-dicarboxylate})_3](\text{C}_{60}^{1-})_2$ values ranging from -120 to -540 $\mu\text{V}/\text{K}$ were measured. The large variation likely has to do with changes in the overall salt stoichiometry. Seebeck coefficients in other materials have been shown to shift or vary because of small concentration changes, similar to doping.³⁶ The stoichiometric variations were confirmed by analyzing UV-vis-NIR data, but a trend between doping levels and Seebeck coefficients was not established and will require further study.

Because of the variability from batch to batch, concentration ratios of cation-to-anion were determined for all 12 salts from UV-Vis-NIR data. A large short-coming was discovered when cation-to-anion ratios were determined. In most cases, since the charge-transfer salts were kinetically precipitated from solution, a non-ideal stoichiometric ratio was isolated. Since ruthenium complexes were used as the reducing agent for C_{60} , and were the only two reagents, it was assumed that very few reaction pathways could exist, and that if oxidation states were correct by UV-Vis-NIR, the stoichiometry would be as predicted. This was a false assumption.

The concentration of ionic species was calculated through Beers law and UV-Vis-NIR data. For all cases, absorbance values for ruthenium ions had to be corrected because C_{60}^{1-} also absorbs in the same range of wavelengths. To make the correction, the molar absorptivity of C_{60}^{1-} was estimated at 410, 471, 501, and 505 nm (λ_{max} values for ruthenium ions) using work published by Lawson *et al.*⁴² At 410 nm, the molar absorptivity was $4500 \text{ M}^{-1}\text{cm}^{-1}$, and 471-505 nm all wavelengths had a very similar absorptivity near $3000 \text{ M}^{-1}\text{cm}^{-1}$. Corrections to the C_{60}^{1-} absorption at 1078 nm were also needed for $[\text{Ru}^{1+}(\text{4,4'-ester substituted bipyridine})_3]$, which has some absorption at 1078 nm.⁴⁵ None of the other ruthenium cations absorb at 1078 nm, so no corrections to C_{60}^{1-} absorptions were needed for those salts.⁴⁵ Since the molar absorptivity of

[Ru¹⁺(4,4'-ester substituted bipyridine)₃] was *ca.* 1/12 the molar absorptivity of C₆₀¹⁻ at 1078 nm, and an equal concentration of each ion was assumed, the absorbance was corrected by subtracting out 1/12 of the absorbance at 1078 nm before calculating the C₆₀¹⁻ concentration. Table 1.5 below summarizes the concentration ratios calculated.

For the Ru¹⁺ salts, in all but one case the ratio of cation-to-anion is smaller than predicted. The ratio could be smaller due to the ruthenium complexes being a mixture of Ru¹⁺ and Ru²⁺. If a mixture of oxidation states for ruthenium were present, the resulting salt would contain more C₆₀¹⁻ to maintain charge neutrality. For Ru²⁺ salts, ratios above and below the predicted cation-to-anion ratio were obtained. This was a surprising find that will require a further and more detailed study. Lastly, the ratios calculated from an X-ray quality single crystal sample were significantly off the predicted cation-to-anion ratio. By correcting for C₆₀¹⁻ absorbance at 410 nm, the cation-to-anion ratio changed from 1:1.06 to 1:1.30. This seems odd, but calculations were double checked and done properly. In the cases of Ru:C₆₀ ratios greater than 1:2, solvent absorbance was the first concern but this concern was omitted because benzonitrile does not absorb in the C₆₀ absorbance range (900-1080 cm⁻¹). A second hypothesis was that oxidative processes (from alcohols or oxygen in the glove box) occurred and the rate of oxidation for the cation was faster than the rate of oxidation of the anion, leading to a lower than expected absorbance for the cation. Clearly, further and more detailed UV-Vis-NIR studies are needed to properly isolate and identify the charge-transfer salts without mixed oxidation states.

Table 1.5. Summary of theoretical cation-to-anion ratios and calculated cation-to-anion ratios for all 12 salts. $[\text{Ru}^{1+}(\text{dimethyl-2,2'}\text{-bipyridine-4,4'}\text{-dicarboxylate})_3]\text{C}_{60}^{1-}$ has two entries, one for a kinetically precipitated sample and another from a single crystal growth that yielded X-ray quality crystals used to solve the structure of $[\text{Ru}^{1+}(\text{dimethyl-2,2'}\text{-bipyridine-4,4'}\text{-dicarboxylate})_3]\text{C}_{60}^{1-}$.

| Concentration ratios calculated from UV-Vis-NIR data | Theoretical Ratio (Ru:C ₆₀) | Calculated Ratio (Ru:C ₆₀) |
|--|--|---|
| $[\text{Ru}^{1+}(\text{diisopropyl-2,2'}\text{-bipyridine-5,5'}\text{-dicarboxylate})_3]\text{C}_{60}^{1-}$ | 1:1 | 1.0:2.6 |
| $[\text{Ru}^{1+}(\text{diethyl-2,2'}\text{-bipyridine-5,5'}\text{-dicarboxylate})_3]\text{C}_{60}^{1-}$ | 1:1 | 1.0:2.0 |
| $[\text{Ru}^{1+}(\text{dimethyl-2,2'}\text{-bipyridine-5,5'}\text{-dicarboxylate})_3]\text{C}_{60}^{1-}$ | 1:1 | 1.0:1.0 |
| $[\text{Ru}^{1+}(\text{dimethyl-2,2'}\text{-bipyridine-4,4'}\text{-dicarboxylate})_3]\text{C}_{60}^{1-}$ (Single Crystal) | 1:1 | 1.0:1.3 |
| $[\text{Ru}^{2+}(\text{diisopropyl-2,2'}\text{-bipyridine-5,5'}\text{-dicarboxylate})_3](\text{C}_{60}^{1-})_2$ | 1:2 | 1.0:1.4 |
| $[\text{Ru}^{2+}(\text{diethyl-2,2'}\text{-bipyridine-5,5'}\text{-dicarboxylate})_3](\text{C}_{60}^{1-})_2$ | 1:2 | 1.0:1.8 |
| $[\text{Ru}^{2+}(\text{dimethyl-2,2'}\text{-bipyridine-5,5'}\text{-dicarboxylate})_3](\text{C}_{60}^{1-})_2$ | 1:2 | 1.0:2.9 |
| $[\text{Ru}^{1+}(\text{diisopropyl-2,2'}\text{-bipyridine-4,4'}\text{-dicarboxylate})_3]\text{C}_{60}^{1-}$ | 1:1 | 1.0:1.5 |
| $[\text{Ru}^{1+}(\text{diethyl-2,2'}\text{-bipyridine-4,4'}\text{-dicarboxylate})_3]\text{C}_{60}^{1-}$ | 1:1 | 1.0:1.5 |
| $[\text{Ru}^{1+}(\text{dimethyl-2,2'}\text{-bipyridine-4,4'}\text{-dicarboxylate})_3]\text{C}_{60}^{1-}$ | 1:1 | 1.0:1.5 |
| $[\text{Ru}^{2+}(\text{diisopropyl-2,2'}\text{-bipyridine-4,4'}\text{-dicarboxylate})_3](\text{C}_{60}^{1-})_2$ | 1:2 | 1.0:3.1 |
| $[\text{Ru}^{2+}(\text{diethyl-2,2'}\text{-bipyridine-4,4'}\text{-dicarboxylate})_3](\text{C}_{60}^{1-})_2$ | 1:2 | 1.0:2.3 |
| $[\text{Ru}^{2+}(\text{dimethyl-2,2'}\text{-bipyridine-4,4'}\text{-dicarboxylate})_3](\text{C}_{60}^{1-})_2$ | 1:2 | 1.0:2.2 |

CONCLUSION

The hypothesis for part 1 of this thesis was that ruthenium tris(bipyridine)/C₆₀-based charge-transfer salts would be a new class of superior thermoelectric materials in terms of tunability and would allow for fundamental study of structure-to-thermoelectric property relationships. The hypothesis was judged by measurements of Seebeck coefficient, electrical conductivity, ligand tunability through NMR, and ruthenium complex and charge-transfer salt tunability through CV and UV-Vis-NIR respectively. The size of the ruthenium cation was tuned through modification of the ligands, tuning the charge density of the cation and changing the distance between donor and acceptor sites. Crystal structure data confirmed that ruthenium-ruthenium distances were greatly affected by ligand appendages. Unexpectedly, an isopropyl based complex afforded closer Ru-Ru distances that corresponds nicely to an increase in electrical conductivity. Salt stoichiometry could also be tuned, which had a significant effect on disproportionation and electrical conductivity. Salts with [Ru(L)₃]²⁺ underwent little disproportionation and also exhibited much lower electrical conductivities on average. Seebeck coefficients ranging from 100 to -400 μV/K were demonstrated, showing that electron and hole carrier materials could be synthesized. Variations in salt stoichiometry proved difficult to control and significantly affected the thermoelectric properties. Because of variations in salt stoichiometry and a lack of synthetically pure charge-transfer salts, the main hypothesis for this section of the thesis is still inconclusive. The class of materials, however, show some promise in that tunability of the class of materials was confirmed, but further studies are still needed.

FUTURE WORK

Future work should be focused on isolation of non-mixed oxidation state salts (i.e. UV-Vis-NIR calculated cation-to-anion ratios that agree with theoretical ratios). If the theoretical salts cannot be isolated by kinetic precipitation, more work should be done in an attempt to recrystallize the product or grow single crystals. In the event that crystallization is not fruitful, UV-Vis-NIR data should be collected for each cation and anion separately. With electronic data files for each cation and anion, along with a spectrum for a mixed oxidation state salt, one could determine the percentage of each oxidation state present in the salt.

X-ray quality single crystal growth may be the best method for reproducible synthesis of a non-mixed oxidation state salt. To increase the likelihood of x-ray quality crystal growth, a substituted fullerene may be more useful. With an appendage on the fullerene cage, the amount of rotation the C_{60} can undergo in the crystal structure should be lowered significantly. Acquiring a substituted C_{60} species may be easy to do since Steven Strauss' group (Chemistry Department, Colorado State University) works with fluorinated fullerene compounds.⁴⁶ Care will need to be taken though, as appendages on the fullerene cage will likely change the potentials of the redox-couples for C_{60} .

Lastly, measuring the thermal properties of the three charge transfer salts for which structural data has been collected would also be important. With values for thermal and electrical conductivity, the phonon contribution to the thermal conductivity could be calculated. It would be interesting to see how the crystal structure influences the phonon contribution to the thermal conductivity.

REFERENCES

- (1) Lawrence Livermore National Laboratory; Department of Energy LLNLUSEnergy2011.png https://flowcharts.llnl.gov/content/energy/energy_archive/energy_flow_2011/LLNLUSEnergy2011.png (accessed Oct 9, 2012).
- (2) Riffat, S. ; Ma, X. *Applied Thermal Engineering* **2003**, *23*, 913–935.
- (3) Bell, L. E. *Science* **2008**, *321*, 1457–1461.
- (4) DiSalvo, F. J. *Science* **1999**, *285*, 703–706.
- (5) Thermoelectrics <http://thermoelectrics.caltech.edu/thermoelectrics/index.html> (accessed Oct 10, 2012).
- (6) Shrestha, S. K.; Conibeer, G.; Chu-Wei Jiang; Konig, D. 6; pp. 28–31.
- (7) Venkatasubramanian, R.; Siivola, E.; Colpitts, T.; O’Quinn, B. *Nature* **2001**, *413*, 597–602.
- (8) Biswas, K.; He, J.; Blum, I. D.; Wu, C.-I.; Hogan, T. P.; Seidman, D. N.; Draid, V. P.; Kanatzidis, M. G. *Nature* **2012**, *489*, 414–418.
- (9) Bux, S. K.; Fleurial, J.-P.; Kaner, R. B. *Chem. Commun.* **2010**, *46*, 8311–8324.
- (10) Culp, S. R.; Simonson, J. W.; Poon, S. J.; Ponnambalam, V.; Edwards, J.; Tritt, T. M. *Applied Physics Letters* **2008**, *93*, 022105–3.
- (11) Grytsiv, A.; Rogl, P.; Berger, S.; Paul, C.; Bauer, E.; Godart, C.; Ni, B.; Abd-Elmeguid, M. M.; Saccone, A.; Ferro, R.; Kaczorowski, D. *Phys. Rev. B* **2002**, *66*, 094411.
- (12) Litvinchuk, A. P.; Nysten, J.; Lorenz, B.; Guloy, A. M.; Haussermann, U. *Journal of Applied Physics* **2008**, *103*, 123524–6.
- (13) Boukai, A. I.; Bunimovich, Y.; Tahir-Kheli, J.; Yu, J.-K.; Goddard III, W. A.; Heath, J. R. *Nature* **2008**, *451*, 168–171.
- (14) Koh, Y. K.; Vineis, C. J.; Calawa, S. D.; Walsh, M. P.; Cahill, D. G. *Applied Physics Letters* **2009**, *94*, 153101–3.
- (15) Condron, C. L.; Kauzlarich, S. M.; Ikeda, T.; Snyder, G. J.; Haarmann, F.; Jeglič, P. *Inorg. Chem.* **2008**, *47*, 8204–8212.
- (16) Sasaki, Y.; Kishimoto, K.; Koyanagi, T.; Asada, H.; Akai, K. *Journal of Applied Physics* **2009**, *105*, 073702–8.
- (17) Hochbaum, A. I.; Chen, R.; Delgado, R. D.; Liang, W.; Garnett, E. C.; Najarian, M.; Majumdar, A.; Yang, P. *Nature* **2008**, *451*, 163–167.
- (18) Vining, C. B. *Nature* **2008**, *451*, 132–133.
- (19) Omar, M. A. *Elementary Solid State Physics*; Addison-Wesley Publishing Company: Boston, MA, 1975.
- (20) Dresselhaus, M. S.; Dresselhaus, G.; Eklund, P. C. *Science of Fullerenes and Carbon Nanotubes*; Academic Press: New York, 1996.
- (21) Chen, G.; Dresselhaus, M. S.; Dresselhaus, G.; Fleurial, J.-P.; Caillat, T. *International Materials Reviews* **2003**, *48*, 45–66.
- (22) Tan, G.; Wang, S.; Tang, X.; Li, H.; Uher, C. *Journal of Solid State Chemistry* **2012**, *196*, 203–208.
- (23) Zhou, L.; Qiu, P.; Uher, C.; Shi, X.; Chen, L. *Intermetallics* **2013**, *32*, 209–213.
- (24) Kleinke, H. *Chem. Mater.* **2009**, *22*, 604–611.
- (25) Ma, Y.; Heijl, R.; Palmqvist, A. *Journal of Materials Science* 1–12.

- (26) Mott, D.; Mai, N. T.; Thuy, N. T. B.; Maeda, Y.; Linh, T. P. T.; Koyano, M.; Maenosono, S. *phys. stat. sol. (a)* **2011**, *208*, 52–58.
- (27) Elliott, C. M.; Hershenhart, E. J. *J. Am. Chem. Soc.* **1982**, *104*, 7519–7526.
- (28) Elliott, C. M.; Prieto, A. L. *Fulleride Salts: Decoupling Thermal and Electrical Conductivity for Thermoelectric Application*; DOE Proposal, 2008.
- (29) Berger, R. M.; McMillin, D. R. *Inorg. Chem.* **1988**, *27*, 4245–4249.
- (30) Kobayashi, H. *Molecular Physics* **1993**, *78*, 909.
- (31) Wagner, M. J.; Dye, J. L.; Perez-Cordero, E.; Buigas, R.; Echegoyen, L. *J. Am. Chem. Soc.* **1995**, *117*, 1318–1323.
- (32) Foss, C. A.; Feldheim, D. L.; Lawson, D. R.; Dorhout, P. K.; Elliott, C. M.; Martin, C. R.; Parkinson, B. A. *Journal of The Electrochemical Society* **1993**, *140*, L84–L86.
- (33) Hong, J.; Shores, M. P.; Elliott, C. M. *Inorg. Chem.* **2010**, *49*, 11378–11385.
- (34) Biner, M.; Buergi, H. B.; Ludi, A.; Roehr, C. *J. Am. Chem. Soc.* **1992**, *114*, 5197–5203.
- (35) Kochanski, G. P.; Hebard, A. F.; Haddon, R. C.; Fiory, A. T. *Science* **1992**, *255*, 184–186.
- (36) Wang, W.; Wang, Z.; Tang, J.; Yang, S.; Jin, H.; Zhao, G.-L.; Li, Q. *Journal of Renewable and Sustainable Energy* **2009**, *1*, 023104–8.
- (37) Xie, Q.; Perez-Cordero, E.; Echegoyen, L. *J. Am. Chem. Soc.* **1992**, *114*, 3978–3980.
- (38) Sheldrick, G. M. *SADABS*; Bruker AXS: Madison, WI.
- (39) Sheldrick, G. M. *SHELXTL-97*; Bruker AXS: Madison, WI, 1997.
- (40) Furue, M.; Maruyama, K.; Oguni, T.; Naiki, M.; Kamachi, M. *Inorg. Chem.* **1992**, *31*, 3792–3795.
- (41) Evans, I. P.; Spencer, A.; Wilkinson, G. *J. Chem. Soc., Dalton Trans.* **1973**, 204–209.
- (42) Lawson, D. R.; Feldheim, D. L.; Foss, C. A.; Dorhout, P. K.; Elliott, C. M.; Martin, C. R.; Parkinson, B. *Journal of The Electrochemical Society* **1992**, *139*, L68–L71.
- (43) Li, C. Phonon Anharmonicity of Ionic Compounds and Metals. Ph.D. Thesis, California Institute of Technology: Pasadena, California, 2012.
- (44) Carbon-based Research at GTRI's EOSL | Nanotechnology Lab
<http://eosl.gtri.gatech.edu/Default.aspx?alias=eosl.gtri.gatech.edu/newnano> (accessed Oct 1, 2012).
- (45) Hershenhart, E. Part 1. An electrochemical comparison of the cobaloxime and Co[C₂(DO)(DOH)_{pn}] model complexes to coenzyme B₁₂; Part 2. Electrochemical and spectral investigations of ring-substituted bipyridines and their complexes with ruthenium. Ph.D. Thesis, University of Vermont: Vermont, 1983.
- (46) Kuvychko, I. V.; Strauss, S. H.; Boltalina, O. V. *Journal of Fluorine Chemistry* **2012**, *143*, 103–108.

APPENDIX 1

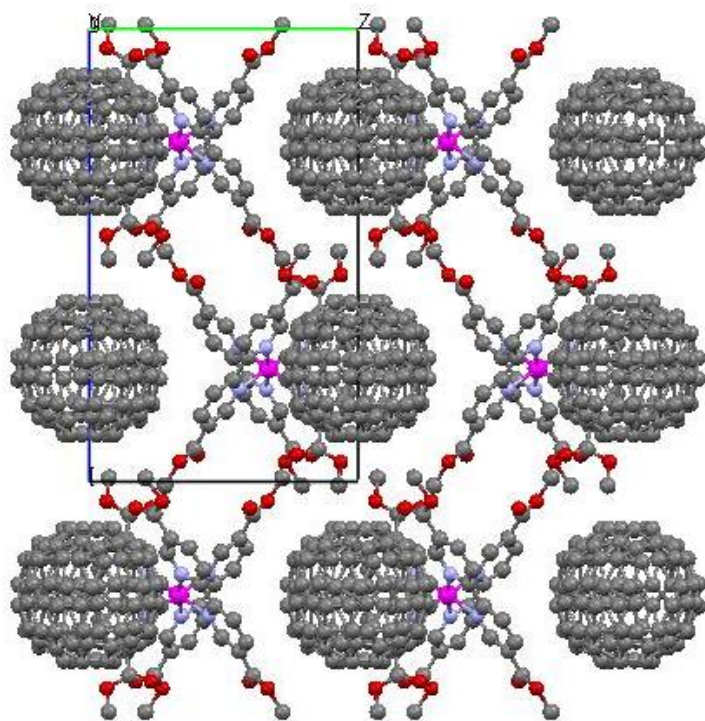
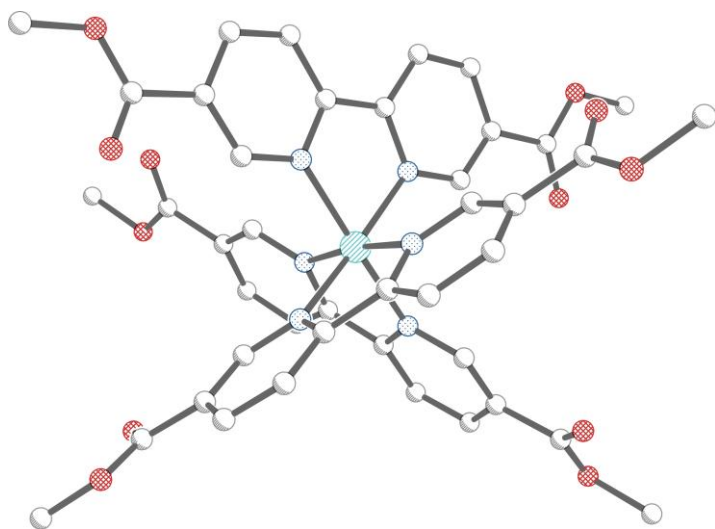


Figure A1.1. Cation structure for $[\text{Ru}^{1+}(\text{dimethyl-2,2'-bipyridine-5,5'-dicarboxylate})_3]\text{C}_{60}^{1-}$ (above) and structure of overall salt (below). Hydrogen omitted for clarity, O is labeled red, N is labeled light blue, and Ru is labeled light blue (above) or magenta (below).

Table A1.1. Crystal data and structure refinement for $[\text{Ru}^{\text{I}+}(\text{dimethyl-2,2'-bipyridine-5,5'-dicarboxylate})_3]\text{C}_{60}^{\text{I-}}$.

| | | |
|---------------------------------|---|------------------------|
| Identification code | ME08 | |
| Empirical formula | $\text{C}_{108} \text{H}_{36} \text{N}_6 \text{O}_{12} \text{Ru}$ | |
| Formula weight | 1710.50 | |
| Temperature | 296(2) K | |
| Wavelength | 0.71073 Å | |
| Crystal system | Trigonal | |
| Space group | P -31c | |
| Unit cell dimensions | $a = 15.5254(3) \text{ \AA}$ | $a = 90^\circ$. |
| | $b = 15.5254(3) \text{ \AA}$ | $b = 90^\circ$. |
| | $c = 22.5633(7) \text{ \AA}$ | $\gamma = 120^\circ$. |
| Volume | $4709.98(19) \text{ \AA}^3$ | |
| Z | 2 | |
| Density (calculated) | 1.206 Mg/m^3 | |
| Absorption coefficient | 0.230 mm^{-1} | |
| F(000) | 1732 | |
| Crystal size | unknown | |
| Theta range for data collection | 1.81 to 20.92°. | |
| Index ranges | $-15 \leq h \leq 15, -15 \leq k \leq 15, -22 \leq l \leq 22$ | |
| Reflections collected | 54300 | |
| Independent reflections | 1625 [R(int) = 0.1289] | |
| Completeness to theta = 20.92° | 96.2 % | |
| Absorption correction | Semi-empirical from equivalents | |

| | |
|--------------------------------------|---------------------------------------|
| Refinement method | Full-matrix least-squares on F^2 |
| Data / restraints / parameters | 1625 / 0 / 202 |
| Goodness-of-fit on F^2 | 3.416 |
| Final R indices [$I > 2\sigma(I)$] | R1 = 0.1450, wR2 = 0.3783 |
| R indices (all data) | R1 = 0.1635, wR2 = 0.3899 |
| Largest diff. peak and hole | 1.478 and -0.578 e. \AA^{-3} |

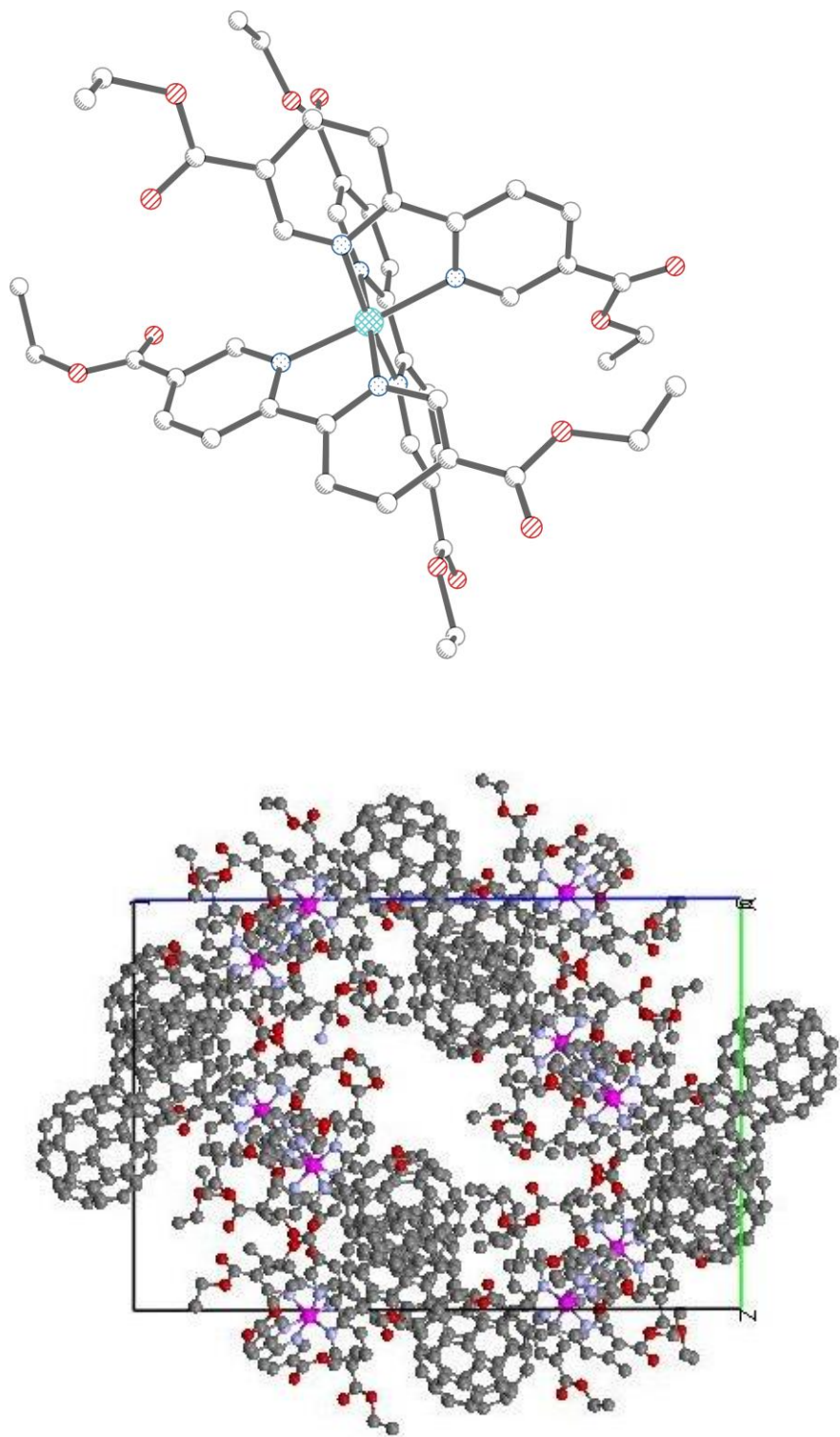


Figure A1.2. Cation structure for $[\text{Ru}^{1+}(\text{diethyl-2,2'-bipyridine-5,5'-dicarboxylate})_3]\text{C}_{60}^{1-}$ (above) and structure of overall salt (below). Hydrogen omitted for clarity, O is labeled red, N is labeled light blue, and Ru is labeled light blue (above) or magenta (below).

Table A1.2. Crystal data and structure refinement for $[\text{Ru}^{1+}(\text{diethyl-2,2'-bipyridine-5,5'-dicarboxylate})_3]\text{C}_{60}^{1-}$

| | | |
|---------------------------------|---|-------------------------|
| Identification code | ME07 | |
| Empirical formula | $\text{C}_{108} \text{H}_{44} \text{N}_6 \text{O}_{12} \text{Ru}$ | |
| Formula weight | 1718.56 | |
| Temperature | 120(2) K | |
| Wavelength | 0.71073 Å | |
| Crystal system | Monoclinic | |
| Space group | P2(1)/n | |
| Unit cell dimensions | $a = 18.936(2) \text{ Å}$ | $a = 90^\circ$. |
| | $b = 25.262(3) \text{ Å}$ | $b = 96.397(4)^\circ$. |
| | $c = 37.641(5) \text{ Å}$ | $g = 90^\circ$. |
| Volume | 17894(4) Å ³ | |
| Z | 8 | |
| Density (calculated) | 1.276 Mg/m ³ | |
| Absorption coefficient | 0.242 mm ⁻¹ | |
| F(000) | 6992 | |
| Crystal size | 0.47 x 0.20 x 0.07 mm ³ | |
| Theta range for data collection | 1.16 to 20.85°. | |
| Index ranges | -18<=h<=18, -24<=k<=17, -37<=l<=37 | |
| Reflections collected | 120527 | |
| Independent reflections | 18287 [R(int) = 0.1633] | |
| Completeness to theta = 20.85° | 97.2 % | |
| Absorption correction | Semi-empirical from equivalents | |

| | |
|--------------------------------------|------------------------------------|
| Max. and min. transmission | 0.9830 and 0.8945 |
| Refinement method | Full-matrix least-squares on F^2 |
| Data / restraints / parameters | 18287 / 0 / 2437 |
| Goodness-of-fit on F^2 | 0.992 |
| Final R indices [$I > 2\sigma(I)$] | R1 = 0.1481, wR2 = 0.3734 |
| R indices (all data) | R1 = 0.2050, wR2 = 0.4247 |
| Largest diff. peak and hole | 1.520 and -2.406 e.Å ⁻³ |

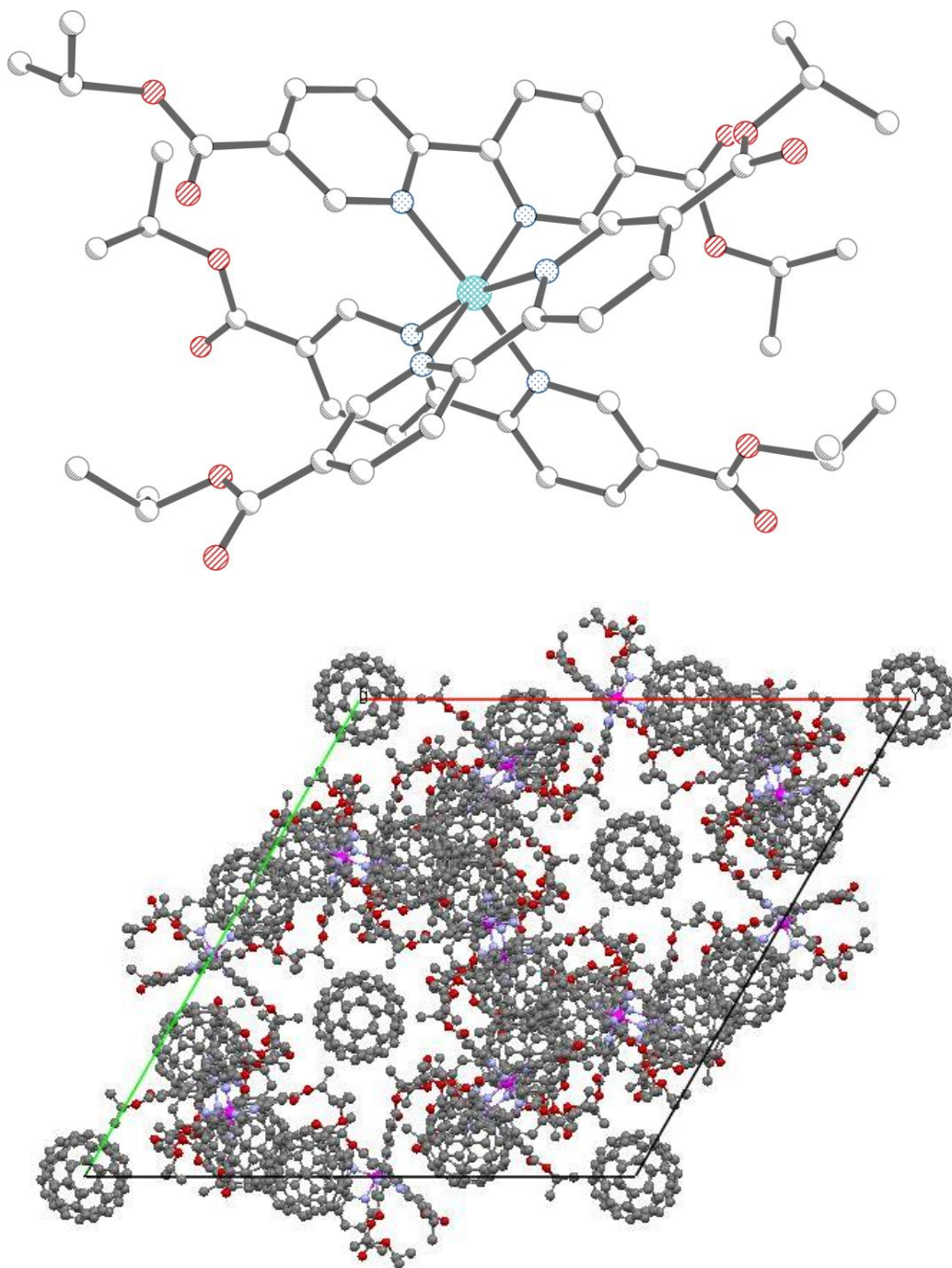


Figure A1.3. Cation structure for $[\text{Ru}^{1+}(\text{diisopropyl-2,2'-bipyridine-5,5'-dicarboxylate})_3]\text{C}_{60}^{1-}$ (above) and structure of overall salt (below). Hydrogen omitted for clarity, O is labeled red, N is labeled light blue, and Ru is labeled light blue (above) or magenta (below).

Table A1.3. Crystal data and structure refinement for $[\text{Ru}^{1+}(\text{diispropyl-2,2'-bipyridine-5,5'-dicarboxylate})_3]\text{C}_{60}^{1-}$.

| | | |
|---------------------------------|---------------------------------------|-----------|
| Identification code | me09 | |
| Empirical formula | C108 H60 N6 O12 Ru | |
| Formula weight | 1734.69 | |
| Temperature | 296(2) K | |
| Wavelength | 0.71073 Å | |
| Crystal system | Rhombohedral | |
| Space group | R-3 | |
| Unit cell dimensions | a = 45.062(2) Å | a = 90°. |
| | b = 45.062(2) Å | b = 90°. |
| | c = 26.6182(12) Å | g = 120°. |
| Volume | 46808(4) Å ³ | |
| Z | 24 | |
| Density (calculated) | 1.477 Mg/m ³ | |
| Absorption coefficient | 0.278 mm ⁻¹ | |
| F(000) | 21360 | |
| Crystal size | 0.290 x 0.265 x 0.096 mm ³ | |
| Theta range for data collection | 1.81 to 24.74°. | |
| Index ranges | -43<=h<=52, -53<=k<=53, -30<=l<=31 | |
| Reflections collected | 175228 | |
| Independent reflections | 17768 [R(int) = 0.0738] | |
| Completeness to theta = 24.74° | 99.8 % | |
| Absorption correction | Semi-empirical from equivalents | |

| | |
|--------------------------------------|--------------------------------------|
| Refinement method | Full-matrix least-squares on F^2 |
| Data / restraints / parameters | 17768 / 0 / 1507 |
| Goodness-of-fit on F^2 | 4.845 |
| Final R indices [$I > 2\sigma(I)$] | R1 = 0.2401, wR2 = 0.5471 |
| R indices (all data) | R1 = 0.2949, wR2 = 0.5776 |
| Largest diff. peak and hole | 13.546 and -11.193 e.Å ⁻³ |

Table A1.4. Atomic coordinates ($\times 10^4$) and equivalent isotropic displacement parameters ($\text{Å}^2 \times 10^3$) for $[\text{Ru}^{1+}(\text{dimethyl-2,2'-bipyridine-5,5'-dicarboxylate})_3]\text{C}_{60}^{1-}$. $U(\text{eq})$ is defined as one third of the trace of the orthogonalized U^{ij} tensor.

| | x | y | z | U(eq) |
|-------|----------|-----------|----------|---------|
| Ru(1) | 6667 | 3333 | 2500 | 49(1) |
| C(1) | 5087(8) | 2190(9) | 3440(6) | 57(3) |
| C(2) | 4420(8) | 1392(10) | 3738(6) | 59(3) |
| C(3) | 4168(10) | 458(12) | 3540(9) | 87(5) |
| C(4) | 4636(9) | 376(9) | 3057(8) | 83(5) |
| C(5) | 5343(8) | 1238(8) | 2754(7) | 64(4) |
| N(1) | 5574(6) | 2149(6) | 2960(5) | 53(3) |
| O(1) | 3361(7) | 646(8) | 4563(4) | 84(3) |
| O(2) | 4024(8) | 2296(10) | 4412(5) | 91(3) |
| C(6) | 3909(11) | 1487(17) | 4279(7) | 85(5) |
| C(7) | 2819(13) | 728(15) | 5084(7) | 115(6) |
| C(8) | 1790(20) | 9620(30) | 3295(12) | 87(9) |
| C(9) | 2350(30) | 11180(30) | 3278(15) | 101(10) |
| C(10) | 2607(18) | 10950(20) | 2730(11) | 77(9) |
| C(11) | 2320(30) | 10320(40) | 2317(18) | 113(11) |
| C(12) | 1680(20) | 9160(20) | 2671(13) | 74(8) |
| C(13) | 620(40) | 8780(30) | 3568(17) | 103(12) |

| | | | | |
|--------|-----------|-----------|----------|----------|
| C(14) | 210(40) | 8090(30) | 3285(18) | 109(13) |
| C(8A) | 1260(30) | 9010(30) | 3302(16) | 69(11) |
| C(9A) | 2210(30) | 10550(30) | 3223(17) | 60(11) |
| C(10A) | 2300(30) | 10080(40) | 2670(20) | 91(14) |
| C(11A) | 2110(20) | 9670(30) | 2270(13) | 54(10) |
| C(12A) | 1180(40) | 8540(50) | 2740(20) | 113(17) |
| C(13A) | 70(60) | 8360(60) | 3560(30) | 102(17) |
| C(14A) | -350(40) | 7880(30) | 3308(16) | 59(11) |
| C(15) | 240(50) | 9320(40) | 3955(7) | 133(8) |
| C(16) | -680(30) | 9050(20) | 3943(7) | 111(7) |
| C(17) | 1410(70) | 10810(70) | 4510(40) | 210(40) |
| C(18) | -1490(50) | 8790(50) | 3660(30) | 120(20) |
| C(17A) | 1850(30) | 11060(40) | 3631(19) | 130(15) |
| C(18A) | -1510(20) | 8150(30) | 3513(14) | 85(11) |
| C(202) | 4280(30) | 8660(30) | 4590(16) | 220(14) |
| C(201) | 3410(30) | 7570(40) | 3580(20) | 254(18) |
| C(200) | 4010(180) | 7520(100) | 2760(90) | 800(200) |
| C(203) | 5230(30) | 9290(30) | 4313(18) | 212(13) |

Table A1.5. Bond lengths [\AA] and angles [$^\circ$].

| | |
|---------------|-----------|
| Ru(1)-N(1) | 2.054(9) |
| Ru(1)-N(1)#1 | 2.054(9) |
| Ru(1)-N(1)#2 | 2.054(9) |
| Ru(1)-N(1)#3 | 2.054(10) |
| Ru(1)-N(1)#4 | 2.054(9) |
| Ru(1)-N(1)#5 | 2.054(9) |
| C(1)-C(2) | 1.333(16) |
| C(1)-N(1) | 1.341(15) |
| C(2)-C(3) | 1.37(2) |
| C(2)-C(6) | 1.50(2) |
| C(3)-C(4) | 1.35(2) |
| C(4)-C(5) | 1.413(18) |
| C(5)-N(1) | 1.355(14) |
| C(5)-C(5)#2 | 1.43(3) |
| O(1)-C(6) | 1.32(2) |
| O(1)-C(7) | 1.49(2) |
| O(2)-C(6) | 1.214(19) |
| C(8)-C(12) | 1.55(4) |
| C(8)-C(13) | 1.73(6) |
| C(9)-C(10) | 1.40(4) |
| C(9)-C(11)#6 | 1.87(7) |
| C(9)-C(14)#7 | 1.90(6) |
| C(10)-C(11) | 1.26(4) |
| C(10)-C(10)#6 | 1.51(5) |
| C(10)-C(11)#6 | 1.90(6) |
| C(11)-C(14)#3 | 1.55(6) |
| C(11)-C(12) | 1.75(6) |
| C(11)-C(9)#6 | 1.87(7) |
| C(11)-C(10)#6 | 1.90(6) |
| C(12)-C(12)#3 | 1.53(6) |
| C(13)-C(14) | 1.12(6) |
| C(13)-C(15) | 1.53(5) |
| C(14)-C(11)#3 | 1.55(6) |
| C(14)-C(9)#8 | 1.90(6) |
| C(8A)-C(12A) | 1.43(6) |

| | |
|---------------------|-----------|
| C(8A)-C(13A) | 1.69(8) |
| C(9A)-C(10A) | 1.49(6) |
| C(9A)-C(14A)#7 | 1.98(5) |
| C(10A)-C(11A) | 1.05(5) |
| C(10A)-C(12A)#3 | 1.95(8) |
| C(11A)-C(12A)#3 | 1.19(7) |
| C(11A)-C(14A)#3 | 1.67(5) |
| C(11A)-C(12A) | 1.94(7) |
| C(12A)-C(12A)#3 | 1.19(10) |
| C(12A)-C(11A)#3 | 1.19(7) |
| C(12A)-C(10A)#3 | 1.95(8) |
| C(13A)-C(14A) | 0.90(7) |
| C(13A)-C(15) | 1.65(9) |
| C(14A)-C(11A)#3 | 1.67(5) |
| C(14A)-C(9A)#8 | 1.98(5) |
| C(15)-C(16) | 1.27(3) |
| C(15)-C(16)#7 | 1.33(3) |
| C(15)-C(18)#7 | 1.47(10) |
| C(15)-C(17)#8 | 1.76(11) |
| C(15)-C(17A)#8 | 1.88(7) |
| C(16)-C(18) | 1.29(8) |
| C(16)-C(15)#8 | 1.33(3) |
| C(16)-C(17A)#8 | 1.50(6) |
| C(16)-C(17)#8 | 1.51(10) |
| C(16)-C(18A) | 1.66(5) |
| C(17)-C(16)#7 | 1.51(10) |
| C(17)-C(15)#7 | 1.76(11) |
| C(18)-C(15)#8 | 1.47(10) |
| C(17A)-C(18A)#7 | 1.15(5) |
| C(17A)-C(16)#7 | 1.50(6) |
| C(17A)-C(15)#7 | 1.88(7) |
| C(18A)-C(17A)#8 | 1.15(5) |
| C(202)-C(203) | 1.44(5) |
| C(200)-C(200)#9 | 1.4(5) |
| C(200)-C(200)#10 | 2.0(3) |
| N(1)-Ru(1)-N(1)#1 | 96.7(4) |
| N(1)-Ru(1)-N(1)#2 | 78.3(5) |
| N(1)#1-Ru(1)-N(1)#2 | 88.7(5) |
| N(1)-Ru(1)-N(1)#3 | 173.1(5) |
| N(1)#1-Ru(1)-N(1)#3 | 78.3(5) |
| N(1)#2-Ru(1)-N(1)#3 | 96.7(4) |
| N(1)-Ru(1)-N(1)#4 | 88.7(5) |
| N(1)#1-Ru(1)-N(1)#4 | 173.1(5) |
| N(1)#2-Ru(1)-N(1)#4 | 96.7(4) |
| N(1)#3-Ru(1)-N(1)#4 | 96.7(4) |
| N(1)-Ru(1)-N(1)#5 | 96.7(4) |
| N(1)#1-Ru(1)-N(1)#5 | 96.7(4) |
| N(1)#2-Ru(1)-N(1)#5 | 173.1(5) |
| N(1)#3-Ru(1)-N(1)#5 | 88.7(5) |
| N(1)#4-Ru(1)-N(1)#5 | 78.3(5) |
| C(2)-C(1)-N(1) | 123.9(11) |
| C(1)-C(2)-C(3) | 119.8(13) |
| C(1)-C(2)-C(6) | 121.4(14) |
| C(3)-C(2)-C(6) | 118.8(14) |
| C(4)-C(3)-C(2) | 118.6(13) |
| C(3)-C(4)-C(5) | 120.0(13) |

| | |
|--------------------------|-----------|
| N(1)-C(5)-C(4) | 119.8(12) |
| N(1)-C(5)-C(5)#2 | 115.4(7) |
| C(4)-C(5)-C(5)#2 | 124.7(8) |
| C(1)-N(1)-C(5) | 117.8(10) |
| C(1)-N(1)-Ru(1) | 126.7(8) |
| C(5)-N(1)-Ru(1) | 115.5(8) |
| C(6)-O(1)-C(7) | 114.4(14) |
| O(2)-C(6)-O(1) | 126.5(16) |
| O(2)-C(6)-C(2) | 119.3(17) |
| O(1)-C(6)-C(2) | 114.1(17) |
| C(12)-C(8)-C(13) | 98(3) |
| C(10)-C(9)-C(11)#6 | 69(2) |
| C(10)-C(9)-C(14)#7 | 117(3) |
| C(11)#6-C(9)-C(14)#7 | 49(2) |
| C(11)-C(10)-C(9) | 144(3) |
| C(11)-C(10)-C(10)#6 | 86(3) |
| C(9)-C(10)-C(10)#6 | 109(3) |
| C(11)-C(10)-C(11)#6 | 119(3) |
| C(9)-C(10)-C(11)#6 | 67(2) |
| C(10)#6-C(10)-C(11)#6 | 41.5(18) |
| C(10)-C(11)-C(14)#3 | 162(5) |
| C(10)-C(11)-C(12) | 105(3) |
| C(14)#3-C(11)-C(12) | 89(3) |
| C(10)-C(11)-C(9)#6 | 96(3) |
| C(14)#3-C(11)-C(9)#6 | 67(3) |
| C(12)-C(11)-C(9)#6 | 149(3) |
| C(10)-C(11)-C(10)#6 | 53(2) |
| C(14)#3-C(11)-C(10)#6 | 110(4) |
| C(12)-C(11)-C(10)#6 | 149(3) |
| C(9)#6-C(11)-C(10)#6 | 43.5(19) |
| C(12)#3-C(12)-C(8) | 135(3) |
| C(12)#3-C(12)-C(11) | 117(3) |
| C(8)-C(12)-C(11) | 94(2) |
| C(14)-C(13)-C(15) | 131(6) |
| C(14)-C(13)-C(8) | 114(5) |
| C(15)-C(13)-C(8) | 109(4) |
| C(13)-C(14)-C(11)#3 | 145(4) |
| C(13)-C(14)-C(9)#8 | 110(4) |
| C(11)#3-C(14)-C(9)#8 | 65(3) |
| C(12A)-C(8A)-C(13A) | 102(4) |
| C(10A)-C(9A)-C(14A)#7 | 128(3) |
| C(11A)-C(10A)-C(9A) | 162(4) |
| C(11A)-C(10A)-C(12A)#3 | 31(3) |
| C(9A)-C(10A)-C(12A)#3 | 136(4) |
| C(10A)-C(11A)-C(12A)#3 | 121(4) |
| C(10A)-C(11A)-C(14A)#3 | 111(4) |
| C(12A)#3-C(11A)-C(14A)#3 | 114(4) |
| C(10A)-C(11A)-C(12A) | 86(4) |
| C(12A)#3-C(11A)-C(12A) | 35(4) |
| C(14A)#3-C(11A)-C(12A) | 140(3) |
| C(12A)#3-C(12A)-C(11A)#3 | 110(7) |
| C(12A)#3-C(12A)-C(8A) | 135(8) |
| C(11A)#3-C(12A)-C(8A) | 103(4) |
| C(12A)#3-C(12A)-C(11A) | 35(5) |
| C(11A)#3-C(12A)-C(11A) | 139(4) |
| C(8A)-C(12A)-C(11A) | 101(4) |

| | |
|---------------------------|-----------|
| C(12A)#3-C(12A)-C(10A)#3 | 82(6) |
| C(11A)#3-C(12A)-C(10A)#3 | 27(2) |
| C(8A)-C(12A)-C(10A)#3 | 124(4) |
| C(11A)-C(12A)-C(10A)#3 | 112(3) |
| C(14A)-C(13A)-C(15) | 144(7) |
| C(14A)-C(13A)-C(8A) | 114(6) |
| C(15)-C(13A)-C(8A) | 91(5) |
| C(13A)-C(14A)-C(11A)#3 | 107(6) |
| C(13A)-C(14A)-C(9A)#8 | 115(6) |
| C(11A)#3-C(14A)-C(9A)#8 | 123(3) |
| C(16)-C(15)-C(16)#7 | 122(3) |
| C(16)-C(15)-C(18)#7 | 151(3) |
| C(16)#7-C(15)-C(18)#7 | 54(5) |
| C(16)-C(15)-C(13) | 119(5) |
| C(16)#7-C(15)-C(13) | 106(5) |
| C(18)#7-C(15)-C(13) | 51(3) |
| C(16)-C(15)-C(13A) | 93(6) |
| C(16)#7-C(15)-C(13A) | 132(5) |
| C(18)#7-C(15)-C(13A) | 78(4) |
| C(13)-C(15)-C(13A) | 28(2) |
| C(16)-C(15)-C(17)#8 | 57(4) |
| C(16)#7-C(15)-C(17)#8 | 132(4) |
| C(18)#7-C(15)-C(17)#8 | 151(4) |
| C(13)-C(15)-C(17)#8 | 115(5) |
| C(13A)-C(15)-C(17)#8 | 94(5) |
| C(16)-C(15)-C(17A)#8 | 53(4) |
| C(16)#7-C(15)-C(17A)#8 | 154.7(19) |
| C(18)#7-C(15)-C(17A)#8 | 116(3) |
| C(13)-C(15)-C(17A)#8 | 68(3) |
| C(13A)-C(15)-C(17A)#8 | 40(3) |
| C(17)#8-C(15)-C(17A)#8 | 70(4) |
| C(15)-C(16)-C(18) | 151(3) |
| C(15)-C(16)-C(15)#8 | 118(3) |
| C(18)-C(16)-C(15)#8 | 69(6) |
| C(15)-C(16)-C(17A)#8 | 85(5) |
| C(18)-C(16)-C(17A)#8 | 80(4) |
| C(15)#8-C(16)-C(17A)#8 | 146(4) |
| C(15)-C(16)-C(17)#8 | 78(5) |
| C(18)-C(16)-C(17)#8 | 125(5) |
| C(15)#8-C(16)-C(17)#8 | 120(4) |
| C(17A)#8-C(16)-C(17)#8 | 87(4) |
| C(15)-C(16)-C(18A) | 124(4) |
| C(18)-C(16)-C(18A) | 38(3) |
| C(15)#8-C(16)-C(18A) | 106(4) |
| C(17A)#8-C(16)-C(18A) | 42(2) |
| C(17)#8-C(16)-C(18A) | 108(4) |
| C(16)#7-C(17)-C(15)#7 | 45(3) |
| C(16)-C(18)-C(15)#8 | 57(3) |
| C(18A)#7-C(17A)-C(16)#7 | 77(4) |
| C(18A)#7-C(17A)-C(15)#7 | 117(4) |
| C(16)#7-C(17A)-C(15)#7 | 42.4(16) |
| C(17A)#8-C(18A)-C(16) | 61(4) |
| C(200)#9-C(200)-C(200)#10 | 75(10) |

Symmetry transformations used to generate equivalent atoms:

#1 -y+1,x-y,z #2 -x+y+1,y,-z+1/2 #3 -y+1,-x+1,-z+1/2
 #4 x,x-y,-z+1/2 #5 -x+y+1,-x+1,z #6 x,x-y+2,-z+1/2
 #7 -y+1,x-y+2,z #8 -x+y-1,-x+1,z #9 -x+y,y,-z+1/2
 #10 x,x-y+1,-z+1/2

Table A1.6. Anisotropic displacement parameters ($\text{\AA}^2 \times 10^3$). The anisotropic displacement factor exponent takes the form: $-2p^2 [h^2 a^{*2} U^{11} + \dots + 2 h k a^* b^* U^{12}]$

| | U ¹¹ | U ²² | U ³³ | U ²³ | U ¹³ | U ¹² |
|-------|-----------------|-----------------|-----------------|-----------------|-----------------|-----------------|
| Ru(1) | 32(1) | 32(1) | 84(2) | 0 | 0 | 16(1) |
| C(1) | 36(7) | 55(8) | 88(9) | -2(7) | -7(7) | 30(7) |
| C(2) | 28(7) | 52(8) | 97(9) | 16(7) | -2(7) | 22(7) |
| C(3) | 38(8) | 86(13) | 146(14) | 35(10) | 22(9) | 37(8) |
| C(4) | 41(7) | 44(8) | 160(15) | 26(8) | 13(9) | 18(7) |
| C(5) | 29(6) | 36(7) | 127(11) | 6(7) | 4(6) | 16(5) |
| N(1) | 37(6) | 36(6) | 91(7) | -6(5) | -2(5) | 21(5) |
| O(1) | 62(6) | 93(7) | 80(6) | 46(6) | 6(5) | 26(5) |
| O(2) | 81(7) | 123(10) | 82(6) | 17(6) | 20(5) | 61(7) |
| C(6) | 57(9) | 123(16) | 92(11) | -4(12) | -19(9) | 59(11) |
| C(7) | 89(12) | 158(17) | 70(9) | 45(10) | 8(9) | 42(12) |
| C(15) | 180(30) | 200(50) | 37(10) | 12(15) | -30(18) | 110(30) |
| C(16) | 140(30) | 140(30) | 49(11) | 42(12) | 31(15) | 70(20) |

Table A1.7. Hydrogen coordinates ($\times 10^4$) and isotropic displacement parameters ($\text{\AA}^2 \times 10^3$).

| | x | y | z | U(eq) |
|-------|------|------|------|-------|
| H(1) | 5224 | 2813 | 3573 | 68 |
| H(3) | 3686 | -105 | 3735 | 105 |
| H(4) | 4492 | -249 | 2924 | 100 |
| H(7A) | 3228 | 1352 | 5280 | 172 |
| H(7B) | 2668 | 193 | 5355 | 172 |
| H(7C) | 2213 | 691 | 4955 | 172 |

Table A1.8. Atomic coordinates ($\times 10^4$) and equivalent isotropic displacement parameters ($\text{\AA}^2 \times 10^3$)

for $[\text{Ru}^{1+}(\text{diethyl-2,2'-bipyridine-5,5'-dicarboxylate})_3]\text{C}_{60}^{1-}$. U(eq) is defined as one third of the trace of the orthogonalized U^{ij} tensor.

| | x | y | z | U(eq) |
|-------|---------|----------|---------|-------|
| Ru(1) | 7559(1) | 9858(1) | 2880(1) | 28(1) |
| N(1) | 8158(8) | 9273(6) | 2677(4) | 27(4) |
| N(2) | 6848(7) | 9571(6) | 2480(4) | 28(4) |
| N(3) | 7083(7) | 9438(6) | 3252(4) | 27(4) |
| N(4) | 6888(7) | 10402(6) | 3061(4) | 27(4) |
| N(5) | 8395(7) | 10122(6) | 3231(4) | 23(3) |

| | | | | |
|-------|-----------|-----------|----------|---------|
| N(6) | 8027(7) | 10384(6) | 2564(4) | 26(4) |
| O(1) | 10349(9) | 8336(7) | 2639(5) | 85(6) |
| O(2) | 10120(8) | 8836(7) | 3107(6) | 70(5) |
| O(3) | 4481(9) | 9403(8) | 1873(5) | 92(6) |
| O(4) | 4766(7) | 9990(7) | 2335(4) | 59(4) |
| O(5) | 7394(17) | 7838(8) | 3448(7) | 160(14) |
| O(6) | 6766(9) | 7868(6) | 3917(4) | 63(4) |
| O(7) | 5692(9) | 12058(6) | 2952(4) | 66(5) |
| O(8) | 6568(9) | 11848(6) | 2630(5) | 71(5) |
| O(9) | 8999(14) | 9411(14) | 4165(10) | 240(30) |
| O(10) | 10004(8) | 9861(7) | 4261(5) | 75(5) |
| O(11) | 8209(14) | 11247(9) | 1441(6) | 128(9) |
| O(12) | 7415(12) | 10619(10) | 1505(5) | 104(7) |
| C(1) | 8814(11) | 9135(7) | 2798(6) | 37(5) |
| C(2) | 9235(12) | 8778(8) | 2630(7) | 47(6) |
| C(3) | 8942(13) | 8576(9) | 2299(7) | 58(7) |
| C(4) | 8246(13) | 8690(9) | 2159(7) | 62(7) |
| C(5) | 7867(11) | 9063(8) | 2368(6) | 41(5) |
| C(6) | 7126(13) | 9181(8) | 2265(5) | 48(6) |
| C(7) | 6661(13) | 8978(10) | 1970(6) | 63(8) |
| C(8) | 5968(14) | 9103(12) | 1914(6) | 77(9) |
| C(9) | 5685(12) | 9482(9) | 2148(5) | 50(6) |
| C(10) | 6150(9) | 9686(7) | 2429(4) | 27(5) |
| C(11) | 9942(13) | 8620(8) | 2775(8) | 56(7) |
| C(12) | 10811(12) | 8679(13) | 3306(10) | 104(12) |
| C(13) | 10878(15) | 8958(14) | 3665(10) | 109(11) |
| C(14) | 4930(15) | 9612(12) | 2099(7) | 70(8) |
| C(15) | 4053(12) | 10180(11) | 2298(7) | 70(7) |
| C(16) | 4008(13) | 10582(12) | 2594(9) | 93(10) |
| C(17) | 7200(10) | 8935(9) | 3326(5) | 38(5) |
| C(18) | 6927(10) | 8659(7) | 3595(5) | 35(5) |
| C(19) | 6500(10) | 8928(9) | 3809(5) | 40(5) |
| C(20) | 6351(8) | 9449(9) | 3728(5) | 30(5) |
| C(21) | 6635(9) | 9697(8) | 3444(5) | 29(5) |
| C(22) | 6489(7) | 10237(7) | 3328(4) | 18(4) |
| C(23) | 5995(10) | 10574(10) | 3454(6) | 48(6) |
| C(24) | 5862(11) | 11057(10) | 3310(6) | 51(6) |
| C(25) | 6246(10) | 11223(8) | 3038(5) | 35(5) |
| C(26) | 6737(8) | 10882(7) | 2924(5) | 26(5) |
| C(27) | 7061(15) | 8085(12) | 3648(7) | 71(8) |
| C(28) | 6890(20) | 7303(12) | 3980(9) | 118(14) |
| C(29) | 6541(17) | 7115(11) | 4266(8) | 92(10) |
| C(30) | 6135(12) | 11756(11) | 2872(6) | 55(7) |
| C(31) | 6480(20) | 12355(14) | 2428(12) | 146(16) |
| C(32) | 7050(40) | 12340(20) | 2204(18) | 330(60) |
| C(33) | 8589(9) | 9920(8) | 3540(6) | 37(5) |
| C(34) | 9248(11) | 10032(8) | 3748(6) | 48(6) |
| C(35) | 9689(10) | 10381(9) | 3617(6) | 42(6) |
| C(36) | 9501(9) | 10606(8) | 3290(6) | 37(6) |
| C(37) | 8852(10) | 10479(7) | 3088(5) | 28(5) |
| C(38) | 8605(9) | 10651(7) | 2736(5) | 31(5) |
| C(39) | 8927(13) | 11057(8) | 2557(6) | 47(6) |
| C(40) | 8700(11) | 11172(8) | 2201(7) | 49(6) |
| C(41) | 8129(11) | 10867(8) | 2023(6) | 43(6) |
| C(42) | 7840(9) | 10491(6) | 2222(5) | 26(5) |
| C(43) | 9444(19) | 9751(14) | 4080(9) | 119(14) |

| | | | | |
|-------|----------|-----------|----------|---------|
| C(46) | 7909(14) | 10958(13) | 1636(8) | 75(8) |
| C(47) | 7180(20) | 10613(18) | 1121(9) | 129(15) |
| C(48) | 7020(40) | 10110(20) | 991(12) | 290(50) |
| Ru(2) | 2638(1) | 3524(1) | 2949(1) | 29(1) |
| N(7) | 1932(7) | 3007(7) | 3130(4) | 28(4) |
| N(8) | 2165(6) | 3981(7) | 3310(3) | 27(4) |
| N(9) | 1925(7) | 3798(6) | 2545(4) | 24(4) |
| N(10) | 3220(7) | 4102(6) | 2735(4) | 25(4) |
| N(11) | 3463(7) | 3281(6) | 3310(4) | 22(4) |
| N(12) | 3138(7) | 2988(6) | 2652(4) | 33(4) |
| O(13) | 545(10) | 1424(10) | 2926(5) | 115(8) |
| O(14) | 1502(9) | 1602(6) | 2634(5) | 64(5) |
| O(15) | 2489(14) | 5571(8) | 3480(6) | 119(9) |
| O(16) | 2050(11) | 5519(7) | 4016(5) | 84(6) |
| O(17) | -424(8) | 3866(7) | 1914(4) | 64(5) |
| O(18) | -134(6) | 3343(6) | 2390(4) | 51(4) |
| O(19) | 5395(8) | 5050(6) | 2671(4) | 56(4) |
| O(20) | 5225(6) | 4523(6) | 3140(4) | 44(4) |
| O(21) | 3924(8) | 3863(7) | 4334(4) | 60(4) |
| O(22) | 5015(6) | 3528(6) | 4382(3) | 43(4) |
| O(23) | 3286(11) | 2057(9) | 1553(5) | 96(7) |
| O(24) | 2665(8) | 2810(7) | 1593(4) | 56(4) |
| C(49) | 1788(9) | 2536(8) | 2973(5) | 33(5) |
| C(50) | 1202(9) | 2230(9) | 3049(5) | 42(6) |
| C(51) | 775(11) | 2410(12) | 3301(7) | 68(8) |
| C(52) | 949(10) | 2892(11) | 3466(6) | 48(6) |
| C(53) | 1519(8) | 3187(9) | 3375(4) | 36(5) |
| C(54) | 1707(9) | 3713(10) | 3501(5) | 38(6) |
| C(55) | 1408(12) | 3943(11) | 3789(6) | 55(6) |
| C(56) | 1588(12) | 4462(13) | 3877(6) | 65(8) |
| C(57) | 2027(11) | 4758(10) | 3665(5) | 44(6) |
| C(58) | 2322(10) | 4492(9) | 3388(6) | 41(5) |
| C(59) | 1038(12) | 1709(10) | 2868(7) | 56(7) |
| C(60) | 1470(20) | 1097(12) | 2430(14) | 160(20) |
| C(61) | 1990(20) | 1030(30) | 2205(18) | 260(50) |
| C(62) | 2221(17) | 5335(11) | 3705(8) | 79(9) |
| C(63) | 2230(30) | 6083(15) | 4079(10) | 144(17) |
| C(64) | 3040(20) | 6150(20) | 4222(15) | 210(30) |
| C(65) | 1248(9) | 3658(8) | 2491(5) | 38(5) |
| C(66) | 761(11) | 3870(9) | 2198(5) | 49(6) |
| C(67) | 1066(11) | 4189(9) | 1954(6) | 54(6) |
| C(68) | 1757(13) | 4333(9) | 2003(6) | 61(7) |
| C(69) | 2173(9) | 4144(8) | 2313(5) | 32(5) |
| C(70) | 2912(10) | 4317(7) | 2412(5) | 36(5) |
| C(71) | 3305(10) | 4662(8) | 2211(6) | 47(6) |
| C(72) | 3978(12) | 4800(8) | 2333(6) | 48(6) |
| C(73) | 4297(10) | 4607(8) | 2668(6) | 40(5) |
| C(74) | 3882(9) | 4257(7) | 2854(5) | 30(5) |
| C(75) | 9(13) | 3694(10) | 2149(6) | 57(7) |
| C(76) | -872(11) | 3125(11) | 2363(6) | 68(8) |
| C(77) | -882(12) | 2718(12) | 2655(7) | 79(9) |
| C(78) | 5029(11) | 4757(9) | 2828(6) | 43(6) |
| C(79) | 5931(9) | 4674(9) | 3318(6) | 53(6) |
| C(80) | 6035(11) | 4343(10) | 3647(7) | 67(8) |
| C(81) | 3622(9) | 3473(7) | 3640(5) | 24(4) |
| C(82) | 4276(8) | 3383(7) | 3852(5) | 27(5) |

| | | | | |
|--------|----------|----------|---------|--------|
| C(83) | 4770(9) | 3064(8) | 3706(5) | 31(5) |
| C(84) | 4607(9) | 2842(8) | 3371(5) | 36(5) |
| C(85) | 3945(8) | 2952(7) | 3178(5) | 23(4) |
| C(86) | 3725(9) | 2736(7) | 2820(5) | 28(5) |
| C(87) | 4059(9) | 2345(8) | 2652(6) | 38(5) |
| C(88) | 3835(11) | 2210(8) | 2305(6) | 41(6) |
| C(89) | 3282(10) | 2483(9) | 2111(6) | 40(5) |
| C(90) | 2944(10) | 2858(8) | 2305(5) | 37(5) |
| C(91) | 4379(7) | 3615(6) | 4207(3) | 19(4) |
| C(92) | 5142(11) | 3727(10) | 4741(7) | 59(7) |
| C(93) | 4881(15) | 3346(9) | 5006(7) | 73(8) |
| C(94) | 3082(12) | 2406(10) | 1730(6) | 48(6) |
| C(95) | 2500(13) | 2844(11) | 1207(6) | 66(8) |
| C(96) | 2158(13) | 3364(11) | 1130(8) | 80(9) |
| C(97) | 1404(12) | 4819(8) | 1010(7) | 53(7) |
| C(98) | -22(9) | 5885(9) | 491(5) | 37(6) |
| C(99) | 1104(10) | 4723(9) | 620(7) | 51(7) |
| C(100) | 125(11) | 5762(12) | 142(7) | 71(8) |
| C(101) | 3188(11) | 6775(9) | 1055(6) | 43(6) |
| C(102) | 2628(12) | 5086(9) | 1230(6) | 52(6) |
| C(103) | 1272(12) | 5555(10) | -274(5) | 48(6) |
| C(104) | 3447(11) | 6645(10) | 448(7) | 54(6) |
| C(105) | 2425(12) | 5971(14) | -265(6) | 74(10) |
| C(106) | 3070(13) | 6032(13) | -50(7) | 62(8) |
| C(107) | 3261(11) | 5319(10) | 1079(6) | 51(7) |
| C(108) | 2430(15) | 6467(10) | 1470(6) | 61(8) |
| C(109) | 1961(13) | 5579(11) | -287(5) | 58(7) |
| C(110) | 2555(13) | 7299(9) | 552(7) | 55(6) |
| C(111) | 2662(15) | 6899(11) | 1233(9) | 84(11) |
| C(112) | 376(10) | 6157(9) | -69(6) | 49(6) |
| C(113) | 783(12) | 6893(12) | 1050(9) | 90(12) |
| C(114) | 3702(10) | 6139(12) | 688(7) | 66(8) |
| C(115) | 1325(14) | 6505(10) | -265(6) | 60(8) |
| C(116) | 43(11) | 6355(12) | 673(10) | 87(11) |
| C(117) | 3308(12) | 5853(10) | 1239(7) | 66(8) |
| C(118) | 421(11) | 6695(9) | 104(7) | 48(6) |
| C(119) | 2020(20) | 7395(10) | 755(8) | 90(11) |
| C(120) | 1149(13) | 5152(12) | 1220(7) | 61(7) |
| C(121) | 2047(15) | 7150(12) | 1138(9) | 88(11) |
| C(122) | 603(14) | 5968(13) | 1236(7) | 71(8) |
| C(123) | 681(13) | 7101(10) | 649(7) | 50(6) |
| C(124) | 2080(15) | 6504(11) | -257(6) | 64(7) |
| C(125) | 1581(16) | 5512(11) | 1463(6) | 69(9) |
| C(126) | 221(11) | 5381(10) | 727(8) | 62(8) |
| C(127) | 1320(20) | 7363(10) | 545(9) | 92(11) |
| C(128) | 2147(13) | 4772(10) | 1023(7) | 60(7) |
| C(129) | 294(13) | 6816(10) | 424(8) | 55(7) |
| C(130) | 1401(12) | 6993(10) | 1213(7) | 65(8) |
| C(131) | 2518(11) | 6859(9) | -34(6) | 49(6) |
| C(132) | 3158(14) | 7007(11) | 661(9) | 80(9) |
| C(133) | 2748(13) | 5965(12) | 1468(6) | 60(7) |
| C(134) | 2222(13) | 7211(9) | 166(6) | 53(6) |
| C(135) | 356(12) | 6514(15) | 986(8) | 87(12) |
| C(136) | 2334(14) | 5488(9) | 1459(5) | 55(7) |
| C(137) | 1672(16) | 6449(14) | 1481(7) | 87(10) |
| C(138) | 3533(14) | 6282(14) | 1031(9) | 95(11) |

| | | | | |
|--------|----------|----------|----------|---------|
| C(139) | 490(12) | 5012(9) | 495(7) | 62(7) |
| C(140) | 1027(11) | 6923(9) | -33(6) | 45(6) |
| C(141) | 1230(14) | 6070(14) | 1452(6) | 82(11) |
| C(142) | 484(14) | 5498(15) | 1074(6) | 83(11) |
| C(143) | 1499(14) | 7247(10) | 178(6) | 54(7) |
| C(144) | 3156(14) | 6536(13) | 117(7) | 80(9) |
| C(145) | 992(13) | 5146(12) | -78(7) | 67(8) |
| C(146) | 905(12) | 6073(12) | -284(6) | 65(8) |
| C(147) | 3609(11) | 5682(10) | 496(8) | 56(7) |
| C(148) | 3356(12) | 5220(10) | 747(9) | 68(8) |
| C(149) | 3301(12) | 5556(15) | 187(10) | 97(13) |
| C(150) | 2934(13) | 4890(10) | 537(7) | 62(7) |
| C(151) | 2870(12) | 5142(10) | 130(7) | 55(7) |
| C(152) | 2328(12) | 4662(8) | 611(8) | 68(8) |
| C(153) | 2260(12) | 5052(14) | -31(9) | 103(15) |
| C(154) | 1648(14) | 4628(10) | 416(7) | 67(7) |
| C(155) | 1603(11) | 4889(8) | 47(6) | 43(6) |
| C(156) | 326(9) | 5158(7) | 102(5) | 27(4) |
| C(157) | 6634(16) | 1596(15) | 4183(10) | 86(10) |
| C(158) | 7160(20) | 1288(12) | 4060(11) | 98(12) |
| C(159) | 6794(16) | 2246(16) | 3762(9) | 87(11) |
| C(160) | 6950(20) | 2860(20) | 3791(13) | 140(20) |
| C(161) | 6602(15) | 2967(17) | 4131(15) | 120(20) |
| C(162) | 6896(19) | 3357(14) | 4343(14) | 110(15) |
| C(163) | 6750(20) | 2850(20) | 4869(9) | 98(12) |
| C(164) | 7531(17) | 3625(12) | 4270(12) | 94(11) |
| C(165) | 8070(20) | 3725(11) | 4568(11) | 95(11) |
| C(166) | 9745(11) | 3079(10) | 4692(9) | 73(9) |
| C(167) | 9698(18) | 3120(20) | 4293(11) | 119(17) |
| C(168) | 9730(19) | 2730(30) | 4066(11) | 180(30) |
| C(169) | 9964(12) | 2223(17) | 4251(10) | 99(16) |
| C(170) | 10039(8) | 2163(9) | 4615(4) | 46(5) |
| C(171) | 9240(20) | 2650(20) | 3766(9) | 101(13) |
| C(172) | 9597(19) | 1810(20) | 4006(11) | 104(16) |
| C(173) | 9180(20) | 2110(20) | 3714(11) | 117(16) |
| C(174) | 8560(20) | 1899(16) | 3598(8) | 99(12) |
| C(175) | 8320(20) | 1357(16) | 3792(10) | 116(15) |
| C(176) | 7946(18) | 2150(12) | 3517(7) | 79(9) |
| C(177) | 7300(30) | 1940(20) | 3603(7) | 118(19) |
| C(178) | 8300(20) | 959(11) | 4328(10) | 90(10) |
| C(179) | 8610(20) | 3413(13) | 3912(9) | 90(10) |
| C(180) | 9771(15) | 1665(16) | 4750(10) | 87(10) |
| C(181) | 9469(19) | 1765(19) | 5081(11) | 118(15) |
| C(182) | 9575(17) | 2404(19) | 5149(8) | 100(12) |
| C(183) | 9057(19) | 2774(18) | 5277(7) | 94(11) |
| C(184) | 8890(20) | 3260(14) | 5098(10) | 95(11) |
| C(185) | 9236(19) | 3393(12) | 4828(10) | 92(10) |
| C(186) | 9944(14) | 2586(13) | 4839(9) | 88(10) |
| C(187) | 7489(17) | 1472(17) | 3781(9) | 85(10) |
| C(188) | 8660(60) | 1157(16) | 4046(13) | 280(60) |
| C(190) | 7750(20) | 1696(16) | 5222(9) | 89(11) |
| C(191) | 7140(30) | 1980(30) | 5139(13) | 140(20) |
| C(192) | 7180(20) | 2520(30) | 5163(11) | 133(18) |
| C(193) | 7810(20) | 2785(14) | 5289(7) | 83(10) |
| C(194) | 9390(20) | 1285(18) | 4494(15) | 130(20) |
| C(195) | 8730(20) | 3678(12) | 4504(10) | 92(10) |

| | | | | |
|--------|-----------|----------|----------|----------|
| C(196) | 8800(20) | 1049(12) | 4623(15) | 104(12) |
| C(197) | 7457(17) | 3052(15) | 3696(9) | 101(13) |
| C(198) | 8550(20) | 1191(10) | 4960(10) | 79(10) |
| C(199) | 7814(18) | 3489(10) | 3934(8) | 73(8) |
| C(200) | 7592(17) | 1022(11) | 4395(11) | 83(9) |
| C(201) | 9027(17) | 3512(13) | 4201(11) | 87(10) |
| C(202) | 7820(30) | 1253(13) | 4983(9) | 92(11) |
| C(203) | 7969(17) | 2707(14) | 3537(6) | 74(9) |
| C(204) | 7351(17) | 1175(11) | 4702(12) | 79(9) |
| C(205) | 8920(20) | 1650(30) | 5199(12) | 170(30) |
| C(206) | 6342(12) | 2500(15) | 4282(11) | 82(10) |
| C(207) | 8360(20) | 1927(15) | 5357(7) | 89(10) |
| C(208) | 6425(16) | 2439(17) | 4645(14) | 100(12) |
| C(209) | 8464(16) | 2500(20) | 5384(7) | 111(15) |
| C(210) | 6605(17) | 1920(19) | 4776(16) | 130(20) |
| C(211) | 7970(40) | 3274(19) | 5110(15) | 170(30) |
| C(212) | 6760(19) | 1548(19) | 4621(18) | 150(20) |
| C(213) | 7810(40) | 3520(20) | 4880(16) | 170(30) |
| C(214) | 8660(30) | 2962(12) | 3666(8) | 92(11) |
| C(215) | 6980(20) | 3287(16) | 4733(15) | 123(17) |
| C(216) | 6438(13) | 2074(14) | 4044(10) | 88(10) |
| C(44) | 10130(20) | 9621(16) | 4657(9) | 47(13) |
| C(45) | 10000 | 10000 | 5000 | 91(16) |
| C(44A) | 9370(20) | 8920(20) | 4353(14) | 56(17) |
| C(45A) | 8900(20) | 8387(19) | 4243(12) | 39(14) |
| C(189) | 9410(30) | 1500(20) | 4150(30) | 220(50) |
| C(300) | 830(20) | 150(19) | 1212(13) | 149(16) |
| C(304) | -430(30) | 780(20) | 962(15) | 159(17) |
| C(302) | 500(30) | 540(20) | 1453(15) | 190(20) |
| C(305) | -140(30) | 840(20) | 1303(16) | 180(20) |
| C(303) | 0(40) | 380(30) | 787(17) | 200(20) |
| C(301) | 510(40) | 110(30) | 870(20) | 240(30) |
| C(310) | 117(15) | 3022(12) | 1271(8) | 84(8) |
| C(309) | 265(18) | 3263(14) | 941(9) | 100(10) |
| C(308) | 540(17) | 2904(13) | 689(8) | 94(9) |
| C(307) | 705(17) | 2396(14) | 775(9) | 97(10) |
| C(306) | 640(20) | 2144(17) | 1108(11) | 130(13) |
| C(312) | 303(18) | 2497(15) | 1349(9) | 102(10) |
| C(313) | 130(20) | 2239(18) | 1672(12) | 135(14) |
| N(20) | 60(20) | 2045(17) | 1950(11) | 176(15) |
| C(314) | 2610(40) | 4270(40) | 4823(18) | 210(30) |
| C(319) | 2390(30) | 3800(30) | 4765(15) | 180(20) |
| C(315) | 2290(40) | 4680(30) | 4871(17) | 220(30) |
| C(318) | 1710(30) | 3600(20) | 4779(15) | 180(20) |
| C(317) | 1170(30) | 4010(20) | 4824(14) | 180(20) |
| C(320) | 3090(60) | 5100(40) | 4970(30) | 360(50) |
| C(321) | -290(80) | 460(70) | 620(50) | 590(90) |
| C(326) | 9000(40) | 8310(30) | 3850(20) | 260(30) |
| C(323) | 9280(50) | 7320(40) | 3840(30) | 350(50) |
| C(322) | 9580(80) | 7650(70) | 3510(50) | 590(100) |
| C(324) | 8910(50) | 7040(40) | 4250(30) | 330(50) |
| C(325) | 8770(40) | 7940(30) | 4303(18) | 240(30) |
| C(329) | 764(11) | 4973(9) | 5023(6) | 105(6) |
| C(327) | 3034(12) | 4166(9) | 5304(6) | 108(6) |
| C(328) | 1454(12) | 4463(10) | 4883(6) | 93(6) |
| C(330) | 1439(11) | 3368(9) | 5221(6) | 104(6) |

| | |
|-------------|-----------|
| C(17)-C(18) | 1.38(3) |
| C(18)-C(19) | 1.38(3) |
| C(18)-C(27) | 1.48(3) |
| C(19)-C(20) | 1.37(3) |
| C(20)-C(21) | 1.40(3) |
| C(21)-C(22) | 1.45(3) |
| C(22)-C(23) | 1.39(3) |
| C(23)-C(24) | 1.35(3) |
| C(24)-C(25) | 1.38(3) |
| C(25)-C(26) | 1.37(3) |
| C(25)-C(30) | 1.49(3) |
| C(28)-C(29) | 1.41(4) |
| C(31)-C(32) | 1.43(5) |
| C(33)-C(34) | 1.43(3) |
| C(34)-C(35) | 1.35(3) |
| C(34)-C(43) | 1.45(4) |
| C(35)-C(36) | 1.37(3) |
| C(36)-C(37) | 1.41(3) |
| C(37)-C(38) | 1.42(3) |
| C(38)-C(39) | 1.40(3) |
| C(39)-C(40) | 1.39(3) |
| C(40)-C(41) | 1.43(3) |
| C(41)-C(42) | 1.36(3) |
| C(41)-C(46) | 1.49(3) |
| C(47)-C(48) | 1.38(6) |
| Ru(2)-N(7) | 2.039(14) |
| Ru(2)-N(9) | 2.039(13) |
| Ru(2)-N(11) | 2.048(13) |
| Ru(2)-N(10) | 2.048(13) |
| Ru(2)-N(12) | 2.052(16) |
| Ru(2)-N(8) | 2.064(14) |
| N(7)-C(49) | 1.34(2) |
| N(7)-C(53) | 1.35(2) |
| N(8)-C(58) | 1.35(2) |
| N(8)-C(54) | 1.37(2) |
| N(9)-C(65) | 1.32(2) |
| N(9)-C(69) | 1.36(2) |
| N(10)-C(74) | 1.34(2) |
| N(10)-C(70) | 1.40(2) |
| N(11)-C(81) | 1.33(2) |
| N(11)-C(85) | 1.37(2) |
| N(12)-C(90) | 1.35(2) |
| N(12)-C(86) | 1.37(2) |
| O(13)-C(59) | 1.22(3) |
| O(14)-C(59) | 1.34(3) |
| O(14)-C(60) | 1.49(3) |
| O(15)-C(62) | 1.19(3) |
| O(16)-C(62) | 1.33(3) |
| O(16)-C(63) | 1.48(4) |
| O(17)-C(75) | 1.22(3) |
| O(18)-C(75) | 1.32(3) |
| O(18)-C(76) | 1.49(2) |
| O(19)-C(78) | 1.21(2) |
| O(20)-C(78) | 1.33(2) |
| O(20)-C(79) | 1.48(2) |
| O(21)-C(91) | 1.207(19) |

| | |
|---------------|-----------|
| O(22)-C(91) | 1.324(18) |
| O(22)-C(92) | 1.44(3) |
| O(23)-C(94) | 1.19(3) |
| O(24)-C(94) | 1.36(3) |
| O(24)-C(95) | 1.45(3) |
| C(49)-C(50) | 1.41(3) |
| C(50)-C(51) | 1.39(3) |
| C(50)-C(59) | 1.50(3) |
| C(51)-C(52) | 1.39(3) |
| C(52)-C(53) | 1.39(3) |
| C(53)-C(54) | 1.44(3) |
| C(54)-C(55) | 1.40(3) |
| C(55)-C(56) | 1.39(3) |
| C(56)-C(57) | 1.43(3) |
| C(57)-C(58) | 1.41(3) |
| C(57)-C(62) | 1.51(4) |
| C(60)-C(61) | 1.38(6) |
| C(63)-C(64) | 1.58(5) |
| C(65)-C(66) | 1.46(3) |
| C(66)-C(67) | 1.40(3) |
| C(66)-C(75) | 1.48(3) |
| C(67)-C(68) | 1.35(3) |
| C(68)-C(69) | 1.42(3) |
| C(69)-C(70) | 1.47(3) |
| C(70)-C(71) | 1.42(3) |
| C(71)-C(72) | 1.35(3) |
| C(72)-C(73) | 1.42(3) |
| C(73)-C(74) | 1.42(3) |
| C(73)-C(78) | 1.50(3) |
| C(76)-C(77) | 1.51(3) |
| C(79)-C(80) | 1.49(3) |
| C(81)-C(82) | 1.42(2) |
| C(82)-C(83) | 1.39(3) |
| C(82)-C(91) | 1.45(2) |
| C(83)-C(84) | 1.38(3) |
| C(84)-C(85) | 1.40(2) |
| C(85)-C(86) | 1.47(3) |
| C(86)-C(87) | 1.37(3) |
| C(87)-C(88) | 1.37(3) |
| C(88)-C(89) | 1.39(3) |
| C(89)-C(90) | 1.40(3) |
| C(89)-C(94) | 1.46(3) |
| C(92)-C(93) | 1.51(3) |
| C(95)-C(96) | 1.48(3) |
| C(97)-C(120) | 1.29(3) |
| C(97)-C(128) | 1.41(3) |
| C(97)-C(99) | 1.53(3) |
| C(98)-C(116) | 1.37(3) |
| C(98)-C(100) | 1.41(3) |
| C(98)-C(126) | 1.59(3) |
| C(99)-C(154) | 1.37(3) |
| C(99)-C(139) | 1.41(3) |
| C(100)-C(112) | 1.39(3) |
| C(100)-C(156) | 1.58(3) |
| C(101)-C(111) | 1.30(3) |
| C(101)-C(138) | 1.41(4) |

| | |
|---------------|---------|
| C(101)-C(132) | 1.59(4) |
| C(102)-C(128) | 1.38(3) |
| C(102)-C(136) | 1.48(3) |
| C(102)-C(107) | 1.50(3) |
| C(103)-C(109) | 1.31(3) |
| C(103)-C(145) | 1.41(3) |
| C(103)-C(146) | 1.48(3) |
| C(104)-C(144) | 1.33(3) |
| C(104)-C(132) | 1.37(3) |
| C(104)-C(114) | 1.61(4) |
| C(105)-C(109) | 1.32(4) |
| C(105)-C(106) | 1.39(3) |
| C(105)-C(124) | 1.50(4) |
| C(106)-C(144) | 1.42(4) |
| C(106)-C(149) | 1.53(4) |
| C(107)-C(148) | 1.31(3) |
| C(107)-C(117) | 1.48(3) |
| C(108)-C(133) | 1.40(4) |
| C(108)-C(137) | 1.44(4) |
| C(108)-C(111) | 1.51(4) |
| C(109)-C(153) | 1.70(4) |
| C(110)-C(119) | 1.36(4) |
| C(110)-C(132) | 1.38(4) |
| C(110)-C(134) | 1.53(3) |
| C(111)-C(121) | 1.34(4) |
| C(112)-C(146) | 1.37(3) |
| C(112)-C(118) | 1.51(3) |
| C(113)-C(135) | 1.26(4) |
| C(113)-C(130) | 1.28(3) |
| C(113)-C(123) | 1.59(4) |
| C(114)-C(147) | 1.36(3) |
| C(114)-C(138) | 1.41(4) |
| C(115)-C(146) | 1.35(3) |
| C(115)-C(124) | 1.43(4) |
| C(115)-C(140) | 1.52(3) |
| C(116)-C(135) | 1.32(4) |
| C(116)-C(129) | 1.60(4) |
| C(117)-C(138) | 1.43(4) |
| C(117)-C(133) | 1.47(4) |
| C(118)-C(129) | 1.29(3) |
| C(118)-C(140) | 1.43(3) |
| C(119)-C(127) | 1.47(4) |
| C(119)-C(121) | 1.57(4) |
| C(120)-C(125) | 1.47(4) |
| C(120)-C(142) | 1.58(4) |
| C(121)-C(130) | 1.35(4) |
| C(122)-C(142) | 1.34(4) |
| C(122)-C(141) | 1.38(4) |
| C(122)-C(135) | 1.71(4) |
| C(123)-C(129) | 1.28(3) |
| C(123)-C(127) | 1.46(4) |
| C(124)-C(131) | 1.43(3) |
| C(125)-C(136) | 1.43(3) |
| C(125)-C(141) | 1.56(4) |
| C(126)-C(142) | 1.38(3) |
| C(126)-C(139) | 1.41(3) |

| | |
|-----------------|---------|
| C(127)-C(143) | 1.49(4) |
| C(128)-C(152) | 1.65(4) |
| C(130)-C(137) | 1.75(4) |
| C(131)-C(134) | 1.33(3) |
| C(131)-C(144) | 1.52(4) |
| C(133)-C(136) | 1.44(3) |
| C(134)-C(143) | 1.38(3) |
| C(137)-C(141) | 1.27(4) |
| C(139)-C(156) | 1.52(3) |
| C(140)-C(143) | 1.39(3) |
| C(145)-C(155) | 1.37(3) |
| C(145)-C(156) | 1.50(3) |
| C(147)-C(149) | 1.28(4) |
| C(147)-C(148) | 1.61(4) |
| C(148)-C(150) | 1.35(4) |
| C(149)-C(151) | 1.33(4) |
| C(150)-C(152) | 1.34(3) |
| C(150)-C(151) | 1.65(4) |
| C(151)-C(153) | 1.26(3) |
| C(152)-C(154) | 1.41(3) |
| C(153)-C(155) | 1.37(3) |
| C(154)-C(155) | 1.53(3) |
| C(156)-C(156)#1 | 1.59(4) |
| C(157)-C(216) | 1.35(4) |
| C(157)-C(158) | 1.39(5) |
| C(157)-C(212) | 1.64(6) |
| C(158)-C(187) | 1.36(5) |
| C(158)-C(200) | 1.57(4) |
| C(159)-C(216) | 1.39(4) |
| C(159)-C(177) | 1.42(6) |
| C(159)-C(160) | 1.59(6) |
| C(160)-C(197) | 1.17(4) |
| C(160)-C(161) | 1.53(6) |
| C(161)-C(162) | 1.35(6) |
| C(161)-C(206) | 1.42(5) |
| C(162)-C(164) | 1.43(5) |
| C(162)-C(215) | 1.47(6) |
| C(163)-C(215) | 1.31(5) |
| C(163)-C(208) | 1.44(5) |
| C(163)-C(192) | 1.55(6) |
| C(164)-C(165) | 1.46(5) |
| C(164)-C(199) | 1.47(4) |
| C(165)-C(195) | 1.30(4) |
| C(165)-C(213) | 1.42(6) |
| C(166)-C(186) | 1.40(4) |
| C(166)-C(185) | 1.39(4) |
| C(166)-C(167) | 1.50(5) |
| C(167)-C(168) | 1.30(7) |
| C(167)-C(201) | 1.62(5) |
| C(168)-C(171) | 1.39(5) |
| C(168)-C(169) | 1.51(7) |
| C(169)-C(170) | 1.37(4) |
| C(169)-C(172) | 1.50(6) |
| C(170)-C(186) | 1.39(3) |
| C(170)-C(180) | 1.47(4) |
| C(171)-C(214) | 1.37(5) |

| | |
|---------------|----------|
| C(171)-C(173) | 1.39(5) |
| C(172)-C(189) | 1.06(7) |
| C(172)-C(173) | 1.48(5) |
| C(173)-C(174) | 1.33(5) |
| C(174)-C(176) | 1.32(4) |
| C(174)-C(175) | 1.64(6) |
| C(175)-C(188) | 1.20(7) |
| C(175)-C(187) | 1.59(5) |
| C(176)-C(177) | 1.40(4) |
| C(176)-C(203) | 1.41(4) |
| C(177)-C(187) | 1.38(5) |
| C(178)-C(200) | 1.41(4) |
| C(178)-C(196) | 1.39(5) |
| C(178)-C(188) | 1.41(6) |
| C(179)-C(201) | 1.29(4) |
| C(179)-C(214) | 1.48(4) |
| C(179)-C(199) | 1.53(4) |
| C(180)-C(181) | 1.45(5) |
| C(180)-C(194) | 1.49(6) |
| C(181)-C(205) | 1.20(5) |
| C(181)-C(182) | 1.64(5) |
| C(182)-C(183) | 1.47(5) |
| C(182)-C(186) | 1.50(5) |
| C(183)-C(209) | 1.42(4) |
| C(183)-C(184) | 1.42(5) |
| C(184)-C(185) | 1.31(4) |
| C(184)-C(211) | 1.75(8) |
| C(185)-C(195) | 1.63(5) |
| C(188)-C(189) | 1.67(11) |
| C(190)-C(207) | 1.33(4) |
| C(190)-C(191) | 1.37(6) |
| C(190)-C(202) | 1.45(5) |
| C(191)-C(192) | 1.36(6) |
| C(191)-C(210) | 1.62(7) |
| C(192)-C(193) | 1.41(6) |
| C(193)-C(209) | 1.45(5) |
| C(193)-C(211) | 1.45(6) |
| C(194)-C(189) | 1.39(9) |
| C(194)-C(196) | 1.41(5) |
| C(195)-C(201) | 1.39(4) |
| C(196)-C(198) | 1.44(5) |
| C(197)-C(203) | 1.48(4) |
| C(197)-C(199) | 1.53(4) |
| C(198)-C(202) | 1.41(5) |
| C(198)-C(205) | 1.59(7) |
| C(200)-C(204) | 1.34(4) |
| C(202)-C(204) | 1.31(4) |
| C(203)-C(214) | 1.49(5) |
| C(204)-C(212) | 1.47(5) |
| C(205)-C(207) | 1.46(5) |
| C(206)-C(208) | 1.37(5) |
| C(206)-C(216) | 1.43(4) |
| C(207)-C(209) | 1.46(5) |
| C(208)-C(210) | 1.43(5) |
| C(210)-C(212) | 1.16(6) |
| C(211)-C(213) | 1.09(7) |

| | |
|------------------|----------|
| C(213)-C(215) | 1.71(8) |
| C(44)-C(45) | 1.65(4) |
| C(45)-C(44)#2 | 1.65(4) |
| C(44A)-C(45A) | 1.63(7) |
| C(45A)-C(325) | 1.19(8) |
| C(45A)-C(326) | 1.51(8) |
| C(300)-C(301) | 1.38(7) |
| C(300)-C(302) | 1.52(6) |
| C(304)-C(305) | 1.35(6) |
| C(304)-C(303) | 1.49(7) |
| C(302)-C(305) | 1.48(7) |
| C(303)-C(301) | 1.20(8) |
| C(303)-C(321) | 0.82(16) |
| C(310)-C(312) | 1.40(4) |
| C(310)-C(309) | 1.44(4) |
| C(309)-C(308) | 1.45(4) |
| C(308)-C(307) | 1.35(4) |
| C(307)-C(306) | 1.42(4) |
| C(306)-C(312) | 1.47(5) |
| C(312)-C(313) | 1.45(5) |
| C(313)-N(20) | 1.18(5) |
| C(314)-C(315) | 1.24(9) |
| C(314)-C(319) | 1.28(8) |
| C(314)-C(327) | 1.92(7) |
| C(319)-C(318) | 1.39(7) |
| C(315)-C(328) | 1.68(7) |
| C(315)-C(320) | 1.84(11) |
| C(318)-C(317) | 1.48(7) |
| C(318)-C(330) | 1.89(6) |
| C(317)-C(328) | 1.28(6) |
| C(320)-N(21)#3 | 2.02(11) |
| C(321)-N(21) | 2.30(18) |
| C(326)-C(325) | 2.03(9) |
| C(323)-C(322) | 1.65(16) |
| C(323)-C(324) | 1.90(12) |
| C(329)-C(328) | 1.95(3) |
| N(21)-C(320)#4 | 2.02(11) |
| N(2)-Ru(1)-N(4) | 95.9(6) |
| N(2)-Ru(1)-N(3) | 90.9(6) |
| N(4)-Ru(1)-N(3) | 77.4(6) |
| N(2)-Ru(1)-N(6) | 95.5(6) |
| N(4)-Ru(1)-N(6) | 94.8(6) |
| N(3)-Ru(1)-N(6) | 170.4(6) |
| N(2)-Ru(1)-N(5) | 171.0(5) |
| N(4)-Ru(1)-N(5) | 91.8(5) |
| N(3)-Ru(1)-N(5) | 95.4(6) |
| N(6)-Ru(1)-N(5) | 79.1(6) |
| N(2)-Ru(1)-N(1) | 79.4(6) |
| N(4)-Ru(1)-N(1) | 174.9(6) |
| N(3)-Ru(1)-N(1) | 100.6(6) |
| N(6)-Ru(1)-N(1) | 87.6(5) |
| N(5)-Ru(1)-N(1) | 93.1(6) |
| N(2)-Ru(1)-Ru(2) | 53.9(4) |
| N(4)-Ru(1)-Ru(2) | 104.1(4) |
| N(3)-Ru(1)-Ru(2) | 44.1(4) |
| N(6)-Ru(1)-Ru(2) | 145.0(4) |

| | |
|-------------------|-----------|
| N(5)-Ru(1)-Ru(2) | 128.5(4) |
| N(1)-Ru(1)-Ru(2) | 71.6(4) |
| C(1)-N(1)-C(5) | 118.5(17) |
| C(1)-N(1)-Ru(1) | 126.5(13) |
| C(5)-N(1)-Ru(1) | 114.5(13) |
| C(10)-N(2)-C(6) | 119.4(16) |
| C(10)-N(2)-Ru(1) | 125.8(12) |
| C(6)-N(2)-Ru(1) | 114.5(13) |
| C(17)-N(3)-C(21) | 117.3(17) |
| C(17)-N(3)-Ru(1) | 124.7(13) |
| C(21)-N(3)-Ru(1) | 117.9(14) |
| C(26)-N(4)-C(22) | 116.2(15) |
| C(26)-N(4)-Ru(1) | 126.7(12) |
| C(22)-N(4)-Ru(1) | 116.7(12) |
| C(33)-N(5)-C(37) | 118.6(16) |
| C(33)-N(5)-Ru(1) | 125.1(12) |
| C(37)-N(5)-Ru(1) | 115.2(12) |
| C(42)-N(6)-C(38) | 117.8(16) |
| C(42)-N(6)-Ru(1) | 127.6(12) |
| C(38)-N(6)-Ru(1) | 114.6(13) |
| C(11)-O(2)-C(12) | 118(2) |
| C(14)-O(4)-C(15) | 117.1(19) |
| C(27)-O(6)-C(28) | 117(2) |
| C(30)-O(8)-C(31) | 118(2) |
| C(43)-O(9)-C(44A) | 112(3) |
| C(43)-O(10)-C(44) | 118(3) |
| C(46)-O(12)-C(47) | 120(2) |
| N(1)-C(1)-C(2) | 125(2) |
| C(3)-C(2)-C(1) | 117(2) |
| C(3)-C(2)-C(11) | 120(2) |
| C(1)-C(2)-C(11) | 124(2) |
| C(4)-C(3)-C(2) | 122(2) |
| C(3)-C(4)-C(5) | 115(2) |
| N(1)-C(5)-C(6) | 116.5(17) |
| N(1)-C(5)-C(4) | 123(2) |
| C(6)-C(5)-C(4) | 120(2) |
| N(2)-C(6)-C(7) | 117(2) |
| N(2)-C(6)-C(5) | 113.6(17) |
| C(7)-C(6)-C(5) | 129.0(19) |
| C(8)-C(7)-C(6) | 123(2) |
| C(7)-C(8)-C(9) | 119(2) |
| C(10)-C(9)-C(8) | 117(2) |
| C(10)-C(9)-C(14) | 122.6(19) |
| C(8)-C(9)-C(14) | 120(2) |
| N(2)-C(10)-C(9) | 123.7(17) |
| O(1)-C(11)-O(2) | 121(2) |
| O(1)-C(11)-C(2) | 128(3) |
| O(2)-C(11)-C(2) | 111.0(19) |
| O(2)-C(12)-C(13) | 108(2) |
| O(3)-C(14)-O(4) | 123(2) |
| O(3)-C(14)-C(9) | 125(2) |
| O(4)-C(14)-C(9) | 112(2) |
| O(4)-C(15)-C(16) | 107(2) |
| N(3)-C(17)-C(18) | 125.1(19) |
| C(19)-C(18)-C(17) | 118(2) |
| C(19)-C(18)-C(27) | 120.4(19) |

| | |
|-------------------|-----------|
| C(17)-C(18)-C(27) | 121(2) |
| C(20)-C(19)-C(18) | 117.4(18) |
| C(19)-C(20)-C(21) | 120.9(18) |
| N(3)-C(21)-C(20) | 120.8(19) |
| N(3)-C(21)-C(22) | 114.0(16) |
| C(20)-C(21)-C(22) | 125.2(16) |
| N(4)-C(22)-C(23) | 120.4(18) |
| N(4)-C(22)-C(21) | 113.6(14) |
| C(23)-C(22)-C(21) | 125.9(16) |
| C(24)-C(23)-C(22) | 121.4(19) |
| C(23)-C(24)-C(25) | 118.7(19) |
| C(26)-C(25)-C(24) | 118.2(19) |
| C(26)-C(25)-C(30) | 120.5(19) |
| C(24)-C(25)-C(30) | 121.4(19) |
| N(4)-C(26)-C(25) | 125.0(18) |
| O(5)-C(27)-O(6) | 124(3) |
| O(5)-C(27)-C(18) | 121(2) |
| O(6)-C(27)-C(18) | 115(2) |
| C(29)-C(28)-O(6) | 112(2) |
| O(7)-C(30)-O(8) | 125(2) |
| O(7)-C(30)-C(25) | 123(2) |
| O(8)-C(30)-C(25) | 112(2) |
| C(32)-C(31)-O(8) | 103(3) |
| N(5)-C(33)-C(34) | 124.2(19) |
| C(35)-C(34)-C(33) | 118(2) |
| C(35)-C(34)-C(43) | 122(2) |
| C(33)-C(34)-C(43) | 120(2) |
| C(34)-C(35)-C(36) | 119.5(18) |
| C(35)-C(36)-C(37) | 121.1(18) |
| N(5)-C(37)-C(36) | 118.6(18) |
| N(5)-C(37)-C(38) | 113.8(16) |
| C(36)-C(37)-C(38) | 127.5(18) |
| N(6)-C(38)-C(39) | 120(2) |
| N(6)-C(38)-C(37) | 116.5(16) |
| C(39)-C(38)-C(37) | 123.8(19) |
| C(40)-C(39)-C(38) | 121(2) |
| C(39)-C(40)-C(41) | 118(2) |
| C(42)-C(41)-C(40) | 116(2) |
| C(42)-C(41)-C(46) | 124(2) |
| C(40)-C(41)-C(46) | 119(2) |
| N(6)-C(42)-C(41) | 126.7(19) |
| O(10)-C(43)-O(9) | 125(3) |
| O(10)-C(43)-C(34) | 119(3) |
| O(9)-C(43)-C(34) | 116(2) |
| O(11)-C(46)-O(12) | 121(3) |
| O(11)-C(46)-C(41) | 126(3) |
| O(12)-C(46)-C(41) | 112(2) |
| C(48)-C(47)-O(12) | 113(3) |
| N(7)-Ru(2)-N(9) | 93.5(6) |
| N(7)-Ru(2)-N(11) | 93.8(5) |
| N(9)-Ru(2)-N(11) | 171.9(5) |
| N(7)-Ru(2)-N(10) | 171.6(6) |
| N(9)-Ru(2)-N(10) | 78.8(6) |
| N(11)-Ru(2)-N(10) | 94.1(5) |
| N(7)-Ru(2)-N(12) | 96.9(6) |
| N(9)-Ru(2)-N(12) | 97.2(6) |

| | |
|-------------------|-----------|
| N(11)-Ru(2)-N(12) | 78.5(6) |
| N(10)-Ru(2)-N(12) | 87.4(6) |
| N(7)-Ru(2)-N(8) | 77.9(6) |
| N(9)-Ru(2)-N(8) | 90.0(5) |
| N(11)-Ru(2)-N(8) | 94.9(5) |
| N(10)-Ru(2)-N(8) | 98.7(6) |
| N(12)-Ru(2)-N(8) | 171.3(6) |
| N(7)-Ru(2)-Ru(1) | 155.1(5) |
| N(9)-Ru(2)-Ru(1) | 89.3(4) |
| N(11)-Ru(2)-Ru(1) | 85.4(4) |
| N(10)-Ru(2)-Ru(1) | 23.8(4) |
| N(12)-Ru(2)-Ru(1) | 107.4(4) |
| N(8)-Ru(2)-Ru(1) | 77.4(4) |
| C(49)-N(7)-C(53) | 119.5(16) |
| C(49)-N(7)-Ru(2) | 122.0(12) |
| C(53)-N(7)-Ru(2) | 117.6(14) |
| C(58)-N(8)-C(54) | 119.9(17) |
| C(58)-N(8)-Ru(2) | 125.3(11) |
| C(54)-N(8)-Ru(2) | 114.6(14) |
| C(65)-N(9)-C(69) | 118.2(15) |
| C(65)-N(9)-Ru(2) | 125.1(12) |
| C(69)-N(9)-Ru(2) | 116.8(11) |
| C(74)-N(10)-C(70) | 117.5(15) |
| C(74)-N(10)-Ru(2) | 126.9(12) |
| C(70)-N(10)-Ru(2) | 115.4(11) |
| C(81)-N(11)-C(85) | 118.0(14) |
| C(81)-N(11)-Ru(2) | 125.8(11) |
| C(85)-N(11)-Ru(2) | 115.5(11) |
| C(90)-N(12)-C(86) | 116.7(17) |
| C(90)-N(12)-Ru(2) | 126.4(13) |
| C(86)-N(12)-Ru(2) | 116.9(13) |
| C(59)-O(14)-C(60) | 121(2) |
| C(62)-O(16)-C(63) | 114(2) |
| C(75)-O(18)-C(76) | 117.6(17) |
| C(78)-O(20)-C(79) | 115.7(16) |
| C(91)-O(22)-C(92) | 117.2(14) |
| C(94)-O(24)-C(95) | 118.4(18) |
| N(7)-C(49)-C(50) | 122(2) |
| C(51)-C(50)-C(49) | 119(2) |
| C(51)-C(50)-C(59) | 119(2) |
| C(49)-C(50)-C(59) | 121(2) |
| C(52)-C(51)-C(50) | 118(2) |
| C(53)-C(52)-C(51) | 121(2) |
| N(7)-C(53)-C(52) | 121(2) |
| N(7)-C(53)-C(54) | 113.2(16) |
| C(52)-C(53)-C(54) | 125.7(18) |
| N(8)-C(54)-C(55) | 122(2) |
| N(8)-C(54)-C(53) | 115.5(17) |
| C(55)-C(54)-C(53) | 122(2) |
| C(56)-C(55)-C(54) | 118(2) |
| C(55)-C(56)-C(57) | 120(2) |
| C(58)-C(57)-C(56) | 118(2) |
| C(58)-C(57)-C(62) | 115(2) |
| C(56)-C(57)-C(62) | 127(2) |
| N(8)-C(58)-C(57) | 121.4(19) |
| O(13)-C(59)-O(14) | 125(3) |

| | |
|-------------------|-----------|
| O(13)-C(59)-C(50) | 124(3) |
| O(14)-C(59)-C(50) | 111.0(19) |
| C(61)-C(60)-O(14) | 115(3) |
| O(15)-C(62)-O(16) | 128(3) |
| O(15)-C(62)-C(57) | 122(2) |
| O(16)-C(62)-C(57) | 110(3) |
| O(16)-C(63)-C(64) | 111(3) |
| N(9)-C(65)-C(66) | 122.6(19) |
| C(67)-C(66)-C(65) | 115.9(19) |
| C(67)-C(66)-C(75) | 123.6(19) |
| C(65)-C(66)-C(75) | 120.1(18) |
| C(68)-C(67)-C(66) | 122(2) |
| C(67)-C(68)-C(69) | 118(2) |
| N(9)-C(69)-C(68) | 123.1(18) |
| N(9)-C(69)-C(70) | 114.5(15) |
| C(68)-C(69)-C(70) | 122.3(19) |
| N(10)-C(70)-C(71) | 120.6(17) |
| N(10)-C(70)-C(69) | 113.5(15) |
| C(71)-C(70)-C(69) | 126.0(18) |
| C(72)-C(71)-C(70) | 120.6(19) |
| C(71)-C(72)-C(73) | 120.3(18) |
| C(74)-C(73)-C(72) | 116.5(18) |
| C(74)-C(73)-C(78) | 120.0(19) |
| C(72)-C(73)-C(78) | 123.5(18) |
| N(10)-C(74)-C(73) | 124.4(18) |
| O(17)-C(75)-O(18) | 124(2) |
| O(17)-C(75)-C(66) | 123(2) |
| O(18)-C(75)-C(66) | 113(2) |
| O(18)-C(76)-C(77) | 106.8(17) |
| O(19)-C(78)-O(20) | 125.6(19) |
| O(19)-C(78)-C(73) | 121(2) |
| O(20)-C(78)-C(73) | 113.3(18) |
| O(20)-C(79)-C(80) | 105.0(16) |
| N(11)-C(81)-C(82) | 124.0(16) |
| C(83)-C(82)-C(81) | 117.1(17) |
| C(83)-C(82)-C(91) | 124.6(15) |
| C(81)-C(82)-C(91) | 118.3(15) |
| C(84)-C(83)-C(82) | 120.0(17) |
| C(83)-C(84)-C(85) | 119.3(18) |
| N(11)-C(85)-C(84) | 121.6(17) |
| N(11)-C(85)-C(86) | 115.3(14) |
| C(84)-C(85)-C(86) | 123.1(17) |
| C(87)-C(86)-N(12) | 120.9(18) |
| C(87)-C(86)-C(85) | 126.5(17) |
| N(12)-C(86)-C(85) | 112.5(16) |
| C(86)-C(87)-C(88) | 120.8(18) |
| C(87)-C(88)-C(89) | 120.8(19) |
| C(90)-C(89)-C(88) | 115.1(19) |
| C(90)-C(89)-C(94) | 122(2) |
| C(88)-C(89)-C(94) | 123(2) |
| N(12)-C(90)-C(89) | 125.3(19) |
| O(21)-C(91)-O(22) | 122.6(14) |
| O(21)-C(91)-C(82) | 123.1(14) |
| O(22)-C(91)-C(82) | 114.3(13) |
| O(22)-C(92)-C(93) | 111.4(19) |
| O(23)-C(94)-O(24) | 124(2) |

| | |
|----------------------|-----------|
| O(23)-C(94)-C(89) | 126(2) |
| O(24)-C(94)-C(89) | 110(2) |
| O(24)-C(95)-C(96) | 107(2) |
| C(120)-C(97)-C(128) | 118(2) |
| C(120)-C(97)-C(99) | 125(2) |
| C(128)-C(97)-C(99) | 106(2) |
| C(116)-C(98)-C(100) | 130(3) |
| C(116)-C(98)-C(126) | 114(2) |
| C(100)-C(98)-C(126) | 106(2) |
| C(154)-C(99)-C(139) | 123(2) |
| C(154)-C(99)-C(97) | 110.1(18) |
| C(139)-C(99)-C(97) | 116(2) |
| C(112)-C(100)-C(98) | 119(3) |
| C(112)-C(100)-C(156) | 122(2) |
| C(98)-C(100)-C(156) | 112(2) |
| C(111)-C(101)-C(138) | 129(3) |
| C(111)-C(101)-C(132) | 116(2) |
| C(138)-C(101)-C(132) | 103(2) |
| C(128)-C(102)-C(136) | 117(2) |
| C(128)-C(102)-C(107) | 121(2) |
| C(136)-C(102)-C(107) | 109(2) |
| C(109)-C(103)-C(145) | 119(2) |
| C(109)-C(103)-C(146) | 115(2) |
| C(145)-C(103)-C(146) | 117(2) |
| C(144)-C(104)-C(132) | 122(3) |
| C(144)-C(104)-C(114) | 115(2) |
| C(132)-C(104)-C(114) | 108(2) |
| C(109)-C(105)-C(106) | 131(3) |
| C(109)-C(105)-C(124) | 113(2) |
| C(106)-C(105)-C(124) | 104(3) |
| C(105)-C(106)-C(144) | 114(3) |
| C(105)-C(106)-C(149) | 115(3) |
| C(144)-C(106)-C(149) | 116(2) |
| C(148)-C(107)-C(117) | 124(3) |
| C(148)-C(107)-C(102) | 119(2) |
| C(117)-C(107)-C(102) | 103(2) |
| C(133)-C(108)-C(137) | 114(2) |
| C(133)-C(108)-C(111) | 120(3) |
| C(137)-C(108)-C(111) | 113(2) |
| C(103)-C(109)-C(105) | 134(3) |
| C(103)-C(109)-C(153) | 102(2) |
| C(105)-C(109)-C(153) | 112(2) |
| C(119)-C(110)-C(132) | 125(3) |
| C(119)-C(110)-C(134) | 108(2) |
| C(132)-C(110)-C(134) | 116(2) |
| C(101)-C(111)-C(121) | 132(3) |
| C(101)-C(111)-C(108) | 115(3) |
| C(121)-C(111)-C(108) | 101(3) |
| C(146)-C(112)-C(100) | 123(2) |
| C(146)-C(112)-C(118) | 113(2) |
| C(100)-C(112)-C(118) | 114(2) |
| C(135)-C(113)-C(130) | 141(4) |
| C(135)-C(113)-C(123) | 94(3) |
| C(130)-C(113)-C(123) | 113(3) |
| C(147)-C(114)-C(138) | 132(3) |
| C(147)-C(114)-C(104) | 111(2) |

| | |
|----------------------|-----------|
| C(138)-C(114)-C(104) | 103(2) |
| C(146)-C(115)-C(124) | 126(3) |
| C(146)-C(115)-C(140) | 110(2) |
| C(124)-C(115)-C(140) | 115(2) |
| C(135)-C(116)-C(98) | 136(3) |
| C(135)-C(116)-C(129) | 100(3) |
| C(98)-C(116)-C(129) | 111(3) |
| C(138)-C(117)-C(133) | 117(3) |
| C(138)-C(117)-C(107) | 118(3) |
| C(133)-C(117)-C(107) | 114(2) |
| C(129)-C(118)-C(140) | 119(2) |
| C(129)-C(118)-C(112) | 128(2) |
| C(140)-C(118)-C(112) | 102.4(19) |
| C(110)-C(119)-C(127) | 112(3) |
| C(110)-C(119)-C(121) | 119(3) |
| C(127)-C(119)-C(121) | 114(3) |
| C(97)-C(120)-C(125) | 125(2) |
| C(97)-C(120)-C(142) | 119(2) |
| C(125)-C(120)-C(142) | 104(2) |
| C(111)-C(121)-C(130) | 126(4) |
| C(111)-C(121)-C(119) | 112(3) |
| C(130)-C(121)-C(119) | 112(3) |
| C(142)-C(122)-C(141) | 121(3) |
| C(142)-C(122)-C(135) | 116(3) |
| C(141)-C(122)-C(135) | 110(3) |
| C(129)-C(123)-C(127) | 120(3) |
| C(129)-C(123)-C(113) | 116(2) |
| C(127)-C(123)-C(113) | 113(2) |
| C(131)-C(124)-C(115) | 122(2) |
| C(131)-C(124)-C(105) | 111(2) |
| C(115)-C(124)-C(105) | 116(2) |
| C(136)-C(125)-C(120) | 117(2) |
| C(136)-C(125)-C(141) | 118(3) |
| C(120)-C(125)-C(141) | 110(2) |
| C(142)-C(126)-C(139) | 128(3) |
| C(142)-C(126)-C(98) | 114(2) |
| C(139)-C(126)-C(98) | 106(2) |
| C(119)-C(127)-C(123) | 127(3) |
| C(119)-C(127)-C(143) | 103(3) |
| C(123)-C(127)-C(143) | 116(3) |
| C(102)-C(128)-C(97) | 124(2) |
| C(102)-C(128)-C(152) | 116(2) |
| C(97)-C(128)-C(152) | 107(2) |
| C(123)-C(129)-C(118) | 127(3) |
| C(123)-C(129)-C(116) | 102(2) |
| C(118)-C(129)-C(116) | 118(2) |
| C(113)-C(130)-C(121) | 139(3) |
| C(113)-C(130)-C(137) | 108(3) |
| C(121)-C(130)-C(137) | 98(2) |
| C(134)-C(131)-C(124) | 120(2) |
| C(134)-C(131)-C(144) | 121(2) |
| C(124)-C(131)-C(144) | 106(2) |
| C(104)-C(132)-C(110) | 123(3) |
| C(104)-C(132)-C(101) | 109(2) |
| C(110)-C(132)-C(101) | 115(2) |
| C(108)-C(133)-C(136) | 122(2) |

| | |
|----------------------|--------|
| C(108)-C(133)-C(117) | 121(2) |
| C(136)-C(133)-C(117) | 105(2) |
| C(131)-C(134)-C(143) | 123(2) |
| C(131)-C(134)-C(110) | 119(2) |
| C(143)-C(134)-C(110) | 105(2) |
| C(113)-C(135)-C(116) | 128(4) |
| C(113)-C(135)-C(122) | 112(3) |
| C(116)-C(135)-C(122) | 108(3) |
| C(133)-C(136)-C(125) | 120(2) |
| C(133)-C(136)-C(102) | 110(2) |
| C(125)-C(136)-C(102) | 118(2) |
| C(141)-C(137)-C(108) | 132(3) |
| C(141)-C(137)-C(130) | 113(3) |
| C(108)-C(137)-C(130) | 101(2) |
| C(114)-C(138)-C(101) | 116(3) |
| C(114)-C(138)-C(117) | 115(3) |
| C(101)-C(138)-C(117) | 118(3) |
| C(126)-C(139)-C(99) | 118(3) |
| C(126)-C(139)-C(156) | 113(2) |
| C(99)-C(139)-C(156) | 122(2) |
| C(143)-C(140)-C(118) | 121(2) |
| C(143)-C(140)-C(115) | 119(2) |
| C(118)-C(140)-C(115) | 107(2) |
| C(137)-C(141)-C(122) | 135(3) |
| C(137)-C(141)-C(125) | 114(3) |
| C(122)-C(141)-C(125) | 101(3) |
| C(122)-C(142)-C(126) | 130(3) |
| C(122)-C(142)-C(120) | 104(2) |
| C(126)-C(142)-C(120) | 114(3) |
| C(134)-C(143)-C(140) | 121(2) |
| C(134)-C(143)-C(127) | 112(2) |
| C(140)-C(143)-C(127) | 116(2) |
| C(104)-C(144)-C(106) | 128(3) |
| C(104)-C(144)-C(131) | 118(3) |
| C(106)-C(144)-C(131) | 106(2) |
| C(155)-C(145)-C(103) | 100(2) |
| C(155)-C(145)-C(156) | 125(2) |
| C(103)-C(145)-C(156) | 127(2) |
| C(115)-C(146)-C(112) | 108(2) |
| C(115)-C(146)-C(103) | 116(2) |
| C(112)-C(146)-C(103) | 119(2) |
| C(149)-C(147)-C(114) | 135(3) |
| C(149)-C(147)-C(148) | 103(3) |
| C(114)-C(147)-C(148) | 109(2) |
| C(107)-C(148)-C(150) | 123(3) |
| C(107)-C(148)-C(147) | 120(2) |
| C(150)-C(148)-C(147) | 107(3) |
| C(147)-C(149)-C(151) | 123(4) |
| C(147)-C(149)-C(106) | 114(3) |
| C(151)-C(149)-C(106) | 113(3) |
| C(152)-C(150)-C(148) | 128(3) |
| C(152)-C(150)-C(151) | 112(2) |
| C(148)-C(150)-C(151) | 106(2) |
| C(153)-C(151)-C(149) | 137(3) |
| C(153)-C(151)-C(150) | 110(3) |
| C(149)-C(151)-C(150) | 100(3) |

| | |
|------------------------|-----------|
| C(150)-C(152)-C(154) | 132(3) |
| C(150)-C(152)-C(128) | 113(2) |
| C(154)-C(152)-C(128) | 103(2) |
| C(151)-C(153)-C(155) | 139(3) |
| C(151)-C(153)-C(109) | 111(3) |
| C(155)-C(153)-C(109) | 96(2) |
| C(99)-C(154)-C(152) | 113(2) |
| C(99)-C(154)-C(155) | 118(2) |
| C(152)-C(154)-C(155) | 114(2) |
| C(145)-C(155)-C(153) | 123(3) |
| C(145)-C(155)-C(154) | 118(2) |
| C(153)-C(155)-C(154) | 111(2) |
| C(145)-C(156)-C(139) | 110.1(17) |
| C(145)-C(156)-C(100) | 106.6(18) |
| C(139)-C(156)-C(100) | 99.6(16) |
| C(145)-C(156)-C(156)#1 | 114.6(18) |
| C(139)-C(156)-C(156)#1 | 114.2(19) |
| C(100)-C(156)-C(156)#1 | 110.3(17) |
| C(216)-C(157)-C(158) | 123(3) |
| C(216)-C(157)-C(212) | 117(4) |
| C(158)-C(157)-C(212) | 105(3) |
| C(187)-C(158)-C(157) | 118(3) |
| C(187)-C(158)-C(200) | 122(4) |
| C(157)-C(158)-C(200) | 107(4) |
| C(216)-C(159)-C(177) | 124(4) |
| C(216)-C(159)-C(160) | 111(4) |
| C(177)-C(159)-C(160) | 116(3) |
| C(197)-C(160)-C(161) | 129(5) |
| C(197)-C(160)-C(159) | 122(5) |
| C(161)-C(160)-C(159) | 98(3) |
| C(162)-C(161)-C(206) | 121(5) |
| C(162)-C(161)-C(160) | 116(3) |
| C(206)-C(161)-C(160) | 113(4) |
| C(161)-C(162)-C(164) | 122(4) |
| C(161)-C(162)-C(215) | 120(4) |
| C(164)-C(162)-C(215) | 104(4) |
| C(215)-C(163)-C(208) | 121(4) |
| C(215)-C(163)-C(192) | 124(5) |
| C(208)-C(163)-C(192) | 100(4) |
| C(162)-C(164)-C(165) | 118(4) |
| C(162)-C(164)-C(199) | 117(4) |
| C(165)-C(164)-C(199) | 114(3) |
| C(195)-C(165)-C(213) | 123(5) |
| C(195)-C(165)-C(164) | 117(3) |
| C(213)-C(165)-C(164) | 107(5) |
| C(186)-C(166)-C(185) | 122(3) |
| C(186)-C(166)-C(167) | 116(3) |
| C(185)-C(166)-C(167) | 111(3) |
| C(168)-C(167)-C(166) | 128(5) |
| C(168)-C(167)-C(201) | 114(4) |
| C(166)-C(167)-C(201) | 102(3) |
| C(167)-C(168)-C(171) | 124(6) |
| C(167)-C(168)-C(169) | 111(4) |
| C(171)-C(168)-C(169) | 113(6) |
| C(170)-C(169)-C(168) | 123(4) |
| C(170)-C(169)-C(172) | 122(3) |

| | |
|----------------------|--------|
| C(168)-C(169)-C(172) | 102(4) |
| C(169)-C(170)-C(186) | 121(3) |
| C(169)-C(170)-C(180) | 116(3) |
| C(186)-C(170)-C(180) | 112(2) |
| C(214)-C(171)-C(168) | 126(5) |
| C(214)-C(171)-C(173) | 118(4) |
| C(168)-C(171)-C(173) | 107(5) |
| C(189)-C(172)-C(169) | 111(6) |
| C(189)-C(172)-C(173) | 126(6) |
| C(169)-C(172)-C(173) | 106(5) |
| C(174)-C(173)-C(171) | 120(4) |
| C(174)-C(173)-C(172) | 115(4) |
| C(171)-C(173)-C(172) | 112(5) |
| C(176)-C(174)-C(173) | 127(4) |
| C(176)-C(174)-C(175) | 103(3) |
| C(173)-C(174)-C(175) | 118(3) |
| C(188)-C(175)-C(187) | 122(6) |
| C(188)-C(175)-C(174) | 124(6) |
| C(187)-C(175)-C(174) | 99(3) |
| C(174)-C(176)-C(177) | 122(4) |
| C(174)-C(176)-C(203) | 116(3) |
| C(177)-C(176)-C(203) | 113(4) |
| C(187)-C(177)-C(176) | 105(5) |
| C(187)-C(177)-C(159) | 114(3) |
| C(176)-C(177)-C(159) | 123(4) |
| C(200)-C(178)-C(196) | 114(3) |
| C(200)-C(178)-C(188) | 130(5) |
| C(196)-C(178)-C(188) | 102(6) |
| C(201)-C(179)-C(214) | 127(4) |
| C(201)-C(179)-C(199) | 116(3) |
| C(214)-C(179)-C(199) | 105(3) |
| C(181)-C(180)-C(170) | 110(3) |
| C(181)-C(180)-C(194) | 117(4) |
| C(170)-C(180)-C(194) | 119(3) |
| C(205)-C(181)-C(180) | 136(5) |
| C(205)-C(181)-C(182) | 105(5) |
| C(180)-C(181)-C(182) | 105(3) |
| C(183)-C(182)-C(186) | 116(3) |
| C(183)-C(182)-C(181) | 127(3) |
| C(186)-C(182)-C(181) | 104(3) |
| C(209)-C(183)-C(184) | 115(4) |
| C(209)-C(183)-C(182) | 111(4) |
| C(184)-C(183)-C(182) | 121(3) |
| C(185)-C(184)-C(183) | 119(4) |
| C(185)-C(184)-C(211) | 127(4) |
| C(183)-C(184)-C(211) | 100(3) |
| C(184)-C(185)-C(166) | 124(4) |
| C(184)-C(185)-C(195) | 113(3) |
| C(166)-C(185)-C(195) | 110(3) |
| C(166)-C(186)-C(170) | 120(3) |
| C(166)-C(186)-C(182) | 117(3) |
| C(170)-C(186)-C(182) | 110(3) |
| C(158)-C(187)-C(177) | 124(4) |
| C(158)-C(187)-C(175) | 117(4) |
| C(177)-C(187)-C(175) | 111(4) |
| C(175)-C(188)-C(178) | 120(9) |

| | |
|----------------------|--------|
| C(175)-C(188)-C(189) | 110(6) |
| C(178)-C(188)-C(189) | 118(6) |
| C(207)-C(190)-C(191) | 121(4) |
| C(207)-C(190)-C(202) | 117(4) |
| C(191)-C(190)-C(202) | 114(4) |
| C(192)-C(191)-C(190) | 119(5) |
| C(192)-C(191)-C(210) | 100(5) |
| C(190)-C(191)-C(210) | 125(5) |
| C(191)-C(192)-C(193) | 122(4) |
| C(191)-C(192)-C(163) | 119(5) |
| C(193)-C(192)-C(163) | 110(5) |
| C(192)-C(193)-C(209) | 121(4) |
| C(192)-C(193)-C(211) | 118(5) |
| C(209)-C(193)-C(211) | 109(5) |
| C(189)-C(194)-C(196) | 125(5) |
| C(189)-C(194)-C(180) | 107(5) |
| C(196)-C(194)-C(180) | 113(4) |
| C(165)-C(195)-C(201) | 131(3) |
| C(165)-C(195)-C(185) | 113(3) |
| C(201)-C(195)-C(185) | 103(3) |
| C(178)-C(196)-C(194) | 107(5) |
| C(178)-C(196)-C(198) | 119(3) |
| C(194)-C(196)-C(198) | 123(5) |
| C(160)-C(197)-C(203) | 119(4) |
| C(160)-C(197)-C(199) | 116(4) |
| C(203)-C(197)-C(199) | 113(3) |
| C(202)-C(198)-C(196) | 120(3) |
| C(202)-C(198)-C(205) | 105(3) |
| C(196)-C(198)-C(205) | 121(4) |
| C(164)-C(199)-C(197) | 120(3) |
| C(164)-C(199)-C(179) | 122(3) |
| C(197)-C(199)-C(179) | 105(3) |
| C(204)-C(200)-C(178) | 128(3) |
| C(204)-C(200)-C(158) | 112(3) |
| C(178)-C(200)-C(158) | 109(4) |
| C(179)-C(201)-C(195) | 119(3) |
| C(179)-C(201)-C(167) | 117(4) |
| C(195)-C(201)-C(167) | 113(3) |
| C(204)-C(202)-C(198) | 121(3) |
| C(204)-C(202)-C(190) | 121(4) |
| C(198)-C(202)-C(190) | 106(3) |
| C(176)-C(203)-C(197) | 126(3) |
| C(176)-C(203)-C(214) | 118(3) |
| C(197)-C(203)-C(214) | 102(3) |
| C(202)-C(204)-C(200) | 118(3) |
| C(202)-C(204)-C(212) | 120(4) |
| C(200)-C(204)-C(212) | 109(4) |
| C(181)-C(205)-C(207) | 138(7) |
| C(181)-C(205)-C(198) | 108(5) |
| C(207)-C(205)-C(198) | 106(4) |
| C(208)-C(206)-C(161) | 119(4) |
| C(208)-C(206)-C(216) | 122(4) |
| C(161)-C(206)-C(216) | 108(4) |
| C(190)-C(207)-C(205) | 106(4) |
| C(190)-C(207)-C(209) | 125(4) |
| C(205)-C(207)-C(209) | 113(4) |

| | |
|----------------------|---------|
| C(206)-C(208)-C(210) | 117(5) |
| C(206)-C(208)-C(163) | 120(3) |
| C(210)-C(208)-C(163) | 113(5) |
| C(183)-C(209)-C(193) | 112(4) |
| C(183)-C(209)-C(207) | 125(4) |
| C(193)-C(209)-C(207) | 112(3) |
| C(212)-C(210)-C(208) | 129(6) |
| C(212)-C(210)-C(191) | 110(5) |
| C(208)-C(210)-C(191) | 108(5) |
| C(213)-C(211)-C(193) | 144(9) |
| C(213)-C(211)-C(184) | 100(6) |
| C(193)-C(211)-C(184) | 105(5) |
| C(210)-C(212)-C(204) | 130(6) |
| C(210)-C(212)-C(157) | 115(5) |
| C(204)-C(212)-C(157) | 106(4) |
| C(211)-C(213)-C(165) | 141(8) |
| C(211)-C(213)-C(215) | 102(7) |
| C(165)-C(213)-C(215) | 104(5) |
| C(171)-C(214)-C(179) | 112(4) |
| C(171)-C(214)-C(203) | 120(3) |
| C(179)-C(214)-C(203) | 115(3) |
| C(163)-C(215)-C(162) | 119(4) |
| C(163)-C(215)-C(213) | 121(5) |
| C(162)-C(215)-C(213) | 106(4) |
| C(157)-C(216)-C(159) | 116(4) |
| C(157)-C(216)-C(206) | 119(4) |
| C(159)-C(216)-C(206) | 111(3) |
| O(10)-C(44)-C(45) | 119(3) |
| C(44)-C(45)-C(44)#2 | 180(3) |
| O(9)-C(44A)-C(45A) | 110(3) |
| C(325)-C(45A)-C(326) | 97(6) |
| C(325)-C(45A)-C(44A) | 149(5) |
| C(326)-C(45A)-C(44A) | 103(4) |
| C(172)-C(189)-C(194) | 145(8) |
| C(172)-C(189)-C(188) | 126(9) |
| C(194)-C(189)-C(188) | 86(4) |
| C(301)-C(300)-C(302) | 117(5) |
| C(305)-C(304)-C(303) | 108(5) |
| C(305)-C(302)-C(300) | 118(5) |
| C(304)-C(305)-C(302) | 122(5) |
| C(301)-C(303)-C(304) | 138(7) |
| C(301)-C(303)-C(321) | 142(10) |
| C(304)-C(303)-C(321) | 80(10) |
| C(303)-C(301)-C(300) | 116(7) |
| C(312)-C(310)-C(309) | 121(3) |
| C(310)-C(309)-C(308) | 115(3) |
| C(307)-C(308)-C(309) | 122(3) |
| C(308)-C(307)-C(306) | 127(3) |
| C(307)-C(306)-C(312) | 111(4) |
| C(310)-C(312)-C(313) | 122(3) |
| C(310)-C(312)-C(306) | 124(3) |
| C(313)-C(312)-C(306) | 114(4) |
| N(20)-C(313)-C(312) | 172(5) |
| C(315)-C(314)-C(319) | 131(9) |
| C(315)-C(314)-C(327) | 98(6) |
| C(319)-C(314)-C(327) | 97(6) |

| | |
|-----------------------|---------|
| C(314)-C(319)-C(318) | 129(7) |
| C(314)-C(315)-C(328) | 102(7) |
| C(314)-C(315)-C(320) | 96(7) |
| C(328)-C(315)-C(320) | 159(6) |
| C(319)-C(318)-C(317) | 114(6) |
| C(319)-C(318)-C(330) | 120(5) |
| C(317)-C(318)-C(330) | 81(4) |
| C(328)-C(317)-C(318) | 112(5) |
| N(21)#3-C(320)-C(315) | 126(7) |
| N(21)-C(321)-C(303) | 146(10) |
| C(45A)-C(326)-C(325) | 36(3) |
| C(322)-C(323)-C(324) | 171(10) |
| C(45A)-C(325)-C(326) | 48(4) |
| C(317)-C(328)-C(315) | 132(4) |
| C(317)-C(328)-C(329) | 111(3) |
| C(315)-C(328)-C(329) | 117(3) |
| C(321)-N(21)-C(320)#4 | 133(5) |

Symmetry transformations used to generate equivalent atoms:

#1 -x,-y+1,-z #2 -x+2,-y+2,-z+1 #3 x+1/2,-y+1/2,z+1/2

#4 x-1/2,-y+1/2,z-1/2

Table A1.10. Anisotropic displacement parameters ($\text{\AA}^2 \times 10^3$). The anisotropic displacement factor exponent takes the form: $-2 \sum_{h^2} [h^2 a^* U^{11} + \dots + 2 h k a^* b^* U^{12}]$

| | U ¹¹ | U ²² | U ³³ | U ²³ | U ¹³ | U ¹² |
|-------|-----------------|-----------------|-----------------|-----------------|-----------------|-----------------|
| Ru(1) | 15(1) | 26(1) | 45(1) | -8(1) | 9(1) | -4(1) |
| N(1) | 18(10) | 29(10) | 37(10) | -6(8) | 13(8) | -8(8) |
| N(2) | 18(9) | 35(10) | 32(9) | -14(8) | 2(7) | -7(7) |
| N(3) | 6(8) | 23(11) | 52(10) | -6(8) | 1(7) | -16(7) |
| N(4) | 22(9) | 21(10) | 37(9) | -12(7) | 1(7) | -15(7) |
| N(5) | 8(8) | 26(9) | 36(10) | -6(8) | 5(7) | -11(7) |
| N(6) | 15(9) | 17(9) | 50(11) | -10(8) | 11(8) | 3(7) |
| O(1) | 68(12) | 46(12) | 153(18) | 11(11) | 64(13) | 22(10) |
| O(2) | 27(9) | 50(11) | 140(17) | -6(11) | 31(10) | 15(8) |
| O(3) | 63(12) | 112(17) | 89(13) | -48(12) | -40(11) | 8(11) |
| O(4) | 23(9) | 73(12) | 76(11) | 1(9) | -8(8) | -8(8) |
| O(5) | 290(40) | 60(16) | 160(20) | 36(14) | 170(30) | 47(18) |
| O(6) | 92(13) | 38(11) | 63(11) | 2(8) | 26(9) | -6(9) |
| O(7) | 68(11) | 59(12) | 74(11) | -12(9) | 16(9) | 49(10) |
| O(8) | 64(11) | 43(11) | 108(14) | 15(10) | 20(11) | 18(9) |
| O(9) | 120(20) | 260(40) | 310(40) | 210(40) | -160(30) | -150(30) |
| O(10) | 35(10) | 99(15) | 85(12) | 9(11) | -23(9) | -32(9) |
| O(11) | 180(20) | 106(19) | 100(16) | 52(14) | 18(16) | -54(17) |
| O(12) | 122(18) | 140(20) | 49(12) | 30(12) | 9(12) | -21(16) |
| C(1) | 41(15) | 23(13) | 55(13) | -1(10) | 36(11) | 2(10) |
| C(2) | 45(16) | 18(13) | 81(19) | 4(12) | 22(14) | -8(11) |
| C(3) | 53(17) | 39(15) | 90(20) | 3(14) | 48(15) | 26(12) |
| C(4) | 59(18) | 39(16) | 92(19) | -32(13) | 30(15) | -25(13) |
| C(5) | 48(14) | 24(13) | 56(15) | -10(11) | 22(12) | -6(11) |
| C(6) | 83(19) | 34(14) | 30(12) | -15(10) | 21(12) | -2(12) |
| C(7) | 50(17) | 63(18) | 77(18) | -55(15) | 6(14) | -4(13) |
| C(8) | 60(19) | 120(30) | 45(15) | -39(16) | -18(13) | -14(17) |

| | | | | | | |
|-------|----------|---------|---------|----------|----------|---------|
| C(9) | 57(16) | 48(15) | 41(13) | -15(11) | -2(12) | 21(12) |
| C(10) | 20(12) | 38(13) | 25(11) | -4(9) | 10(9) | -8(9) |
| C(11) | 49(17) | 10(13) | 120(20) | 3(13) | 50(16) | 6(12) |
| C(12) | 13(13) | 90(20) | 210(40) | 20(20) | -5(17) | 37(14) |
| C(13) | 60(20) | 100(30) | 160(30) | -20(20) | -10(20) | 10(18) |
| C(14) | 70(20) | 80(20) | 61(17) | -15(16) | -5(16) | 8(16) |
| C(15) | 47(16) | 68(19) | 93(19) | -15(16) | -6(13) | 17(13) |
| C(16) | 44(16) | 100(30) | 140(30) | 0(20) | 13(17) | 26(16) |
| C(17) | 30(12) | 51(17) | 33(12) | -9(11) | -4(9) | -4(11) |
| C(18) | 38(12) | 19(13) | 47(13) | 2(10) | 3(10) | -6(10) |
| C(19) | 39(13) | 49(16) | 30(12) | 4(11) | -12(10) | -12(11) |
| C(20) | 2(9) | 57(16) | 30(11) | -11(10) | 5(8) | -5(9) |
| C(21) | 7(10) | 47(15) | 33(11) | -15(10) | -1(9) | -6(9) |
| C(22) | -1(8) | 38(13) | 17(8) | -9(8) | 4(6) | -3(8) |
| C(23) | 25(12) | 62(18) | 58(14) | -1(13) | 16(11) | 5(12) |
| C(24) | 27(13) | 62(18) | 67(16) | -1(13) | 21(12) | 23(12) |
| C(25) | 23(11) | 26(13) | 55(14) | -2(10) | -5(10) | 12(10) |
| C(26) | 4(9) | 24(13) | 49(12) | 4(10) | 1(8) | -5(8) |
| C(27) | 90(20) | 90(20) | 46(15) | 20(15) | 39(15) | 10(17) |
| C(28) | 180(40) | 70(20) | 120(30) | 12(19) | 90(30) | 20(20) |
| C(29) | 130(30) | 41(19) | 100(20) | 0(16) | 20(20) | -23(18) |
| C(30) | 38(14) | 80(20) | 47(15) | -11(14) | 8(12) | 5(14) |
| C(31) | 190(40) | 70(30) | 190(40) | 60(30) | 90(30) | 50(20) |
| C(32) | 380(90) | 260(70) | 400(90) | 290(70) | 270(80) | 200(70) |
| C(33) | 20(12) | 40(14) | 52(15) | -20(12) | 4(10) | -9(10) |
| C(34) | 32(13) | 32(14) | 76(16) | 13(12) | -4(12) | -13(11) |
| C(35) | 28(12) | 51(15) | 43(14) | -15(12) | -13(10) | 1(11) |
| C(36) | 0(10) | 26(12) | 88(17) | -24(12) | 21(10) | -17(8) |
| C(37) | 33(13) | 7(11) | 46(13) | -14(9) | 13(10) | -7(9) |
| C(38) | 23(12) | 12(11) | 64(15) | -11(10) | 28(11) | -5(9) |
| C(39) | 76(17) | 18(13) | 51(15) | -4(10) | 21(13) | 16(12) |
| C(40) | 36(14) | 22(13) | 90(20) | -3(12) | 31(13) | -2(11) |
| C(41) | 29(13) | 38(14) | 66(16) | 22(12) | 24(12) | 21(11) |
| C(42) | 16(10) | 4(10) | 60(15) | 0(9) | 16(10) | 8(8) |
| C(43) | 110(30) | 110(30) | 120(30) | 30(20) | -90(20) | -40(20) |
| C(46) | 56(17) | 90(20) | 80(20) | 8(19) | 20(16) | -12(16) |
| C(47) | 130(30) | 170(40) | 90(30) | 50(30) | -10(20) | 10(30) |
| C(48) | 470(110) | 200(60) | 150(40) | -110(40) | -160(60) | 210(70) |
| Ru(2) | 11(1) | 33(1) | 43(1) | 11(1) | 6(1) | 2(1) |
| N(7) | 11(8) | 39(12) | 35(9) | 13(8) | 3(7) | -4(7) |
| N(8) | -5(7) | 69(13) | 19(6) | 25(7) | 5(5) | -3(7) |
| N(9) | 10(9) | 32(10) | 30(9) | 13(7) | 5(7) | 12(7) |
| N(10) | 15(9) | 24(9) | 37(9) | 10(7) | 11(7) | -3(7) |
| N(11) | 2(8) | 25(9) | 38(10) | 6(7) | -1(7) | 2(7) |
| N(12) | 6(8) | 50(11) | 44(11) | 13(9) | 7(7) | -4(8) |
| O(13) | 75(14) | 170(20) | 101(15) | 23(14) | -3(11) | -90(15) |
| O(14) | 56(11) | 31(10) | 104(13) | -3(9) | 1(10) | -21(8) |
| O(15) | 200(30) | 58(15) | 111(18) | -16(12) | 78(18) | 7(15) |
| O(16) | 115(16) | 46(13) | 92(14) | -21(10) | 23(12) | 19(11) |
| O(17) | 37(9) | 96(14) | 57(10) | 20(10) | -9(8) | 20(9) |
| O(18) | 14(7) | 89(12) | 49(9) | 17(9) | -3(6) | -5(7) |
| O(19) | 48(10) | 42(10) | 81(11) | 12(8) | 23(9) | -20(8) |
| O(20) | 10(7) | 56(10) | 66(10) | 8(8) | 1(7) | 0(6) |
| O(21) | 43(10) | 76(12) | 59(10) | 0(9) | -10(8) | 20(9) |
| O(22) | 20(8) | 57(10) | 48(9) | -6(7) | -9(7) | 12(7) |
| O(23) | 109(17) | 103(17) | 71(13) | -45(12) | -8(11) | 24(13) |

| | | | | | | |
|--------|---------|---------|---------|----------|---------|---------|
| O(24) | 57(10) | 67(12) | 43(10) | -5(8) | -4(8) | 6(9) |
| C(49) | 9(10) | 42(15) | 48(12) | 31(11) | -3(9) | -12(9) |
| C(50) | 5(10) | 72(18) | 48(13) | 22(12) | 1(10) | 5(11) |
| C(51) | 10(12) | 120(30) | 70(17) | 51(17) | -1(12) | -16(14) |
| C(52) | 1(11) | 80(20) | 64(15) | 0(14) | -1(10) | 6(11) |
| C(53) | 1(9) | 89(17) | 21(8) | 17(9) | 3(7) | 2(10) |
| C(54) | 0(10) | 72(18) | 39(13) | 5(12) | -11(9) | 17(10) |
| C(55) | 40(14) | 70(20) | 50(15) | 9(14) | -1(12) | -3(13) |
| C(56) | 29(14) | 120(30) | 47(15) | 4(16) | 7(12) | 47(16) |
| C(57) | 36(13) | 69(19) | 27(12) | -6(11) | 3(10) | 17(12) |
| C(58) | 16(11) | 44(16) | 63(15) | 9(12) | 7(10) | 8(11) |
| C(59) | 26(14) | 62(19) | 77(18) | 20(15) | -7(13) | -6(13) |
| C(60) | 120(30) | 20(20) | 340(60) | -90(30) | -10(40) | -31(19) |
| C(61) | 90(30) | 350(90) | 350(80) | -270(80) | 80(40) | -10(40) |
| C(62) | 120(30) | 50(20) | 70(20) | -7(16) | 40(18) | 30(17) |
| C(63) | 220(50) | 110(30) | 120(30) | -40(20) | 70(30) | 50(30) |
| C(64) | 110(40) | 190(50) | 330(70) | -160(50) | 90(40) | -50(30) |
| C(65) | 9(11) | 56(15) | 45(13) | 2(11) | -11(9) | 7(10) |
| C(66) | 45(15) | 64(17) | 40(13) | 21(12) | 9(11) | -2(12) |
| C(67) | 33(14) | 65(17) | 58(15) | 35(13) | -22(11) | 3(12) |
| C(68) | 73(19) | 49(17) | 59(16) | 14(12) | 3(14) | -11(13) |
| C(69) | 25(12) | 46(14) | 23(11) | 7(10) | -1(9) | 15(10) |
| C(70) | 40(13) | 19(12) | 51(14) | 12(10) | 15(11) | -10(10) |
| C(71) | 25(13) | 45(15) | 68(15) | 31(11) | 0(11) | -17(10) |
| C(72) | 58(16) | 33(14) | 54(14) | 19(11) | 17(12) | -19(12) |
| C(73) | 40(13) | 24(12) | 58(14) | 4(10) | 20(11) | -20(10) |
| C(74) | 20(12) | 25(12) | 44(12) | -9(9) | 1(9) | -1(9) |
| C(75) | 49(16) | 76(19) | 47(15) | 24(14) | 13(13) | 2(14) |
| C(76) | 26(14) | 120(20) | 61(15) | 22(15) | 0(11) | -2(14) |
| C(77) | 27(14) | 120(20) | 90(20) | 17(18) | 2(13) | -32(14) |
| C(78) | 34(14) | 40(15) | 56(15) | -6(12) | 10(12) | -15(12) |
| C(79) | 5(11) | 49(15) | 108(19) | 9(14) | 11(11) | -5(9) |
| C(80) | 20(13) | 65(19) | 110(20) | 19(16) | -14(13) | 2(12) |
| C(81) | 24(11) | 17(11) | 33(12) | 15(9) | 15(9) | 7(8) |
| C(82) | 10(10) | 32(12) | 40(12) | 8(9) | 11(9) | 10(8) |
| C(83) | 4(10) | 38(13) | 48(13) | 12(10) | -4(9) | -12(9) |
| C(84) | 14(11) | 43(14) | 54(14) | 8(11) | 15(10) | -4(9) |
| C(85) | 4(10) | 28(12) | 39(12) | 19(9) | 5(9) | 0(8) |
| C(86) | 7(10) | 25(12) | 53(13) | -2(10) | 11(9) | -7(9) |
| C(87) | 8(10) | 36(13) | 68(15) | 14(11) | 2(10) | 10(9) |
| C(88) | 34(13) | 21(13) | 69(17) | -16(11) | 10(12) | -9(10) |
| C(89) | 13(11) | 50(15) | 58(15) | -4(12) | 18(11) | -8(10) |
| C(90) | 24(11) | 44(14) | 44(14) | 16(11) | 4(10) | -20(10) |
| C(91) | -1(8) | 32(11) | 29(8) | 6(7) | 10(7) | 22(8) |
| C(92) | 16(12) | 70(19) | 90(20) | -12(15) | -5(12) | -4(11) |
| C(93) | 120(20) | 24(15) | 77(18) | -7(12) | -3(16) | -4(14) |
| C(94) | 50(15) | 53(17) | 40(15) | -11(13) | 11(12) | -14(13) |
| C(95) | 56(16) | 90(20) | 49(16) | 3(14) | -6(12) | -19(15) |
| C(96) | 43(16) | 90(20) | 100(20) | 34(18) | -4(15) | 13(15) |
| C(97) | 56(18) | 16(13) | 90(20) | -1(12) | 39(15) | -6(11) |
| C(98) | 4(10) | 71(18) | 36(12) | -14(12) | -3(8) | -7(10) |
| C(99) | 2(11) | 45(15) | 100(20) | 14(13) | -16(12) | -7(10) |
| C(100) | 18(13) | 110(30) | 80(20) | -5(18) | -22(12) | -22(14) |
| C(101) | 22(13) | 30(15) | 73(17) | -11(12) | -21(12) | -4(11) |
| C(102) | 47(15) | 44(16) | 60(15) | 16(13) | -16(13) | 1(12) |
| C(103) | 29(15) | 73(19) | 42(13) | -15(12) | -2(11) | -18(13) |

| | | | | | | |
|--------|---------|---------|---------|----------|---------|---------|
| C(104) | 27(13) | 64(18) | 72(18) | -7(14) | 12(13) | -23(12) |
| C(105) | 27(15) | 160(30) | 43(14) | -20(16) | 20(12) | -19(19) |
| C(106) | 36(16) | 100(20) | 56(16) | 11(17) | 21(13) | 16(16) |
| C(107) | 29(14) | 70(20) | 51(15) | 4(13) | -11(11) | 31(13) |
| C(108) | 100(20) | 34(17) | 41(14) | 29(12) | -24(13) | -32(16) |
| C(109) | 44(17) | 100(20) | 32(13) | 3(13) | -6(11) | -25(16) |
| C(110) | 51(16) | 30(15) | 80(19) | -19(12) | -1(14) | 9(12) |
| C(111) | 47(19) | 70(20) | 130(30) | -90(20) | -7(18) | -13(16) |
| C(112) | 15(12) | 40(15) | 85(17) | 25(13) | -18(12) | -17(10) |
| C(113) | 8(14) | 110(20) | 160(30) | -100(20) | 11(16) | -23(14) |
| C(114) | 2(11) | 110(30) | 80(19) | 0(18) | -13(11) | 14(12) |
| C(115) | 73(19) | 42(17) | 56(15) | 17(13) | -28(13) | -41(16) |
| C(116) | 9(12) | 90(30) | 160(30) | -70(20) | 22(16) | 8(13) |
| C(117) | 32(15) | 56(19) | 100(20) | 30(16) | -53(15) | -18(13) |
| C(118) | 24(13) | 55(17) | 65(17) | -8(13) | 1(12) | 36(12) |
| C(119) | 170(40) | 27(17) | 70(20) | -29(14) | 20(20) | -6(18) |
| C(120) | 41(15) | 90(20) | 48(15) | 18(16) | -4(13) | -30(16) |
| C(121) | 40(20) | 90(20) | 140(30) | -90(20) | 22(18) | -9(17) |
| C(122) | 44(17) | 120(30) | 64(17) | -23(19) | 46(15) | -6(18) |
| C(123) | 46(16) | 38(16) | 68(18) | -5(14) | 6(14) | 14(13) |
| C(124) | 80(20) | 53(18) | 61(16) | 20(14) | 23(15) | 15(17) |
| C(125) | 100(20) | 70(20) | 44(15) | 35(14) | 47(16) | 61(19) |
| C(126) | 14(12) | 57(18) | 120(20) | -40(17) | 32(14) | -19(11) |
| C(127) | 120(30) | 22(17) | 120(30) | -20(15) | -30(20) | 20(17) |
| C(128) | 53(18) | 48(17) | 82(18) | 18(14) | 14(15) | 9(13) |
| C(129) | 43(15) | 28(15) | 90(20) | 12(15) | -3(16) | 20(12) |
| C(130) | 26(16) | 70(20) | 100(20) | -61(16) | 11(13) | 15(13) |
| C(131) | 19(12) | 41(16) | 84(17) | 18(14) | -8(12) | -7(12) |
| C(132) | 54(19) | 47(19) | 140(30) | -16(19) | 42(19) | -26(15) |
| C(133) | 38(15) | 80(20) | 59(16) | 21(14) | -7(12) | -24(15) |
| C(134) | 58(18) | 33(15) | 70(18) | 10(12) | 14(14) | 25(12) |
| C(135) | 8(13) | 150(30) | 110(20) | -90(30) | 17(14) | 1(17) |
| C(136) | 90(20) | 46(16) | 31(13) | 20(11) | 0(13) | -10(15) |
| C(137) | 70(20) | 130(30) | 61(17) | -46(19) | 30(15) | -20(20) |
| C(138) | 32(16) | 120(30) | 120(30) | -20(20) | -38(17) | -49(19) |
| C(139) | 44(15) | 33(16) | 110(20) | 12(14) | 13(14) | -21(12) |
| C(140) | 35(14) | 37(15) | 59(15) | 13(12) | -15(12) | 11(11) |
| C(141) | 56(18) | 150(30) | 44(15) | -25(16) | 30(13) | -80(20) |
| C(142) | 60(20) | 160(30) | 29(14) | -19(17) | 6(13) | -80(20) |
| C(143) | 69(19) | 51(17) | 42(15) | 10(12) | 8(13) | 23(14) |
| C(144) | 56(18) | 130(30) | 51(17) | -35(17) | 9(14) | -57(18) |
| C(145) | 43(17) | 90(20) | 65(17) | -22(16) | 1(13) | -19(16) |
| C(146) | 18(13) | 100(30) | 70(17) | 8(15) | -3(12) | 17(15) |
| C(147) | 15(12) | 57(18) | 100(20) | -49(16) | 9(13) | -6(11) |
| C(148) | 24(14) | 47(18) | 130(30) | -8(18) | -7(16) | 6(12) |
| C(149) | 1(13) | 150(30) | 140(30) | -80(30) | 8(16) | 1(17) |
| C(150) | 43(16) | 44(16) | 100(20) | 1(15) | 20(14) | 8(14) |
| C(151) | 23(15) | 66(18) | 83(18) | -28(15) | 34(13) | -7(13) |
| C(152) | 37(16) | 11(13) | 150(30) | 5(14) | -4(17) | 2(11) |
| C(153) | 4(14) | 160(30) | 150(30) | -120(30) | 7(15) | 2(16) |
| C(154) | 60(20) | 47(17) | 90(20) | -10(14) | 3(16) | -19(13) |
| C(155) | 35(16) | 33(13) | 61(15) | -21(11) | 9(11) | 13(11) |
| C(156) | 22(11) | 24(11) | 36(11) | -11(9) | 7(8) | 8(8) |
| C(157) | 41(18) | 90(30) | 120(30) | 40(20) | -18(18) | -39(18) |
| C(158) | 80(30) | 50(20) | 160(40) | -10(20) | -20(30) | -50(20) |
| C(159) | 42(18) | 160(40) | 56(19) | 30(20) | -22(15) | -30(20) |

| | | | | | | |
|--------|----------|----------|---------|---------|---------|----------|
| C(160) | 40(20) | 210(50) | 160(40) | 140(40) | -30(20) | -20(30) |
| C(161) | 27(17) | 60(30) | 260(60) | 70(30) | -40(30) | -12(17) |
| C(162) | 70(30) | 60(30) | 210(40) | 90(30) | 90(30) | 70(20) |
| C(163) | 90(20) | 130(40) | 80(20) | -20(30) | 30(20) | 60(30) |
| C(164) | 60(20) | 60(20) | 160(40) | 30(20) | -20(30) | 27(17) |
| C(165) | 110(30) | 33(19) | 150(30) | -9(18) | 70(30) | 6(17) |
| C(166) | 17(13) | 22(16) | 180(30) | -19(17) | 13(16) | -2(11) |
| C(167) | 60(20) | 210(50) | 80(30) | 40(30) | 0(20) | -100(30) |
| C(168) | 50(20) | 450(110) | 60(30) | 0(40) | 20(20) | -90(40) |
| C(169) | 0(13) | 170(40) | 130(30) | 110(30) | 25(16) | 35(18) |
| C(170) | -2(9) | 102(18) | 36(9) | 17(10) | -1(6) | 10(9) |
| C(171) | 90(30) | 150(40) | 70(20) | 50(30) | 50(20) | 20(30) |
| C(172) | 30(20) | 190(50) | 100(30) | -40(30) | 32(19) | 30(30) |
| C(173) | 60(30) | 190(50) | 110(30) | 60(30) | 60(20) | 60(30) |
| C(174) | 80(30) | 150(40) | 70(20) | 10(20) | 42(19) | 70(30) |
| C(175) | 190(50) | 90(30) | 70(20) | -30(20) | 30(30) | 60(30) |
| C(176) | 110(30) | 60(20) | 71(19) | -12(15) | 10(17) | 19(19) |
| C(177) | 120(40) | 190(50) | 35(17) | 20(20) | -10(20) | -120(40) |
| C(178) | 140(40) | 37(19) | 90(30) | -4(17) | 30(30) | 18(19) |
| C(179) | 120(30) | 70(20) | 80(20) | 40(20) | 10(20) | -40(20) |
| C(180) | 35(18) | 100(30) | 120(30) | 30(20) | 10(20) | 46(18) |
| C(181) | 40(20) | 170(40) | 150(30) | 90(30) | 0(20) | 70(20) |
| C(182) | 60(20) | 170(40) | 60(20) | 0(20) | -43(17) | 20(20) |
| C(183) | 100(30) | 130(40) | 53(18) | -10(20) | -6(17) | -60(20) |
| C(184) | 130(30) | 60(20) | 90(30) | -40(20) | 10(20) | -40(20) |
| C(185) | 110(30) | 60(20) | 100(30) | -23(19) | 0(20) | -50(20) |
| C(186) | 51(18) | 100(30) | 110(30) | -60(20) | -27(18) | 2(17) |
| C(187) | 80(20) | 100(30) | 80(20) | -50(20) | 26(19) | -20(20) |
| C(188) | 740(170) | 50(30) | 80(30) | 30(20) | 200(70) | 130(60) |
| C(190) | 70(20) | 130(30) | 70(20) | 30(20) | 29(19) | -40(20) |
| C(191) | 60(30) | 220(60) | 130(40) | 80(40) | 50(30) | -40(40) |
| C(192) | 60(30) | 230(60) | 120(30) | 50(40) | 80(30) | 30(40) |
| C(193) | 110(30) | 100(30) | 45(17) | -13(17) | 37(19) | 20(20) |
| C(194) | 100(30) | 100(30) | 200(50) | 70(40) | 100(40) | 70(30) |
| C(195) | 120(30) | 50(20) | 100(30) | -20(18) | 10(30) | -30(20) |
| C(196) | 100(30) | 40(20) | 180(40) | 40(20) | 30(30) | 41(19) |
| C(197) | 49(19) | 140(30) | 110(20) | 100(20) | -21(18) | -20(20) |
| C(198) | 110(30) | 8(15) | 110(30) | 41(16) | -20(30) | -9(16) |
| C(199) | 110(30) | 35(17) | 70(20) | 40(14) | -18(19) | -11(16) |
| C(200) | 60(20) | 41(18) | 140(30) | 34(19) | 0(20) | -10(15) |
| C(201) | 70(20) | 80(20) | 100(30) | 30(20) | -10(20) | -31(19) |
| C(202) | 140(40) | 60(20) | 70(20) | 23(18) | 10(20) | -40(20) |
| C(203) | 70(20) | 110(30) | 39(15) | 32(15) | 7(14) | 40(20) |
| C(204) | 70(20) | 40(19) | 130(30) | 18(19) | 30(20) | -14(16) |
| C(205) | 60(30) | 320(90) | 120(30) | 140(50) | -10(30) | 60(40) |
| C(206) | 8(13) | 110(30) | 130(30) | -40(30) | -11(15) | 24(15) |
| C(207) | 130(40) | 100(30) | 37(16) | 39(16) | 0(18) | -10(30) |
| C(208) | 47(19) | 110(30) | 160(40) | 30(30) | 70(20) | 0(20) |
| C(209) | 50(20) | 250(50) | 37(16) | 0(20) | 5(13) | -40(30) |
| C(210) | 23(19) | 80(30) | 300(70) | 50(40) | 80(30) | 10(20) |
| C(211) | 360(110) | 60(30) | 130(40) | -40(30) | 130(60) | -20(40) |
| C(212) | 60(30) | 90(40) | 320(80) | 100(40) | 100(40) | 10(20) |
| C(213) | 270(80) | 100(40) | 170(50) | -10(30) | 160(60) | 30(40) |
| C(214) | 180(40) | 50(20) | 52(18) | 35(16) | 40(20) | 0(20) |
| C(215) | 90(30) | 70(30) | 230(60) | 40(30) | 90(30) | 50(20) |
| C(216) | 24(15) | 90(30) | 140(30) | 30(20) | -38(18) | -12(15) |

| | | | | | | |
|--------|---------|---------|----------|---------|---------|--------|
| C(44) | 50(30) | 50(30) | 30(20) | 30(20) | -20(19) | 0(20) |
| C(45) | 20(20) | 150(40) | 100(30) | -10(30) | 23(19) | 0(20) |
| C(44A) | 20(20) | 60(40) | 90(40) | -20(30) | -10(20) | 20(20) |
| C(45A) | 10(20) | 60(30) | 50(30) | 30(20) | 20(20) | 20(20) |
| C(189) | 130(50) | 130(50) | 440(140) | -40(60) | 240(70) | 10(40) |

Table A1.11. Hydrogen coordinates ($\times 10^4$) and isotropic displacement parameters ($\text{\AA}^2 \times 10^3$).

| | x | y | z | U(eq) |
|--------|-------|-------|------|-------|
| H(1) | 9011 | 9286 | 3012 | 45 |
| H(3) | 9219 | 8361 | 2169 | 69 |
| H(4) | 8035 | 8539 | 1948 | 74 |
| H(7) | 6847 | 8749 | 1811 | 76 |
| H(8) | 5676 | 8949 | 1727 | 93 |
| H(10) | 5968 | 9915 | 2589 | 32 |
| H(12A) | 11199 | 8780 | 3173 | 124 |
| H(12B) | 10826 | 8299 | 3341 | 124 |
| H(13A) | 11293 | 8832 | 3810 | 164 |
| H(13B) | 10464 | 8888 | 3783 | 164 |
| H(13C) | 10920 | 9333 | 3629 | 164 |
| H(15A) | 3724 | 9891 | 2321 | 84 |
| H(15B) | 3937 | 10345 | 2066 | 84 |
| H(16A) | 4179 | 10425 | 2819 | 140 |
| H(16B) | 3523 | 10690 | 2597 | 140 |
| H(16C) | 4294 | 10884 | 2552 | 140 |
| H(17) | 7490 | 8750 | 3185 | 46 |
| H(19) | 6319 | 8762 | 4001 | 48 |
| H(20) | 6058 | 9639 | 3864 | 35 |
| H(23) | 5750 | 10463 | 3641 | 57 |
| H(24) | 5519 | 11275 | 3392 | 61 |
| H(26) | 6985 | 10994 | 2738 | 31 |
| H(28A) | 6728 | 7107 | 3765 | 142 |
| H(28B) | 7399 | 7241 | 4032 | 142 |
| H(29A) | 6651 | 7340 | 4470 | 138 |
| H(29B) | 6696 | 6761 | 4325 | 138 |
| H(29C) | 6038 | 7116 | 4197 | 138 |
| H(31A) | 6022 | 12372 | 2285 | 175 |
| H(31B) | 6529 | 12657 | 2588 | 175 |
| H(32A) | 6851 | 12294 | 1960 | 493 |
| H(32B) | 7361 | 12055 | 2276 | 493 |
| H(32C) | 7304 | 12670 | 2227 | 493 |
| H(33) | 8280 | 9685 | 3634 | 45 |
| H(35) | 10119 | 10469 | 3748 | 50 |
| H(36) | 9807 | 10846 | 3199 | 44 |
| H(39) | 9296 | 11251 | 2677 | 57 |
| H(40) | 8914 | 11440 | 2082 | 59 |
| H(42) | 7474 | 10289 | 2107 | 31 |
| H(47A) | 6759 | 10833 | 1075 | 155 |
| H(47B) | 7548 | 10765 | 994 | 155 |
| H(48A) | 7443 | 9896 | 1025 | 429 |
| H(48B) | 6860 | 10131 | 741 | 429 |
| H(48C) | 6660 | 9957 | 1117 | 429 |
| H(49) | 2083 | 2408 | 2811 | 40 |

| | | | | |
|--------|-------|------|------|-----|
| H(51) | 387 | 2214 | 3358 | 81 |
| H(52) | 679 | 3019 | 3639 | 58 |
| H(55) | 1098 | 3753 | 3916 | 66 |
| H(56) | 1423 | 4618 | 4076 | 78 |
| H(58) | 2633 | 4672 | 3256 | 49 |
| H(60A) | 1497 | 805 | 2598 | 197 |
| H(60B) | 1006 | 1076 | 2288 | 197 |
| H(63A) | 1934 | 6226 | 4252 | 173 |
| H(63B) | 2122 | 6279 | 3858 | 173 |
| H(64A) | 3322 | 6093 | 4031 | 310 |
| H(64B) | 3164 | 5905 | 4411 | 310 |
| H(64C) | 3116 | 6508 | 4311 | 310 |
| H(65) | 1076 | 3415 | 2646 | 45 |
| H(67) | 785 | 4307 | 1751 | 64 |
| H(68) | 1953 | 4548 | 1839 | 73 |
| H(71) | 3098 | 4794 | 1994 | 56 |
| H(72) | 4234 | 5022 | 2198 | 57 |
| H(74) | 4082 | 4126 | 3073 | 36 |
| H(76A) | -996 | 2963 | 2131 | 82 |
| H(76B) | -1210 | 3405 | 2394 | 82 |
| H(77A) | -491 | 2478 | 2646 | 118 |
| H(77B) | -1321 | 2525 | 2622 | 118 |
| H(77C) | -840 | 2892 | 2883 | 118 |
| H(79A) | 5943 | 5048 | 3378 | 64 |
| H(79B) | 6298 | 4602 | 3164 | 64 |
| H(80A) | 5687 | 4438 | 3803 | 101 |
| H(80B) | 6502 | 4402 | 3767 | 101 |
| H(80C) | 5981 | 3976 | 3583 | 101 |
| H(81) | 3282 | 3678 | 3735 | 28 |
| H(83) | 5210 | 2999 | 3835 | 37 |
| H(84) | 4931 | 2623 | 3275 | 43 |
| H(87) | 4443 | 2169 | 2774 | 45 |
| H(88) | 4055 | 1932 | 2198 | 49 |
| H(90) | 2555 | 3033 | 2187 | 45 |
| H(92A) | 4902 | 4064 | 4756 | 71 |
| H(92B) | 5647 | 3786 | 4801 | 71 |
| H(93A) | 4375 | 3380 | 5002 | 110 |
| H(93B) | 5104 | 3426 | 5242 | 110 |
| H(93C) | 4997 | 2991 | 4944 | 110 |
| H(95A) | 2181 | 2561 | 1120 | 79 |
| H(95B) | 2931 | 2817 | 1091 | 79 |
| H(96A) | 1686 | 3358 | 1200 | 120 |
| H(96B) | 2136 | 3436 | 878 | 120 |
| H(96C) | 2431 | 3635 | 1261 | 120 |

Table A1.12. Atomic coordinates ($\times 10^4$) and equivalent isotropic displacement parameters ($\text{\AA}^2 \times 10^3$) for $[\text{Ru}^{1+}(\text{diispropyl-2,2'-bipyridine-5,5'-dicarboxylate})_3]\text{C}_{60}^{1-}$. $U(\text{eq})$ is defined as one third of the trace of the orthogonalized U^{ij} tensor.

| | x | y | z | U(eq) |
|-------|---------|---------|---------|--------|
| Ru(1) | 4670(1) | -11(1) | 6826(1) | -12(1) |
| C(1) | 3905(5) | -410(5) | 7077(8) | 9(4) |

| | | | | |
|-------|----------|-----------|----------|--------|
| C(2) | 3560(5) | -610(5) | 6964(8) | 7(4) |
| C(3) | 3453(6) | -637(6) | 6465(9) | 19(5) |
| C(4) | 3701(6) | -466(7) | 6093(9) | 20(5) |
| C(5) | 4045(5) | -271(5) | 6233(8) | 11(5) |
| C(6) | 4321(6) | -94(6) | 5878(8) | 12(5) |
| C(7) | 4273(6) | -67(7) | 5347(9) | 19(5) |
| C(8) | 4545(6) | 114(6) | 5041(9) | 20(5) |
| C(9) | 4881(6) | 280(6) | 5241(9) | 16(5) |
| C(10) | 4913(6) | 244(6) | 5764(8) | 13(5) |
| C(11) | 3296(6) | -791(5) | 7350(8) | 12(5) |
| C(12) | 3188(6) | -937(7) | 8227(9) | 21(5) |
| C(13) | 3034(8) | -1318(7) | 8206(11) | 34(7) |
| C(14) | 3392(8) | -775(8) | 8698(10) | 36(7) |
| C(15) | 5177(6) | 493(6) | 4932(9) | 17(5) |
| C(16) | 5777(6) | 901(7) | 4931(10) | 25(6) |
| C(17) | 5769(9) | 1237(8) | 4838(13) | 46(8) |
| C(18) | 6072(7) | 953(8) | 5252(12) | 38(7) |
| C(19) | 4818(5) | 720(6) | 6761(9) | 15(5) |
| C(20) | 4949(6) | 1057(6) | 6935(9) | 19(5) |
| C(21) | 5006(6) | 1112(6) | 7444(9) | 22(5) |
| C(22) | 4917(6) | 836(7) | 7768(9) | 22(6) |
| C(23) | 4778(6) | 506(6) | 7562(9) | 14(5) |
| C(24) | 4671(6) | 199(6) | 7853(8) | 15(5) |
| C(25) | 4587(6) | 168(7) | 8371(8) | 18(5) |
| C(26) | 4467(7) | -146(7) | 8598(9) | 25(6) |
| C(27) | 4429(6) | -421(7) | 8334(9) | 19(5) |
| C(28) | 4516(5) | -373(6) | 7820(8) | 13(5) |
| C(29) | 5010(7) | 1330(6) | 6553(11) | 24(6) |
| C(30) | 5216(9) | 1926(7) | 6450(12) | 42(8) |
| C(31) | 4921(10) | 1970(10) | 6469(16) | 63(11) |
| C(32) | 5544(10) | 2218(9) | 6657(18) | 69(12) |
| C(33) | 4305(6) | -762(7) | 8569(9) | 24(6) |
| C(34) | 4197(9) | -1333(8) | 8420(12) | 41(8) |
| C(35) | 3822(10) | -1550(9) | 8444(15) | 58(10) |
| C(36) | 4360(12) | -1464(10) | 8032(14) | 61(11) |
| C(37) | 5434(6) | 493(6) | 6866(8) | 12(5) |
| C(38) | 5777(6) | 605(6) | 6757(8) | 12(5) |
| C(39) | 5867(6) | 374(6) | 6590(9) | 18(5) |
| C(40) | 5618(6) | 31(6) | 6534(8) | 14(5) |
| C(41) | 5279(5) | -70(6) | 6654(8) | 11(5) |
| C(42) | 4995(5) | -418(6) | 6606(8) | 11(5) |
| C(43) | 5035(6) | -708(6) | 6526(9) | 19(5) |
| C(44) | 4750(6) | -1023(6) | 6486(8) | 15(5) |
| C(45) | 4432(6) | -1059(6) | 6536(9) | 15(5) |
| C(46) | 4402(6) | -771(6) | 6615(8) | 13(5) |
| C(47) | 6040(6) | 978(6) | 6805(9) | 18(5) |
| C(48) | 6114(8) | 1540(7) | 6974(13) | 41(8) |
| C(49) | 6043(9) | 1673(9) | 6470(19) | 72(13) |
| C(50) | 5995(10) | 1637(9) | 7410(16) | 65(11) |
| C(51) | 4117(7) | -1402(7) | 6495(10) | 25(6) |
| C(52) | 3494(7) | -1694(7) | 6423(12) | 32(7) |
| C(53) | 3374(9) | -1830(9) | 6939(15) | 57(10) |
| C(54) | 3277(8) | -1585(10) | 6148(14) | 52(9) |
| N(1) | 4147(4) | -247(4) | 6721(7) | 7(4) |
| N(2) | 4647(4) | 69(4) | 6065(6) | 7(4) |
| N(3) | 4743(4) | 457(4) | 7052(7) | 10(4) |

| | | | | |
|--------|----------|----------|----------|---------|
| N(4) | 4628(4) | -79(5) | 7590(6) | 10(4) |
| N(5) | 5187(4) | 166(5) | 6808(6) | 9(4) |
| N(6) | 4677(4) | -452(4) | 6664(6) | 6(3) |
| O(1) | 2994(4) | -929(4) | 7268(6) | 16(4) |
| O(2) | 3434(4) | -776(4) | 7809(6) | 13(3) |
| O(3) | 5166(4) | 512(5) | 4476(6) | 21(4) |
| O(4) | 5466(4) | 665(4) | 5204(6) | 18(4) |
| O(5) | 4934(6) | 1270(5) | 6128(8) | 43(5) |
| O(6) | 5148(5) | 1629(4) | 6770(7) | 34(5) |
| O(7) | 4226(5) | -824(5) | 9006(7) | 36(5) |
| O(8) | 4301(5) | -987(5) | 8241(7) | 28(4) |
| O(9) | 6341(4) | 1095(5) | 6718(8) | 36(5) |
| O(10) | 5895(4) | 1163(4) | 6938(8) | 30(5) |
| O(11) | 4122(5) | -1664(5) | 6476(9) | 39(5) |
| O(12) | 3831(4) | -1375(4) | 6452(8) | 29(4) |
| C(100) | 3217(8) | 2596(7) | 4340(8) | 29(7) |
| C(101) | 3280(8) | 2597(8) | 6995(9) | 34(7) |
| C(102) | 2376(7) | 2193(7) | 5974(12) | 33(7) |
| C(103) | 3909(7) | 3391(7) | 5208(11) | 31(7) |
| C(104) | 3422(8) | 3442(6) | 5429(11) | 31(7) |
| C(105) | 3620(8) | 3393(7) | 5029(11) | 31(7) |
| C(106) | 3080(9) | 1752(7) | 5890(11) | 35(7) |
| C(107) | 3245(10) | 2888(9) | 6903(9) | 42(9) |
| C(108) | 3091(8) | 2036(8) | 6687(11) | 34(7) |
| C(109) | 3261(8) | 2316(8) | 4433(9) | 31(7) |
| C(110) | 2601(8) | 1813(7) | 6142(12) | 36(7) |
| C(111) | 2889(8) | 1807(7) | 6314(11) | 33(7) |
| C(112) | 4131(7) | 3007(8) | 5362(13) | 39(8) |
| C(113) | 3798(8) | 2928(9) | 4618(11) | 38(8) |
| C(114) | 2504(7) | 2036(8) | 6336(12) | 40(8) |
| C(115) | 3995(7) | 3155(8) | 5003(11) | 36(7) |
| C(116) | 2358(7) | 2094(9) | 5466(15) | 46(9) |
| C(117) | 3418(8) | 3163(7) | 4644(11) | 31(7) |
| C(118) | 3499(8) | 2926(7) | 4444(9) | 34(7) |
| C(119) | 4026(7) | 2668(8) | 5220(12) | 35(7) |
| C(120) | 3063(9) | 3256(8) | 5394(14) | 46(9) |
| C(121) | 2992(8) | 2275(7) | 6893(9) | 29(7) |
| C(122) | 3597(7) | 2617(8) | 6869(9) | 32(7) |
| C(123) | 3060(20) | 3169(13) | 6311(15) | 90(20) |
| C(124) | 3584(10) | 3477(7) | 5899(14) | 49(9) |
| C(125) | 2903(10) | 2570(10) | 4457(9) | 44(9) |
| C(126) | 2683(12) | 2013(13) | 4777(15) | 75(15) |
| C(127) | 4153(7) | 3103(9) | 5863(15) | 47(9) |
| C(128) | 2974(14) | 2012(9) | 4647(12) | 59(13) |
| C(129) | 2704(8) | 2260(8) | 6726(10) | 34(7) |
| C(130) | 3560(14) | 2350(17) | 4621(14) | 86(17) |
| C(131) | 2487(8) | 2527(9) | 6110(13) | 43(8) |
| C(132) | 2586(9) | 2784(11) | 5774(19) | 63(12) |
| C(133) | 2918(10) | 1719(7) | 5444(14) | 50(10) |
| C(134) | 3540(17) | 3186(9) | 6668(13) | 69(17) |
| C(135) | 3446(9) | 1948(8) | 5959(13) | 39(8) |
| C(136) | 3821(11) | 2598(14) | 4757(15) | 73(14) |
| C(137) | 3870(9) | 2899(14) | 6633(11) | 68(15) |
| C(138) | 2453(9) | 2355(17) | 5098(13) | 76(17) |
| C(139) | 3473(15) | 2049(11) | 5037(15) | 65(14) |
| C(140) | 3508(19) | 2276(19) | 6668(15) | 120(30) |

| | | | | |
|--------|-----------|----------|-----------|-----------|
| C(141) | 2870(10) | 3110(9) | 5840(20) | 69(14) |
| C(142) | 3010(20) | 2930(20) | 4660(16) | 150(40) |
| C(143) | 4030(10) | 3310(10) | 6055(19) | 73(13) |
| C(144) | 3104(15) | 1859(9) | 5007(13) | 67(14) |
| C(145) | 2968(12) | 2891(16) | 6711(13) | 76(15) |
| C(146) | 3921(11) | 3448(8) | 5748(18) | 77(15) |
| C(147) | 3953(9) | 2530(13) | 6125(16) | 59(13) |
| C(148) | 2654(11) | 2294(18) | 4681(14) | 81(17) |
| C(149) | 2569(9) | 2696(14) | 5220(20) | 78(17) |
| C(150) | 3637(10) | 2095(9) | 5480(20) | 74(15) |
| C(151) | 3827(15) | 3178(13) | 6549(15) | 86(18) |
| C(152) | 2703(11) | 2610(13) | 6599(17) | 81(15) |
| C(153) | 3930(8) | 2421(9) | 5590(20) | 69(15) |
| C(154) | 4054(8) | 2852(14) | 6238(15) | 68(13) |
| C(155) | 3580(20) | 2167(13) | 6370(30) | 130(30) |
| C(156) | 3426(16) | 3349(10) | 6333(15) | 68(13) |
| C(157) | 2928(16) | 3035(11) | 4980(20) | 100(20) |
| C(158) | 2480(10) | 1851(15) | 5370(40) | 150(40) |
| C(159) | 2631(14) | 1751(10) | 5460(40) | 140(40) |
| C(200) | 1498(14) | -2(15) | 4970(20) | 110(20) |
| C(201) | 1754(9) | 271(8) | 5307(13) | 44(8) |
| C(202) | 1958(15) | 236(13) | 5571(17) | 68(13) |
| C(203) | 2174(14) | 470(20) | 5830(19) | 90(20) |
| C(204) | 2198(11) | 797(14) | 5862(13) | 100(20) |
| C(205) | 1943(11) | 834(9) | 5550(14) | 58(10) |
| C(206) | 1736(7) | 568(9) | 5293(12) | 41(8) |
| C(207) | 1206(12) | -7(12) | 8250(18) | 73(12) |
| C(208) | 1301(10) | 123(9) | 7728(13) | 49(9) |
| C(209) | 1616(11) | 197(10) | 7547(18) | 66(11) |
| C(210) | 1692(10) | 307(11) | 7076(17) | 62(11) |
| C(211) | 1471(11) | 345(9) | 6767(14) | 59(10) |
| C(212) | 1142(11) | 277(9) | 6945(16) | 59(11) |
| C(213) | 1065(10) | 166(10) | 7437(15) | 54(9) |
| C(300) | 338(7) | 203(13) | 6198(10) | 100(18) |
| C(301) | 100(20) | 366(13) | 6190(20) | 170(40) |
| C(302) | -13(13) | 691(11) | 5606(18) | 64(12) |
| C(303) | 217(15) | 647(12) | 5890(20) | 94(17) |
| C(304) | 566(16) | 734(16) | 5660(40) | 130(30) |
| C(305) | 589(18) | 864(13) | 5190(30) | 110(20) |
| C(306) | 797(13) | 736(14) | 4930(60) | 190(60) |
| C(307) | 895(11) | 539(14) | 5020(30) | 110(30) |
| C(308) | 821(11) | 360(13) | 5570(30) | 100(20) |
| C(309) | 660(20) | 460(20) | 5860(40) | 240(70) |
| N(7) | 1307(12) | -259(14) | 4710(20) | 113(16) |
| N(8) | 1129(13) | -110(13) | 8633(18) | 123(18) |
| C(400) | 2989(6) | 7386(7) | 8650(5) | 289(15) |
| C(401) | 3181(4) | 7182(3) | 8625(10) | 296(11) |
| C(402) | 3734(15) | 7491(7) | 8095(7) | 670(50) |
| C(403) | 4019(8) | 7700(8) | 7218(9) | 370(20) |
| C(404) | 3293(6) | 7412(4) | 7584(4) | 301(8) |
| C(405) | 3720(130) | 7540(70) | 6400(200) | 1100(600) |
| Ru(1A) | 5325(8) | 28(8) | 3194(11) | 600(20) |

Table A1.13. Bond lengths [\AA] and angles [$^\circ$].

| | |
|----------------|-----------|
| Ru(1)-Ru(1A)#1 | 0.11(3) |
| Ru(1)-N(4) | 2.054(17) |
| Ru(1)-N(6) | 2.048(16) |
| Ru(1)-N(3) | 2.055(17) |
| Ru(1)-N(2) | 2.068(16) |
| Ru(1)-N(1) | 2.063(17) |
| Ru(1)-N(5) | 2.052(16) |
| Ru(1)-Ru(1A) | 10.08(3) |
| C(1)-N(1) | 1.35(3) |
| C(1)-C(2) | 1.39(3) |
| C(2)-C(3) | 1.40(3) |
| C(2)-C(11) | 1.47(3) |
| C(3)-C(4) | 1.40(3) |
| C(4)-C(5) | 1.40(3) |
| C(5)-N(1) | 1.36(3) |
| C(5)-C(6) | 1.44(3) |
| C(6)-N(2) | 1.37(3) |
| C(6)-C(7) | 1.44(3) |
| C(7)-C(8) | 1.35(4) |
| C(8)-C(9) | 1.41(3) |
| C(9)-C(10) | 1.42(3) |
| C(9)-C(15) | 1.45(3) |
| C(10)-N(2) | 1.32(3) |
| C(11)-O(1) | 1.20(3) |
| C(11)-O(2) | 1.36(3) |
| C(12)-O(2) | 1.48(3) |
| C(12)-C(13) | 1.50(4) |
| C(12)-C(14) | 1.51(4) |
| C(15)-O(3) | 1.22(3) |
| C(15)-O(4) | 1.35(3) |
| C(16)-O(4) | 1.46(3) |
| C(16)-C(18) | 1.50(4) |
| C(16)-C(17) | 1.55(4) |
| C(19)-N(3) | 1.31(3) |
| C(19)-C(20) | 1.40(3) |
| C(20)-C(21) | 1.38(4) |
| C(20)-C(29) | 1.51(4) |
| C(21)-C(22) | 1.40(4) |
| C(22)-C(23) | 1.40(3) |
| C(23)-N(3) | 1.37(3) |
| C(23)-C(24) | 1.44(3) |
| C(24)-N(4) | 1.36(3) |
| C(24)-C(25) | 1.42(3) |
| C(25)-C(26) | 1.38(4) |
| C(26)-C(27) | 1.36(4) |
| C(27)-C(28) | 1.41(3) |
| C(27)-C(33) | 1.48(4) |
| C(28)-N(4) | 1.31(3) |
| C(29)-O(5) | 1.18(3) |
| C(29)-O(6) | 1.30(3) |
| C(30)-C(31) | 1.44(5) |
| C(30)-O(6) | 1.48(3) |
| C(30)-C(32) | 1.51(5) |
| C(33)-O(7) | 1.21(3) |

| | |
|---------------|---------|
| C(33)-O(8) | 1.33(3) |
| C(34)-O(8) | 1.46(4) |
| C(34)-C(35) | 1.47(5) |
| C(34)-C(36) | 1.54(5) |
| C(37)-N(5) | 1.34(3) |
| C(37)-C(38) | 1.40(3) |
| C(38)-C(39) | 1.37(3) |
| C(38)-C(47) | 1.50(3) |
| C(39)-C(40) | 1.39(3) |
| C(40)-C(41) | 1.39(3) |
| C(41)-N(5) | 1.38(3) |
| C(41)-C(42) | 1.45(3) |
| C(42)-N(6) | 1.37(3) |
| C(42)-C(43) | 1.42(3) |
| C(43)-C(44) | 1.36(3) |
| C(44)-C(45) | 1.37(3) |
| C(45)-C(46) | 1.39(3) |
| C(45)-C(51) | 1.49(3) |
| C(46)-N(6) | 1.36(3) |
| C(47)-O(9) | 1.21(3) |
| C(47)-O(10) | 1.34(3) |
| C(48)-O(10) | 1.48(3) |
| C(48)-C(50) | 1.44(5) |
| C(48)-C(49) | 1.57(6) |
| C(51)-O(11) | 1.20(3) |
| C(51)-O(12) | 1.36(3) |
| C(52)-O(12) | 1.48(3) |
| C(52)-C(54) | 1.49(4) |
| C(52)-C(53) | 1.49(4) |
| N(1)-Ru(1A)#1 | 2.08(3) |
| N(2)-Ru(1A)#1 | 2.04(3) |
| N(3)-Ru(1A)#1 | 2.15(3) |
| N(4)-Ru(1A)#1 | 2.10(3) |
| N(5)-Ru(1A)#1 | 2.02(3) |
| N(6)-Ru(1A)#1 | 1.95(3) |
| C(100)-C(125) | 1.39(4) |
| C(100)-C(109) | 1.40(4) |
| C(100)-C(118) | 1.42(4) |
| C(101)-C(107) | 1.42(4) |
| C(101)-C(122) | 1.42(4) |
| C(101)-C(121) | 1.41(4) |
| C(102)-C(131) | 1.38(4) |
| C(102)-C(116) | 1.41(5) |
| C(102)-C(114) | 1.47(4) |
| C(103)-C(115) | 1.41(4) |
| C(103)-C(105) | 1.39(4) |
| C(103)-C(146) | 1.46(5) |
| C(104)-C(124) | 1.42(4) |
| C(104)-C(120) | 1.40(5) |
| C(104)-C(105) | 1.47(4) |
| C(105)-C(117) | 1.42(4) |
| C(106)-C(133) | 1.36(5) |
| C(106)-C(135) | 1.44(5) |
| C(106)-C(111) | 1.51(4) |
| C(107)-C(145) | 1.35(5) |
| C(107)-C(134) | 1.48(7) |

| | |
|---------------|----------|
| C(108)-C(111) | 1.39(4) |
| C(108)-C(121) | 1.46(4) |
| C(108)-C(140) | 1.63(8) |
| C(109)-C(130) | 1.37(5) |
| C(109)-C(128) | 1.45(5) |
| C(110)-C(114) | 1.38(5) |
| C(110)-C(111) | 1.39(5) |
| C(110)-C(159) | 1.86(10) |
| C(112)-C(127) | 1.39(5) |
| C(112)-C(119) | 1.41(5) |
| C(112)-C(115) | 1.46(4) |
| C(113)-C(118) | 1.42(4) |
| C(113)-C(115) | 1.41(5) |
| C(113)-C(136) | 1.58(6) |
| C(114)-C(129) | 1.41(4) |
| C(116)-C(158) | 1.47(7) |
| C(116)-C(138) | 1.42(6) |
| C(117)-C(118) | 1.39(4) |
| C(117)-C(142) | 1.61(10) |
| C(119)-C(153) | 1.39(5) |
| C(119)-C(136) | 1.48(5) |
| C(120)-C(157) | 1.41(6) |
| C(120)-C(141) | 1.42(5) |
| C(121)-C(129) | 1.34(4) |
| C(122)-C(137) | 1.40(5) |
| C(122)-C(140) | 1.48(7) |
| C(123)-C(156) | 1.41(7) |
| C(123)-C(141) | 1.47(7) |
| C(123)-C(145) | 1.53(6) |
| C(124)-C(156) | 1.33(6) |
| C(124)-C(146) | 1.64(7) |
| C(125)-C(148) | 1.33(7) |
| C(125)-C(142) | 1.56(7) |
| C(126)-C(148) | 1.36(7) |
| C(126)-C(128) | 1.36(7) |
| C(126)-C(158) | 1.79(10) |
| C(127)-C(154) | 1.40(6) |
| C(127)-C(143) | 1.40(6) |
| C(128)-C(144) | 1.46(6) |
| C(129)-C(152) | 1.62(6) |
| C(130)-C(136) | 1.20(6) |
| C(130)-C(139) | 1.64(7) |
| C(131)-C(132) | 1.35(5) |
| C(131)-C(152) | 1.55(6) |
| C(132)-C(149) | 1.52(7) |
| C(132)-C(141) | 1.40(6) |
| C(133)-C(144) | 1.39(5) |
| C(133)-C(159) | 1.37(7) |
| C(134)-C(151) | 1.35(7) |
| C(134)-C(156) | 1.41(5) |
| C(135)-C(155) | 1.39(6) |
| C(135)-C(150) | 1.49(6) |
| C(137)-C(151) | 1.38(8) |
| C(137)-C(154) | 1.42(6) |
| C(138)-C(149) | 1.39(7) |
| C(138)-C(148) | 1.54(6) |

| | |
|---------------------|----------|
| C(139)-C(150) | 1.36(6) |
| C(139)-C(144) | 1.44(7) |
| C(140)-C(155) | 1.07(8) |
| C(142)-C(157) | 1.10(7) |
| C(143)-C(146) | 1.26(6) |
| C(143)-C(151) | 1.54(6) |
| C(145)-C(152) | 1.27(6) |
| C(147)-C(154) | 1.32(6) |
| C(147)-C(153) | 1.48(7) |
| C(147)-C(155) | 1.78(9) |
| C(149)-C(157) | 1.71(8) |
| C(150)-C(153) | 1.43(6) |
| C(158)-C(159) | 1.01(8) |
| C(200)-N(7) | 1.25(6) |
| C(200)-C(201) | 1.49(6) |
| C(201)-C(202) | 1.23(6) |
| C(201)-C(206) | 1.38(5) |
| C(202)-C(203) | 1.23(8) |
| C(203)-C(204) | 1.42(8) |
| C(204)-C(205) | 1.49(7) |
| C(205)-C(206) | 1.29(5) |
| C(207)-N(8) | 1.10(6) |
| C(207)-C(208) | 1.49(6) |
| C(208)-C(213) | 1.41(5) |
| C(208)-C(209) | 1.37(5) |
| C(209)-C(210) | 1.33(6) |
| C(210)-C(211) | 1.36(6) |
| C(211)-C(212) | 1.44(6) |
| C(212)-C(213) | 1.38(5) |
| C(300)-C(301)#2 | 1.23(9) |
| C(300)-C(309) | 1.61(14) |
| C(300)-C(301) | 1.58(10) |
| C(301)-C(300)#3 | 1.23(9) |
| C(301)-C(303) | 1.36(8) |
| C(302)-C(308)#3 | 1.38(7) |
| C(302)-C(303) | 1.38(7) |
| C(302)-C(306)#4 | 1.48(14) |
| C(303)-C(304) | 1.55(10) |
| C(304)-C(305) | 1.37(10) |
| C(304)-C(309) | 1.59(10) |
| C(305)-C(307)#4 | 1.26(10) |
| C(305)-C(306) | 1.49(9) |
| C(306)-C(307) | 1.20(9) |
| C(306)-C(302)#5 | 1.48(14) |
| C(307)-C(305)#5 | 1.26(10) |
| C(307)-C(308) | 1.62(10) |
| C(308)-C(309) | 1.27(11) |
| C(308)-C(302)#2 | 1.38(7) |
| C(402)-C(404) | 2.28(5) |
| Ru(1A)-N(4)#1 | 2.10(3) |
| Ru(1A)-N(6)#1 | 1.95(3) |
| Ru(1A)-N(3)#1 | 2.15(3) |
| Ru(1A)-N(2)#1 | 2.04(3) |
| Ru(1A)-N(1)#1 | 2.08(3) |
| Ru(1A)-N(5)#1 | 2.02(3) |
| Ru(1A)#1-Ru(1)-N(4) | 114(10) |

| | |
|-----------------------|-----------|
| Ru(1A)#1-Ru(1)-N(6) | 20(10) |
| N(4)-Ru(1)-N(6) | 96.1(7) |
| Ru(1A)#1-Ru(1)-N(3) | 157(10) |
| N(4)-Ru(1)-N(3) | 79.6(8) |
| N(6)-Ru(1)-N(3) | 169.8(7) |
| Ru(1A)#1-Ru(1)-N(2) | 73(10) |
| N(4)-Ru(1)-N(2) | 171.1(7) |
| N(6)-Ru(1)-N(2) | 89.5(7) |
| N(3)-Ru(1)-N(2) | 96.0(7) |
| Ru(1A)#1-Ru(1)-N(1) | 100(10) |
| N(4)-Ru(1)-N(1) | 93.5(7) |
| N(6)-Ru(1)-N(1) | 92.3(7) |
| N(3)-Ru(1)-N(1) | 97.1(7) |
| N(2)-Ru(1)-N(1) | 79.3(7) |
| Ru(1A)#1-Ru(1)-N(5) | 69(10) |
| N(4)-Ru(1)-N(5) | 94.7(7) |
| N(6)-Ru(1)-N(5) | 78.8(7) |
| N(3)-Ru(1)-N(5) | 92.2(7) |
| N(2)-Ru(1)-N(5) | 93.2(7) |
| N(1)-Ru(1)-N(5) | 168.6(7) |
| Ru(1A)#1-Ru(1)-Ru(1A) | 51(10) |
| N(4)-Ru(1)-Ru(1A) | 163.2(5) |
| N(6)-Ru(1)-Ru(1A) | 70.7(5) |
| N(3)-Ru(1)-Ru(1A) | 111.6(6) |
| N(2)-Ru(1)-Ru(1A) | 25.6(5) |
| N(1)-Ru(1)-Ru(1A) | 97.4(5) |
| N(5)-Ru(1)-Ru(1A) | 72.9(5) |
| N(1)-C(1)-C(2) | 122.6(19) |
| C(1)-C(2)-C(3) | 119(2) |
| C(1)-C(2)-C(11) | 122.8(19) |
| C(3)-C(2)-C(11) | 117.9(19) |
| C(4)-C(3)-C(2) | 118(2) |
| C(3)-C(4)-C(5) | 119(2) |
| N(1)-C(5)-C(4) | 122(2) |
| N(1)-C(5)-C(6) | 114.7(18) |
| C(4)-C(5)-C(6) | 123(2) |
| N(2)-C(6)-C(7) | 118(2) |
| N(2)-C(6)-C(5) | 117.1(18) |
| C(7)-C(6)-C(5) | 124(2) |
| C(8)-C(7)-C(6) | 121(2) |
| C(7)-C(8)-C(9) | 120(2) |
| C(10)-C(9)-C(8) | 117(2) |
| C(10)-C(9)-C(15) | 121(2) |
| C(8)-C(9)-C(15) | 122(2) |
| N(2)-C(10)-C(9) | 123(2) |
| O(1)-C(11)-O(2) | 124(2) |
| O(1)-C(11)-C(2) | 124(2) |
| O(2)-C(11)-C(2) | 112.3(18) |
| O(2)-C(12)-C(13) | 110(2) |
| O(2)-C(12)-C(14) | 105.2(19) |
| C(13)-C(12)-C(14) | 114(2) |
| O(3)-C(15)-O(4) | 124(2) |
| O(3)-C(15)-C(9) | 124(2) |
| O(4)-C(15)-C(9) | 112(2) |
| O(4)-C(16)-C(18) | 106(2) |
| O(4)-C(16)-C(17) | 108(2) |

| | |
|-------------------|-----------|
| C(18)-C(16)-C(17) | 113(3) |
| N(3)-C(19)-C(20) | 124(2) |
| C(21)-C(20)-C(19) | 117(2) |
| C(21)-C(20)-C(29) | 125(2) |
| C(19)-C(20)-C(29) | 118(2) |
| C(22)-C(21)-C(20) | 120(2) |
| C(23)-C(22)-C(21) | 119(2) |
| N(3)-C(23)-C(22) | 121(2) |
| N(3)-C(23)-C(24) | 114.7(18) |
| C(22)-C(23)-C(24) | 124(2) |
| N(4)-C(24)-C(25) | 120(2) |
| N(4)-C(24)-C(23) | 115.8(18) |
| C(25)-C(24)-C(23) | 124(2) |
| C(26)-C(25)-C(24) | 118(2) |
| C(25)-C(26)-C(27) | 121(2) |
| C(26)-C(27)-C(28) | 118(2) |
| C(26)-C(27)-C(33) | 122(2) |
| C(28)-C(27)-C(33) | 120(2) |
| N(4)-C(28)-C(27) | 123(2) |
| O(5)-C(29)-O(6) | 127(2) |
| O(5)-C(29)-C(20) | 123(2) |
| O(6)-C(29)-C(20) | 110(2) |
| C(31)-C(30)-O(6) | 108(3) |
| C(31)-C(30)-C(32) | 116(3) |
| O(6)-C(30)-C(32) | 104(3) |
| O(7)-C(33)-O(8) | 124(3) |
| O(7)-C(33)-C(27) | 124(3) |
| O(8)-C(33)-C(27) | 112(2) |
| O(8)-C(34)-C(35) | 112(3) |
| O(8)-C(34)-C(36) | 103(3) |
| C(35)-C(34)-C(36) | 113(3) |
| N(5)-C(37)-C(38) | 122(2) |
| C(39)-C(38)-C(37) | 119(2) |
| C(39)-C(38)-C(47) | 121(2) |
| C(37)-C(38)-C(47) | 120(2) |
| C(38)-C(39)-C(40) | 120(2) |
| C(39)-C(40)-C(41) | 119(2) |
| N(5)-C(41)-C(40) | 121(2) |
| N(5)-C(41)-C(42) | 114.6(17) |
| C(40)-C(41)-C(42) | 124(2) |
| N(6)-C(42)-C(43) | 121(2) |
| N(6)-C(42)-C(41) | 114.5(18) |
| C(43)-C(42)-C(41) | 124.0(19) |
| C(44)-C(43)-C(42) | 119(2) |
| C(43)-C(44)-C(45) | 120(2) |
| C(44)-C(45)-C(46) | 120(2) |
| C(44)-C(45)-C(51) | 121(2) |
| C(46)-C(45)-C(51) | 120(2) |
| N(6)-C(46)-C(45) | 123(2) |
| O(9)-C(47)-O(10) | 125(2) |
| O(9)-C(47)-C(38) | 124(2) |
| O(10)-C(47)-C(38) | 111.2(18) |
| O(10)-C(48)-C(50) | 105(3) |
| O(10)-C(48)-C(49) | 104(3) |
| C(50)-C(48)-C(49) | 113(3) |
| O(11)-C(51)-O(12) | 125(2) |

| | |
|----------------------|-----------|
| O(11)-C(51)-C(45) | 123(2) |
| O(12)-C(51)-C(45) | 112(2) |
| O(12)-C(52)-C(54) | 103(2) |
| O(12)-C(52)-C(53) | 110(2) |
| C(54)-C(52)-C(53) | 115(3) |
| C(1)-N(1)-C(5) | 118.6(18) |
| C(1)-N(1)-Ru(1) | 126.0(14) |
| C(5)-N(1)-Ru(1) | 114.9(14) |
| C(1)-N(1)-Ru(1A)#1 | 126.8(16) |
| C(5)-N(1)-Ru(1A)#1 | 113.6(16) |
| Ru(1)-N(1)-Ru(1A)#1 | 2.9(9) |
| C(10)-N(2)-C(6) | 120.6(18) |
| C(10)-N(2)-Ru(1) | 126.0(15) |
| C(6)-N(2)-Ru(1) | 113.3(14) |
| C(10)-N(2)-Ru(1A)#1 | 125.4(17) |
| C(6)-N(2)-Ru(1A)#1 | 113.7(16) |
| Ru(1)-N(2)-Ru(1A)#1 | 2.8(9) |
| C(19)-N(3)-C(23) | 118.7(19) |
| C(19)-N(3)-Ru(1) | 126.3(15) |
| C(23)-N(3)-Ru(1) | 113.8(15) |
| C(19)-N(3)-Ru(1A)#1 | 125.5(17) |
| C(23)-N(3)-Ru(1A)#1 | 114.3(17) |
| Ru(1)-N(3)-Ru(1A)#1 | 1.1(9) |
| C(28)-N(4)-C(24) | 119.8(19) |
| C(28)-N(4)-Ru(1A)#1 | 122.8(17) |
| C(24)-N(4)-Ru(1A)#1 | 116.7(17) |
| C(28)-N(4)-Ru(1) | 125.1(15) |
| C(24)-N(4)-Ru(1) | 114.2(15) |
| Ru(1A)#1-N(4)-Ru(1) | 2.6(9) |
| C(37)-N(5)-C(41) | 118.3(17) |
| C(37)-N(5)-Ru(1A)#1 | 128.3(17) |
| C(41)-N(5)-Ru(1A)#1 | 112.5(16) |
| C(37)-N(5)-Ru(1) | 125.7(15) |
| C(41)-N(5)-Ru(1) | 115.3(14) |
| Ru(1A)#1-N(5)-Ru(1) | 2.8(9) |
| C(46)-N(6)-C(42) | 117.2(17) |
| C(46)-N(6)-Ru(1A)#1 | 127.3(17) |
| C(42)-N(6)-Ru(1A)#1 | 115.5(17) |
| C(46)-N(6)-Ru(1) | 126.7(14) |
| C(42)-N(6)-Ru(1) | 116.1(14) |
| Ru(1A)#1-N(6)-Ru(1) | 1.1(10) |
| C(11)-O(2)-C(12) | 116.1(17) |
| C(15)-O(4)-C(16) | 116.7(18) |
| C(29)-O(6)-C(30) | 117(2) |
| C(33)-O(8)-C(34) | 118(2) |
| C(47)-O(10)-C(48) | 119(2) |
| C(51)-O(12)-C(52) | 118(2) |
| C(125)-C(100)-C(109) | 119(3) |
| C(125)-C(100)-C(118) | 113(3) |
| C(109)-C(100)-C(118) | 117(3) |
| C(107)-C(101)-C(122) | 118(3) |
| C(107)-C(101)-C(121) | 116(3) |
| C(122)-C(101)-C(121) | 114(3) |
| C(131)-C(102)-C(116) | 122(3) |
| C(131)-C(102)-C(114) | 110(3) |
| C(116)-C(102)-C(114) | 117(3) |

| | |
|----------------------|--------|
| C(115)-C(103)-C(105) | 119(3) |
| C(115)-C(103)-C(146) | 121(3) |
| C(105)-C(103)-C(146) | 107(3) |
| C(124)-C(104)-C(120) | 120(3) |
| C(124)-C(104)-C(105) | 110(3) |
| C(120)-C(104)-C(105) | 118(3) |
| C(117)-C(105)-C(103) | 120(3) |
| C(117)-C(105)-C(104) | 115(3) |
| C(103)-C(105)-C(104) | 113(3) |
| C(133)-C(106)-C(135) | 124(3) |
| C(133)-C(106)-C(111) | 110(3) |
| C(135)-C(106)-C(111) | 112(3) |
| C(101)-C(107)-C(145) | 127(4) |
| C(101)-C(107)-C(134) | 117(3) |
| C(145)-C(107)-C(134) | 104(4) |
| C(111)-C(108)-C(121) | 119(3) |
| C(111)-C(108)-C(140) | 125(3) |
| C(121)-C(108)-C(140) | 102(3) |
| C(100)-C(109)-C(130) | 123(4) |
| C(100)-C(109)-C(128) | 117(3) |
| C(130)-C(109)-C(128) | 109(4) |
| C(114)-C(110)-C(111) | 122(3) |
| C(114)-C(110)-C(159) | 123(3) |
| C(111)-C(110)-C(159) | 100(3) |
| C(110)-C(111)-C(108) | 119(3) |
| C(110)-C(111)-C(106) | 112(3) |
| C(108)-C(111)-C(106) | 116(3) |
| C(127)-C(112)-C(119) | 122(3) |
| C(127)-C(112)-C(115) | 118(3) |
| C(119)-C(112)-C(115) | 109(3) |
| C(118)-C(113)-C(115) | 119(3) |
| C(118)-C(113)-C(136) | 125(3) |
| C(115)-C(113)-C(136) | 102(3) |
| C(110)-C(114)-C(129) | 118(3) |
| C(110)-C(114)-C(102) | 117(3) |
| C(129)-C(114)-C(102) | 114(3) |
| C(103)-C(115)-C(113) | 121(3) |
| C(103)-C(115)-C(112) | 115(3) |
| C(113)-C(115)-C(112) | 113(3) |
| C(102)-C(116)-C(158) | 115(5) |
| C(102)-C(116)-C(138) | 117(3) |
| C(158)-C(116)-C(138) | 115(5) |
| C(105)-C(117)-C(118) | 121(3) |
| C(105)-C(117)-C(142) | 124(3) |
| C(118)-C(117)-C(142) | 100(3) |
| C(113)-C(118)-C(117) | 119(3) |
| C(113)-C(118)-C(100) | 115(3) |
| C(117)-C(118)-C(100) | 116(3) |
| C(153)-C(119)-C(112) | 118(3) |
| C(153)-C(119)-C(136) | 121(4) |
| C(112)-C(119)-C(136) | 107(3) |
| C(157)-C(120)-C(104) | 116(4) |
| C(157)-C(120)-C(141) | 113(4) |
| C(104)-C(120)-C(141) | 118(3) |
| C(129)-C(121)-C(108) | 119(3) |
| C(129)-C(121)-C(101) | 119(3) |

| | |
|----------------------|--------|
| C(108)-C(121)-C(101) | 111(3) |
| C(137)-C(122)-C(101) | 124(3) |
| C(137)-C(122)-C(140) | 116(4) |
| C(101)-C(122)-C(140) | 106(4) |
| C(156)-C(123)-C(141) | 123(4) |
| C(156)-C(123)-C(145) | 102(4) |
| C(141)-C(123)-C(145) | 123(5) |
| C(156)-C(124)-C(104) | 126(4) |
| C(156)-C(124)-C(146) | 120(4) |
| C(104)-C(124)-C(146) | 103(3) |
| C(148)-C(125)-C(100) | 122(4) |
| C(148)-C(125)-C(142) | 120(4) |
| C(100)-C(125)-C(142) | 103(4) |
| C(148)-C(126)-C(128) | 120(4) |
| C(148)-C(126)-C(158) | 106(5) |
| C(128)-C(126)-C(158) | 121(5) |
| C(112)-C(127)-C(154) | 119(3) |
| C(112)-C(127)-C(143) | 125(4) |
| C(154)-C(127)-C(143) | 102(4) |
| C(126)-C(128)-C(109) | 120(3) |
| C(126)-C(128)-C(144) | 117(4) |
| C(109)-C(128)-C(144) | 109(4) |
| C(121)-C(129)-C(114) | 122(3) |
| C(121)-C(129)-C(152) | 120(3) |
| C(114)-C(129)-C(152) | 103(3) |
| C(136)-C(130)-C(109) | 131(6) |
| C(136)-C(130)-C(139) | 107(4) |
| C(109)-C(130)-C(139) | 110(5) |
| C(132)-C(131)-C(102) | 123(4) |
| C(132)-C(131)-C(152) | 117(4) |
| C(102)-C(131)-C(152) | 109(3) |
| C(131)-C(132)-C(149) | 118(4) |
| C(131)-C(132)-C(141) | 124(4) |
| C(149)-C(132)-C(141) | 107(4) |
| C(144)-C(133)-C(106) | 121(4) |
| C(144)-C(133)-C(159) | 111(5) |
| C(106)-C(133)-C(159) | 117(5) |
| C(107)-C(134)-C(151) | 121(3) |
| C(107)-C(134)-C(156) | 110(5) |
| C(151)-C(134)-C(156) | 118(5) |
| C(155)-C(135)-C(106) | 119(5) |
| C(155)-C(135)-C(150) | 114(5) |
| C(106)-C(135)-C(150) | 113(3) |
| C(130)-C(136)-C(119) | 132(5) |
| C(130)-C(136)-C(113) | 108(4) |
| C(119)-C(136)-C(113) | 109(3) |
| C(151)-C(137)-C(122) | 116(4) |
| C(151)-C(137)-C(154) | 112(4) |
| C(122)-C(137)-C(154) | 121(5) |
| C(149)-C(138)-C(116) | 123(3) |
| C(149)-C(138)-C(148) | 116(5) |
| C(116)-C(138)-C(148) | 108(5) |
| C(150)-C(139)-C(144) | 121(4) |
| C(150)-C(139)-C(130) | 125(4) |
| C(144)-C(139)-C(130) | 100(4) |
| C(155)-C(140)-C(122) | 140(8) |

| | |
|----------------------|--------|
| C(155)-C(140)-C(108) | 103(7) |
| C(122)-C(140)-C(108) | 107(3) |
| C(123)-C(141)-C(132) | 117(4) |
| C(123)-C(141)-C(120) | 117(4) |
| C(132)-C(141)-C(120) | 114(5) |
| C(157)-C(142)-C(125) | 135(8) |
| C(157)-C(142)-C(117) | 105(7) |
| C(125)-C(142)-C(117) | 108(4) |
| C(146)-C(143)-C(127) | 118(5) |
| C(146)-C(143)-C(151) | 116(5) |
| C(127)-C(143)-C(151) | 114(5) |
| C(133)-C(144)-C(139) | 119(4) |
| C(133)-C(144)-C(128) | 118(5) |
| C(139)-C(144)-C(128) | 112(4) |
| C(152)-C(145)-C(107) | 119(5) |
| C(152)-C(145)-C(123) | 113(5) |
| C(107)-C(145)-C(123) | 113(5) |
| C(143)-C(146)-C(103) | 123(5) |
| C(143)-C(146)-C(124) | 119(4) |
| C(103)-C(146)-C(124) | 107(3) |
| C(154)-C(147)-C(153) | 121(3) |
| C(154)-C(147)-C(155) | 125(4) |
| C(153)-C(147)-C(155) | 99(4) |
| C(125)-C(148)-C(126) | 122(4) |
| C(125)-C(148)-C(138) | 117(5) |
| C(126)-C(148)-C(138) | 112(5) |
| C(138)-C(149)-C(132) | 117(3) |
| C(138)-C(149)-C(157) | 124(4) |
| C(132)-C(149)-C(157) | 104(4) |
| C(139)-C(150)-C(135) | 122(4) |
| C(139)-C(150)-C(153) | 119(5) |
| C(135)-C(150)-C(153) | 108(5) |
| C(137)-C(151)-C(134) | 124(4) |
| C(137)-C(151)-C(143) | 100(5) |
| C(134)-C(151)-C(143) | 125(5) |
| C(145)-C(152)-C(131) | 127(5) |
| C(145)-C(152)-C(129) | 118(5) |
| C(131)-C(152)-C(129) | 104(3) |
| C(119)-C(153)-C(150) | 116(4) |
| C(119)-C(153)-C(147) | 118(3) |
| C(150)-C(153)-C(147) | 114(4) |
| C(147)-C(154)-C(127) | 121(4) |
| C(147)-C(154)-C(137) | 115(4) |
| C(127)-C(154)-C(137) | 112(5) |
| C(140)-C(155)-C(135) | 142(8) |
| C(140)-C(155)-C(147) | 102(6) |
| C(135)-C(155)-C(147) | 104(6) |
| C(124)-C(156)-C(123) | 115(4) |
| C(124)-C(156)-C(134) | 121(5) |
| C(123)-C(156)-C(134) | 110(5) |
| C(142)-C(157)-C(120) | 142(8) |
| C(142)-C(157)-C(149) | 106(6) |
| C(120)-C(157)-C(149) | 102(5) |
| C(159)-C(158)-C(116) | 151(8) |
| C(159)-C(158)-C(126) | 94(8) |
| C(116)-C(158)-C(126) | 99(6) |

| | |
|--------------------------|-----------|
| C(158)-C(159)-C(133) | 157(10) |
| C(158)-C(159)-C(110) | 92(9) |
| C(133)-C(159)-C(110) | 101(4) |
| N(7)-C(200)-C(201) | 170(7) |
| C(202)-C(201)-C(206) | 123(4) |
| C(202)-C(201)-C(200) | 124(5) |
| C(206)-C(201)-C(200) | 113(4) |
| C(201)-C(202)-C(203) | 122(5) |
| C(202)-C(203)-C(204) | 123(4) |
| C(205)-C(204)-C(203) | 115(4) |
| C(206)-C(205)-C(204) | 116(4) |
| C(205)-C(206)-C(201) | 121(3) |
| N(8)-C(207)-C(208) | 178(7) |
| C(213)-C(208)-C(209) | 122(4) |
| C(213)-C(208)-C(207) | 119(4) |
| C(209)-C(208)-C(207) | 119(4) |
| C(210)-C(209)-C(208) | 118(4) |
| C(209)-C(210)-C(211) | 123(4) |
| C(210)-C(211)-C(212) | 121(4) |
| C(211)-C(212)-C(213) | 116(3) |
| C(208)-C(213)-C(212) | 120(4) |
| C(301)#2-C(300)-C(309) | 115(5) |
| C(301)#2-C(300)-C(301) | 131(5) |
| C(309)-C(300)-C(301) | 104(4) |
| C(300)#3-C(301)-C(303) | 123(9) |
| C(300)#3-C(301)-C(300) | 109(5) |
| C(303)-C(301)-C(300) | 113(6) |
| C(308)#3-C(302)-C(303) | 125(5) |
| C(308)#3-C(302)-C(306)#4 | 99(5) |
| C(303)-C(302)-C(306)#4 | 121(5) |
| C(302)-C(303)-C(304) | 119(6) |
| C(302)-C(303)-C(301) | 119(6) |
| C(304)-C(303)-C(301) | 110(6) |
| C(305)-C(304)-C(309) | 130(9) |
| C(305)-C(304)-C(303) | 109(5) |
| C(309)-C(304)-C(303) | 108(8) |
| C(307)#4-C(305)-C(304) | 125(7) |
| C(307)#4-C(305)-C(306) | 124(9) |
| C(304)-C(305)-C(306) | 101(9) |
| C(307)-C(306)-C(302)#5 | 111(8) |
| C(307)-C(306)-C(305) | 136(10) |
| C(302)#5-C(306)-C(305) | 104(8) |
| C(306)-C(307)-C(305)#5 | 134(10) |
| C(306)-C(307)-C(308) | 120(9) |
| C(305)#5-C(307)-C(308) | 92(6) |
| C(309)-C(308)-C(302)#2 | 113(8) |
| C(309)-C(308)-C(307) | 112(7) |
| C(302)#2-C(308)-C(307) | 119(6) |
| C(308)-C(309)-C(304) | 120(10) |
| C(308)-C(309)-C(300) | 124(7) |
| C(304)-C(309)-C(300) | 104(6) |
| N(4)#1-Ru(1A)-N(6)#1 | 97.8(15) |
| N(4)#1-Ru(1A)-N(3)#1 | 76.4(13) |
| N(6)#1-Ru(1A)-N(3)#1 | 170.1(19) |
| N(4)#1-Ru(1A)-N(2)#1 | 166.4(19) |
| N(6)#1-Ru(1A)-N(2)#1 | 93.1(15) |

| | |
|----------------------|-----------|
| N(3)#1-Ru(1A)-N(2)#1 | 93.9(14) |
| N(4)#1-Ru(1A)-N(1)#1 | 91.6(14) |
| N(6)#1-Ru(1A)-N(1)#1 | 94.6(14) |
| N(3)#1-Ru(1A)-N(1)#1 | 93.5(15) |
| N(2)#1-Ru(1A)-N(1)#1 | 79.5(13) |
| N(4)#1-Ru(1A)-N(5)#1 | 94.3(14) |
| N(6)#1-Ru(1A)-N(5)#1 | 82.0(14) |
| N(3)#1-Ru(1A)-N(5)#1 | 90.4(14) |
| N(2)#1-Ru(1A)-N(5)#1 | 95.1(14) |
| N(1)#1-Ru(1A)-N(5)#1 | 173.5(19) |
| N(4)#1-Ru(1A)-Ru(1) | 165.4(12) |
| N(6)#1-Ru(1A)-Ru(1) | 71.7(10) |
| N(3)#1-Ru(1A)-Ru(1) | 112.4(10) |
| N(2)#1-Ru(1A)-Ru(1) | 28.1(9) |
| N(1)#1-Ru(1A)-Ru(1) | 99.2(10) |
| N(5)#1-Ru(1A)-Ru(1) | 74.6(10) |

Symmetry transformations used to generate equivalent atoms:

#1 -x+1,-y,-z+1 #2 -x+y,-x,z #3 -y,x-y,z
 #4 x-y,x,-z+1 #5 y,-x+y,-z+1

Table A1.14. Anisotropic displacement parameters ($\text{\AA}^2 \times 10^3$). The anisotropic displacement factor exponent takes the form: $-2 \sum h^2 a^* 2U^{11} + \dots + 2 h k a^* b^* U^{12}$]

| | U ¹¹ | U ²² | U ³³ | U ²³ | U ¹³ | U ¹² |
|-------|-----------------|-----------------|-----------------|-----------------|-----------------|-----------------|
| Ru(1) | -11(1) | -3(1) | -19(1) | -3(1) | 0(1) | 0(1) |
| C(1) | 12(11) | 12(11) | 10(11) | 2(9) | 1(9) | 11(9) |
| C(2) | 8(11) | 7(10) | 5(10) | -4(8) | -2(8) | 3(9) |
| C(3) | 13(12) | 26(13) | 14(12) | 3(10) | -5(10) | 8(11) |
| C(4) | 15(12) | 29(14) | 10(11) | 1(10) | -5(10) | 6(11) |
| C(5) | 9(11) | 9(11) | 13(11) | 0(9) | -6(9) | 3(9) |
| C(6) | 17(12) | 23(12) | 2(10) | -4(9) | -8(9) | 14(10) |
| C(7) | 19(13) | 31(14) | 9(12) | -1(10) | -13(10) | 14(11) |
| C(8) | 18(12) | 27(14) | 11(12) | 2(10) | -5(10) | 10(11) |
| C(9) | 23(13) | 19(12) | 12(12) | -4(10) | 0(10) | 15(11) |
| C(10) | 18(12) | 15(11) | 8(11) | -3(9) | -3(9) | 11(10) |
| C(11) | 15(12) | 8(10) | 12(11) | 1(9) | 0(9) | 6(9) |
| C(12) | 16(12) | 28(14) | 12(12) | 10(11) | 8(10) | 7(11) |
| C(13) | 33(16) | 37(17) | 27(15) | 7(13) | -4(13) | 13(14) |
| C(14) | 39(17) | 48(18) | 10(13) | -4(12) | 2(12) | 13(15) |
| C(15) | 22(13) | 20(12) | 13(13) | -3(10) | 3(10) | 14(11) |
| C(16) | 19(13) | 30(15) | 22(14) | 11(12) | 10(11) | 8(12) |
| C(17) | 43(19) | 33(17) | 50(20) | 19(16) | 15(17) | 12(15) |
| C(18) | 15(14) | 45(18) | 43(18) | 10(15) | 1(13) | 6(13) |
| C(19) | 6(10) | 15(12) | 25(13) | -10(10) | -5(10) | 6(9) |
| C(20) | 18(13) | 22(13) | 17(13) | 0(10) | 2(10) | 11(11) |
| C(21) | 22(13) | 18(13) | 25(14) | -6(11) | -4(11) | 10(11) |
| C(22) | 16(12) | 33(15) | 17(12) | -17(11) | -6(10) | 12(11) |
| C(23) | 8(11) | 17(12) | 16(12) | -10(10) | -3(9) | 6(10) |
| C(24) | 14(11) | 34(14) | 1(10) | -16(10) | -6(9) | 15(11) |
| C(25) | 20(13) | 34(15) | 8(11) | -1(11) | -3(10) | 20(12) |
| C(26) | 25(14) | 52(17) | 6(12) | -1(12) | 5(10) | 27(13) |
| C(27) | 9(11) | 28(14) | 19(13) | 6(11) | -1(10) | 9(11) |

| | | | | | | |
|--------|---------|--------|---------|---------|---------|--------|
| C(28) | 11(11) | 23(13) | 9(11) | 1(10) | -1(9) | 12(10) |
| C(29) | 24(14) | 17(13) | 30(16) | 5(12) | 5(12) | 9(11) |
| C(30) | 70(20) | 25(16) | 28(16) | 6(13) | -10(16) | 22(16) |
| C(31) | 70(30) | 60(30) | 70(30) | 30(20) | 30(20) | 50(20) |
| C(32) | 60(20) | 26(18) | 100(30) | 10(20) | 10(20) | 6(17) |
| C(33) | 18(13) | 39(16) | 13(13) | 8(12) | -1(10) | 14(12) |
| C(34) | 60(20) | 35(17) | 32(17) | 0(14) | -11(15) | 27(17) |
| C(35) | 80(30) | 37(19) | 50(20) | 11(17) | 10(20) | 23(19) |
| C(36) | 100(30) | 50(20) | 50(20) | -5(18) | -10(20) | 50(20) |
| C(37) | 14(11) | 18(12) | 8(11) | 2(9) | 5(9) | 11(10) |
| C(38) | 10(11) | 19(12) | 5(10) | -4(9) | 3(9) | 5(10) |
| C(39) | 10(11) | 27(13) | 17(12) | 3(10) | 5(10) | 9(11) |
| C(40) | 18(12) | 25(13) | 7(11) | -5(9) | 1(9) | 17(11) |
| C(41) | 5(10) | 20(12) | 11(11) | 5(9) | -1(8) | 9(9) |
| C(42) | 9(11) | 24(12) | 12(11) | -1(9) | -5(9) | 16(10) |
| C(43) | 18(13) | 22(13) | 20(13) | 1(10) | -2(10) | 13(11) |
| C(44) | 25(13) | 17(12) | 10(11) | 7(9) | 3(10) | 14(11) |
| C(45) | 14(12) | 12(11) | 17(12) | 4(9) | 0(10) | 5(10) |
| C(46) | 14(11) | 21(12) | 9(11) | 5(9) | 4(9) | 11(10) |
| C(47) | 13(12) | 22(13) | 17(12) | -7(10) | 1(10) | 7(10) |
| C(48) | 22(15) | 16(14) | 70(20) | -4(14) | 10(15) | -4(12) |
| C(49) | 40(20) | 29(18) | 140(40) | 20(20) | 10(20) | 8(16) |
| C(50) | 60(20) | 40(20) | 80(30) | -30(20) | 10(20) | 12(17) |
| C(51) | 24(14) | 26(15) | 24(13) | -1(11) | -1(11) | 13(12) |
| C(52) | 17(13) | 20(14) | 48(18) | -11(13) | 1(13) | 2(11) |
| C(53) | 36(19) | 40(20) | 70(30) | 35(19) | 12(18) | 7(16) |
| C(54) | 24(16) | 60(20) | 60(20) | -12(19) | -18(16) | 17(17) |
| N(1) | 5(9) | 13(9) | 10(9) | -3(7) | -6(7) | 9(8) |
| N(2) | 12(9) | 13(9) | 2(8) | 3(7) | -2(7) | 11(8) |
| N(3) | 7(9) | 10(9) | 17(10) | -10(8) | -1(8) | 8(8) |
| N(4) | 6(9) | 24(11) | -2(8) | -2(8) | 2(7) | 7(8) |
| N(5) | 2(8) | 25(10) | 5(9) | -2(8) | 1(7) | 10(8) |
| N(6) | 10(9) | 4(8) | 7(8) | -6(7) | -3(7) | 6(7) |
| O(1) | 7(8) | 19(8) | 17(8) | 2(7) | 1(7) | 3(7) |
| O(2) | 6(7) | 17(8) | 11(8) | 1(6) | -1(6) | 2(6) |
| O(3) | 24(9) | 32(10) | 11(9) | 5(7) | 4(7) | 16(8) |
| O(4) | 17(9) | 24(9) | 10(8) | 6(7) | 5(7) | 8(7) |
| O(5) | 73(16) | 16(10) | 33(12) | -1(9) | -5(11) | 17(10) |
| O(6) | 43(12) | 12(9) | 39(11) | 1(8) | -2(9) | 7(9) |
| O(7) | 44(12) | 42(12) | 20(11) | 14(9) | 8(9) | 21(10) |
| O(8) | 37(11) | 27(10) | 23(10) | 11(8) | 3(8) | 17(9) |
| O(9) | 12(10) | 32(11) | 55(13) | -13(10) | 9(9) | 3(8) |
| O(10) | 11(8) | 9(8) | 63(14) | -6(9) | 0(9) | -2(7) |
| O(11) | 22(10) | 15(10) | 78(16) | -5(10) | 3(10) | 6(8) |
| O(12) | 10(8) | 14(9) | 58(13) | -5(9) | 6(9) | 1(7) |
| C(100) | 52(19) | 29(15) | -1(11) | -7(10) | 0(11) | 15(14) |
| C(101) | 56(19) | 49(19) | -2(11) | 0(11) | 6(12) | 27(16) |
| C(102) | 13(13) | 31(15) | 54(19) | -3(14) | 6(13) | 9(12) |
| C(103) | 24(14) | 22(14) | 33(16) | 15(12) | 5(12) | 0(12) |
| C(104) | 50(18) | 10(12) | 37(16) | 5(12) | 0(14) | 18(13) |
| C(105) | 41(17) | 15(13) | 33(16) | 8(12) | 6(13) | 10(12) |
| C(106) | 70(20) | 13(13) | 30(16) | 9(12) | 8(15) | 23(14) |
| C(107) | 80(30) | 70(20) | 1(12) | -8(13) | -4(14) | 60(20) |
| C(108) | 35(17) | 33(16) | 31(16) | 27(14) | 12(13) | 14(14) |
| C(109) | 48(18) | 47(18) | 9(12) | -6(12) | 5(12) | 32(16) |
| C(110) | 34(17) | 13(13) | 40(18) | 6(13) | 8(14) | -4(12) |

| | | | | | | |
|--------|----------|---------|----------|----------|----------|---------|
| C(111) | 57(19) | 18(14) | 28(16) | 19(12) | 25(15) | 21(14) |
| C(112) | 6(13) | 45(18) | 60(20) | 14(16) | 11(13) | 6(12) |
| C(113) | 50(20) | 50(20) | 22(15) | 23(14) | 30(14) | 36(17) |
| C(114) | 22(15) | 38(18) | 41(18) | 16(15) | 13(14) | 1(13) |
| C(115) | 22(14) | 43(18) | 30(16) | 21(14) | 14(13) | 7(13) |
| C(116) | 11(14) | 60(20) | 60(20) | -28(19) | -9(15) | 11(14) |
| C(117) | 34(16) | 29(15) | 24(15) | 20(12) | -2(13) | 12(13) |
| C(118) | 51(18) | 34(16) | 5(12) | 13(11) | 8(12) | 11(14) |
| C(119) | 20(14) | 47(19) | 46(18) | 5(15) | 15(13) | 23(14) |
| C(120) | 70(20) | 39(18) | 60(20) | 28(17) | 19(19) | 52(19) |
| C(121) | 46(18) | 39(16) | 2(11) | 7(11) | 11(12) | 21(14) |
| C(122) | 35(16) | 55(19) | 10(12) | -3(13) | -11(11) | 26(15) |
| C(123) | 240(70) | 80(30) | 30(20) | 10(20) | 40(30) | 140(50) |
| C(124) | 70(30) | 13(15) | 50(20) | -6(15) | -14(19) | 16(16) |
| C(125) | 70(20) | 90(30) | -4(12) | 0(14) | -6(13) | 60(20) |
| C(126) | 50(30) | 70(30) | 40(20) | -20(20) | -10(20) | -20(20) |
| C(127) | 13(15) | 50(20) | 60(20) | -15(19) | -4(15) | -1(14) |
| C(128) | 140(40) | 27(18) | 18(16) | -22(14) | -30(20) | 50(20) |
| C(129) | 39(17) | 34(16) | 19(14) | 8(12) | 19(13) | 11(14) |
| C(130) | 90(40) | 170(60) | 30(20) | -50(30) | 0(20) | 100(40) |
| C(131) | 32(17) | 60(20) | 60(20) | 3(17) | 28(16) | 35(16) |
| C(132) | 50(20) | 70(30) | 110(40) | 30(30) | 30(20) | 60(20) |
| C(133) | 80(30) | 4(13) | 60(20) | -9(14) | -10(20) | 16(15) |
| C(134) | 170(50) | 30(20) | 20(18) | -31(16) | -60(30) | 60(30) |
| C(135) | 60(20) | 31(16) | 50(20) | 15(15) | 2(17) | 41(16) |
| C(136) | 60(30) | 130(40) | 50(20) | -40(30) | 20(20) | 50(30) |
| C(137) | 33(19) | 120(40) | 8(15) | 1(19) | -13(14) | 0(20) |
| C(138) | 15(17) | 180(50) | 22(17) | -20(30) | -14(14) | 40(30) |
| C(139) | 140(40) | 60(30) | 40(20) | 10(20) | 40(30) | 90(30) |
| C(140) | 260(70) | 220(70) | 30(20) | -20(30) | -40(30) | 240(70) |
| C(141) | 50(20) | 40(20) | 140(40) | 20(20) | 50(30) | 39(19) |
| C(142) | 350(120) | 220(70) | 20(20) | -30(30) | -70(40) | 260(90) |
| C(143) | 40(20) | 50(20) | 90(30) | -10(20) | -10(20) | -10(18) |
| C(144) | 150(50) | 24(18) | 29(18) | -4(15) | 20(20) | 50(20) |
| C(145) | 70(30) | 160(50) | 29(19) | -20(20) | 2(19) | 90(40) |
| C(146) | 70(30) | 14(16) | 90(30) | 4(19) | -40(20) | -24(16) |
| C(147) | 24(18) | 90(30) | 60(20) | 50(30) | 3(17) | 30(20) |
| C(148) | 40(20) | 170(60) | 30(20) | -30(30) | -27(18) | 50(30) |
| C(149) | 22(17) | 110(40) | 120(40) | 80(30) | 20(20) | 50(20) |
| C(150) | 50(20) | 40(20) | 160(50) | 20(30) | 40(30) | 50(20) |
| C(151) | 100(40) | 60(30) | 30(20) | -10(20) | -30(20) | -20(30) |
| C(152) | 50(30) | 120(40) | 70(30) | -40(30) | 40(20) | 40(30) |
| C(153) | 24(17) | 50(20) | 150(50) | 30(30) | 10(20) | 31(17) |
| C(154) | 8(15) | 130(40) | 50(20) | -10(30) | -17(15) | 20(20) |
| C(155) | 220(70) | 80(30) | 150(60) | -70(40) | -150(60) | 120(40) |
| C(156) | 140(40) | 40(20) | 40(20) | -10(18) | 0(30) | 50(30) |
| C(157) | 170(50) | 60(30) | 100(40) | -40(30) | -110(40) | 90(30) |
| C(158) | 10(20) | 70(40) | 310(100) | -130(50) | -30(40) | -10(20) |
| C(159) | 60(30) | 9(18) | 340(110) | -20(30) | -100(50) | 10(20) |
| C(200) | 90(40) | 90(40) | 90(40) | -30(30) | 40(30) | 0(30) |
| C(201) | 50(20) | 26(16) | 41(19) | 7(15) | 22(17) | 11(15) |
| C(202) | 100(40) | 80(30) | 50(30) | 10(20) | 20(30) | 70(30) |
| C(203) | 70(30) | 190(60) | 60(30) | 80(40) | 50(30) | 100(40) |
| C(204) | 50(30) | 100(40) | 20(18) | -20(20) | 15(18) | -50(30) |
| C(205) | 90(30) | 31(19) | 50(20) | 13(17) | 10(20) | 30(20) |
| C(206) | 20(14) | 60(20) | 38(18) | 20(16) | 5(13) | 17(15) |

| | | | | | | |
|--------|------------|----------|------------|-----------|------------|----------|
| C(207) | 70(30) | 80(30) | 60(30) | 0(20) | 0(20) | 30(30) |
| C(208) | 60(20) | 50(20) | 34(18) | -2(16) | -5(17) | 28(19) |
| C(209) | 60(30) | 50(20) | 100(30) | -20(20) | -20(20) | 30(20) |
| C(210) | 30(20) | 80(30) | 60(30) | -20(20) | -11(19) | 20(20) |
| C(211) | 70(30) | 50(20) | 37(19) | 5(16) | 14(19) | 20(20) |
| C(212) | 70(30) | 40(20) | 70(30) | 0(19) | -20(20) | 30(20) |
| C(213) | 50(20) | 60(20) | 60(20) | -4(19) | 3(18) | 35(19) |
| C(300) | 45(16) | 300(60) | 37(15) | -80(20) | -4(13) | 150(30) |
| C(301) | 300(100) | 40(30) | 90(40) | 0(30) | 120(50) | 30(40) |
| C(302) | 80(30) | 40(20) | 80(30) | 0(20) | 0(30) | 30(20) |
| C(303) | 100(40) | 50(30) | 130(50) | -40(30) | -30(40) | 30(30) |
| C(304) | 70(40) | 70(40) | 250(90) | -100(50) | -110(50) | 40(30) |
| C(305) | 80(40) | 40(30) | 160(70) | -30(40) | 30(50) | -10(30) |
| C(306) | 30(30) | 40(30) | 450(190) | -60(60) | 20(60) | -10(20) |
| C(307) | 40(20) | 40(30) | 230(90) | 10(40) | 10(30) | 10(20) |
| C(308) | 40(20) | 60(30) | 190(70) | 10(40) | -50(30) | 10(20) |
| C(309) | 190(80) | 220(80) | 410(160) | -260(110) | -280(110) | 180(80) |
| N(7) | 80(30) | 130(40) | 130(40) | -30(40) | 10(30) | 60(30) |
| N(8) | 120(40) | 120(40) | 70(30) | 20(30) | 10(30) | 20(30) |
| C(400) | 370(20) | 450(30) | -283(6) | 190(9) | -11(6) | -43(16) |
| C(401) | 160(10) | -268(5) | 1030(30) | -396(11) | 168(13) | 0(6) |
| C(402) | 1500(110) | 128(19) | -117(9) | -147(12) | -400(30) | 40(30) |
| C(403) | 630(40) | 210(20) | 69(15) | 460(20) | 66(16) | 52(19) |
| C(404) | 2000(20) | 213(10) | -267(5) | 117(5) | -400(8) | 1335(16) |
| C(405) | 1100(1000) | 500(300) | 2000(1500) | -400(600) | -400(1000) | 600(500) |
| Ru(1A) | 570(40) | 570(40) | 610(50) | 0(30) | 10(30) | 250(30) |

Table A1.15. Hydrogen coordinates ($\times 10^4$) and isotropic displacement parameters ($\text{\AA}^2 \times 10^3$).

| | x | y | z | U(eq) |
|--------|------|-------|------|-------|
| H(1) | 3973 | -387 | 7411 | 11 |
| H(3) | 3222 | -766 | 6381 | 23 |
| H(4) | 3637 | -481 | 5758 | 24 |
| H(7) | 4053 | -175 | 5214 | 23 |
| H(8) | 4512 | 129 | 4699 | 24 |
| H(10) | 5131 | 348 | 5903 | 15 |
| H(12) | 3006 | -880 | 8196 | 25 |
| H(13A) | 2919 | -1402 | 7890 | 51 |
| H(13B) | 2872 | -1421 | 8475 | 51 |
| H(13C) | 3211 | -1376 | 8239 | 51 |
| H(14A) | 3538 | -867 | 8768 | 54 |
| H(14B) | 3238 | -822 | 8975 | 54 |
| H(14C) | 3528 | -531 | 8651 | 54 |
| H(16) | 5784 | 799 | 4609 | 30 |
| H(17A) | 5554 | 1183 | 4686 | 69 |
| H(17B) | 5954 | 1384 | 4619 | 69 |
| H(17C) | 5793 | 1351 | 5153 | 69 |
| H(18A) | 6068 | 1059 | 5563 | 57 |
| H(18B) | 6283 | 1098 | 5079 | 57 |
| H(18C) | 6055 | 735 | 5319 | 57 |
| H(19) | 4782 | 681 | 6418 | 18 |
| H(21) | 5104 | 1333 | 7572 | 26 |

| | | | | |
|--------|------|-------|------|-----|
| H(22) | 4949 | 869 | 8112 | 26 |
| H(25) | 4612 | 356 | 8552 | 22 |
| H(26) | 4410 | -171 | 8937 | 29 |
| H(28) | 4493 | -559 | 7636 | 16 |
| H(30) | 5253 | 1880 | 6103 | 51 |
| H(31A) | 4716 | 1750 | 6469 | 94 |
| H(31B) | 4921 | 2099 | 6181 | 94 |
| H(31C) | 4929 | 2092 | 6770 | 94 |
| H(32A) | 5637 | 2405 | 6422 | 104 |
| H(32B) | 5707 | 2143 | 6710 | 104 |
| H(32C) | 5498 | 2293 | 6970 | 104 |
| H(34) | 4296 | -1320 | 8752 | 49 |
| H(35A) | 3731 | -1450 | 8671 | 86 |
| H(35B) | 3764 | -1774 | 8561 | 86 |
| H(35C) | 3727 | -1567 | 8115 | 86 |
| H(36A) | 4292 | -1441 | 7700 | 91 |
| H(36B) | 4286 | -1700 | 8098 | 91 |
| H(36C) | 4606 | -1331 | 8059 | 91 |
| H(37) | 5375 | 651 | 6983 | 14 |
| H(39) | 6095 | 446 | 6515 | 21 |
| H(40) | 5676 | -128 | 6418 | 16 |
| H(43) | 5252 | -683 | 6502 | 23 |
| H(44) | 4772 | -1215 | 6424 | 18 |
| H(46) | 4184 | -797 | 6636 | 16 |
| H(48) | 6356 | 1608 | 7006 | 49 |
| H(49A) | 6104 | 1578 | 6192 | 108 |
| H(49B) | 6178 | 1918 | 6459 | 108 |
| H(49C) | 5804 | 1603 | 6449 | 108 |
| H(50A) | 5788 | 1638 | 7330 | 97 |
| H(50B) | 6167 | 1861 | 7518 | 97 |
| H(50C) | 5950 | 1475 | 7676 | 97 |
| H(52) | 3516 | -1865 | 6223 | 38 |
| H(53A) | 3511 | -1920 | 7071 | 86 |
| H(53B) | 3139 | -2009 | 6927 | 86 |
| H(53C) | 3396 | -1649 | 7152 | 86 |
| H(54A) | 3295 | -1385 | 6306 | 78 |
| H(54B) | 3042 | -1766 | 6155 | 78 |
| H(54C) | 3353 | -1532 | 5806 | 78 |
| H(202) | 1949 | 25 | 5576 | 81 |
| H(203) | 2328 | 434 | 6013 | 106 |
| H(204) | 2360 | 973 | 6060 | 115 |
| H(205) | 1935 | 1036 | 5542 | 70 |
| H(206) | 1571 | 576 | 5094 | 49 |
| H(209) | 1770 | 171 | 7747 | 79 |
| H(210) | 1906 | 362 | 6951 | 75 |
| H(211) | 1535 | 415 | 6436 | 70 |
| H(212) | 990 | 306 | 6743 | 71 |
| H(213) | 857 | 120 | 7576 | 65 |

**PART 2: SYNTHESIS AND CHARACTERIZATION OF POLYMER THIN FILMS FOR
USE AS A LITHIUM-ION BATTERY SEPARATOR MATERIAL**

CHAPTER 2: AQUEOUS ELECTRODEPOSITION OF POLY(ETHYLENE GLYCOL) DIACRYLATE FOR USE AS A LITHIUM-ION BATTERY SEPARATOR MATERIAL

INTRODUCTION

Portable energy storage has become a necessity across the world, and the demand for better and smaller energy storage systems will continue to grow well into the future. The global market for energy storage is expected to grow from \$39.7 billion in 2011 to \$69.1 billion by 2016, nearly doubling in 5 years.¹ The expected growth and continuous demand is driven by a constant thirst for electronic devices and toys, ranging from smart phones to electric vehicles. The demand for high energy storage doesn't stop at electronic devices and toys that make our lives easier or more enjoyable. The basis of a smart grid, which would revolutionize the entire power grid, hinges on high power-density storage. Optimization of alternative energy sources such as wind and solar require these energy storage systems as well.

Portable energy storage can be divided into two categories, chemical energy storage in the form of batteries and electrical energy storage in the form of capacitors. Structurally, capacitors and batteries are very similar. Each is composed of two electrodes, a cathode and an anode, separated by an electronically insulating material. This material is referred to as the separator in a battery and the dielectric in a capacitor. In a battery, the anode and cathode must be two different materials, but in a capacitor they can be the same material. A battery stores the energy in the form of a chemical potential, the potential difference between the anode and cathode. Chemical reactions (redox processes) occur at the cathode and anode when charging or discharging the battery, and the electrons generated or consumed in the reaction provide the electrical energy the battery outputs. In a capacitor, electrical charge is built up on the surface of

the electrodes, negative charge on the cathode and positive on the anode, giving rise to a potential difference between the anode and cathode. When the anode and cathode are electrically connected, the charges flow to recombine giving rise to electrical energy. In a capacitor, no chemical reactions take place, a stark contrast to batteries, where reactions take place in the bulk of the material. Because no chemical reactions take place, discharging a capacitor occurs extremely quickly compared to batteries. Since the time taken to discharge a given amount of energy is much lower, the power of the device is increased. Figure 2.1 is a useful graph for comparing batteries and capacitors.² Shown in Figure 2.1, capacitors discharge very quickly and exhibit large power density, which is why capacitors are optimal at delivering

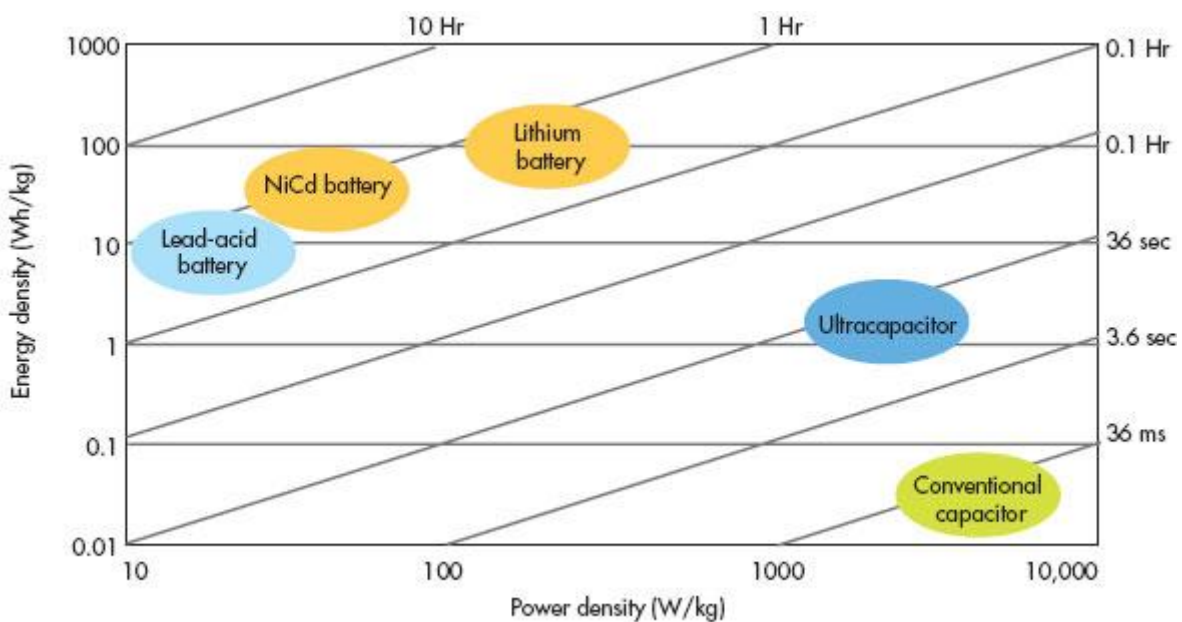


Figure 2.1. Ragone plot² used to compare batteries and capacitors. Energy density is plotted versus power density, both on log scales. The diagonal lines represent discharge times. Figure reproduced from reference 2.

large amounts of power for short periods of time. In contrast, batteries are efficient at delivering moderate amounts of power over longer periods of time, at a constant voltage ideally. This is because batteries undergo chemical reactions at the anode and cathode; the process occurs much

more slowly than capacitive discharge. The benefit batteries have is that chemical reactions at the anode and cathode occur throughout the bulk of the material, unlike a capacitor. This is why batteries have higher energy densities, which means more energy can be stored for a given amount of mass. Since common electronic devices require small amounts of energy over long periods of time, batteries have dominated the energy storage market.¹

With the emergence of electric vehicles and increasing power needs for portable electronic equipment, standard battery technology cannot meet the power demand of the near future. One approach could be to switch over to capacitors, where research on supercapacitors (referred to as ultracapacitors in Figure 2.1) has been fruitful.³⁻⁵ The issue with the supercapacitor approach is that it is not possible to improve energy density of supercapacitors because capacitors only undergo surface charging and not chemical reactions in the bulk of the material. A better approach would be to structurally modify a battery (high surface area) which would combine the best properties of both, high energy density *and* high power density.

Battery technology has already advanced significantly with the introduction of lithium-ion batteries, storing 2-3 times more energy per weight than nickel metal hydride rechargeable batteries.⁶ But this improvement only scratches at the surface of the potential for lithium-ion batteries. Current lithium-ion batteries are all composed of layered architectures, regardless of how they are packaged, seen in figure 2.2.⁷ The thin films have low surface areas due to their two dimensional geometry and the films are microns thick which enables modest power densities at best.^{8,9}

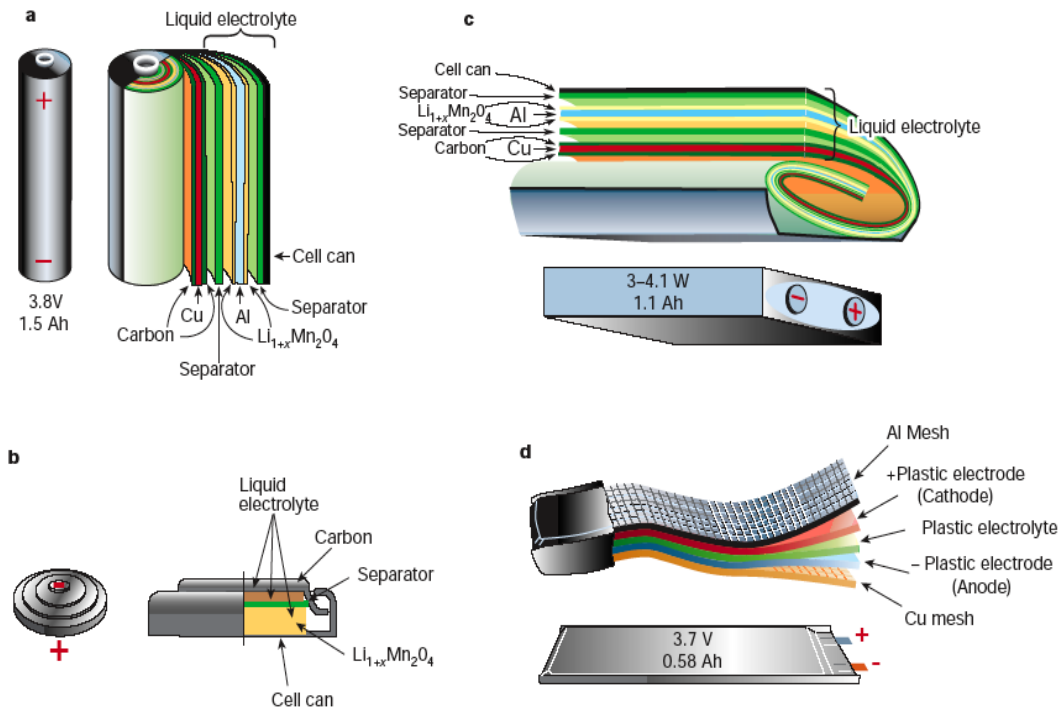


Figure 2.2. Different types of lithium-ion batteries and how they are packaged; a, cylindrical; b, coin; c, prismatic; d, flat.

To increase the power of lithium-ion batteries, the distance between the cathode and anode (separator thickness) must be minimized while also maximizing the surface area of the cathode and anode. A thin separator minimizes the time it takes for lithium diffusion through the separator. The time taken for diffusion is related to the square of the separator thickness, see equation below. In this equation, t is the time for diffusion (sec), L is the length of diffusion or

$$t \approx L^2/D \quad (\text{Eq. 2.1})$$

separator thickness (cm), and D is the diffusion coefficient (cm^2/sec). A high surface area electrode affords more surface sites for lithiation/delithiation of the anode or cathode. It also increases the surface area to volume ratio, which means the diffusion path through the cathode or anode is decreased. Decreasing the diffusion distance that Li^+ travels in the cathode or anode is important because lithium diffusion coefficients through cathode/anode materials range between

10^{-8} and 10^{-10} cm²/sec, which are lower values than polymer-based materials (10^{-7} cm²/sec). Transport through the separator and lithiation/delithiation are the two rate-limiting processes in lithium-ion batteries. A battery with low surface area electrodes and a thin separator will be limited by the lithiation/delithiation processes while a battery with high surface area electrodes and a thick separator will be limited by lithium transport through the separator. Therefore, in order to maximize the power density of a lithium-ion battery it is imperative to address both issues simultaneously with a goal of achieving fast and comparable rates. This can be achieved by developing a high-surface-area, three-dimensional-structured, battery.¹⁰

High-surface-area anode and cathode materials have already been fabricated through the synthesis of nanoparticles, nanotubes, or nanowires.^{6,11-14} The problem that still plagues this field is the development of a conformal, nanoscale material that can perform as a separator between the cathode and anode. This issue has been a major challenge for several reasons. First, nanoscale materials are fragile and hard to work with. The separator cannot be made independently of the anode or cathode since assembly would be essentially impossible with such a thin material; therefore, the separator needs to be fabricated in-situ. Second, the separator needs to conformally coat the 3-D nanostructure. Coating structures such as nanowires limits fabrication methods. Some work has been done using atomic layer deposition to coat electrodes with a thin ceramic layer (Al₂O₃) to minimize solvent decomposition and solid electrolyte interface (SEI) formation, but the method is slow and not cost effective for commercial use.^{15,16} Third, controlling the thickness of the separator can be difficult, especially for films only tens of nanometers thick. For polymerizations, this usually requires a self-limiting polymerization mechanism to avoid incomplete or non-uniform film coverage. Fourth, regardless of thickness,

the separator must be able to handle the physical stresses that occur during charging/discharging as expansion/contraction processes occur. If the separator cannot withstand these stresses the battery will short. Fifth, the separator has to be electronically insulating with nanoscale thickness, and also conduct ions. These challenges are great and progress in the field of nanoscale separators has therefore been slow.

Commercially available separator materials do not meet the criteria listed above and, therefore, are not suitable for nanostructured cells. Commercial separators are too thick for any nanostructured application, usually 20-25 microns.¹⁷ This includes separators made by industry leaders including Celgard, Asahi Hipore, and Tonen Setala.¹⁷ Furthermore, the separators are not solid-state, but require plasticizer doped with a lithium salt. Plasticizing leads to unwanted side effects such as the deposition of a solid electrolyte interface (SEI) due to decomposition of the organic liquid electrolyte. SEI formation can affect cycle life, operating temperature, and safety, and therefore must be carefully controlled or altogether avoided.¹⁸ SEI formation can be avoided through a solid-state separator, which has no organic plasticizers. The focus commercially has been on improving safety through improved strength, puncture resistance and thermal stability, not on fundamental advancements in solid-state separators.^{17,19}

Academically, there has been some progress in the field of solid-state separators, but more work is needed. Ceramic and polymer electrolytes comprise the current literature on solid state electrolytes.²⁰ Ceramic materials are rigid and brittle, undesirable properties for a battery due to contraction and expansion of the cathode/anode.²¹ Therefore ceramic materials were not investigated. The largest barrier to overcome in solid-state electrolytes is the low ionic conductivity they exhibit ($\leq 10^{-5}$ S/cm at 25 °C) compared to liquid based separators ($\geq 10^{-4}$ S/cm at 25 °C).²²⁻²⁴ It should be noted that a large percentage (*ca.* 15%) of the published literature on

solid-state electrolytes make claims of solid-state electrolytes which ultimately contain plasticizers, ionic liquids, or components that are liquid at room temperature, all of which are not true solid-state electrolytes and none will be viewed or reported as such in this dissertation.²⁵⁻²⁸

A few strategies have been used to improve the ionic conductivity of solid electrolytes, although ion conductivity still remains very low. One approach is to synthesize lithium salt doped polymer films, the most common polymer for this has been polyethylene oxide (PEO) because the repeating ethylene oxide units are good at dissolving salts.^{6,22} MacCallum *et al.* reported an ionic conductivity for PEO:LiClO₄ (8:1 respectively) of 1×10^{-7} at room temperature, typical of solid polymer electrolytes (for PEO, $M_n = 5 \times 10^6$ g/mol, the average molecular weight of the polymer). One reason salt-polymer composites have low conductivity is that they crystallize, and most ion conduction is believed to occur through amorphous regions.²⁴ To suppress crystallization, inorganic nanocomposites such as Al₂O₃, SiO₂, or TiO₂ have been incorporated into polymer films. Incorporation of nanocomposites has been shown to decrease crystallization, increase the transference number (i.e., the fraction of the migration current carried by lithium ions) and increase cycling capacity in polymer electrolytes.^{6,29} Kang *et al.* reported an ionic conductivity of 5.8×10^{-5} S/cm at 30 °C for a highly crosslinked polysiloxane-g-oligo(ethylene oxide) film.²⁸

Again, the transference number is the fraction of the migration current carried by lithium ions. The transference number is measured using non-blocking electrodes such as Li_(m) because cation intercalation is needed. The equation for transference number is given below, where t_+ is the transference number, I_+ is the cation migration current (steady state current), and I_0 is the initial current as described below.

$$t_+ = I_+/I_0 \quad (\text{Eq. 2.2})$$

In a dc polarization experiment, a constant potential is applied and a subsequent current is passed (I_0). After a certain time has passed, the anions establish a concentration gradient and current because of anion migration is minimized since the anions cannot intercalate into the cathode/anode. The current approaches steady state (I_+) and is due to Li^+ migration only. Transference numbers are reported as a value (0-1) where 1 refers to a system in which all initial current is due to lithium migration only (the ideal situation). Solid polymer electrolytes typically have low transference numbers (≤ 0.3).^{30,31}

Another approach to improving solid electrolytes is to synthesize extremely thin films. Rhodes *et al.* has published work on electrodeposited poly(phenylene oxide) based films that are less than 100 nm thick.^{32,33} Although the films exhibit low ion conductivity (7×10^{-10} S/cm), the distance the lithium has to traverse (in one dimension) is two orders of magnitude less compared to commercial separators.³² Furthermore, it has been hypothesized that ion conductivity can be dramatically altered because the electric double layer of each electrode overlaps with each other when film thickness is less than 50 nm, establishing field-driven fluxes in the electrolyte.³²

Aside from having high ionic conductivity, a solid polymer electrolyte would ideally possess the following characteristics:

- An ionic transference number as close to 1 as possible. If transference numbers could approach unity, all the current would be carried by lithium ions and concentration polarization effects would be minimized; hence a higher power density could then be achieved.²²

- High thermal, electrochemical, and chemical stability are also important. Many cathode and anode materials undergo thermal runaway in the range of 150-200 °C, which suggests that operating temperatures must be kept below 150 °C for safety. Therefore, a polymer separator needs to be stable up to *ca.* 150 °C. Operating voltages in lithium batteries range from 3.2-4.6 V vs Li⁺ so the separator needs to be stable up to 5 V vs Li⁺. Lastly, the separator needs to be chemically stable under atmospheric conditions in cases where a battery pack is punctured and exposed to atmospheric conditions. In most cases, solid polymer electrolytes already outperform liquid-based electrolytes when it comes to stability.
- A low glass transition temperature (T_g), well below room temperature is also desirable (≤ -40 °C). A low T_g allows for the polymer matrix to move on the microscopic level, facilitating ion mobility in the matrix.²³
- A good mechanical strength must be achieved so that the cathode and anode remain physically separated in abusive environments.
- The separator needs to be compatible with electrode materials to avoid reactions at the interfaces such as oxide formation, which would increase resistance across the interface. Most polymer electrolytes are compatible with electrode materials.

Expansion and contraction of the anode and cathode is also a concern that must be considered. Expansion/contraction when lithiating/delithiating occurs for all anode and cathode materials.^{34,35} The separator must therefore be able to handle the physical stresses or the battery will short if the separator becomes pulverized. A proper polymer-based separator can handle such stresses due to the viscoelastic properties of polymers.³⁶ This is in stark contrast to ceramic-based separator materials, which are brittle.²¹ The viscoelastic properties allow polymers to be viewed

as viscous liquids and elastic solids, which allow for movement of the polymer when a stress is applied. In the case of a battery it should allow the separator to maintain a physical separation between cathode and anode even during the expansion/contraction processes. Therefore a polymer based separator is ideal in regards to expansion/contraction processes.^{24,37} Coating 3-D structures with a polymer coating is another issue that must be addressed.

Whether the cathode/anode is composed of nanoparticles or a nanowire array, achieving a thin, conformal coating of the active electrode material with a separator material remains a significant challenge. Recall that gas-phase depositions are a possible coating strategy but the approach is slow and costly.^{15,16} Electrodeposition is another method that can achieve conformal coatings on three dimensional structured surfaces.^{32,33} Electrodeposition can afford thin and conformal polymer films if the electrode becomes insulating as the polymerization occurs, leading to self limiting behavior; that is, polymerization occurs more rapidly over regions of highest electrical conductivity (i.e., bare surfaces) which results in a complete, uniform modification of the conducting surface. Furthermore, electrodeposition affords intimate contact between electrode and separator, which should improve charge transport across the interface.³² The applied potential and deposition time can be varied to alter the film thickness in a predictable manner.³⁸ Lastly, electrodeposition can often be performed on the bench top and in an aqueous solvent in short amounts of time, unlike gas-phase depositions.

Performing the deposition in an aqueous media has advantages relative to organic solvents. Using an aqueous solvent is more environmentally benign and has fewer health hazards relative to organic solvents. The aqueous media can be easily doped with a lithium salt; with proper choice of monomer, the lithium salts can get incorporated into the polymer matrix during polymerization. By choosing monomers with functionalities that help solvate lithium salts, such

chain and the lithium salt within the polymer matrix. Furthermore, it has been demonstrated that Li^+ ions coordinate to 5-6 O atoms in neighboring PEO strands in crystalline regions.^{24,44} Also, ion vacancies in crystalline regions of PEO/ LiClO_4 mixtures has been reported to improve conductivity.^{24,45} Vacancies refer to open sites that lithium ions can “hop to” as a means of conduction. We hypothesized that 13 PEO units would be sufficient to accommodate 2 Li^+ ions per monomer unit with at least one vacant site remaining, if short range crystallinity was observed.

The focus of this study, then, is the reductive electrodeposition of a thin polymer film onto an active electrode for potential use as a lithium-ion battery separator. The hypothesis of this chapter is that reductive electrodeposition of poly(ethylene glycol) diacrylate out of an aqueous solution containing lithium supporting electrolyte will afford a salt-doped solid-state separator material that conformally coats 3-D structures, exhibits high electronic resistance and high ionic conductivity. The hypothesis will be tested through SEM imaging to examine how conformal coatings will be, along with impedance spectroscopy to determine electronic and ionic conductivities. Aside from the main hypothesis, a few other significant parameters will be investigated. In this study polymer thickness will be monitored as a function of monomer concentration, deposition time, and deposition temperature. Scanning electron microscopy (SEM) images and stylus profilometry will be used to determine polymer thickness and to view surface morphology. The crystallinity of the polymer will be evaluated using x-ray diffraction (XRD). Salt doping will be investigated with x-ray photoelectron spectroscopy (XPS) analysis. Differential scanning calorimetry (DSC) and thermal gravimetric analysis (TGA) measurements will be performed to determine break down temperature and glass transition temperature (T_g) respectively. Infrared (IR) spectroscopy will be used to determine completeness of

polymerization and dryness of polymer sample. Table 2.1 below summarizes the physical observables that will be used to judge the separator material along with ideal values and the best reported literature values, where applicable.^{23,32,46}

Table 2.1. A summary of the physical properties that will be used as criteria to judge PEGDA films. Included are ideal values along with some of the best reported values in literature.

| Physical Property | Ideal | Reported in Lit. |
|---------------------------|---------------------|---|
| Reductively Polymerized | yes | yes (polymers in general, not PEGDA) (Ref 46) |
| Electronic Conductivity | zero | 7×10^{-12} S/cm (Ref 32) |
| Ionic Conductivity | $\geq 10^{-2}$ S/cm | 1.6×10^{-4} S/cm (Ref 23) |
| Conformal/Uniform Coating | yes | 21 ± 2 nm (Ref 32) |
| Thickness | 10-50 nm | 21-43 nm (Ref 32) |
| Grafted | yes | yes (Ref 46) |
| Tg | -100 °C | -80 °C (Ref 23) |

EXPERIMENTAL

CHEMICALS

Poly(ethylene glycol) diacrylate (PEGDA, MW = 700 g/mol, Aldrich) was purified by running through a column of De-Hibit 200 (Polyscience, Inc.). Lithium perchlorate (95 %, Aldrich) was used as received. Isobutyronitrile, bromine, and phosphorus tribromide were used as received from Aldrich. The radical initiator α -bromoisobutyronitrile (BrIBN) was synthesized using the method published by Stevens.⁴⁷ Indium tin oxide (Delta Technologies, Limited; Rs = 4-8 Ω) was washed with aqueous NaOH (1 M) followed by distilled water prior to use.

APPARATUS

Polymerizations and impedance measurements were carried out using a GAMRY Instruments Reference 3000 potentiostat/galvanostat. X-ray photoelectron spectroscopy (XPS) measurements were performed using Physical Electronics ESCA 5800 system (Physical Electronics, Chanhassen, MN). Monochromatic Al K α (E = 1486.6 eV) was employed as the X-ray source. Scanning electron microscopy (SEM) measurements were performed using a Joel JSM 6500F field emission microscope equipped with a Thermo Noran energy-dispersive spectrophotometer (EDS). X-ray diffraction (XRD) measurements were performed using a Scintag X-2 (Cu X-ray source). Infrared spectroscopy (IR) measurements were performed using Nicolet 380 FT-IR spectrophotometer with a Smart Performer ZnSe ATR accessory. Thermal gravimetric analysis (TGA) measurements were performed using a TGA 2950 Thermogravimetric analyzer (TA instruments). Differential scanning calorimetry (DSC) measurements were performed using a DSC 2920 Modulated DSC (TA instruments). Battery cycling was carried out using a Maccor Model 4200 battery cycler. Topographical mapping was performed using a JOEL DektakXT stylus profilometer.

ELECTRODEPOSITION

A two-compartment electrochemical cell was used for polymerization, very similar to a standard fritted H-cell. The working compartment was degassed with nitrogen for 10 minutes prior to deposition to remove dioxygen, a known radical scavenger. A deposition potential of -1.25 V vs SSCE was chosen which allows for initiator reduction, but minimizes water reduction which would form H₂ at the electrode and interfere with polymerization. The solutions were magnetically stirred during deposition to replenish monomer at the surface of the electrode and

minimize the depletion region that forms near the electrode surface. Polymer thickness was monitored as a function of monomer concentration (0.05 – 0.5 M), deposition time (5 – 60 min), and deposition temperature (2 °C or 25 °C). The supporting electrolyte concentration was varied from 0.1 – 1.0 M to determine if in-situ salt doping concentration could be controlled. Bromoisobutyronitrile, the radical initiator, was held constant at 0.01 M for all experiments.⁴⁷ All depositions onto copper antimonide electrodes (planar or foam) were done with 0.2 M PEGDA solutions and deposition time was one hour.

Impedance measurements were carried out with a frequency range of 1 Hz to 1 MHz with an amplitude voltage of 10 mV vs open circuit potential (OCP). The OCP was measured for 100 seconds prior to the impedance measurement.

To determine the thickness of the polymer films deposited on ITO, side view images were taken using SEM. Samples were dipped in liquid nitrogen for 30 sec prior to breaking. Samples were side mounted for SEM viewing and a 10 nm layer of gold was sputtered onto the samples. Images were taken in multiple locations on the sample and each image included multiple thickness measurements. Measurements were compiled using Origin to calculate means and standard deviations.

RESULTS AND DISCUSSION

The hypothesis of this chapter is that reductive electrodeposition of poly(ethylene glycol) diacrylate out of an aqueous solution containing lithium supporting electrolyte will afford a salt-doped solid-state separator material that conformally coats 3-D structures, exhibits high electronic resistance and high ionic conductivity. The hypothesis will be tested through SEM

imaging to examine how conformal coatings will be, along with impedance spectroscopy to determine electronic and ionic conductivities. Aside from the main hypothesis, a few other significant parameters will be investigated such as film thickness dependences (through SEM and profilometry), film atomic makeup (through XPS), completeness of polymerization and dryness of sample (through FTIR), crystallinity of polymer film (through XRD) and breakdown and glass transition temperatures of the polymer film (through TGA and DSC, respectively).

A radical initiator was required in the polymerizations because the monomer alone did not polymerize at a potential less negative than water reduction. The first radical initiator investigated was potassium persulfate ($K_2S_2O_8$). This initiator was problematic in that, depending on the substrate, polymerization sometimes occurred spontaneously without applying a potential. Therefore, the more stable radical initiator, BrIBN, was employed. Cyclic voltammetry (CV) data (Figure 2.4) indicated that the initiator was reduced at potentials more negative than ca. -1.0 V vs SSCE. Two peaks were observed in the voltammogram. The peak around -800 mV vs SSCE was not observed in CV data of BrIBN published by Agarwal *et al.* indicating an impurity in the BrIBN after synthesis and purification.⁴⁸ The BrIBN was distilled and its purity confirmed by NMR, so it is unclear what the impurity is. Regardless, the radical initiator performed as intended.

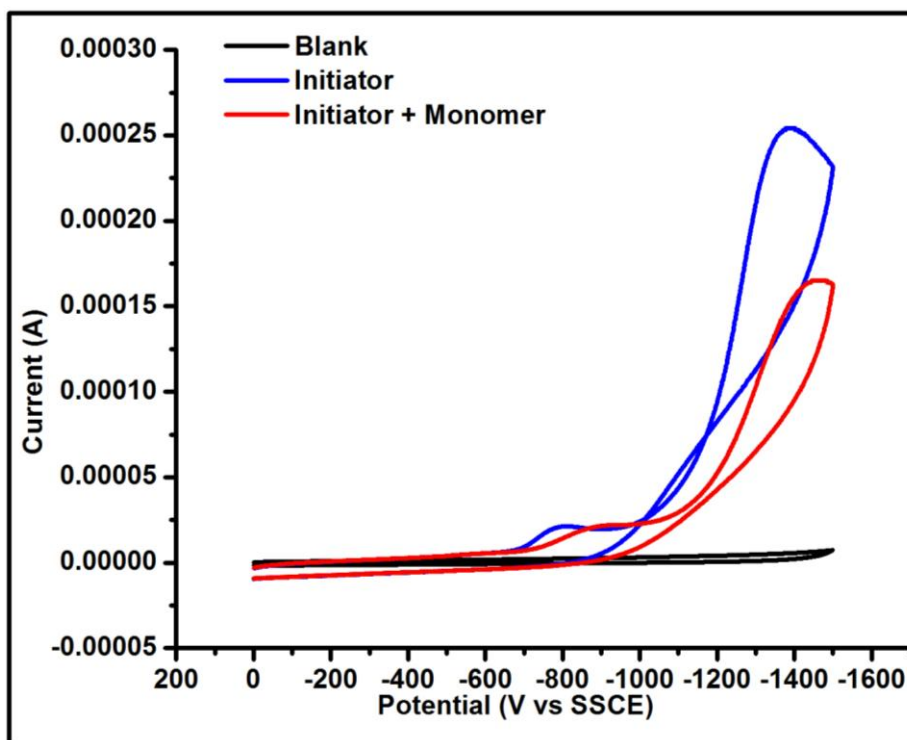


Figure 2.4. Cyclic Voltammetry data taken for radical initiator (BrIBN) and initiator plus monomer (PEGDA 700). CV was taken in a solution of 0.1 M LiClO₄ in degassed H₂O; scan rate = 100 mV/sec, working electrode = glassy carbon.

During polymerization the polymer layer swells allowing additional monomer and initiator to reach the electrode surface facilitating further polymerization. Simultaneously, supporting electrolyte in solution partitions into the growing polymer establishing an equilibrium between the polymer and solution. When the electrode is removed from solution and dried, that salt is expected to become entrapped in the polymer matrix leading to enhanced, in-situ salt doping. Deposition baths with 0.1, 0.5, and 1.0 M LiClO₄ supporting electrolyte were used to test this hypothesis. Although salt doping of the isolated polymer matrix was confirmed by XPS (Figure 2.5), there was no significant change to the ionic conductivity of the resulting film. The salt doping was confirmed by the presence of chlorine in the polymer matrix. Lithium was not detected, but lithium is difficult to detect by XPS in low concentrations because of its low

photoelectric cross section with Al K α excitation.⁴⁹ This was interpreted as only a small amount of supporting electrolyte can get incorporated into the polymer matrix and higher concentrations in solution do not necessarily mean a higher concentration of lithium salt will partition into the polymer matrix. It is likely that lithium perchlorate prefers an aqueous media over a polymer matrix media and therefore, the bulk of supporting electrolyte does not partition into the polymer matrix and remains in solution.

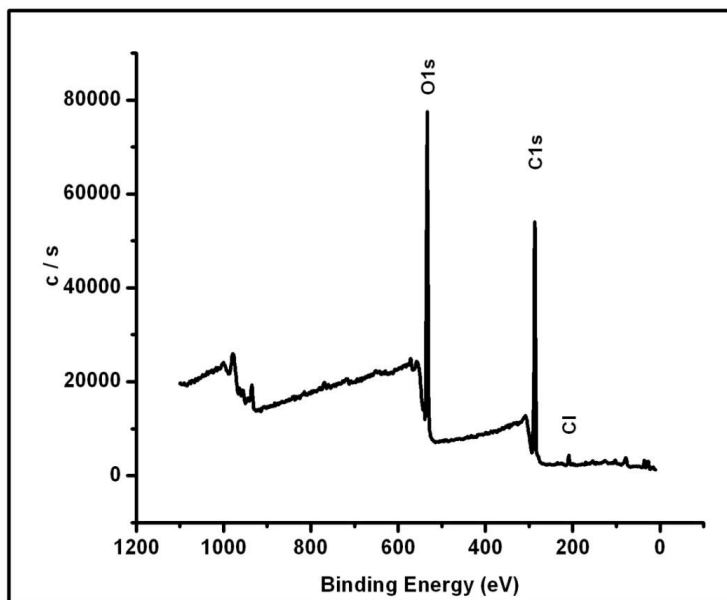


Figure 2.5. XPS spectra for PEGDA 700 deposited onto Cu₂Sb planar substrate. The chlorine peak is from salt doping with LiClO₄. Lithium is extremely hard to detect by XPS in low concentrations, which is probably why none was detected.⁴⁶

Infrared spectroscopy (Figure 2.6) was used to determine if either free monomer or water was trapped in the polymer matrix after drying at 40 °C for 16 hours. From IR data it is clear that no significant amounts of monomer (C-C double bond stretching frequency ca. 1635 cm⁻¹) or

water (OH stretching frequency ca. 3200-3650 cm^{-1}) are trapped in the polymer layer after drying the sample. This is important because monomer or water trapped in the matrix would behave as a solvent for the lithium salt and the separator would no longer be truly solid-state. Water removal is especially important for Li ion cell construction because of the voltages achieved during cycling of the cell. The voltages are large enough to reduce water at the cathode and oxidize water at the anode.

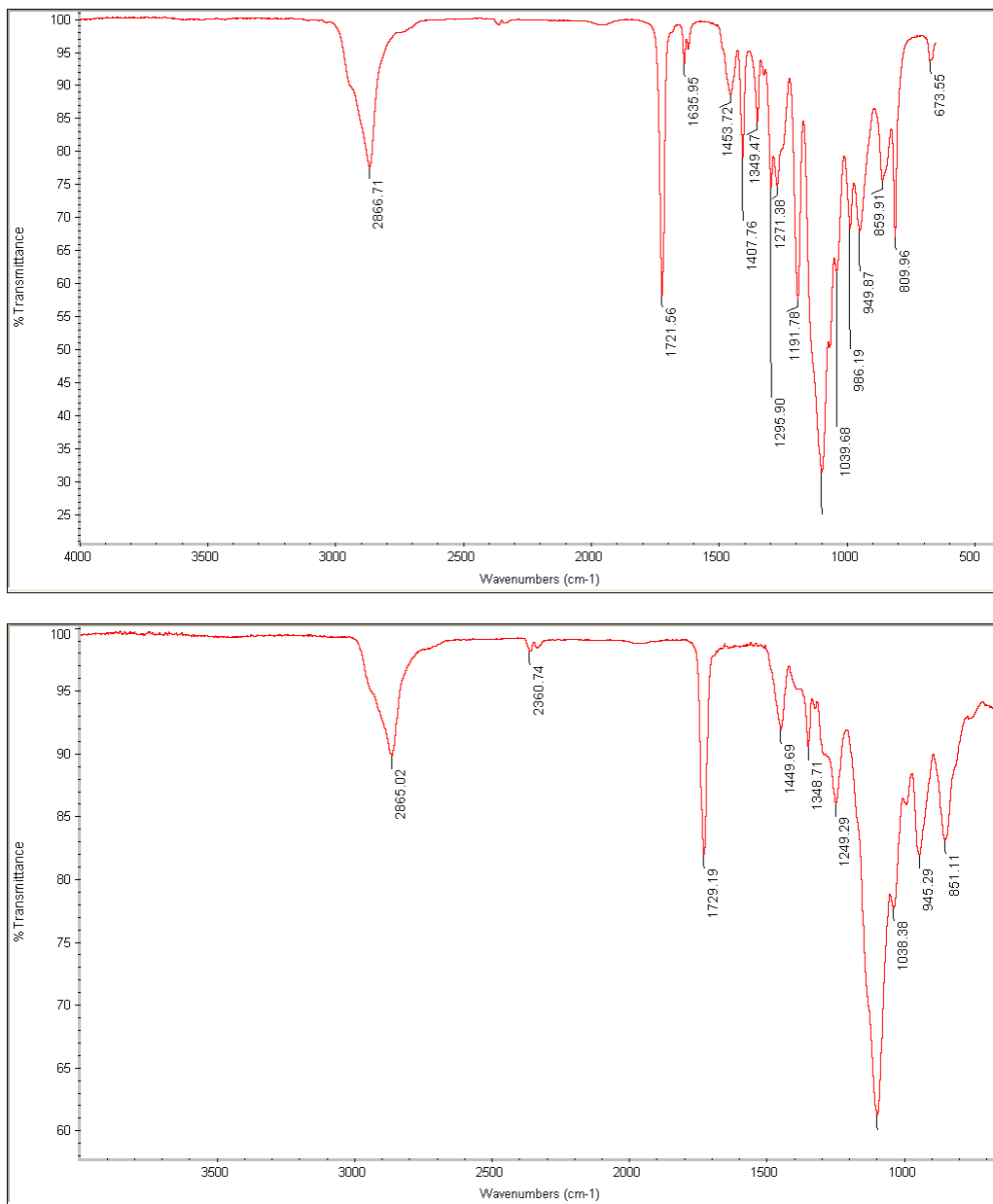


Figure 2.6. IR data; Top) IR spectra for PEGDA (monomer, MW= 700 g/mol), there is a band at 1635.95 that can be assigned to C-C double bond stretching. Bottom) IR spectra of the polymer film after drying at 40 °C for 16 hrs in a vacuum oven. Note the band at 1635.95 is no longer visible nor are bands associated with water (3200-3650 cm^{-1}) apparent, the latter indicating the dryness of the sample.

Seen in Figure 2.7, the deposited polymer thickness was measured as a function of deposition time (a), deposition temperature (b), and monomer concentration (c). Because the polymer system swells in the aqueous solvent, its thickness increased with deposition time as monomer continuously reached the electrode surface and is polymerized. It is unclear at this time why the polymer thickness did not increase significantly when the deposition time was increased from 15 to 30 minutes, but the variation in thickness from sample to sample did increase. This is evidence that thickness of polymer may be more difficult to control as thickness increases.

Polymer film thickness was also monitored as a function of deposition temperature. This was of interest because at lower temperatures there should be slower polymerization and diffusion rates, leading to possibly less variation in film thickness. A limited range of temperatures were available for study. First, the solvent inherently limited the temperature to between 0-100 °C. Additionally, however, the ITO slides underwent an undetermined reaction at 50 °C during the polymerization, which turned the electrode an iridescent color with no polymer layer being formed. Thus, efforts to deposit from solutions above 50 °C were not attempted. Moreover, already at 25 °C there was a noticeable increase in the variability in thickness from sample-to-sample, so efforts were focused on lower temperatures. By lowering the deposition temperature from room temperature to 2 °C, the polymer film thickness was decreased along with the variation in film thickness. This is due to slower diffusion and slower polymerization rates.⁵⁰⁻⁵² While the trend with temperature appears consistent with the arguments made above, the effect was not particularly dramatic (at least at the lower end of the accessible range) and deposition temperature was deemed to not be the best way to tune the thickness of the film.

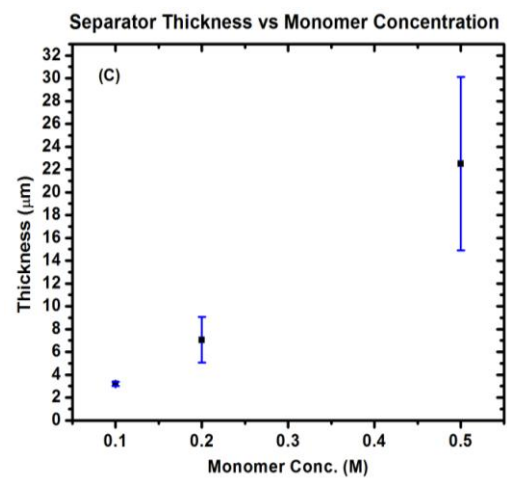
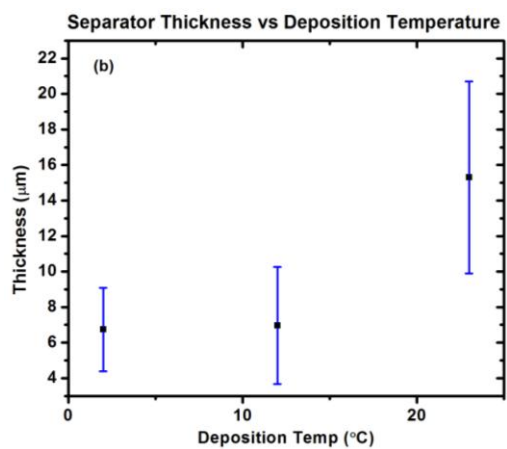
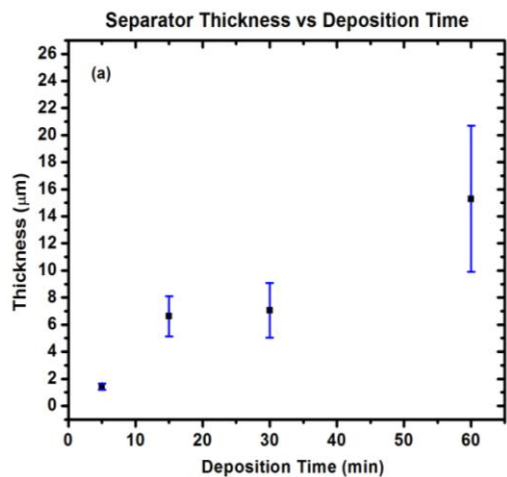


Figure 2.7. Graphs show deposited polymer thickness as a function of: time (a), deposition temperature (b), and monomer concentration (c). Error bars are shown in blue.

The effect of monomer concentration on the deposition was investigated at room temperature and with a deposition time of 30 min. Monomer concentrations of 0.05, 0.1, 0.2, and 0.5 M were examined. A significant effect on the thickness of the resulting polymer was observed. At low concentration, 0.05 M, no polymer layer formed on the ITO surface probably because only small oligomeric chains form which retain solubility in the aqueous media. Film thickness increased as monomer concentration increased beyond 0.05 M. As with increased deposition time and temperature, variation in film thickness also increased with increasing monomer concentration, as indicated by the error bars in Figure 3. With a monomer concentration of 0.5 M, the polymer thickness was greatly increased along with the sample-to-sample variation. The data indicate that there might be an optimal monomer concentration of 0.1-0.2 M, above which large variations in thickness are observed and below which no polymer film forms on the active electrode surface.

Figure 2.8 shows SEM images highlighting the change in surface morphology. Polymers deposited from 0.1 M monomer solutions exhibited a smooth and ripple-free surface (see, however, the repeat experiment described below). Polymers deposited from 0.2 M monomer solutions exhibit a smooth surface with noticeable ripples. Polymers deposited from 0.5 M monomer solutions exhibit a very rough surface composed of densely packed ripples. Repeated experiments follow these trends, although films deposited from 0.1 M and 0.2 M have both afforded smooth and rippled surfaces. The films are rippled or smooth prior to any drying step, so the phenomenon has been narrowed to the deposition itself. Further confusion arose when repeated depositions from the same mother-liquor solution produced both wrinkled and smooth

films. It was clear that at 0.5 M monomer concentration, the films were always extremely wrinkled, as seen in Figure 2.8. Further study is needed to determine what causes the ripples and how to minimize the ripples.

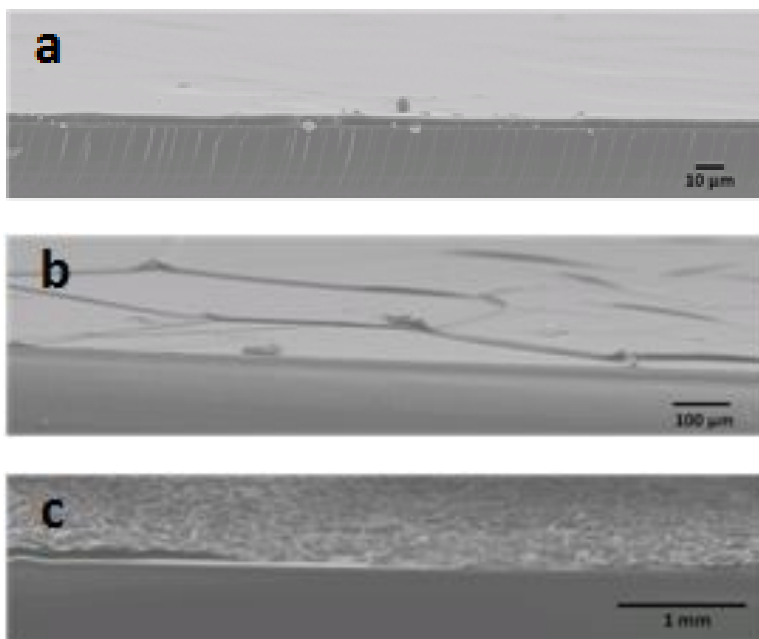


Figure 2.8. SEM images; top to bottom, a) polymer film deposited from 0.1 M monomer solution; b) polymer film deposited from 0.2 M monomer solution; c) polymer film deposited from 0.5 M monomer solution.

It is possible that as the polymerization proceeds, there may be density/composition gradients that develop within the polymer as a function of distance from the electrode which could impede transport of more monomer and/or initiator to the electrode surface. Moreover, free-radical polymerizations can be difficult to control because of the multiple propagation and termination pathways that can be taken, such as chain transfer or backbiting.³⁶ It is likely that, as the interior composition of the polymer changes, the mechanistic details of the polymerization could change for local environmental reasons, such as crystallite formation and subsequent

changes in diffusion rates and chain mobility. In any event, the variation in thickness from sample-to-sample increases with thickness irrespective of what parameter is changed to increase thickness (i.e., time, temperature or monomer concentration).

Electrochemical impedance spectroscopy was used to determine the ionic conductivity of various polymer films. Two methods were used. In/Ga eutectic was used to make a soft contact measurement with the polymer and ITO was the counter/reference electrode. This method was used by Rhodes *et al.* to measure impedance of ultrathin films.³² A gold/polymer/gold sandwich type setup, common in the literature, was also used.²⁹ Polymer was electrodeposited onto a gold substrate, dried and stored in a desiccator, and a gold rod (1 mm diameter) was used as the probe electrode. For In/Ga, since film thickness varied by SEM and the film thickness directly underneath the In/Ga during measurements was not known, the smallest thickness value was used since this would give the lower limit for the ionic conductivity, see Eq. 2.3, on page 89. For the gold/polymer/gold measurement the thickness was determined with a stylus profilometer and a thin region was selected for measurement for the same reason. Shown in Figure 2.9 is the fitted Nyquist plot of the impedance, using the In/Ga eutectic, along with SEM images used to determine thickness. This method was problematic in that the system was not under equilibrium conditions, as seen by the change in open circuit potential (OCP) prior to the impedance measurement (Figure 2.10). Because of the instability in OCP with time, measurements had to be taken as quickly as possible. It is possible that the liquid eutectic undergoes an unwanted reaction with the polymer or migrates into the polymer matrix.

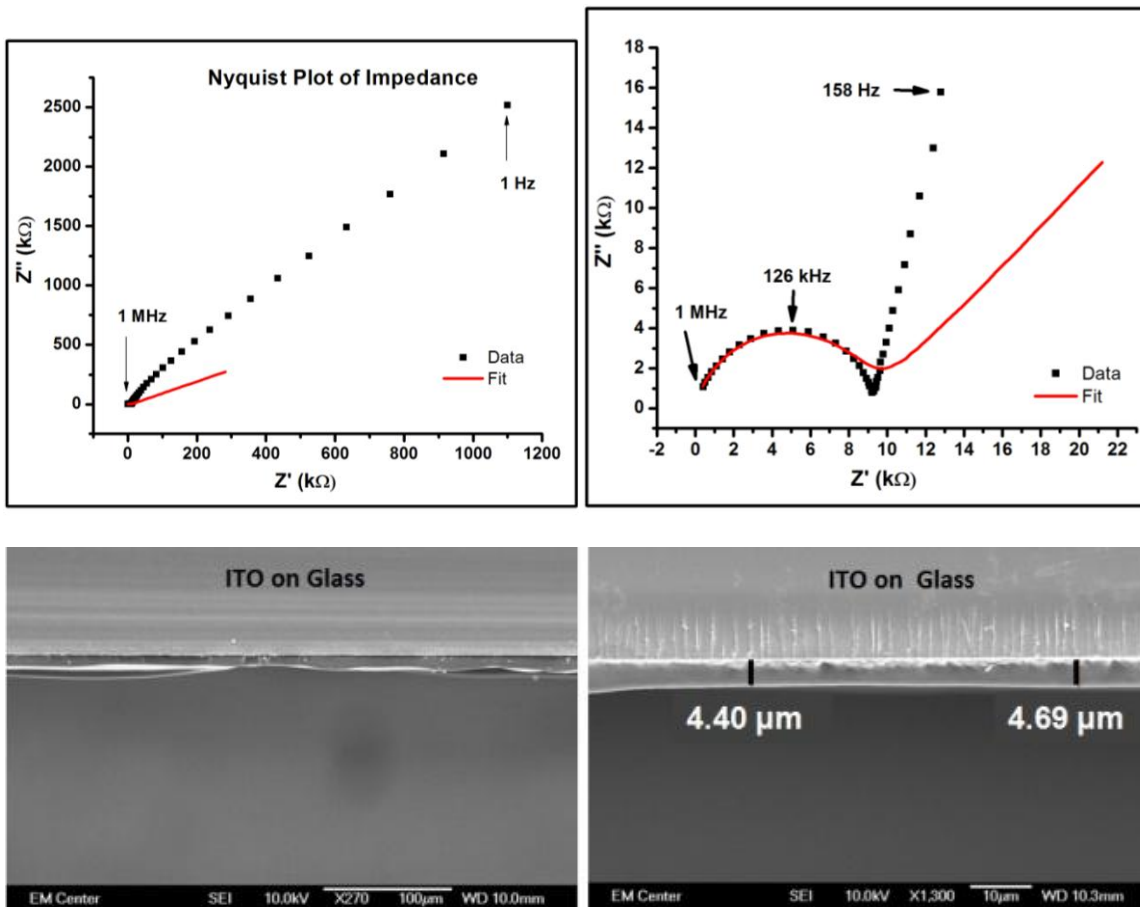


Figure 2.9. Nyquist plots of the impedance for the In/Ga eutectic method (top left: entire Nyquist plot; top right: high frequency region of the Nyquist plot) along with SEM images used to determine thickness; inset shows impedance over entire frequency range.

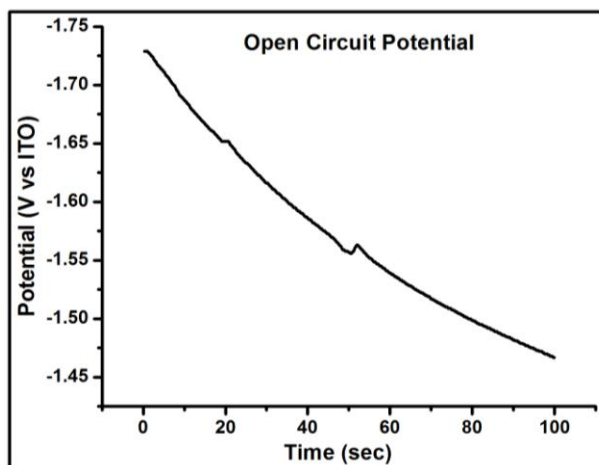


Figure 2.10. Open circuit potential for In/Ga soft contact method prior to impedance measurement.

Consequently, the two different contact methods were employed for comparison. Figure 2.11 shows the fitted Nyquist plot using a gold sandwich method. Figure 2.12 shows the profilometry mapping used to determine the thickness of the film for the gold sandwich sample. In the high frequency range a semicircle can be modeled using a constant phase element (CPE) in parallel with a resistor (see the equivalent circuit in Figure 2.13).

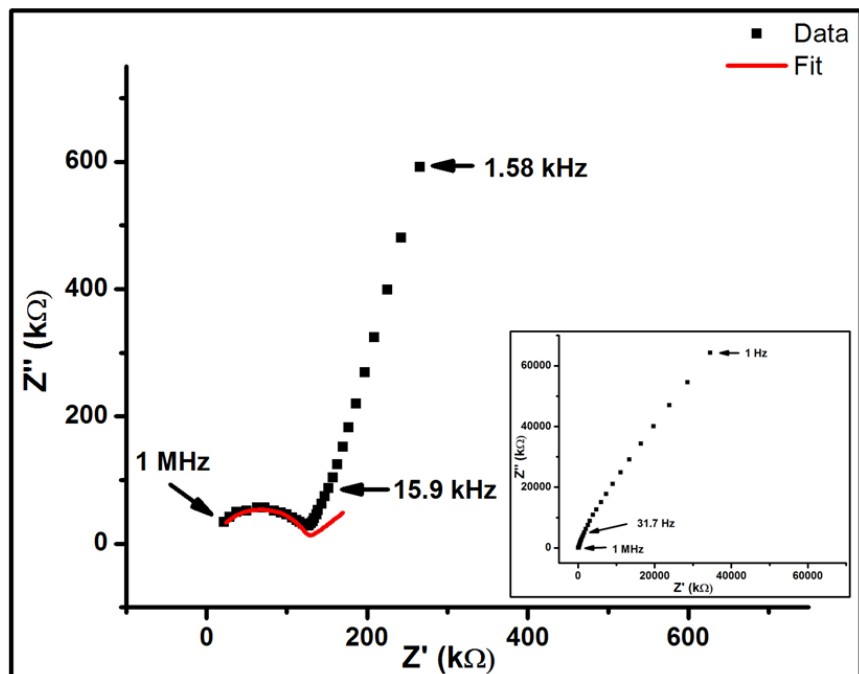


Figure 2.11. Nyquist plots of the impedance for the gold sandwich method; inset shows impedance over entire frequency range. The film thickness was determined from Figure 2.12.

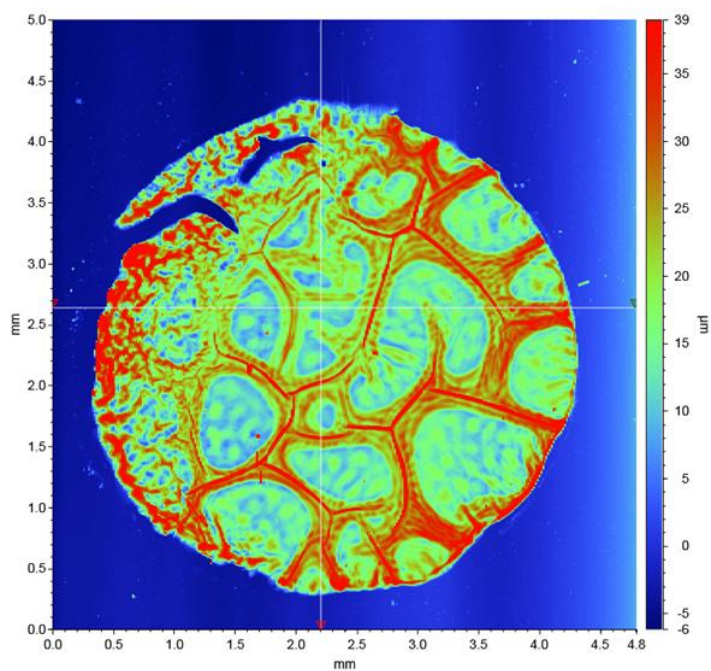


Figure 2.12. Topographical map of polymer layer deposited from 0.2 M monomer bath onto a gold substrate. The film exhibits significant surface rippling. X and Y direction thickness profiles can be found in the Appendix 2 (pg 182).

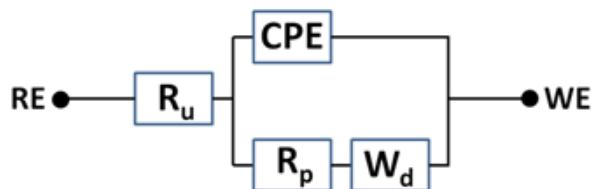


Figure 2.13. Equivalent circuit used to model the impedance data. R_u = uncompensated resistance, R_p = polarization resistance, CPE = constant phase element, W_d = Warburg diffusion.⁵¹

The semicircle in the Nyquist plot (Figure 2.9 and Figure 2.11) is depressed, which is believed to be due to a combination of Cole-Cole distributions in the polymer separator along with leaky or imperfect interfacial capacitance.^{53,54} The Cole-Cole distribution is a distribution of relaxation times and is related to ethoxy chain rotation being influenced by the Li^+ , which in turn increases chain entanglement.⁵⁵ Cole-Cole distributions, which have been discussed for $LiClO_4/PEO$ systems, give rise to a depressed semicircle in the Nyquist plot.^{53,55} Leaky or imperfect interfacial capacitance also gives rise to a depressed semicircle.⁵⁴ Furthermore, leaky interfacial capacitance gives rise to slopes more positive than -1 and maximum phase shifts which do not reach -90° in the Bode plots (not shown), as was seen for this separator material.⁵⁴ Beyond this high frequency semicircle, a diffusional tail can be seen. This tail is not ideal (not at a 45° angle) for Warburg diffusion, making modeling difficult.⁵⁶ One reason could be the effect of the blocking electrodes, leading to a slope between 45° and 90° .⁵⁷ A blocking electrode behaves like a capacitor: charge cannot intercalate the electrodes and only builds up on the surface of the electrode, and the response seen in a Nyquist plot is a line with a slope of 90° (a vertical line). If Warburg diffusion and blocking electrode effects were both occurring over the same frequency range, the averaging of the signals could lead to a line with a slope between 45° and 90° . A second reason for the non-ideal diffusional tail could be a variation in the chemical diffusion

coefficient. This behavior has been seen in insertion cathodes (LiCoO_2 and LiFePO_4) for different levels of charging/discharging and was attributed to variation in the diffusion coefficient as a result of variable stoichiometry of the active material.⁵⁸ Since the polymer separator has some short range order according to XRD (Figure 2.14), there is the possibility for variation in the diffusion coefficient.

051612Polymer

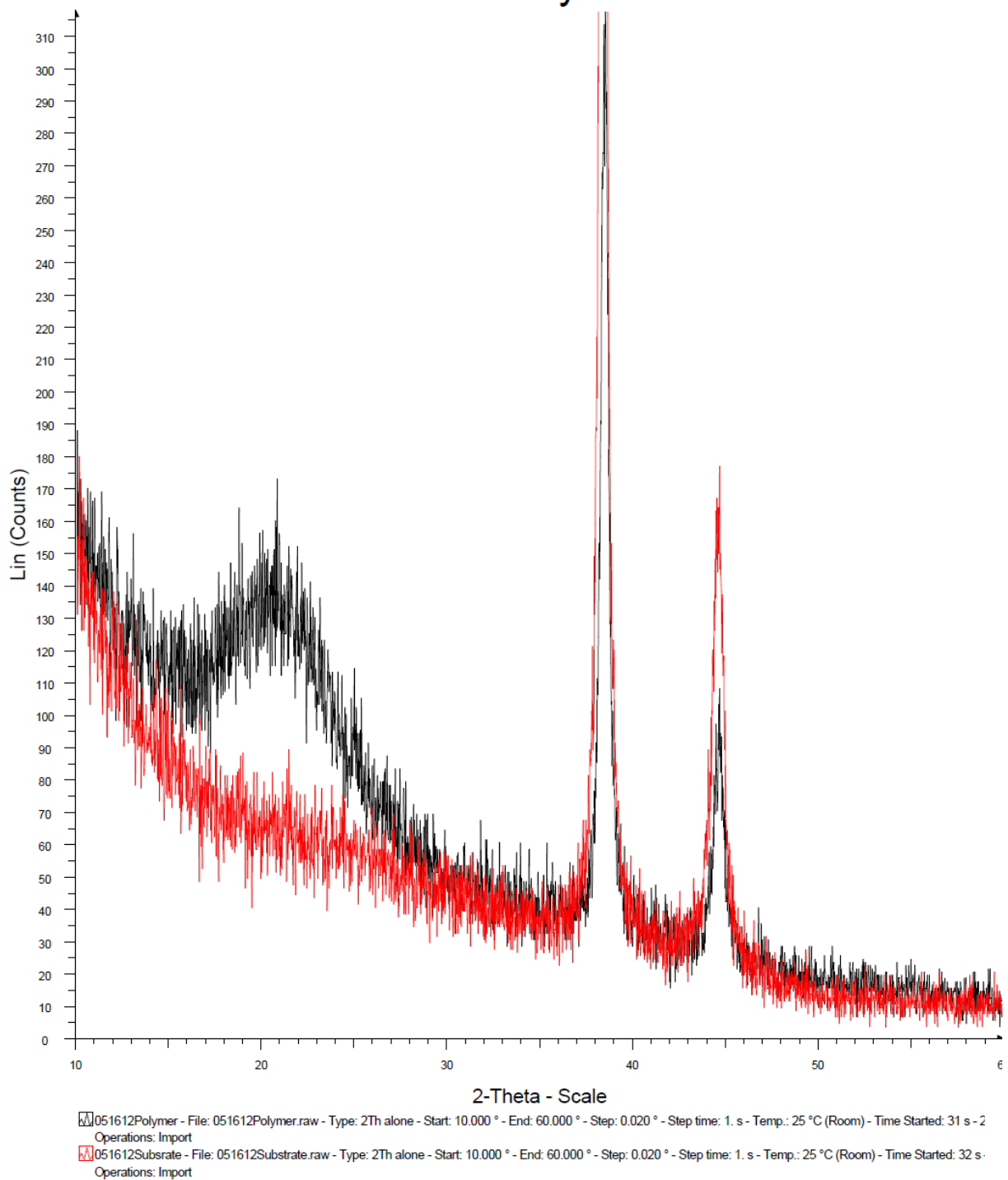


Figure 2.14. XRD data for separator material deposited on gold. Red trace is just the substrate (gold) and black trace is polymer plus substrate. A peak around 20 2θ is evidence of short range crystallinity.

Using the fit values for the polarization resistance (R_p) the ionic conductivity was calculated using the equation below; where σ = ionic conductivity, d = separator thickness, SA = surface area of working electrode, and R_p = polarization resistance.

$$\sigma = d/(SA * R_p) \quad (\text{Eq. 2.3})$$

The surface area was held constant for the In/Ga experiment by using a glass tube with a diameter of 3 mm to contain the In/Ga. Electrical contact to the In/Ga was achieved with a tungsten wire. Using this method, with a film thickness of 4.4 μm , an ionic conductivity of 6.5×10^{-7} S/cm was calculated. Using a gold rod with diameter of 1 mm, with a film thickness of 5.0 μm , an ionic conductivity of 5.8×10^{-7} S/cm was calculated. Both methods are in good agreement with one another with an average ionic conductivity of 6.1×10^{-7} S/cm. These values are impressive given that no salt doping steps were needed. For comparison, MacCallum *et al.* reported an ionic conductivity of 1×10^{-7} S/cm for an amorphous PEO/LiClO₄ separator.⁵⁹ These values is similar to most solid polymer electrolytes, but still 2-3 orders of magnitude lower than the leading solid state separators, poly(dimethylsiloxane/PEO) copolymers.²³ Further work is needed to increase the ionic conductivity of the PEGDA/LiClO₄ separator material.

Linear sweep voltammetry (LSV) was used to determine the electronic conductivity of the polymer film; the linear sweep can be seen in Figure 2.15. The LSV data was collected on the same sample that the soft contact impedance data was collected, directly after collecting the impedance data. With a surface area of 0.0707 cm^2 and using the lower limit thickness of 4.4 μm ,

an electronic conductivity of 3.5×10^{-8} S/cm was calculated. For a 10 micron thick separator, this value would calculate to 0.14 mA of current for a 4 V battery using Ohms law. This value of leakage current is too high and further work is needed to decrease the electronic conductivity.

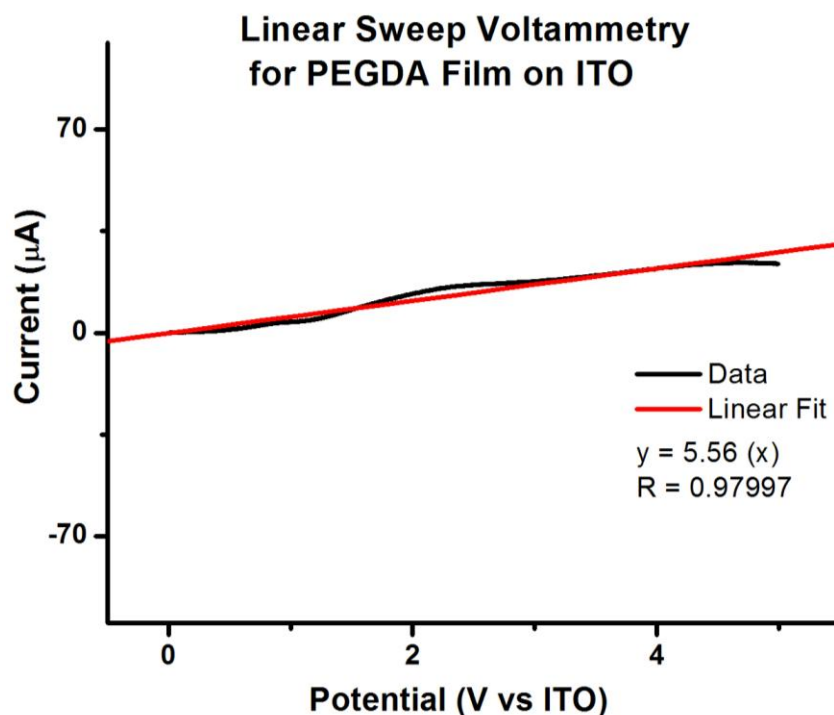


Figure 2.15. Linear sweep voltammetry for PEGDA film on ITO. Data was collected using the same setup as the soft-contact impedance measurement.

PEDGA 700 was also deposited onto Cu_2Sb planar and 3-D foam architectures in attempts to construct full lithium-ion cells and cycle them. Cu_2Sb was chosen because it has great promise as an anode material for lithium-ion batteries.⁶⁰ In a full cell with LiCoO_2 cathodes, the Cu_2Sb was the anode material, but in half cells with $\text{Li}_{(m)}$, the Cu_2Sb was the cathode material. In either case, planar or foam structure, 1.0 M LiClO_4 dissolved in ethyl carbonate:dimethyl carbonate (1:1) was needed as a plasticizer because the solid-state ionic conductivity was too low to cycle a solid state cell. Although the separator does conformally coat

all substrates, constructing a full cell proved problematic and was not accomplished on planar or foam substrates. On planar Cu_2Sb that had been electrodeposited onto copper foil, a half cell vs lithium was successfully constructed and cycled. The cell was charged at a rate of $C/3.5$ and discharged at a rate of $5C$ for 10 cycles. The two charging plateaus for copper antimonide can be seen, and occurred at the proper voltages vs $\text{Li}_{(m)}$. The data showed the separator material allowed good chemical communication between the anode and cathode, that significant interfacial resistances were not growing with time and were not present when cell was constructed, and that the separator material was not degrading over 10 cycles. The cycling data is shown in Figure 2.16.

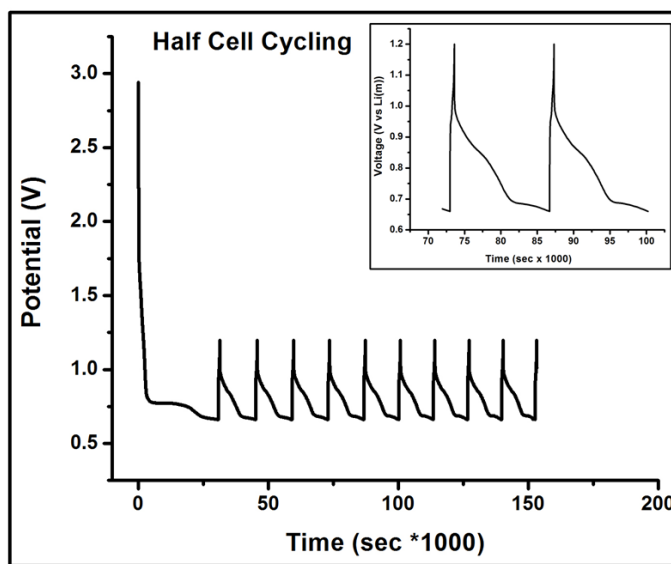


Figure 2.16. Cycling data for half cell vs. lithium, 10 cycles total; charged at $C/3.5$ and discharged at $5C$.

For the foam architecture, a half cell was not possible since once the Cu_2Sb was coated with the separator, it was not possible to fill the remaining void space with lithium metal. Attempts to make a full cell with a LiCoO_2 based slurry typically led to shorting as the polymer layer had to endure multiple cycles of swelling and drying, due to solvent in the slurry, which in

turn led to cracking and shorting of the device. A full cell of this type was freeze fractured using $N_2(l)$ and side view SEM images confirmed a fairly uniform coating of the polymer on the foam structure (Figure 2.17). The triangular shape was a piece of the Cu_2Sb coated copper foam. The deposited polymer layer is a dark smooth layer *ca.* 4 μm in thickness that can be seen coating the foam. Outside of this layer the remaining area is the $LiCoO_2$ based matrix. The result is very interesting because it shows that a uniform coating was applied to a three dimensional structure even though the electric field coming from the 3-D working electrode during the deposition was expected to be non-uniform. In other words, the non-uniform electric field present during the deposition did not lead to thick polymer deposits at points of higher electric field and thin polymer deposits at points with lower electric field.

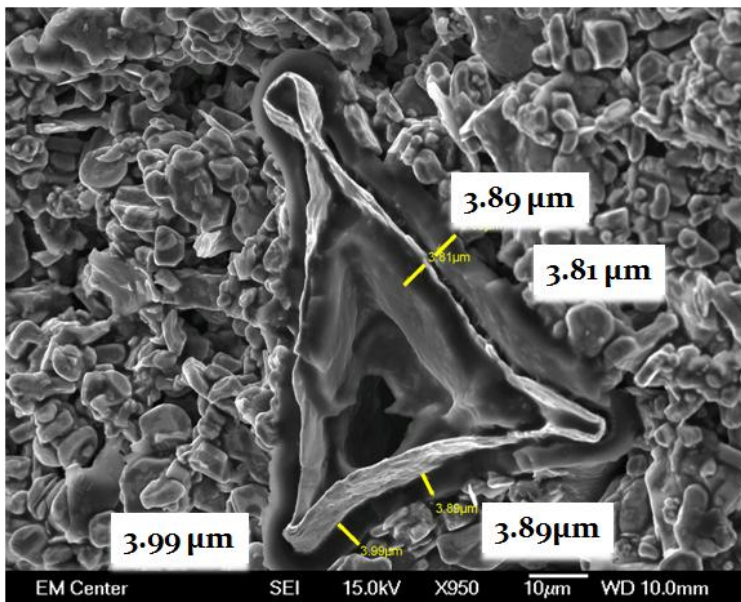


Figure 2.17. SEM image of polymer separator coating a 3-D structure (triangular piece) after void space was filled with a $LiCoO_2$ based cathode slurry and dried (outer micron particles). The sample was freeze fractured to expose interior for imaging.

Thermogravimetric analysis (TGA, Figure 2.18) and differential scanning calorimetry (DSC, Figure 2.19) were used to determine the break-down and glass transition temperatures, respectively, of the electrodeposited polymer. A glass transition temperature (T_g) of -40 °C was determined from DSC data. This value is in fair agreement with literature published by Priola *et al.* who reported a T_g of -47.5 °C and -55.3 °C for UV-cured PEDGA 600.⁶¹ The glass transition temperature is important because the ionic conductivity will decrease as the polymer loses chain mobility. A breakdown temperature of 200 °C was determined from TGA data. The breakdown temperature is important for functionality and safety. If the polymer cannot maintain structural rigidity at the temperature extremes of operation, then the cell will short.

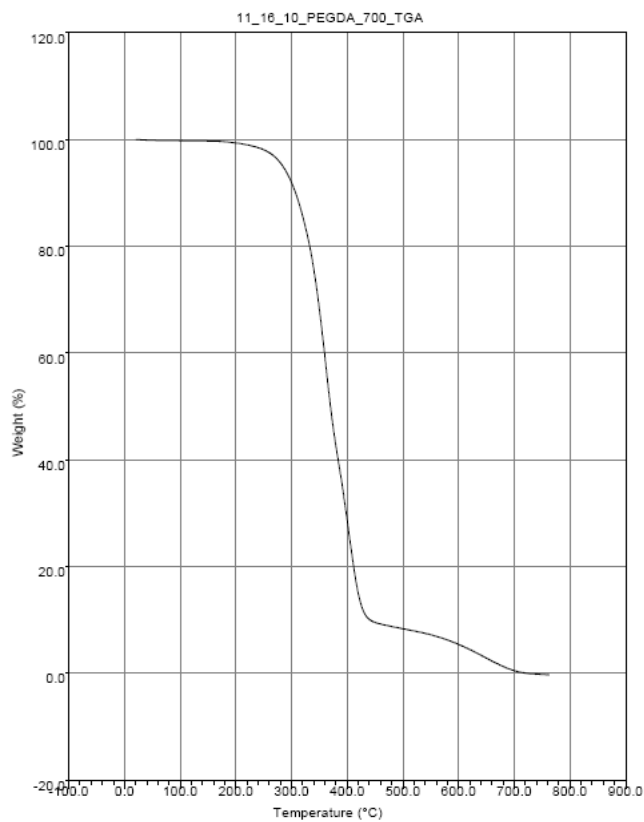


Figure 2.18. Thermogravimetric analysis shows a breakdown temperature of *ca.* 200 °C.

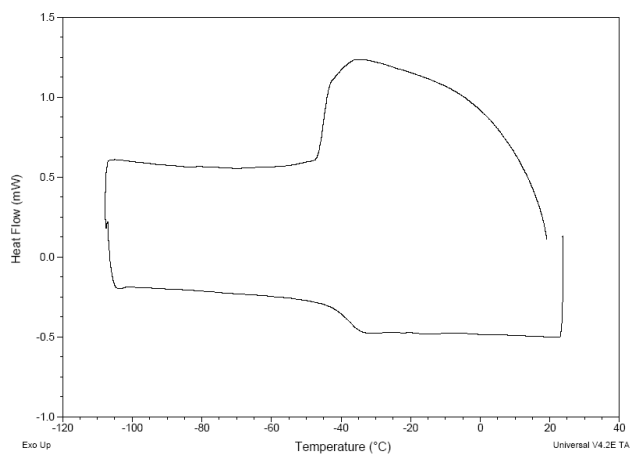


Figure 2.19. Differential scanning calorimetry shows a glass transition temperature of *ca.* -40 °C.

CONCLUSION

The monomer chosen was poly(ethylene glycol) diacrylate which afforded a highly amorphous polymer film when electrodeposited onto ITO out of aqueous solution. It is worth noting that XRD data do suggest some short range crystallinity, likely due to ethylene glycol units forming a helical structure around Li^+ ions.⁴³ The thickness of the polymer film deposited was monitored as a function of monomer concentration, deposition time, and deposition temperature. As expected, thickness of film is directly related to all three variables; a thicker film was afforded by an increase in temperature, monomer concentration, or deposition time. Film thickness varies significantly from sample to sample and that variability increased with thickness. At low monomer concentration (0.05 M), no polymer formed on the surface of the electrode. It was also noticed that 0.1 M monomer concentration led to a smoother polymer surface as seen by SEM, while higher monomer concentrations increased the roughness of the polymer surface.

The hypothesis of this chapter was that reductive electrodeposition of poly(ethylene glycol) diacrylate out of an aqueous solution containing lithium supporting electrolyte would afford a salt-doped solid-state separator material that conformally coated 3-D structures, exhibited high electronic resistance and high ionic conductivity. Polymer films were successfully electrodeposited out of aqueous solutions onto ITO, gold, and Cu_2Sb substrates (both 2-D and 3-D). Film deposition was confirmed by XPS and SEM/profilometry data. Impedance data show an average ionic conductivity of 6.1×10^{-7} S/cm. This value is impressive given the fact that no post-polymerization salt-doping steps or plasticizer were necessary, but further work is needed to increase the ionic conductivity. XPS data confirms that LiClO_4 does get incorporated into the polymer matrix during polymerization. Linear sweep voltammetry was used to determine the

electronic conductivity of the polymer film, which was 3.5×10^{-8} S/cm. For a 10 micron thick separator, this value of electronic conductivity would calculate to 0.14 mA of current for a 4 V battery using Ohms law. This value of leakage current is too high and further work is needed to decrease the electronic conductivity. TGA and DSC data show the polymer film has a large operating window (-40 to 200 °C) which is potentially good for practical application.

Table 2.2 below summarizes criteria that were used to judge the PEGDA films. As can be seen in the table, a PEGDA-based separator material does not meet the ideal physical properties for a lithium ion battery separator material. PEGDA can be reductively polymerized out of an aqueous solution though a radical initiator. PEGDA-based solid-state films are plagued by low ionic conductivity as are most solid-state polymer electrolytes, but when plasticized half-cell cycling was demonstrated. The film coatings are much thicker than desired and thicknesses vary significantly. Films are not grafted, which increases the likelihood of faults and shorts in a final battery cell. The glass transition temperature is low enough to be satisfactory, allowing for segmental motion of the polymer and ionic conductivity at room temperature. The electronic conductivity is also low enough, but not ideal for commercial application because battery shelf-life would be affected as the battery could self-discharge over time.

Table 2.2. A summary of the physical properties that were used as criteria to judge PEGDA films. Included are ideal values along with some of the best reported values in literature.

| Physical Property | PEGDA | Ideal | Reported in Lit. |
|---------------------------|---------------------------|---------------------|---|
| Reductively Polymerized | yes | yes | yes (polymers in general, not PEGDA) (Ref 46) |
| Electronic Conductivity | 3.5×10^{-8} S/cm | zero | 7×10^{-12} S/cm (Ref 32) |
| Ionic Conductivity | 6.1×10^{-7} S/cm | $\geq 10^{-2}$ S/cm | 1.6×10^{-4} S/cm (Ref 23) |
| Conformal/Uniform Coating | 9.0 ± 5.5 μ m | yes | 21 ± 2 nm (Ref 32) |
| Thickness | 1-20 μ m | 10-50 nm | 21-43 nm (Ref 32) |
| Grafted | no | yes | yes (Ref 46) |
| Tg | -40 °C | -100 °C | -80 °C (Ref 23) |

FUTURE WORK

Future work on PEGDA based films should be focused on transferring what has been learned here and applying it to a more fruitful system. Electrodeposition as a technique to coat a 3-D structure with a separator material was demonstrated and could be applied elsewhere. To identify possible systems that would be more fruitful, the table of criteria (Table 2.1 or Table 2.2) should be used. Focus should be made on affording nanoscale separator materials that are grafted to the electrode surface. Self-limiting polymerizations should be investigated as they produce extremely thin and uniform coatings.^{32,33} Once a nanoscale and grafted separator film can be deposited, focus should be made on increasing the ionic conductivity of the separator material. Methods to increase the ionic conductivity include: addition of flexible PEO-based arms to increase segmental motion of the polymer and enhance lithium diffusion rates; incorporation of inorganic components which has been shown to increase transference numbers and ionic conductivity²³; use of different lithium salts, which has been shown to affect ionic conductivity⁶²; incorporation of anionic polymers that act as hopping sites for lithium ions²⁵.

REFERENCES

- (1) Energy Storage Technologies Market: Type, Applications and Strategic Opportunities (Forecast to 2016), Market Research Report: MarketsandMarkets <http://www.marketsandmarkets.com/Market-Reports/high-power-energy-storage-advanced-technologies-and-global-market-research-95.html> (accessed Sep 20, 2012).
- (2) Tuite, D. Get The Lowdown On Ultracapacitors <http://electronicdesign.com/content/topic/get-the-lowdown-on-ultracapacitors17465/catpath/power> (accessed Sep 20, 2012).
- (3) Wei, W.; Cui, X.; Chen, W.; Ivey, D. G. *Chem. Soc. Rev.* **2011**, *40*, 1697–1721.
- (4) Wang, G.; Zhang, L.; Zhang, J. *Chem. Soc. Rev.* **2012**, *41*, 797–828.
- (5) Bose, S.; Kuila, T.; Mishra, A. K.; Rajasekar, R.; Kim, N. H.; Lee, J. H. *J. Mater. Chem.* **2012**, *22*, 767–784.
- (6) Bruce, P. G.; Scrosati, B.; Tarascon, J.-M. *Angew. Chem. Int. Ed.* **2008**, *47*, 2930–2946.
- (7) Tarascon, J.-M.; Armand, M. *Nature* **2001**, *414*, 359–367.
- (8) Lee, S. W.; Yabuuchi, N.; Gallant, B. M.; Chen, S.; Kim, B.; Hammond, P. T.; Shao-Horn, Y. *nature nanotechnology* **2010**, *116*, 531–537.
- (9) Long, J. W.; Dunn, B.; Rolison, D. R.; White, H. S. *Chemical Reviews* **2004**, *104*, 4463–4492.
- (10) Arthur, T. S.; Bates, D. J.; Cirigliano, N.; Johnson, D. C.; Malati, P.; Mosby, J. M.; Perre, E.; Rawls, M. T.; Prieto, A. L.; Dunn, B. *Mrs Bulletin* **2011**, *36*, 523–531.
- (11) Chockla, A. M.; Klavetter, K. C.; Mullins, C. B.; Korgel, B. A. *ACS Appl. Mater. Interfaces* **2012**, *4*, 4658–4664.
- (12) Yiping, T.; Xiaoxu, T.; Guangya, H.; Huazhen, C.; Guoqu, Z. *Electrochimica Acta* **2012**, *78*, 154–159.
- (13) Kang, C.; Lahiri, I.; Baskaran, R.; Kim, W.-G.; Sun, Y.-K.; Choi, W. *Journal of Power Sources* **2012**, *219*, 364–370.
- (14) Pei, B.; Yao, H.; Zhang, W.; Yang, Z. *Journal of Power Sources* **2012**, *220*, 317–323.
- (15) Leung, K.; Qi, Y.; Zavadil, K. R.; Jung, Y. S.; Dillon, A. C.; Cavanagh, A. S.; Lee, S.-H.; George, S. M. *J. Am. Chem. Soc.* **2011**, *133*, 14741–14754.
- (16) Woo, J. H.; Trevey, J. E.; Cavanagh, A. S.; Choi, Y. S.; Kim, S. C.; George, S. M.; Oh, K. H.; Lee, S.-H. *Journal of The Electrochemical Society* **2012**, *159*, A1120–A1124.
- (17) Arora, P.; Zhang, Z. M. *Chemical Reviews* **2004**, *104*, 4419–4462.
- (18) Verma, P.; Maire, P.; Novák, P. *Electrochimica Acta* **2010**, *55*, 6332–6341.
- (19) Huang, X. *Journal of Solid State Electrochemistry* **2011**, *15*, 649–662.
- (20) Yang, M.; Hou, J. *Membranes* **2012**, *2*, 367–383.
- (21) Tilley, R. *Understanding Solids The Science of Materials*; John Wiley & Sons, Inc.: West Sussex PO19 8SQ, England, 2004.
- (22) Agrawal, R. C.; Pandey, G. P. *J. Phys. D: Appl. Phys.* **2008**, *41*, 223001/1–223001/18.
- (23) Meyer, W. H. *Advanced Materials* **1998**, *10*, 439–448.
- (24) Bruce, P. G. *Solid State Ionics* **2008**, *179*, 752–760.
- (25) Kang, W. C.; Park, H. G.; Kim, K. C.; Ryu, S. W. *Electrochimica Acta* **2009**, *54*, 4540–4544.
- (26) Park, C.-H.; Park, M.; Yoo, S.-I.; Joo, S.-K. *Journal of Power Sources* **2006**, *158*, 1442–1446.

- (27) Rajendran, S.; Uma, T. *Bulletin of Materials Science* **2000**, *23*, 27–29.
- (28) Kang, Y.; Lee, W.; Hack Suh, D.; Lee, C. *Journal of Power Sources* **2003**, *119-121*, 448–453.
- (29) Bronstein, L. M.; Joo, C.; Karlinsey, R.; Ryder, A.; Zwanziger, J. W. *Chemistry of Materials* **2001**, *13*, 3678–3684.
- (30) Goodenough, J. B. *Solid State Ionics* **1994**, *69*, 184–198.
- (31) Song, M.-K.; Cho, J.-Y.; Cho, B. W.; Rhee, H.-W. *Journal of Power Sources* **2002**, *110*, 209–215.
- (32) Rhodes, C. P.; Long, J. W.; Doescher, M. S.; Fontanella, J. J.; Rolison, D. R. *J. Phys. Chem. B* **2004**, *108*, 13079–13087.
- (33) Rhodes, C. P.; Long, J. W.; Rolison, D. R. *Electrochemical and Solid State Letters* **2005**, *8*, A579–A584.
- (34) Trahey, L.; Kung, H. H.; Thackeray, M. M.; Vaughey, J. T. *Eur. J. Inorg. Chem.* **2011**, *2011*, 3984–3988.
- (35) Ryu, I.; Choi, J. W.; Cui, Y.; Nix, W. D. *Journal of the Mechanics and Physics of Solids* **2011**, *59*, 1717–1730.
- (36) Painter, P. C.; Coleman, M. M. *Fundamentals of Polymer Science an Introductory Text*; Second.; CRC Press: Boca Raton, 1997.
- (37) Scrosati, B. *Applications of Electroactive Polymers*; Chapman and Hall: London, 1993.
- (38) Cram, S. L. *S. J. Appl. Poly. Sci.* **2003**, *87*, 765–773.
- (39) Qiu, W.; Ma, X.; Yang, Q.; Fu, Y.; Zong, X. *Journal of Power Sources* **2004**, *138*, 245–252.
- (40) Reale, P.; Panero, S.; Scrosati, B. *Journal of the Electrochemical Society* **2005**, *152*, A1949–A1954.
- (41) Kum, K.-S.; Song, M.-K.; Kim, Y.-T.; Kim, H.-S.; Cho, B.-W.; Rhee, H.-W. *Electrochimica Acta* **2004**, *50*, 285–288.
- (42) Yang, C.-M.; Kim, H.-S.; Na, B.-K.; Kum, K.-S.; Cho, B. W. *Journal of Power Sources* **2006**, *156*, 574–580.
- (43) Andreev, Y. G.; Bruce, P. G. *Electrochimica Acta* **2000**, *45*, 1417–1423.
- (44) Gadjourova, Z. A.; Andreev, Y. G.; Tunstall, D. P.; Bruce, P. G. *Nature* **2001**, *412*, 520–523.
- (45) Staunton, A. E.; Andreev, Y. G.; Bruce, P. G. *Faraday Discussions* **2007**, *134*, 143–156.
- (46) Danda, C. K.; Cai, R.; Wang, W.; Baba, A.; Advincula, R. C. *Polymeric Materials: Science and Engineering* **2008**, *98*, 444–445.
- (47) Stevens, C. L. *JACS* **1948**, *70*, 165–167.
- (48) Agarwal, R.; Bell, J. P. *J. Appl. Polym. Sci.* **1999**, *71*, 1665–1675.
- (49) Södergren, S.; Siegbahn, H.; Rensmo, H.; Lindström, H.; Hagfeldt, A.; Lindquist, S.-E. *J. Phys. Chem. B* **1997**, *101*, 3087–3090.
- (50) Nagaraja, G. K.; Demappa, T.; Mahadevaiah J. *Appl. Polym. Sci.* **2008**, *110*, 3395–3400.
- (51) Bergert, U.; Buback, M.; Heyne, J. *Macromol. Rapid Commun.* **1995**, *16*, 275–281.
- (52) Farrington Daniels; Robert A. Alberty *Physical Chemistry*; Third.; John Wiley & Sons, Inc., 1967.
- (53) Cole, K. S.; Cole, R. H. *J. Chem. Phys.* **1941**, *9*, 341–351.
- (54) Taylor, R.; Spotnitz, R.; Kendig, M.; Buchheit, R.; Loveday, D.; Contu, F. *A Short Course on Electrochemical Impedance Spectroscopy: Theory, Applications, and Laboratory Instruction* **2012**.

- (55) Salomon, M.; Xu, M.; Eyring, E. M.; Petrucci, S. *J. Phys. Chem.* **1994**, *98*, 8234–8244.
- (56) Liu, Y.; Zhao, R.; Ghaffari, M.; Lin, J.; Liu, S.; Cebeci, H.; De Villoria, R. G.; Montazami, R.; Wang, D.; Wardle, B. L.; Heflin, J. R.; Zhang, Q. M. *Sensors and Actuators A: Physical* **2012**, *181*, 70–76.
- (57) Ahmad, A.; Rahman, M. Y. A.; Suait, M. S. *Journal of Applied Polymer Science* **2012**, *124*, 4222–4229.
- (58) Atebamba, J.-M.; Moskon, J.; Pejovnik, S.; Gaberscek, M. *J. Electrochem. Soc.* **2010**, *157*, A1218–A1228.
- (59) Maccallum, J. R.; Smith, M. J.; Vincent, C. A. *Solid State Ionics* **1984**, *11*, 307–312.
- (60) Mosby, J. M.; Prieto, A. L. *Journal of the American Chemical Society* **2008**, *130*, 10656–10661.
- (61) Priola, A.; Gozzelino, G.; Ferrero, F.; Malucelli, G. *Polymer* **1993**, *34*, 3653–3657.
- (62) Niedzicki, L.; Kasprzyk, M.; Kuziak, K.; Żukowska, G. Z.; Armand, M.; Bukowska, M.; Marcinek, M.; Szczeciński, P.; Wiczorek, W. *Journal of Power Sources* **2009**, *192*, 612–617.

CHAPTER 3: SYNTHESIS AND CHARACTERIZATION OF DIAZONIUM SALTS WITH A POLY(ETHYLENE GLYCOL) APPENDAGE AND FILMS AFFORDED BY ELECTRODEPOSITION FOR USE AS A LITHIUM-ION BATTERY SEPARATOR MATERIAL

INTRODUCTION

As outlined in Chapter 2, there are many challenges to developing a nanoscale separator material for lithium-ion batteries. First, nanoscale materials are fragile and hard to work with. The separator cannot be made independently of the anode or cathode since assembly would be essentially impossible with such a thin material; therefore, the separator needs to be fabricated in situ. Second, the separator needs to conformally coat the 3-D nanostructure. Coating structures such as nanowires also limits fabrication methods. Some work has been done using atomic layer deposition to coat electrodes with a thin ceramic layer (Al_2O_3) to minimize solvent decomposition and solid electrolyte interface (SEI) formation, but the method is time-intensive and not cost effective for commercial use.^{1,2} Third, controlling the thickness of the separator can be difficult, especially for films only 10s of nanometers thick. For polymerizations, this usually requires a self-limiting polymerization mechanism to avoid incomplete or non-uniform film coverage. Fourth, regardless of thickness, the separator must be able to handle the physical stresses that occur during charging/discharging during which expansion/contraction processes occur. If the separator cannot withstand these stresses the battery will short. Fifth, the separator has to be electronically insulating when less than 100 nm thick, but also must be ionically conducting. These challenges are great so that progress in the field of nanoscale separators has been slow.

A PEGDA based film, as determined in chapter 2, does not meet the criteria for a nanoscale separator material for four reasons. Film thickness was difficult to control and afforded films with micron thicknesses in all cases. Furthermore, none of the PEGDA films underwent grafting and commonly shorted when constructing a full cell. Lastly, the films exhibited low ionic conductivity unless salt-doped plasticizer was added. However, the deposition method proved to be a good approach to conformally coat a three-dimensional electrode structure and allowed for in-situ salt doping of the deposited polymer.

With this in mind, a new approach was taken that focused on achieving nanoscale polymer films that would be grafted to the electrode surface. Diazonium salts were chosen because they have been shown to graft to electrode surfaces and exhibit great self-limiting deposition characteristics.³⁻⁵ Diazonium salts can be deposited out of acidic aqueous conditions ($\text{pH} \leq 3$) if the monomers are soluble.⁵ The grafting of diazonium salts involves a $1e^-$ reduction of the diazonium functional group followed by loss of $\text{N}_{2(g)}$ and phenyl radical formation.⁵ The phenyl radical then reacts with the electrode surface to form a chemical bond. Diazonium salts have been electro-grafted onto many electrode materials such as carbon, metals, oxides, semiconductors, and polymers.⁵ In summary, diazonium salts were chosen because they should afford a grafted and conformal coating of ideal thickness for a nanoscale three-dimensional architecture lithium-ion battery.

To test the hypothesis that a diazonium-based film would be grafted, nanoscale in thickness, and function as a lithium-ion battery separator material, four diazonium salt based monomers were synthesized and electrodeposited. To judge the deposited films, thickness was determined by profilometry or SEM imaging, grafting was determined by impedance

spectroscopy on sonicated samples, and impedance spectroscopy was used to determine ionic and electronic conductivities. Table 3.1 summarizes criteria that were used to judge the diazonium-based films along with the best reported values in literature.⁶⁻⁸

Table 3.1. A summary of the physical properties that were used as criteria to judge diazonium-based films. Included are ideal values along with some of the best reported values in literature.

| Physical Property | Ideal | Reported in Lit. |
|---------------------------|---------------------|-----------------------------------|
| Reductively Polymerized | yes | yes (polymers in general) (Ref 8) |
| Electronic Conductivity | zero | 7×10^{-12} S/cm (Ref 7) |
| Ionic Conductivity | $\geq 10^{-2}$ S/cm | 1.6×10^{-4} S/cm (Ref 6) |
| Conformal/Uniform Coating | yes | 21 ± 2 nm (Ref 7) |
| Thickness | 10-50 nm | 21-43 nm (Ref 7) |
| Grafted | yes | yes (Ref 8) |
| Tg | -100 °C | -80 °C (Ref 6) |

Three of the four monomers have never been reported in the literature and none have been used in lithium-ion battery separator applications. The monomers are: 4-(2-(2-(2-methoxyethoxy)ethoxy)ethyl)benzene diazonium tetrafluoroborate (p-triethoxy, synthesized by Bahr *et al.*⁹), 2-(2-(2-(2-methoxyethoxy)ethoxy)ethyl)benzene diazonium tetrafluoroborate (o-triethoxy), 4-(polyethylene glycol)benzene diazonium tetrafluoroborate (p-PEG), and 2-(polyethylene glycol)benzene diazonium tetrafluoroborate (o-PEG). The p-PEG and o-PEG short hand notation will be used for the remainder of this chapter. The structures are provided in Figure 3.1.

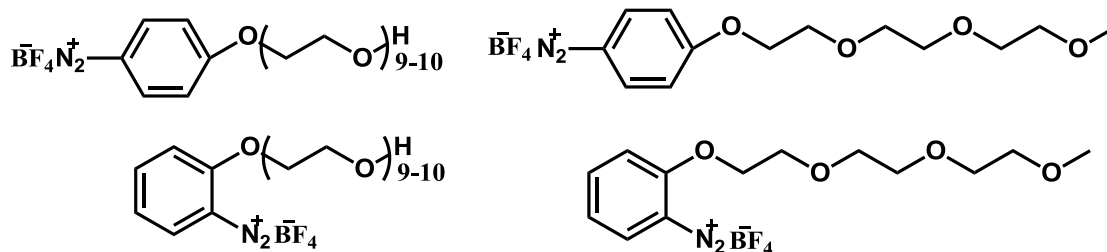


Figure 3.1. Monomer structures. Top left: p-PEG; bottom left: o-PEG; top right: p-triethoxy; bottom right: o-triethoxy.

EXPERIMENTAL

CHEMICALS

Dichloromethane was purged with nitrogen and dried over 4 Å molecular sieves before storing in a glove box. All other reagents were obtained commercially and used as received.

APPARATUS

Cyclic voltammetry (CV) and chronoamperometry experiments were carried out using a CH Instruments Electrochemical Workstation Model 750 D. Impedance measurements were carried out using a GAMRY Instruments Reference 3000 potentiostat/galvanostat. Nuclear magnetic resonance spectroscopy was carried out using a Varian Mercury-Inova 300 NMR Spectrometer Systems. Infrared spectroscopy (IR) measurements were performed using Nicolet 380 FT-IR spectrophotometer using KBr pellets.

SYNTHESES

All syntheses were modified from a publication by Bahr *et al.* who reported the synthesis of the p-triethoxy salt.⁹ For the diazotization reaction, the method published by Tang *et al.* was found to be more repeatable, yielded more product, and the product was a higher purity according to NMR.¹⁰ For increased purity, a silica column was employed on the o-PEG salt with 5 % MeOH in CH₂Cl₂ (by volume) as the eluent. Each diazonium salt synthesis involves 4 steps starting from an alcohol, see Figure 3.2. This reaction scheme is therefore useful for many starting materials as long as an alcohol group is present.

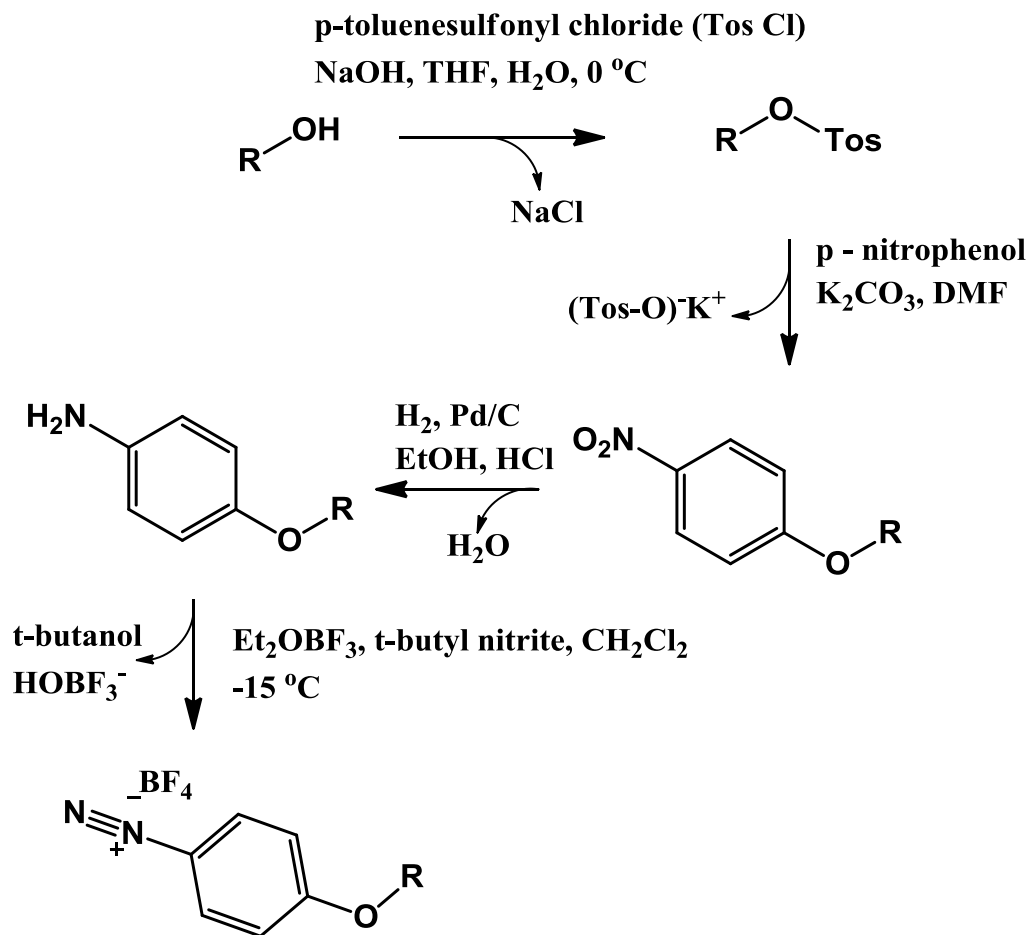


Figure 3.2. Reaction scheme used to synthesize diazonium salts starting from an alcohol. The reaction is applicable to many alcohols.^{6,7}

2-(2-(2-Methoxyethoxy)ethoxy)ethyl p-toluenesulfonate (1) was synthesized using the method published by Bahr *et al.*⁹ A clear and colorless oil was afforded at 93 % yield. ¹H NMR (CDCl₃) δ: 7.80 (d, 2H), 7.35 (d, 2H), 4.14 (t, 2H), 3.68 (t, 2H), 3.64 to 3.54 (m, 6H), 3.52 (t, 2H), 3.37 (s, 3H), 2.49 (s, 3H).

Poly(ethylene glycol) p-toluenesulfonate (2) was synthesized following the method published by Bahr *et al.*⁹ Polyethylene glycol (Mn = 400 g/mol) was used instead of tri(ethylene glycol)monomethyl ether. A clear and colorless oil was afforded at 82 % yield. ¹H NMR (CDCl₃) δ: 7.61 (d, 2H), 7.15 (d, 2H), 3.95 (t, 2H), 3.33 to 3.53 (m, 16H), 2.24 (s, 3H).

4-(2-(2-(2-Methoxyethoxy)ethoxy)ethyl)nitrobenzene (3) was synthesized using the method published by Bahr *et al.*⁹ One modification was made, that being 5 % methanol in dichloromethane (by volume) was used as the eluent for the column chromatography. A clear and light yellow oil was afforded at 82 % yield. ¹H NMR (CDCl₃) δ: 8.18 (d, 2H), 6.99 (d, 2H), 4.23 (t, 2H), 3.90 (t, 2H), 3.80 to 3.60 (m, 6H), 3.55 (t, 2H), 3.38 (s, 3H).

2-(2-(2-(2-Methoxyethoxy)ethoxy)ethyl)nitrobenzene (4) was synthesized following the method published by Bahr *et al.*; except o-nitrophenol was used instead of p-nitrophenol and 5 % methanol in dichloromethane (by volume) was used as the eluent for the column chromatography.⁹ A yellow oil was afforded at 82 % yield. ¹H NMR (CDCl₃) δ: 7.81 (d, 1H), 7.51 (t, 1H), 7.12 (d, 1H), 7.03 (t, 1H), 4.27 (t, 2H), 3.91 (t, 2H), 3.76 (t, 2H), 3.65 (m, 4H), 3.55 (t, 2H), 3.38 (s, 3H).

4-(polyethylene glycol)nitrobenzene (5) was synthesized following the method published by Bahr *et al.*; except polyethylene glycol was used instead of tri(ethylene glycol)monomethyl ether and 5 % methanol in dichloromethane (by volume) was used as the eluent for the column chromatography.⁹ A yellow oil was afforded at 56 % yield. ¹H NMR (CDCl₃) δ: 8.25 (d, 2H), 7.02 (d, 2H), 4.26 (t, 2H), 3.93 (t, 2H), 3.75 (m, 4H), 3.75 to 3.62 (m, 14H).

2-(polyethylene glycol)nitrobenzene (6) was synthesized following the method published by Bahr *et al.*; except polyethylene glycol was used instead of tri(ethylene glycol)monomethyl ether, o-nitrophenol was used instead of p-nitrophenol, and 5 % methanol in dichloromethane (by volume) was used as the eluent for the column chromatography.⁹ A yellow oil was afforded at 63 % yield. ¹H NMR (CDCl₃) δ: 7.84 (d, 1H), 7.52 (t, 1H), 7.12 (d, 1H), 7.03 (t, 1H), 4.27 (t, 2H), 3.91 (t, 2H), 3.74 (m, 4H), 3.74 to 3.60 (m, 20H).

4-(2-(2-(2-Methoxyethoxy)ethoxy)ethyl)aniline (7) was synthesized using the method published by Bahr *et al.*⁹ “Acidic ethanol” used in the synthesis was obtained by adding 2 mL conc. HCl to 50 mL EtOH which was the same for all the aniline syntheses.

2-(2-(2-(2-Methoxyethoxy)ethoxy)ethyl)aniline (8) was synthesized following the method published by Bahr *et al.*; except compound **4** was used as the starting material instead of compound **3**.⁹ A reddish-brown oil was recovered at 94 % yield. ¹H NMR (CDCl₃) δ: 6.85 (m, 4H), 4.17 (t, 2H), 3.84 (t, 2H), 3.73 (t, 2H), 3.68 (m, 4H), 3.58 (t, 2H), 3.40 (s, 3H). IR (neat) 3470, 3360, 3202, 2877, 1619, 1511, 1461, 1352, 1281, 1223, 1118, 947, 851, and 747 cm⁻¹.

4-(polyethylene glycol)aniline (9) was synthesized following the method published by Bahr *et al.*; except compound **5** was used as the starting material instead of compound **3**.⁹ A reddish-brown oil was recovered at 88 % yield. ¹H NMR (CDCl₃) δ: 6.80 (m, 4H), 4.04 (t, 2H), 3.82 (m, 4H), 3.75 to 3.55 (m, 30H). IR (neat) 3440, 3356, 2872, 1636, 1511, 1465, 1356, 1294, 1244, 1118, 943, 834, and 730 cm⁻¹.

2-(polyethylene glycol)aniline (10) was synthesized following the method published by Bahr *et al.*; except compound **6** was used as the starting material instead of compound **3**.⁹ A light brown oil was recovered at 98 % yield. ¹H NMR (CDCl₃) δ: 6.83 (m, 4H), 4.16 (t, 2H), 3.85 (t, 2H), 3.73 (m, 4H), 3.72 to 3.60 (m, 28H). IR (neat) 3465, 3361, 2872, 1619, 1507, 1461, 1352, 1281, 1223, 1123, 947, 843, and 742 cm⁻¹.

4-(2-(2-(2-Methoxyethoxy)ethoxy)ethyl)benzene diazonium tetrafluoroborate (11; p-triethoxy) was synthesized using the method published by Tang *et al.*¹⁰ A reddish-brown tarry product was recovered at 95 % yield. ¹H NMR (d-acetone) δ: 8.75 (d, 2H), 7.55 (d, 2H), 4.55 (t, 2H), 3.92 (t, 2H), 3.67 (t, 2H), 3.58 (m, 4H), 3.46 (t, 2H), 3.27 (s, 3H). IR (neat) 3115, 3060, 2893, 2250, 1582, 1490, 1455, 1340, 1286, 1072, 938, 847, and 742 cm⁻¹.

2-(2-(2-(2-Methoxyethoxy)ethoxy)ethyl)benzene diazonium tetrafluoroborate (12; o-triethoxy) was synthesized following the method published by Tang *et al.*¹⁰ A reddish-brown tarry product was recovered at 84 % yield. ¹H NMR (d-acetone) δ: 8.59 (d, 1H), 8.31 (t, 1H), 7.82 (d, 1H), 7.54 (t, 1H), 4.75 (t, 2H), 4.02 (t, 2H), 3.72 (t, 2H), 3.62 (m, 4H), 3.51 (t, 2H), 3.32 (s, 3H). IR (neat) 3110, 2885, 2267, 1594, 1569, 1490, 1452, 1352, 1310, 1085, 939, 851, and 768 cm⁻¹.

4-(polyethylene glycol)benzene diazonium tetrafluoroborate (13; p-PEG) was synthesized following the method published by Tang *et al.*¹⁰ A reddish-brown tarry product was recovered at 78 % yield. ¹H NMR (d-acetone) δ: 8.80 (d, 2H), 7.60 (d, 2H), 4.58 (t, 2H), 3.93 (t, 2H), 3.67 to 3.47 (m, 30H). IR (neat) 3110, 2885, 2258, 1586, 1511, 1452, 1344, 1290, 1089, 955, 847, and 734 cm⁻¹.

2-(polyethylene glycol)benzene diazonium tetrafluoroborate (14; o-PEG) was synthesized following the method published by Tang *et al.*¹⁰ A reddish-brown tarry product was recovered at 27 %, the low final yield was due to column purification. ¹H NMR (d-acetone) δ : 8.61 (d, 1H), 8.30 (t, 1H), 7.82 (d, 1H), 7.54 (t, 1H), 4.76 (t, 2H), 3.98 (t, 2H), 3.72 to 3.52 (m, 32H). IR (neat) 3110, 2885, 2267, 1590, 1569, 1494, 1356, 1297, 1089, 951, 838, 767, and 734 cm⁻¹

ELECTROCHEMICAL TECHNIQUES

Cyclic voltammetry and film depositions (chronoamperometry) were performed using a glass cyclic voltammetry cell comprised of a working and reference compartment connected by a Luggin capillary. The working compartment was degassed with nitrogen for 5 minutes to remove oxygen from the compartment prior to CV or deposition. The electrolyte solution was composed of 0.1 M tetrabutylammonium hexafluorophosphate (TBAPF₆) in acetonitrile. Acetonitrile (99.9 %) was purchased from Macron Chemicals and used as received. Acetonitrile was used because the monomers had limited solubility in aqueous solutions. Acetonitrile was used to demonstrate proof-of-concept; and it is likely that water solubility could be enhanced by choice of different anions for the monomers. The monomer concentration was chosen to be 10 mM which was high enough for modification of the electrode surface. At low concentrations, ca. 1 mM, it had been reported that surface modification does not occur.¹¹ After each deposition, the modified GC electrode was sonicated for 15 minutes in neat acetonitrile to remove any non-grafted components in the film. Impedance spectroscopy was performed using a soft contact method (In/Ga eutectic) published by Rhodes *et al.*¹² The diazonium modified GC electrode was lowered into a pool of In/Ga eutectic. Gold evaporated onto glass was used as a plate to hold the In/Ga and provide good electrical contact to the eutectic. The frequency range was 1 Hz to 1 MHz with a voltage amplitude of 10 mV.

RESULTS AND DISCUSSION

The hypothesis of this chapter of the thesis was that a diazonium-based film would be grafted, nanoscale in thickness and function as a lithium-ion battery separator material. To judge the deposited films, grafting was determined by impedance spectroscopy on sonicated samples, thickness was determined by profilometry or SEM imaging, and impedance spectroscopy was used to determine ionic and electronic conductivities. To test the hypothesis, four diazonium salt based monomers were synthesized and electrodeposited.

Monomer structure was an important consideration, so each monomer was chosen for multiple reasons. All of the monomers have a diazonium “head” that can undergo grafting to multiple types of electrode surfaces such as carbon, metals, semiconductors, oxides, as well as to polymers.^{5,13} Having a diazonium functionality allows for direct reduction of the monomer onto the electrode surface without the use of a radical initiator. Furthermore, electropolymerization of diazonium salts show great self-limiting characteristics which produce very thin films.³⁻⁵ The “tail” of connecting ethylene glycol repeating units was chosen to incorporate ion mobility in a film afforded by the monomer. Two different tail lengths were synthesized to evaluate if tail length affected ionic conductivity or electrical resistivity. The position of the tail on the benzene ring was also investigated for the same reasons. In a para-position it was thought that the benzene rings of the diazoniums might pack more tightly onto the electrode surface leading to a film with higher density. Steric hindrance has been shown to influence packing density in a predictable manner for self assembled mono-layers.^{14,15} A denser film should exhibit a lower ionic conductivity and a greater electrical resistivity. Furthermore, with a PEG-type tail in the para-position it might prove difficult to get lithium ions close to the electrode surface for intercalation.

In contrast, with a tail in the ortho-position, the PEG tail would be directly adjacent to the electrode surface and not blocked by the benzene rings, potentially allowing for better ion mobility very near the electrode surface. The PEG tail in the ortho-position should also lead to a less dense film because the benzene rings of the diazoniums cannot pack as tightly onto the electrode surface due to steric hindrance. To summarize, the secondary hypothesis of this chapter is that monomer structure will influence ionic conductivity and electrical resistivity through PEG tail length and position on the benzene ring. The secondary hypothesis will be judged through impedance spectroscopy and redox shut-off experiments.

Infrared spectroscopy was used to identify important functional groups during the synthesis of the diazonium monomers. The nitro stretching peak (ca. 1500 cm^{-1}) was difficult to identify prior to the hydrogenation step because multiple stretching peaks were present near 1500 cm^{-1} and the peak nearest to 1500 cm^{-1} was present for each intermediate product.¹⁶ IR was successfully used to identify the amine stretching frequency ($3250\text{-}3500\text{ cm}^{-1}$) after hydrogenation of the nitrobenzene intermediate to confirm success of the reduction reaction to the aromatic amine.¹⁷ After the diazotizing reaction, the amine peaks were greatly suppressed and a sharp peak at 2260 cm^{-1} was present, consistent with the stretching frequency of the diazonium functional group.¹⁸

Cyclic voltammetry was used to determine the reduction potentials of the diazonium salts (Figure 3.3). All diazonium salts exhibit a broad irreversible reduction peak, common for diazonium salts.^{4,19} All peaks occur in the range of -0.5 to -0.9 V vs SSCE, therefore the depositions were performed at -1.0 V vs SSCE. As seen in Figure 3.3, the o-PEG does show an impurity wave at ca. -1.6 V vs SSCE.

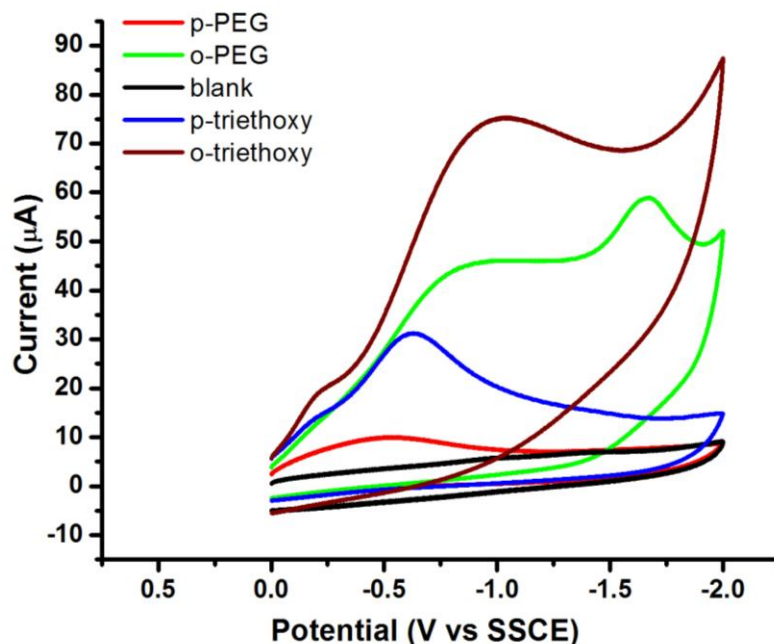


Figure 3.3. Cyclic voltammograms for all four diazonium salts; CVs were taken in a solution of 0.1 M tetrabutylammonium hexafluorophosphate in acetonitrile, scan rate = 100 mV/sec, the glassy-carbon electrode was polished using 0.3 μm β -alumina on a polishing pad before each scan.

This was surprising since o-PEG was the only diazonium salt purified by column chromatography; by depositing at -1.0 V electrochemical reactions with the impurity were likely avoided. Ortho substituted diazonium salts have more negative reduction potentials, perhaps due to the close proximity of the electron-donating ether group to the diazonium functional group. In general, electron-donating groups on the benzene ring shifts the reduction potential to more negative values while an electron-withdrawing groups shifts the reduction potential to more positive values. The concentration of diazonium salt was the same for all the cyclic voltammograms, but the peak current in the CV varied significantly for the monomers. The self-limiting abilities of each of the monomers may be a reason for the different peak heights. Comparing the four diazonium salts, there is excellent correlation between lower current in the voltammogram and lower current at the end of the deposition.

Chronoamperometry was used to deposit the diazonium based films onto a GC electrode. Deposition curves can be seen in Figure 3.4 (a and b). Insets show the current drop on a log scale for better comparison. After 15 minutes the current dropped at least 2 orders of magnitude in all cases and as high as 5 orders of magnitude for p-PEG. This shows the remarkable self-limiting nature of diazonium based films. As expected, para substituted diazonium salts showed better shutoff current and better self-limiting properties. This is likely due to the ability of the benzene rings of the diazonium to pack more tightly onto the electrode surface because of a lack of steric hindrance. The PEG based monomers also lead to better self-limiting properties, likely due to the longer chain length on the tail, hindering the ability of fresh monomer to transport to the electrode surface.

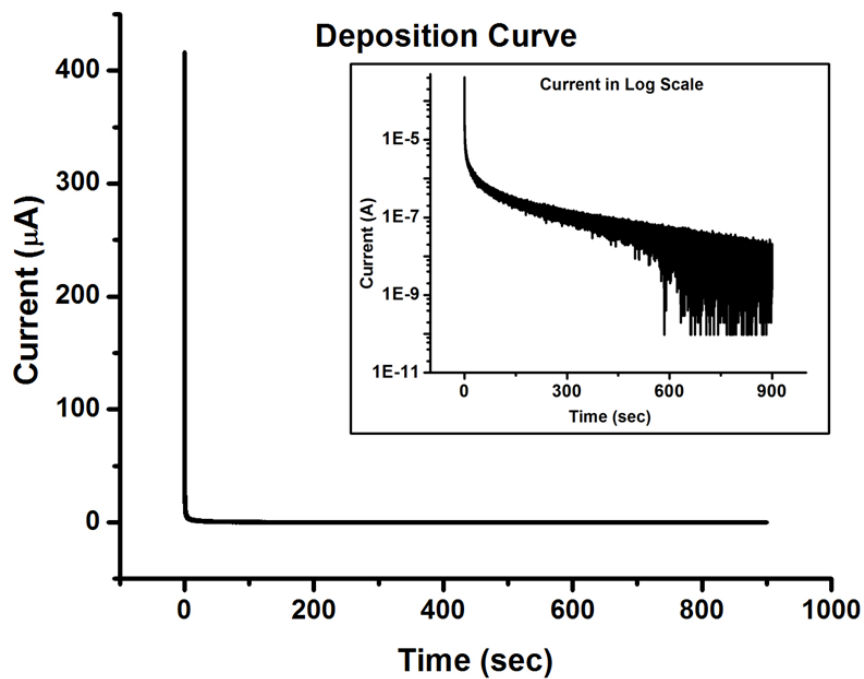
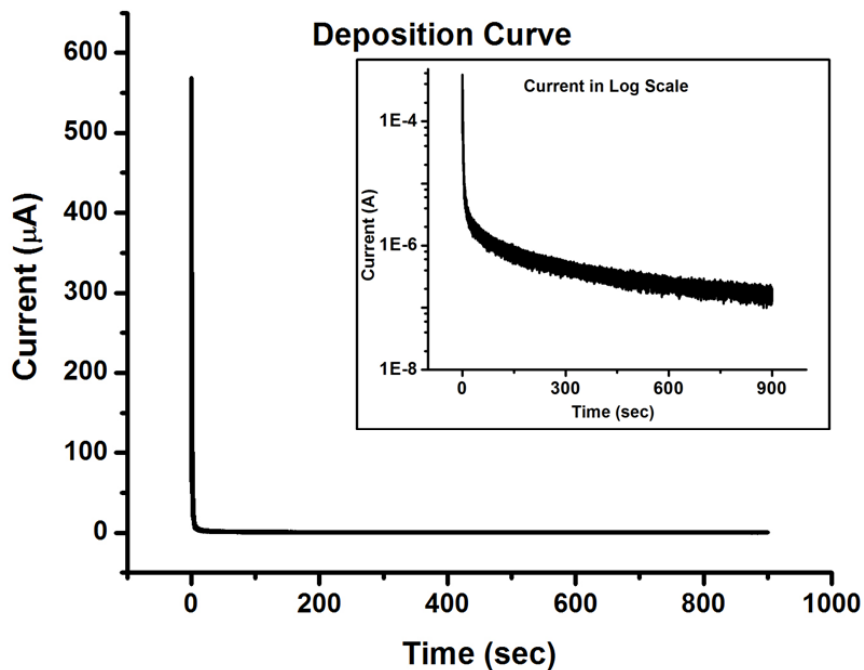


Figure 3.4.a. Deposition curves, inset shows current decrease on a log scale for clarity; top) 2-(polyethylene glycol)benzene diazonium tetrafluoroborate (o-PEG); bottom) 4-(polyethylene glycol)benzene diazonium tetrafluoroborate (p-PEG). The noise is due to very low current, which was near the limitations of the potentiostat.

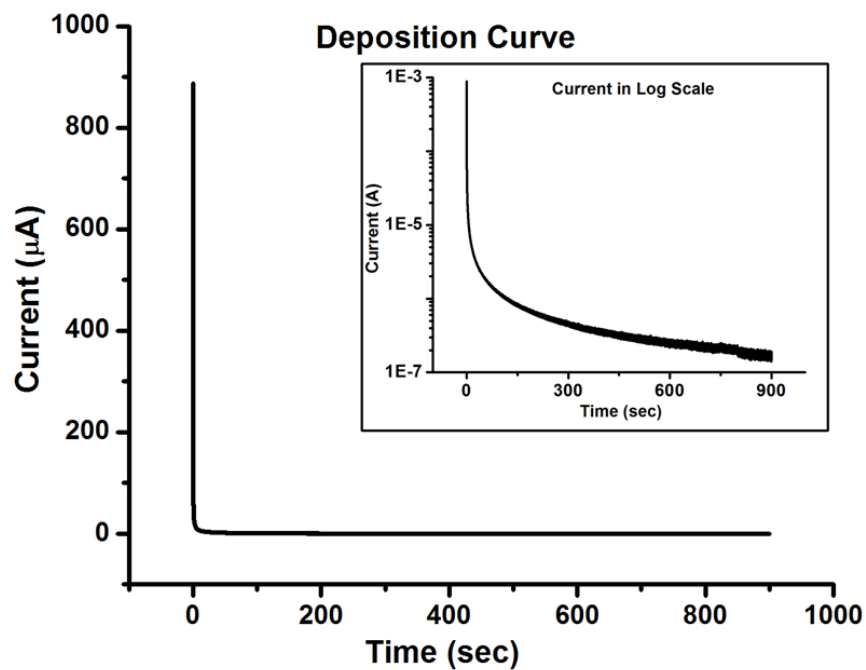
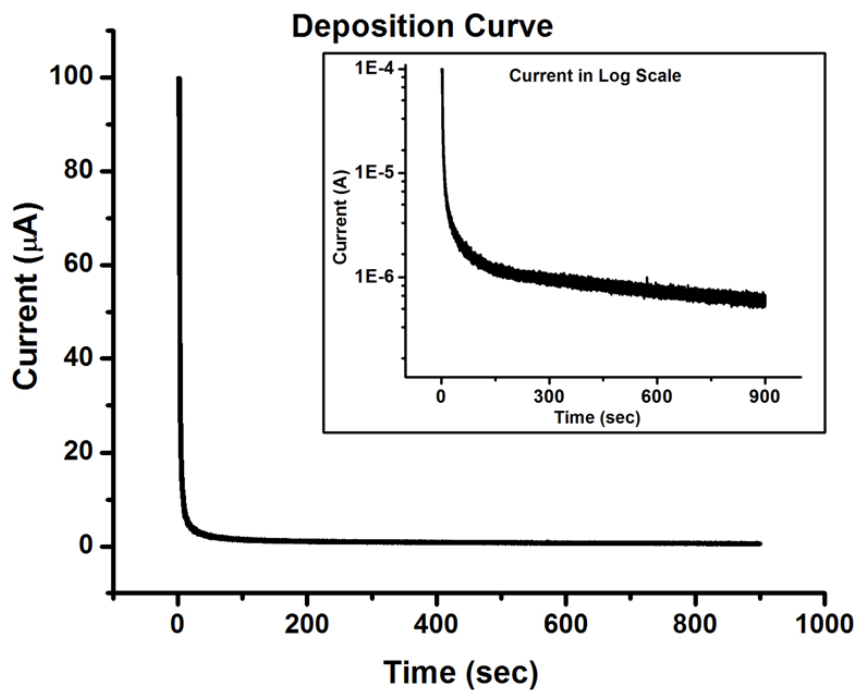


Figure 3.4.b. Deposition curves, inset shows current decrease on a log scale for clarity; top) 2-(2-(2-(2-methoxyethoxy)ethoxy)ethyl)benzene diazonium tetrafluoroborate (*o*-triethoxy); bottom) 4-(2-(2-(2-methoxyethoxy)ethoxy)ethyl)benzene diazonium tetrafluoroborate (*p*-triethoxy).

After each deposition, the coated GC electrode was sonicated in neat acetonitrile for 15 minutes before any characterization. The purpose of sonication was to remove any non-grafted components from the film. If the film itself was not grafted, the film would wash off under sonication because of the extreme agitation. The films are grafted and strongly adhered to the electrode surface because no impedance tests resulted in a shorted circuit (*vide infra*).

Impedance spectroscopy was used to determine the electronic resistance and ionic conductivity of the films. None of the films exhibit a diffusional (Warburg) tail at low frequency in the Nyquist plot (Figure 3.5); hence, none of the films exhibited ionic conductivity.^{20,21} This is not surprising since the films should be void of any ions. Attempts to measure impedance with plasticized films (1.0 M LiClO₄ in EC/DMC) were unsuccessful because an oxide layer formed instantly on the In/Ga eutectic upon contact with the plasticizer. It should be noted that ion permeation through the film is suggested by redox probe experiments (Figure 3.6 and 3.7).

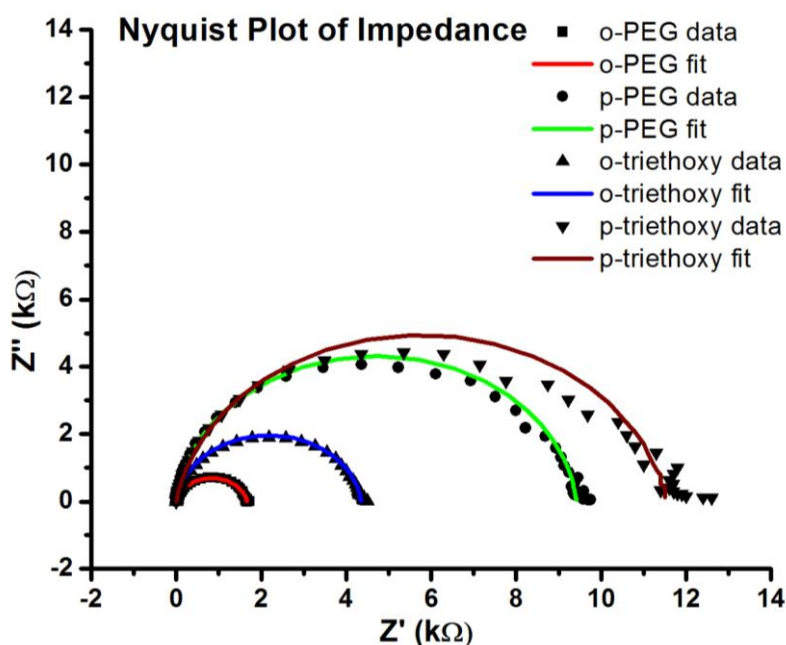


Figure 3.5. Nyquist plotted impedance data with fits for all four diazonium-based films deposited.

A depressed semicircle at medium to high frequency can be modeled with a resistor in parallel with a capacitor, a simple Randles circuit. The semicircle is slightly depressed or flattened, which is likely due to leaky or imperfect interfacial capacitance.²¹ Resistance values for the films can be found in Table 3.2. The values are all in the k Ω range, which is comparable to nanoscale poly(phenylene oxide)-type films deposited by Rhodes *et al.*¹² Para-substituted films exhibit higher resistances than their ortho counterpart. We hypothesize that the difference in resistance is due to the ability of the benzene rings to pack more tightly onto the electrode surface because of less steric hindrance. The shorter PEG tail also led to an increase in resistance of the film, consistent with less steric hindrance and tighter packing onto the electrode surface.

Table 3.2. Summary of resistance, capacitance, thickness, and resistivity values for all four diazonium-based films. Values obtained from impedance spectroscopy.

| Film | Resistance (k Ω) | Capacitance (nF) | Thickness (nm) | Resistivity (k Ω *cm) |
|-------------|--------------------------|------------------|----------------|------------------------------|
| p-triethoxy | 11.5 \pm 0.1 | 59.0 \pm 0.3 | 2.9 \pm 0.2 | 2.8 \pm 0.2 E+06 |
| o-triethoxy | 4.34 \pm 0.02 | 54.0 \pm 0.3 | 3.1 \pm 0.2 | 9.9 \pm 0.6 E+05 |
| p-PEG | 9.40 \pm 0.05 | 53.0 \pm 0.2 | 3.2 \pm 0.2 | 2.1 \pm 0.1 E+06 |
| o-PEG | 1.66 \pm 0.01 | 17.0 \pm 0.1 | 10 \pm 1 | 1.2 \pm 0.1 E+05 |

The thickness of the films was calculated using the capacitance values, determined by impedance spectroscopy. Using the equation for capacitance, seen below, the thickness was calculated.

$$C = \kappa * \epsilon_0 * A/D \quad (\text{Eq. 3.1})$$

In the equation above, C = capacitance (F), κ = dielectric constant, ϵ_0 = permittivity of free space (F/cm), A = area of electrode (cm²), and D = film/dielectric thickness (cm). The dielectric constant of the films was estimated to be 2.7 \pm 0.2, which is an average of 4 dielectric constants of polymer films with some molecular architecture similarities to the ones prepared here. The 4

polymers and dielectric constants were: poly(phenylene oxide), 2.59; polycarbonate, 2.92; azopolymer with aliphatic and aromatic fragments, 2.5; poly(phenylene oxide), 2.77.^{12,22,23} The area of the electrode was constant throughout all experiments and was equal to 0.71 cm². The capacitance values were determined using the same fit and plot as the resistance values, seen in Table 3.1. All films were extremely thin, as expected based on their self-limiting property. Three films (o-triethoxy, p-triethoxy, and p-PEG) were estimated to be (based on the above calculation) 3 nm thick while o-PEG was estimated to be 10 nm thick. Attempts to measure the thickness of the films using profilometry or SEM imaging were unsuccessful because the film thicknesses were below the lower limit of the instruments.

Using the calculated thicknesses and the measured resistances, the resistivity was calculated for all four films (Table 3.1). All films exhibit high resistivity values (1200- 28000 MΩ/cm) consistent with being insulators.²⁴ It is difficult to compare these values with commercially available separators or ideal values because those resistivity values are reported as a Gurley number, which is the air permeability.²⁵ Air permeability is proportional to resistivity of a separator for a given morphology.²⁵ Since morphology of the diazonium based films is not known, a Gurley number could not be calculated, and a comparison could not be made. Attempts to perform solid state linear sweep voltammetry on the films (not shown) resulted in a breakdown of the separator near 1.5 V (using same setup as impedance measurement with reference shorted to auxiliary). Therefore, even with high resistivity values, these particular films are not thick enough to hold up to the voltages of typical lithium cells (*ca.* 3.2 V).

Ferrocene and 1, 1', 3, 3'-tetra-*t*-butyl ferrocene were used as probe molecules to test the deposited films for pinholes or incomplete coverage. The ferrocene probes showed a small irreversible anodic peak for all four films (Figures 3.6 and 3.7). This data was inconclusive with regard to pinholes, which is why 1, 1', 3, 3'-tetra-*t*-butyl ferrocene was also used. The larger and bulkier 1, 1', 3, 3'-tetra-*t*-butyl ferrocene did not penetrate the polymer film, as seen by the lack of current in the probe experiments, with an exception for *o*-triethoxy (Figure 3.7). If pinholes did exist, ferrocene and 1, 1', 3, 3'-tetra-*t*-butyl ferrocene probe molecules would give similar responses. This was not the case for any film.

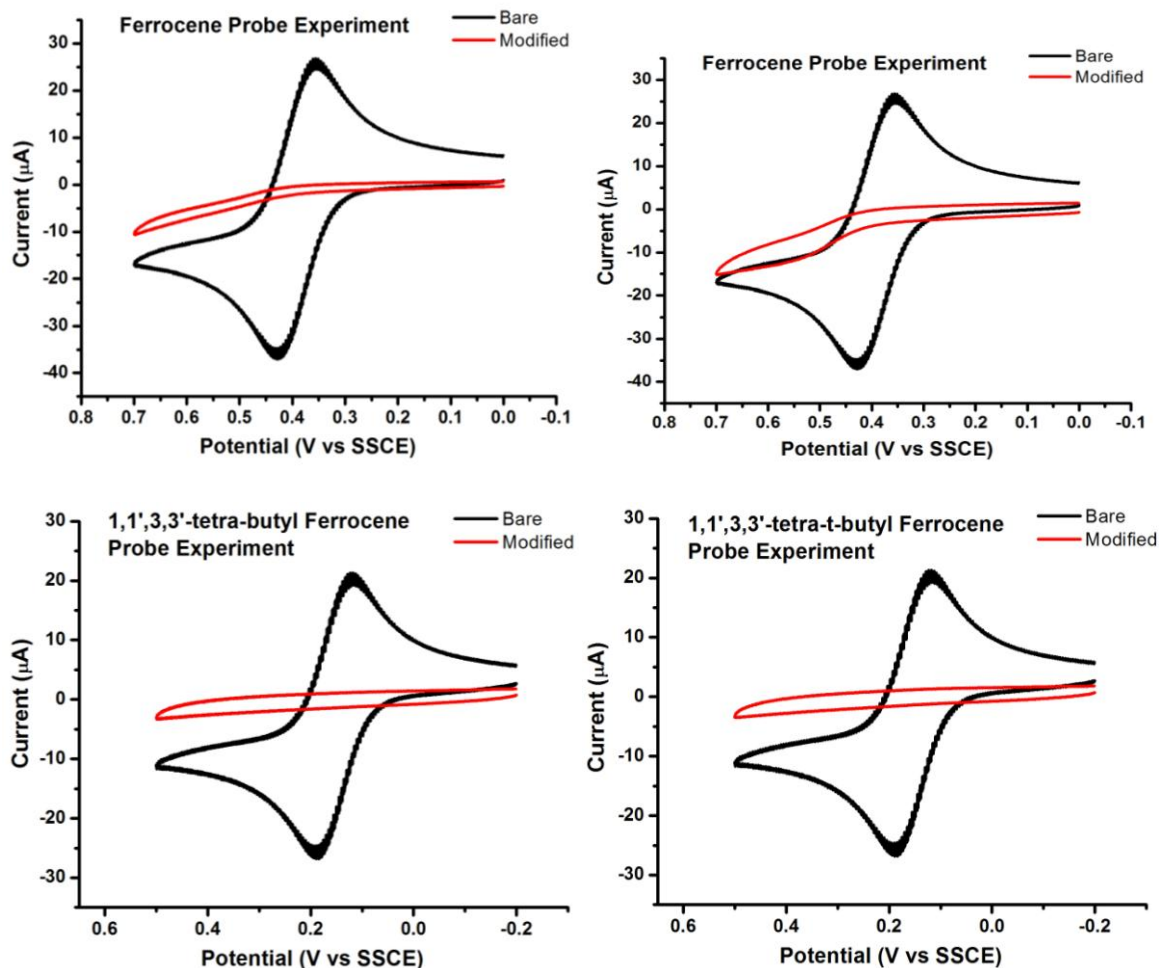


Figure 3.6. Cyclic voltammograms from ferrocene and 1,1',3,3'-tetra-t-butyl ferrocene probe experiments for p-PEG film (left) and o-PEG film (right).

Although o-triethoxy films were more electrically resistive than o-PEG, the probe experiment suggests o-triethoxy is better at allowing molecules, and probably ions, to transport to the electrode surface. Further evidence for this is seen in the deposition curves, which show worse shut off/blocking effects for o-triethoxy. The data suggests that o-triethoxy would be more suitable as a separator material for ionic reasons, but would also require the thickest film because it exhibited the lowest resistivity. The fact that ferrocene was able to reach the electrode surface

and oxidize, for all films, is worth noting. This suggests that diffusion of molecules or ions through the film is possible and likely has a size dependency, which would be good since the afforded films target use is as lithium-ion battery separators.

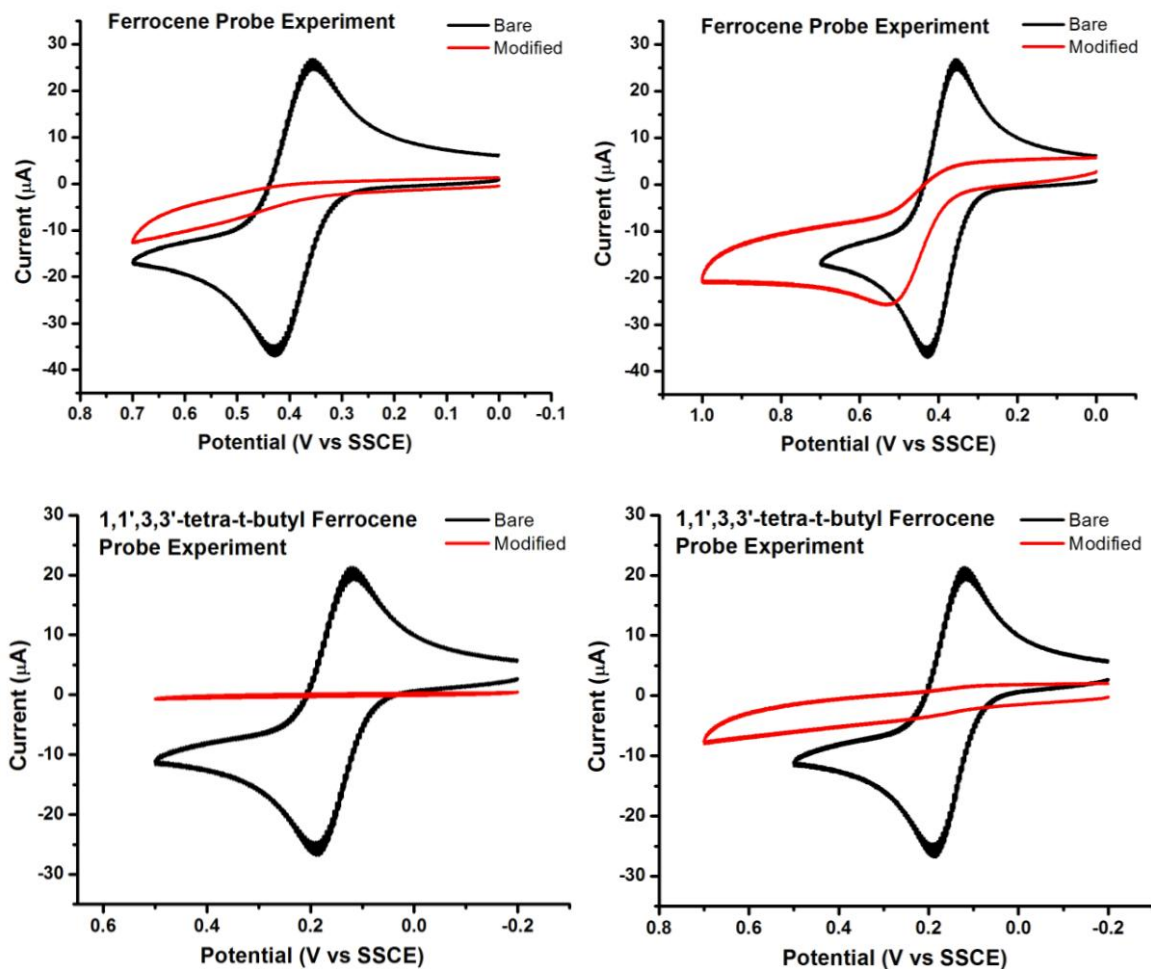


Figure 3.7. Cyclic voltammograms from ferrocene and 1,1',3,3'-tetra-t-butyl ferrocene probe experiments for p-triethoxy film (left) and o-triethoxy film (right).

Comparing ortho vs. para substitution in Figure 3.6 and 3.7, the data suggest that para substituted films are better at blocking the electrode from probe molecules than ortho substituted. The main reason for investigating ortho and para substitutions was to see if a ortho positioned tail would facilitate movement of ions/molecules to the electrode surface better than a para

position. As expected, with the tail in the ortho position it becomes easier to pass molecules, and likely ions, to the electrode surface. We hypothesize that the tail in the ortho position causes steric hindrance and the benzene heads cannot pack as tightly onto the electrode surface, leaving space for the transport. Furthermore, substitution at the ortho position forces the PEG tail to be directly adjacent to the electrode surface, possibly facilitating molecule and ion movement very near the electrode surface.

Glass transition temperature (T_g) is also an important consideration for a separator material because the ionic conductivity will be very low as the polymer loses chain mobility. Due to the extremely thin nature of the diazonium-based films, it was not possible to isolate a large enough sample size for differential scanning calorimetry.

CONCLUSION

The hypothesis of this chapter of the thesis was that a diazonium-based film would be grafted, nanoscale in thickness and function as a lithium-ion battery separator material. To judge the deposited films, thickness was to be determined by profilometry or SEM imaging, grafting was determined by impedance spectroscopy on sonicated samples, and impedance spectroscopy was used to determine ionic and electronic conductivities. The secondary hypothesis of this chapter was that monomer structure would influence ionic conductivity and electrical resistivity through PEG tail length and position on the benzene ring. The secondary hypothesis was judged through impedance spectroscopy and redox shut-off experiments. Table 3.3 summarizes the criteria used to judge the diazonium-based films and how they performed.

Table 3.3. A summary of the physical properties that were used as criteria to judge diazonium-based films. Included are ideal values along with some of the best reported values in literature.

| Physical Property | Diazo-film | Ideal | Reported in Lit. |
|---------------------------|----------------------------|---------------------|-----------------------------------|
| Reductively Polymerized | yes | yes | yes (polymers in general) (Ref 8) |
| Electronic Conductivity | 3.6×10^{-10} S/cm | zero | 7×10^{-12} S/cm (Ref 7) |
| Ionic Conductivity | none | $\geq 10^{-2}$ S/cm | 1.6×10^{-4} S/cm (Ref 6) |
| Conformal/Uniform Coating | Conformal | yes | 21 ± 2 nm (Ref 7) |
| Thickness | 3-10 nm | 10-50 nm | 21-43 nm (Ref 7) |
| Grafted | yes | yes | yes (Ref 8) |
| Tg | unknown | -100 °C | -80 °C (Ref 6) |

A new class of monomers with a diazonium functional group was successfully synthesized and characterized. The monomers have a diazonium head group that can undergo grafting to multiple surfaces and also leads to a self-limiting polymerization. The grafting was confirmed by impedance measurements on sonicated films. The monomers have a PEG based tail that should facilitate ion movement through the film. Films afforded from para-substituted diazonium salts exhibit higher resistivity values than ortho substituted and blocked the electrode better during redox shut-off experiments. Therefore para substitution decreases transport (probe molecules or monomer) to the electrode surface but increases electrical resistivity. In other words, ortho substitution helps facilitate mobility through the film while para substitution increases electrical resistivity of the film. Film thickness could not be determined by SEM imaging or profilometry because the thickness was below the limitations of the instruments. Estimated thicknesses were calculated based on capacitance values. The films were extremely thin (3-10 nm), grafted, conformal, pinhole free, and exhibited resistivity values as high as 28000

MΩ/cm. Increasing the thickness of the films is still desired as this would increase the voltage window the films can operate in. The films are a good start toward a nanoscale lithium-ion battery separator material that undergoes grafting to the electrode surface.

FUTURE WORK

Future work should be focused on increasing the thickness of the diazonium-based films. To increase the film thickness a few approaches could be taken. First, a large enough over-potential could form a radical on the benzene ring that is grafted to the electrode surface. Another monomer unit could then react at the radical site and the polymerization would continue. Likewise, the over-potential could also allow for reduction of a diazonium monomer in solution that would in turn react with the already grafted film. Diazonium-based film thickness has been reported to depend on applied potential.^{26,27} A second approach would be to add in a smaller diazonium monomer such as methoxy diazonium tetrafluoroborate. If steric hindrance is blocking further monomer to react with the depositing film, a small tailed diazonium may still be able to react and act as a new site that a PEG-based diazonium could then react with. This approach could increase film thickness, but also may increase film density and decrease ion/molecule mobility in the film. Third, by increasing the deposition time the film thickness could increase. This approach was attempted twice in some preliminary work, but the longest deposition was only 1 hr, which did not produce a thicker film. In a recent publication by Lehr *et al.*, two growth mechanisms were hypothesized for diazonium film formation.²⁸ One mechanism is a potential and substrate dependant mechanism and the second is a slow-growth in which film thickness increased with time. Without continuing to apply a potential and simply leaving the

substrate in a diazonium-based solution, the film thickness continued to increase for at least 13 hrs.²⁸ Therefore, an attempt should be made to deposit for 6 and/or 12 hours to determine if a long deposition approach could be used to produce thicker diazonium-based films.

REFERENCES

- (1) Leung, K.; Qi, Y.; Zavadil, K. R.; Jung, Y. S.; Dillon, A. C.; Cavanagh, A. S.; Lee, S.-H.; George, S. M. *J. Am. Chem. Soc.* **2011**, *133*, 14741–14754.
- (2) Woo, J. H.; Trevey, J. E.; Cavanagh, A. S.; Choi, Y. S.; Kim, S. C.; George, S. M.; Oh, K. H.; Lee, S.-H. *Journal of The Electrochemical Society* **2012**, *159*, A1120–A1124.
- (3) Adenier, A.; Combellas, C.; Kanoufi, F.; Pinson, J.; Podvorica, F. I. *Chem. Mater.* **2006**, *18*, 2021–2029.
- (4) Allongue, P.; Delamar, M.; Desbat, B.; Fagebaume, O.; Hitmi, R.; Pinson, J.; Saveant, J. M. *Journal of the American Chemical Society* **1997**, *119*, 201–207.
- (5) Belanger, D.; Pinson, J. *Chem. Soc. Rev.* **2011**, *40*, 3995–4048.
- (6) Meyer, W. H. *Advanced Materials* **1998**, *10*, 439–448.
- (7) Rhodes, C. P.; Long, J. W.; Doescher, M. S.; Fontanella, J. J.; Rolison, D. R. *J. Phys. Chem. B* **2004**, *108*, 13079–13087.
- (8) Danda, C. K.; Cai, R.; Wang, W.; Baba, A.; Advincula, R. C. *Polymeric Materials: Science and Engineering* **2008**, *98*, 444–445.
- (9) Bahr, J. L.; Yang, J.; Kosynkin, D. V.; Bronikowski, M. J.; Smalley, R. E.; Tour, J. M. *J. Am. Chem. Soc.* **2001**, *123*, 6536–6542.
- (10) Tang, Z.; Zhang, Y.; Wang, T.; Wang, W. *Synlett* **2010**, *2010*, 804–808.
- (11) Andrieux, C. P.; Pinson, J. *J. Am. Chem. Soc.* **2003**, *125*, 14801–14806.
- (12) Rhodes, C. P.; Long, J. W.; Rolison, D. R. *Electrochemical and Solid State Letters* **2005**, *8*, A579–A584.
- (13) Pinson, J.; Podvorica, F. *Chem. Soc. Rev.* **2005**, *34*, 429–439.
- (14) Weidner, T.; Bretthauer, F.; Ballav, N.; Motschmann, H.; Orendi, H.; Bruhn, C.; Siemeling, U.; Zharnikov, M. *Langmuir* **2008**, *24*, 11691–11700.
- (15) Elbing, M.; Błaszczuk, A.; Von Hänisch, C.; Mayor, M.; Ferri, V.; Grave, C.; Rampi, M. A.; Pace, G.; Samorì, P.; Shaporenko, A.; Zharnikov, M. *Adv. Funct. Mater.* **2008**, *18*, 2972–2983.
- (16) Kuhn, A.; Von Eschwege, K. G.; Conradie, J. *J. Phys. Org. Chem.* **2012**, *25*, 58–68.
- (17) Brown, W. H.; Foote, C. S. *Organic Chemistry*; Second.; Saunders College Publishing: Orlando, Florida.
- (18) Nuttall, R. ; Roberts, E. ; Sharp, D. W. . *Spectrochimica Acta* **1961**, *17*, 947–952.
- (19) Creager, S. E.; Liu, B.; Mei, H.; DesMarteau, D. *Langmuir* **2006**, *22*, 10747–10753.
- (20) Atebamba, J.-M.; Moskon, J.; Pejovnik, S.; Gaberscek, M. *J. Electrochem. Soc.* **2010**, *157*, A1218–A1228.
- (21) Taylor, R.; Spotnitz, R.; Kendig, M.; Buchheit, R.; Loveday, D.; Contu, F. A Short Course on Electrochemical Impedance Spectroscopy: Theory, Applications, and Laboratory Instruction **2012**.
- (22) Tokarzewski, L.; Dziewiecka, B. *J. Polym. Sci. Polym. Chem. Ed.* **1981**, *19*, 1577–1580.
- (23) *CRC Handbook of Chemistry and Physics*; 92nd ed.; CRC Press, 2011.
- (24) Resistivity - Cost http://www-materials.eng.cam.ac.uk/mpsite/interactive_charts/resistivity-cost/NS6Chart.html (accessed Aug 27, 2012).
- (25) Arora, P.; Zhang, Z. M. *Chemical Reviews* **2004**, *104*, 4419–4462.
- (26) Downard, A. J. *Langmuir* **2000**, *16*, 9680–9682.

- (27) Brooksby, P. A.; Downard, A. J. *Langmuir* **2004**, *20*, 5038–5045.
- (28) Lehr, J.; Williamson, B. E.; Downard, A. J. *J. Phys. Chem. C* **2011**, *115*, 6629–6634.

APPENDIX 2

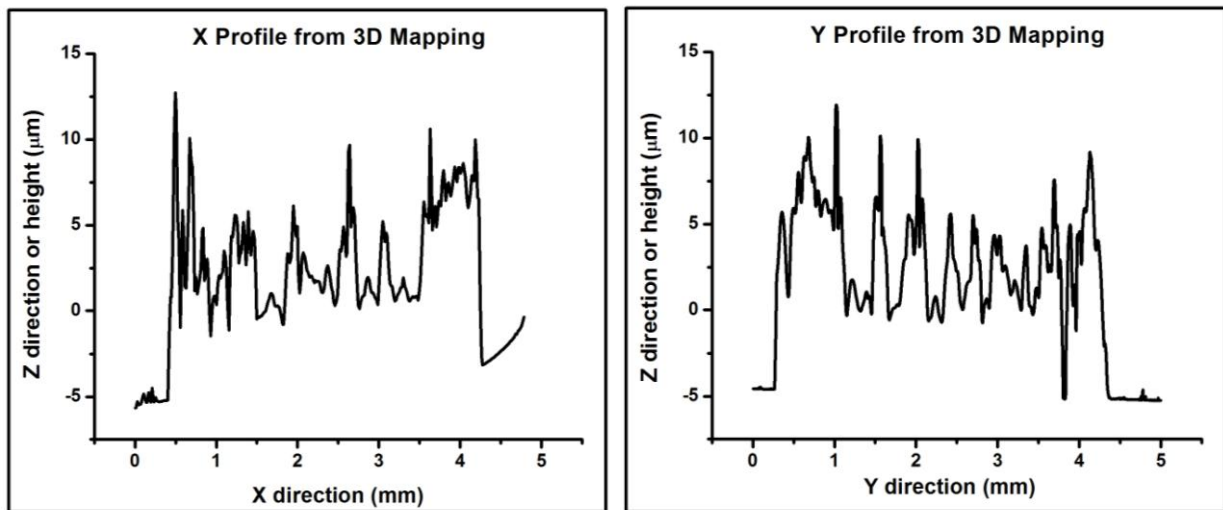


Figure A2.1. X and Y profiles for topographical map (Figure 2.12) used to determine the thickness of the PEGDA film.